



This work is protected by copyright and other intellectual property rights and duplication or sale of all or part is not permitted, except that material may be duplicated by you for research, private study, criticism/review or educational purposes. Electronic or print copies are for your own personal, non-commercial use and shall not be passed to any other individual. No quotation may be published without proper acknowledgement. For any other use, or to quote extensively from the work, permission must be obtained from the copyright holder/s.

**Towards monitoring of the progress of
chemical reactions using a novel plasma-
assisted desorption ionisation mass
spectrometry methodology**

Jasim Mohammed Shamar Jamur

Thesis submitted to Keele University for the Degree of Doctor of Philosophy

March 2018

Keele University

Abstract

A novel method for monitoring of pharmaceutically relevant reactions using PADI-MS has been developed in this study. The visible non-thermal plasma plume from a coaxial helium gas flow non-thermal RF plasma was optimised using a range of samples. PADI-MS was found to be a powerful analytical technique for pharmaceutically relevant solid and liquid samples and can readily be adapted for use in reaction monitoring. This study has determined that PADI-MS is fast, easy to set up and requires little or no sample preparation. PADI-MS has significant advantages over other techniques as it is faster, more sensitive and more convenient and suitable for investigation of complex molecules and mixtures. However, two limitations of PADI-MS are that the plasma can affect the sample surface chemistry upon exposure and quantification is not always trivial.

A number of other analytical methods were used in conjunction with PADI-MS: TLC, HPLC, FTIR and Raman spectroscopy. Chapter 3 investigated PADI-MS and Raman analysis of paracetamol tablet as model for pharmaceutically relevant solids. Raman microscopy was used to develop an understanding of how the plasma affects the sample surface. The plasma effect was also studied by examining changes in PADI-MS spectra.

In Chapter 4, PADI-MS acquisition settings were improved by adding water vapour to the outer He flow gas and increasing the plasma power to 8 W, optimising the analysis of mixture solutions from TLC plates. Although molecules could be identified with optimum sensitivity after separation, this may not be necessary, unless the highest possible sensitivity is required.

Chapter 5 deals with PADI-MS for direct analysis of pharmaceutical compounds in solid and liquid forms from glass slides and cotton swabs. PADI-MS was determined to be

suitable for analysis of pharmaceutical tablets from solutions via both substrates, with distinct advantages for the latter.

The final Chapter studied PADI-MS for the monitoring of imine formation as model pharmaceutical reaction. Both FTIR and PADI-MS were successfully used, but the latter is faster and more versatile. TLC and HPLC could not be used for this reaction. PADI-MS was successfully used for this reaction using cotton swabs without preparation or pre-concentration of sample solutions.

Contents

Abstract	I
Abbreviations	XV
Publications and presentations	XVII
Acknowledgements	XIX
CHAPTER 1: Introduction.....	1
1.1. General introduction	2
1.2. Reaction monitoring	3
1.3. Pharmaceutical applications of separation techniques	4
1.3.1. Chromatography.....	4
1.3.1.1. Thin layer chromatography (TLC)	5
1.3.1.2. High-performance liquid chromatography (HPLC)	9
1.3.1.2.1. HPLC components	10
1.3.1.2.2. Types of columns in HPLC	12
1.3.1.2.3. Types of HPLC detectors.....	13
1.3.1.2.4. Types of HPLC	15
A) Normal phase HPLC	15
B) Reverse phase HPLC	15
1.4. Pharmaceutical applications of spectroscopic techniques.....	16
1.4.1. Spectrophotometry	16
1.4.1.1. Ultraviolet-visible (UV/Vis) spectroscopy	16
1.4.1.1.1. UV/Vis instrumentation	17
1.4.2. Vibrational spectroscopies	19
1.4.2.1. Infrared spectroscopy (IR).....	19
1.4.2.1.1. Basic principles of IR spectroscopy	21
1.4.2.1.2. Steps of generating the FTIR spectrum	22
1.4.2.2. Raman spectroscopy	23
1.4.2.2.1. Basic principles of Raman spectroscopy	23
1.5. Mass spectrometry (MS)	26
1.5.1. Practical steps in mass spectrometry	28
1.5.2. Hyphenated techniques using mass spectrometry.....	30
1.5.2.1. LC/MS instrumentation	31
1.5.3. Ambient mass spectrometry (AMS).....	32
1.5.3.1. Plasma-based ambient mass spectrometry.....	34

1.5.3.2. Ambient mass spectrometry techniques	37
1.5.3.2.1. Desorption electrospray ionisation (DESI).....	37
1.5.3.2.2. Direct analysis in real time (DART).....	37
1.5.3.2.3. Low-temperature plasma probe (LTP).....	38
1.5.3.2.4. Plasma assisted desorption ionisation-mass spectrometry (PADI-MS)	
39	
References	42
CHAPTER 2: Experimental details	63
2.1. Chemicals	64
2.2. Standard and Sample Preparation.....	64
2.3. Experimental techniques	64
2.3.1. Chromatographic techniques.....	64
2.3.1.1. Thin layer chromatography (TLC)	64
2.3.1.2. High-performance liquid chromatography (HPLC)	64
2.3.2. Spectroscopic techniques	65
2.3.2.1. Ultraviolet-visible (UV/Vis) spectrophotometer	65
2.3.3. Vibrations spectroscopy techniques	65
2.3.3.1. Fourier transform infrared spectroscopy (FTIR)	65
2.3.3.2. Raman spectroscopy	65
2.3.4. Plasma-assisted desorption ionisation-Mass spectrometry (PADI-MS)	65
References	68
CHAPTER 3: PADI Plasma-substrate interaction studied by PADI-MS and Raman spectroscopy using paracetamol tablets as a model system	69
Abstract	70
3.1. Introduction	71
3.2. Materials and methods.....	74
3.2.1. Apparatus:.....	74
3.2.2. Chemicals:.....	75
3.2.3. Preparation of samples:	75
3.2.4. Procedure:	75
3.3. Results and discussion	78
3.3.1. Method development and optimisation of PADI-MS and Raman spectroscopy conditions	78
3.3.2. Exposure of sample to plasma flame	78

3.3.3.	Raman microscopy.....	81
3.3.3.1.	Identification of functional groups of paracetamol.....	81
3.3.3.2.	Effect of visible plasma on the chemistry of paracetamol tablets	83
3.3.4.	Plasma-assisted desorption ionisation mass spectrometry (PADI-MS).....	88
3.3.4.1.	Identification of fragment and adduct peaks of paracetamol.....	88
3.3.4.2.	Effect of plasma flame on paracetamol tablet chemistry using PADI-MS	91
3.4.	Conclusions	95
	References	97
	CHAPTER 4: PADI Mass spectrometry analysis of mixtures from TLC plates.....	101
	Abstract	102
4.1.	Introduction	103
4.2.	Materials and methods.....	108
4.2.1.	Apparatus:	108
4.2.2.	Chemicals:.....	108
4.2.3.	Preparation of sample solutions:	109
4.2.4.	Standard TLC plates:.....	109
4.2.5.	Procedure:	109
4.3.	Results and discussion.....	112
4.3.1.	Optimised conditions used for all following experiments	112
4.3.1.1.	Plasma Power.....	112
4.3.1.2.	Plasma pencil to sample distance.....	113
4.3.1.3.	Carrier gas flow rate	114
4.3.1.4.	Carrier gas additives	114
4.3.2.	Time dependence of plasma interaction.....	119
4.3.3.	Analysis of Mixtures	122
4.3.3.1.	Method A: Analysis without separation of spots.....	122
4.3.3.2.	Method B: Analysis after separation of spots.....	130
4.3.4.	Quantification.....	135
4.3.4.1.	Practical evaluation.....	138
4.4.	Conclusions	141
	References	143
	CHAPTER 5: Plasma-assisted desorption ionisation mass spectrometry – PADI-MS for the analysis of pharmaceutical solids and liquids from glass slides and cotton swabs.....	147

Abstract	148
5.1. Introduction:	149
5.2. Materials and methods.....	152
5.2.1. Apparatus:	152
5.2.2. Chemicals and materials:	153
5.2.3. Preparation of sample solutions:	153
5.2.4. Procedure:	154
5.3. Results and discussion:.....	154
5.3.1. Method development and optimisation of PADI-MS conditions	154
5.3.2. Analysis of pure and tablets	155
5.3.2.1. Plasma-sample interaction time	160
5.3.3. Analysis of individual compounds/mixtures from glass slides.....	165
5.3.4. Analysis of mixtures from cotton swabs.....	172
5.3.5. Quantification.....	181
5.4. Conclusions	183
References	186
CHAPTER 6: PADI mass spectrometry for the monitoring of imine (Schiff base)	
formation as a model of pharmaceutical reaction mixtures	189
Abstract	190
6.1. Introduction	191
6.2. Materials and methods.....	194
6.2.1. Apparatus:	194
6.2.1.1. UV-Vis spectrophotometer	194
6.2.1.2. Thin layer chromatography (TLC)	194
6.2.1.3. High performance liquid chromatography (HPLC).....	194
6.2.1.4. Fourier transform infrared spectroscopy (FTIR)	195
6.2.1.5. Plasma assisted desorption ionisation mass spectrometry (PADI-MS).....	195
6.2.2. Chemicals:.....	195
6.2.3. Schiff base reaction	196
6.2.4. Monitoring Methods	197
6.2.4.1. Monitoring of the Schiff base formation by TLC.....	197
6.2.4.2. Monitoring of the Schiff base reaction by HPLC	197
6.2.4.3. Monitoring of the Schiff base reaction by FTIR.....	198
6.2.4.4. Monitoring of the Schiff base reaction by PADI-MS.....	198

6.3. Results and discussion.....	198
6.3.1. Wavelength measurements of the starting materials and product using UV-Vis spectrophotometry.....	198
6.3.2. Reaction monitoring of imine formation using TLC.....	200
6.3.3. Reaction monitoring of imine formation using HPLC.....	201
6.3.4. Reaction monitoring of imine formation using FTIR spectroscopy.....	205
6.3.5. Reaction monitoring of imine formation using PADI-MS.....	211
6.3.5.1. Para-anisidine and 4-nitrobenzaldehyde standards.....	211
6.3.5.2. Analysis of reaction mixtures.....	215
6.4. Conclusions.....	220
References.....	222
CHAPTER 7: General discussions and conclusions.....	226

Index of Figures

Chapter 1

Figure 1. 1. Schematic diagram of high-pressure liquid chromatography (HPLC).	10
Figure 1. 2. Schematic diagram of a UV/Vis Spectrophotometer.....	18
Figure 1. 3. Schematic diagram of an FT spectrometer.	22
Figure 1. 4. Schematic illustration of excitation states of molecules via Rayleigh, Stokes and anti-Stokes Raman scattering.	25
Figure 1. 5. Components of a mass spectrometer.	28
Figure 1. 6. Schematic diagram of mass spectrometer linked to LC.	32
Figure 1. 7. Components of traditional ways to produce ions of samples.	33

Chapter 2

Figure 2. 1. Schematic of the PADI probe and source in operation.....	67
Figure 2. 2. Schematic diagram of PADI-MS instrument.....	67

Chapter 3

Figure 3. 1. Thermal camera images of a sample of paracetamol tablet during exposure to the plasma at different times: a 5 secs; b 15 secs; c 35 secs; d 1 min; e 3 min and f 5 min.	77
Figure 3. 2. Photo of the PADI source in operation using helium directly from a cylinder with flow rate of 224 mL/min, and the distance between the plasma flame and sample was 5 mm.	79
Figure 3. 3. Photos of paracetamol tablets after exposure to room temperature non-thermal plasma flame (from 10 secs to 300 secs) at 7W.....	79
Figure 3. 4. Spot size of PADI plasma as a function of plasma exposure time.	80
Figure 3. 5. Molecular structure for paracetamol.....	81
Figure 3. 6. Raman spectrum of 500 mg 0-seconds paracetamol tablet (without exposure to plasma).	82
Figure 3. 7. Raman spectra of C=O, aryl CC and CNH stretch-bend of paracetamol tablets after exposure to NTP at different times: 10 secs, 20 secs, 30 secs, 50 secs, 1 min, 2 min, 3 min and 5 min.	84
Figure 3. 8. Raman spectra of CNH stretch-open, C-O-H (OH substitution) and aryl CH bend of paracetamol tablets after exposure to NTP at different times: 10 secs, 20 secs, 30 secs, 50 secs, 1 min, 2 min, 3 min and 5 min.....	85
Figure 3. 9. Raman spectra of aryl CH wag and ring deformation of paracetamol tablets after exposure to NTP at different times: 10 secs, 20 secs, 30 secs, 50 secs, 1 min, 2 min, 3 min and 5 min.	85
Figure 3. 10. Peak height measurements of the vibration peaks for paracetamol tablet with a total acquisition time of 5 minutes using Raman microscopy.	86
Figure 3. 11. Intensity ratios measurement of C=O/aryl CH bend of paracetamol tablet (500 mg) with an acquisition time of 5 minutes using Raman microscopy.....	87

Figure 3. 12. Intensity ratios measurement of C=O/CNH stretch open of paracetamol tablet (500 mg) with an acquisition time of 5 minutes using Raman microscopy.....	88
Figure 3. 13. PADI-MS spectra of background and pure paracetamol at exposure time to plasma with an acquisition time of 1 minute.	90
Figure 3. 14. PADI-MS spectra of paracetamol tablet at different exposure times to plasma with an acquisition time of 5 minutes.	90
Figure 3. 15. PADI-MS signal intensity for [M+H] ⁺ in pure paracetamol.....	91
Figure 3. 16. PADI-MS signal intensity for [M+H] ⁺ in paracetamol tablet with a total acquisition time of 5 minutes.	92
Figure 3. 17. Signal intensity of adduct and fragment peaks for each sample of paracetamol tablet against acquisition time up to 5 minutes in 5 seconds intervals 5, 45, 85, 115, 195 and 295 seconds.	93
Figure 3. 18. Signal intensity ratios of adduct and fragment peaks of paracetamol tablet by a factor of 152/77, 302/77 and 169/77 with acquisition time up to 5 minutes using PADI-MS.....	94

Chapter 4

Figure 4. 1. Signal intensity of [M+H] ⁺ in paracetamol tablet against different plasma power using helium added with a total acquisition time of 1 minute.	113
Figure 4. 2. Signal intensity of [M+H] ⁺ in paracetamol tablet against different plasma pencil to sample distance using helium added with a total acquisition time of 1 minute. .	114
Figure 4. 3. PADI-MS spectra of single paracetamol (5 µg/µL) using dry helium (b) and helium added with water vapour (c) with a total acquisition time of 1 minute. Arrows indicate diagnostic peaks that link to paracetamol.....	117
Figure 4. 4. Signal intensity of protonated paracetamol m/z = 152 (5 µg/µL) against time using dry helium and added with water vapour in 5 seconds intervals 0-5, 10-15 and 20-25 seconds.	117
Figure 4. 5. Signal intensity of protonated caffeine m/z = 195 (5 µg/µL) against time using dry helium and added with water vapour in 5 seconds intervals 0-5, 10-15 and 20-25 seconds.	118
Figure 4. 6. The signal intensity of pure paracetamol and caffeine solutions (both 5 µg/µL) deposited on a TLC plate using helium added with water vapour in 5 seconds intervals 0-5, 10-15, 20-25, 30-35, 40-45 and 55-60 seconds using thermal couple.	120
Figure 4. 7. Intensity ratios for paracetamol and caffeine by a factor of 152/194 (both 5 µg/µL) applied and measured separately using helium added with water vapour in 5 seconds intervals 0-5, 10-15, 20-25, 30-35, 40-45 and 55-60 seconds.....	121
Figure 4. 8. Intensity ratios for paracetamol and caffeine by a factor of 152/195 (both 5 µg/µL) applied and measured separately using helium added with water vapour in 5 seconds intervals 0-5, 10-15, 20-25, 30-35, 40-45 and 55-60 seconds.....	121
Figure 4. 9. Intensity ratios for caffeine by a factor of 195/194 (5 µg/µL) measured using helium added with water vapour in 5 seconds intervals 0-5, 10-15, 20-25, 30-35, 40-45 and 55-60 seconds.....	122

Figure 4. 10. PADI-MS spectra for the mixture solution of paracetamol and caffeine (both 2.5 $\mu\text{g}/\mu\text{L}$) from TLC plates using helium added with water vapour (a), dry helium (b) and background (c) with acquisition time of 1 minute.	124
Figure 4. 11. Signal intensity of protonated paracetamol ($[\text{M}+\text{H}]^+$ m/z 152) (2.5 $\mu\text{g}/\mu\text{L}$) in the mixture solution from TLC plate using dry helium and added with water vapour in 5 seconds intervals 0-5, 10-15 and 20-25 seconds.	124
Figure 4. 12. Signal intensity of protonated caffeine ($[\text{M}+\text{H}]^+$ m/z 195) (2.5 $\mu\text{g}/\mu\text{L}$) in the mixture solution from TLC plate using dry helium and added with water vapour in 5 seconds intervals 0-5, 10-15 and 20-25 seconds.	125
Figure 4. 13. Signal intensity of mixed solutions (1:1) paracetamol and caffeine (both 2.5 $\mu\text{g}/\mu\text{L}$) using helium added with water vapour in 5 seconds intervals 0-5, 10-15, 20-25, 30-35, 40-45 and 55-60 seconds.	127
Figure 4. 14. PADI-MS spectra (20-500 m/z) of mixed solutions (1:1) paracetamol and caffeine (both 2.5 $\mu\text{g}/\mu\text{L}$) (a) and single paracetamol (5 $\mu\text{g}/\mu\text{L}$) from TLC plates using helium added with water vapour before separation of spots with a total acquisition time of 1 minute.	128
Figure 4. 15. PADI-MS spectrum of Panadol solution containing 50 mg/mL paracetamol and 6.5 mg/mL caffeine deposited on the TLC plate using helium added with water vapour before separation of spots with a total acquisition time of 1 minute.	129
Figure 4. 16. PADI-MS data of Panadol solution containing 50 mg/mL paracetamol and 6.5 mg/mL of caffeine deposited on the TLC plate using helium added with water vapour before separation of spots with a total acquisition time of 1 minute.	130
Figure 4. 17. PADI-MS spectra of individual spots of paracetamol (a) and caffeine (b) (both 5 $\mu\text{g}/\mu\text{L}$) on the TLC plate after separation of spots with a total acquisition time of 1 minute.	132
Figure 4. 18. PADI-MS spectra of paracetamol and caffeine spots (a and b respectively) (both 2.5 $\mu\text{g}/\mu\text{L}$) on the TLC plate after separation of spots with a total acquisition time of 1 minute.	132
Figure 4. 19. PADI-MS spectra of paracetamol spot in the mixture solution (2.5 $\mu\text{g}/\mu\text{L}$) on the TLC plate in 5 seconds intervals 0-5 (b), 30-35 (c) and 55-60 seconds (d) after separation of spots with a total acquisition time of 1 minute.	133
Figure 4. 20. Signal intensity of different mixture concentrations of protonated paracetamol m/z = 152 measured from TLC plates after separation of spots with a total acquisition time of 1 minute.	133
Figure 4. 21. Intensity ratios by a ratio of 152/195 of 1:1 mixed of paracetamol and caffeine (both 2.5 $\mu\text{g}/\mu\text{L}$) applied using TLC plate after separation of spots with a total acquisition time of 1 minute.	134
Figure 4. 22. Signal intensity of 1:1 mixture of $[\text{2M}+\text{2H}]^+$ m/z 304 and $\text{M}+\text{O}-\text{H}$ m/z 166 for paracetamol (2.5 $\mu\text{g}/\mu\text{L}$) using TLC plate after separation of spots with a total acquisition time of 1 minute.	135
Figure 4. 23. Plot of mass spectrum intensity versus concentrations of aqueous 1:1 paracetamol and caffeine without separation of the spots with a total acquisition time of 30-35 seconds.	137

Figure 4. 24. Plot of mass spectrum intensity versus concentrations of aqueous 1:1 paracetamol and caffeine after separation of spots with a total acquisition time of 30-35 seconds.	137
Figure 4. 25. PADI-MS spectra of aqueous 1:1 paracetamol and caffeine using dry TLC plate (both 2.5 µg/µL) after separation of spots with a total acquisition time of 1 minute.	139
Figure 4. 26. Signal intensity of different mixture concentrations of paracetamol in aqueous 1:1 solution measured from dry TLC plates after separation of spots with a total acquisition time of 1 minute.	140
Figure 4. 27. Plot of mass spectrum intensity versus concentrations of aqueous 1:1 paracetamol and caffeine solution after separation of spots using dry TLC plate with a total acquisition time of 30-35 seconds.	140

Chapter 5

Figure 5. 1. PADI-MS spectra of background (a) and pure paracetamol (b) with a total acquisition time of 1 minute.	156
Figure 5. 2. PADI-MS spectra of background (a) and pure caffeine (b) with a total acquisition time of 1 minute.	156
Figure 5. 3. PADI-MS signal intensity for [M+H] ⁺ in pure paracetamol.	157
Figure 5. 4. PADI-MS signal intensity for [M+H] ⁺ in pure caffeine.	157
Figure 5. 5. PADI-MS spectra of (a) Panadol tablet containing 500 mg paracetamol and 65 mg caffeine; (b) paracetamol tablet containing 500 mg paracetamol; (c) no sample with a total acquisition time of 1 minute.	159
Figure 5. 6. Signal intensity of [H+M] ⁺ in paracetamol tablet versus time upon binning of data in 5 seconds intervals up to a total acquisition time of 60 seconds.	160
Figure 5. 7. Signal intensity of [H+M] ⁺ (m/z = 152; left y-axis) and caffeine ions (m/z = 194; right y-axis) in a Panadol tablet versus time with a total acquisition time of 1 minute.	162
Figure 5. 8. Signal intensity of caffeine molecular ion in Pro Plus tablet contains 50 mg versus time caffeine with a total acquisition time of 1 minute.	163
Figure 5. 9. Signal intensity of protonated paracetamol in Panadol tablet in 5 seconds intervals 0-5, 5-10, 10-15, 15-20, 20-25, 25-30, 30-35, 35-40, 40-45, 45-50, 50-55 and 55-60 seconds.	164
Figure 5. 10. Signal intensity of protonated paracetamol in Panadol tablet in accumulated seconds 0-5, 0-10, 0-15, 0-20, 0-25, 0-30, 0-35, 0-40, 0-45, 0-50, 0-55 and 0-60 seconds.	164
Figure 5. 11. Signal intensity of single paracetamol and caffeine (both 5 µg/µL) using glass slide with a total acquisition time of 1 minute.	166
Figure 5. 12. Signal intensity ratios of paracetamol and caffeine solutions (m/z 152/194) (both 5 µg/µL) applied from the glass slide and measured separately using outer He added with water vapour in 5 seconds intervals 0-5, 10-15, 20-25, 30-35, 40-45 and 55-60 seconds.	167

Figure 5. 13. Signal intensity ratios of single protonated caffeine and pure caffeine molecular ion solutions by a factor of (m/z 194/195) (both 5 µg/µL) applied from glass slide using added with water vapour in 5 seconds intervals 0-5, 10-15, 25-30, 30-35, 40-45 and 55-60 seconds.	167
Figure 5. 14. PADI-MS spectra of 1:1 mixed of paracetamol and caffeine of 0.1 µg/µL (a), 0.01 µg/µL (b) and no sample (c), using glass slide with a total acquisition time of 1 minute.	170
Figure 5. 15. Signal intensity of an aqueous 1:1 mixture of paracetamol and caffeine (both 2.5 µg/µL) using a glass slide with a total acquisition time of 1 minute.	170
Figure 5. 16. PADI-MS spectra of background (a) and Panadol solution (b) using a glass slide with a total acquisition time of 1 minute.	171
Figure 5. 17. Signal intensity ratio by a factor of 152/195 of 1:1 mixed of paracetamol and caffeine (both 0.1 µg/µL) applied using glass slides and measured in 5 seconds intervals 0-5, 10-15, 20-25, 30-35, 40-45 and 55-60 seconds.	171
Figure 5. 18. Signal intensity of single paracetamol and caffeine (both 5 µg/µL) using cotton swabs with a total acquisition time of 1 minute.	173
Figure 5. 19. Signal intensity ratios by a factor of (m/z 194/195) of single caffeine molecular ion and single protonated caffeine solutions (both 5 µg/µL) applied from cotton swabs using added with water vapour in 5 seconds intervals 0-5, 10-15, 20-25, 25-30, 30-35, 35-40 and 45-50 seconds.	174
Figure 5. 20. PADI-MS spectra of 1:1 mix with paracetamol and caffeine of (a) 2.5 µg/µL, (b) 0.01 µg/µL and (c) blank using cotton swabs with a total acquisition time of 1 minute.	175
Figure 5. 21. Signal intensity of various concentrations of paracetamol in mixture solutions from cotton swabs with a total acquisition time of 1 minute.	176
Figure 5. 22. Signal intensity ratios by a factor of m/z 152/195 of the mixture of paracetamol and caffeine solution (both 2.5 µg/µL) applied from cotton swabs using added with water vapour in 5 seconds intervals 0-5, 10-15, 20-25, 30-35, 40-45 and 55-60 seconds.	177
Figure 5. 23. PADI-MS spectra of a 1:1 mixture of paracetamol and caffeine (both 2.5 µg/µL) in 5 seconds intervals 0-5 (a), 10-15 (b), 20-25 (c), 30-35 (d), 40-45 (e) and 55-60 seconds (f) using cotton swabs.	178
Figure 5. 24. Signal intensity of diagnostic peaks of a paracetamol/caffeine mixture (both 2.5 µg/µL) applied using cotton swabs and measured in 5 seconds intervals 0-5, 10-15, 20-25, 30-35, 40-45 and 55-60 seconds.	179
Figure 5. 25. PADI-MS spectrum of Panadol solution (containing paracetamol and caffeine 50 µg/µL and 6.5 µg/µL) using cotton swab and measured in 5 seconds intervals 30-35 seconds.	180
Figure 5. 26. Signal intensity of protonated paracetamol and caffeine molecular ions in Panadol solution from cotton swab using added with water vapour in 5 seconds intervals 0-5, 10-15, 20-25, 30-35, 40-45 and 55-60 seconds.	180
Figure 5. 27. Calibration plot of mass intensity versus concentrations of standard mixture solutions of protonated paracetamol and caffeine molecular ion using glass slides.	182

Figure 5. 28. Calibration plots of mass intensity versus concentrations of standard mixture solutions of protonated paracetamol and caffeine molecular ion using a cotton swab.183

Chapter 6

Figure 6. 1. The schematic reaction of the imine formation.	196
Figure 6. 2. UV/Vis spectra of 4-nitrobenzaldehyde (a), para-anisidine (b) and product (N-4-MP-1-4-NPM) (c) (10 mmol each).	199
Figure 6. 3. HPLC chromatogram for para-anisidine and 4-nitrobenzaldehyde (both 5 mmol) using ODS-C18 column 150 mm × 4.6 mm, acetonitrile and deionised water (25%: 75%, v/v) mobile phase, flow rate of 1 mL/min and detection at a wavelength of 300 nm.	203
Figure 6. 4. HPLC chromatograms for the reaction mixtures (both 2.5 mmole) at different reaction times using conditions as for Figure 6. 4.	204
Figure 6. 5. FTIR spectrum of 4-nitrobenzaldehyde (solid).	206
Figure 6. 6. FTIR spectrum of para-anisidine (solid).	206
Figure 6. 7. FTIR spectra for reactants 4-nitrobenzaldehyde (a) , para-anisidine (b) and reaction mixtures during reaction times: 5 min (c), 15 min (d), 30 min (e), 45 min (f), 60 min (g) and 120 min (h).	209
Figure 6. 8. Ratios of the normalised area for C=O/C=C during reaction time.	210
Figure 6. 9. Ratios of the normalised area for C=O/C=N during reaction time.	210
Figure 6. 10. Peak height for 4-nitrobenzaldehyde m/z 152 and para-anisidine m/z 124 using different substrates with a total acquisition time of 1 minute.	213
Figure 6. 11. PADI-MS spectra of 4-nitrobenzaldehyde (a) and para-anisidine (b) using cotton swabs with a total acquisition time of 1 minute.	214
Figure 6. 12. Signals intensity of protonated 4-nitrobenzaldehyde and protonated para-anisidine using cotton swabs in 5 second intervals 0-5, 10-15, 20-25, 30-35, 40-45 and 55-60 seconds.	214
Figure 6. 13. PADI-MS spectra of the reaction mixtures over reaction times in 5 seconds intervals of 30-35 seconds.	216
Figure 6. 14. Reaction progress of the synthesis of N-4-MP-1-4-NPM over reaction time in 5 seconds intervals of 30-35 seconds.	216
Figure 6. 15. Peak intensity ratios of 4-nitrobenzaldehyde, para-anisidine and the product by a factor of 256/152 and 256/124 over reaction time with an acquisition time of 30-35 seconds.	218
Figure 6. 16. Signal intensity of [M+H] ⁺ m/z 152 for 4-nitrobenzaldehyde over different reaction times with an acquisition time of 55 seconds.	218
Figure 6. 17. Signal intensity of [M+H] ⁺ m/z 124 for para-anisidine over different reaction times with an acquisition time of 55 seconds.	219
Figure 6. 18. Signal intensity of N-4-MP-1-4-NPM with an acquisition time of 60 seconds at different reaction times.	219

Index of Tables

Chapter 3

Table 3. 1. Vibrations of paracetamol molecule in Raman spectrum Figure 3.5.....	83
Table 3. 2. Diagnostic, adduct and fragment peaks of paracetamol.....	91

Chapter 4

Table 4. 1. Concentrations and amounts of paracetamol and caffeine in the mixtures used for methods A and B.	111
Table 4. 2. The amount of molecule per mole in the solution of an individual and a mixture of paracetamol/caffeine.	111
Table 4. 3. Diagnostic, adduct and fragment peaks of paracetamol and caffeine.	118

Chapter 5

Table 5. 1. The optimal conditions of PADI probe for analysing of individual and paracetamol /caffeine mixtures in liquid.....	155
Table 5. 2. Diagnostic peaks for paracetamol and caffeine.....	159

Abbreviations

AMS	Ambient mass spectrometry
APIs	Active pharmaceutical ingredients
CD	Chiral detector
CDD	Corona discharge detector
CE-MS	Capillary electrophoresis mass spectrometry
CI	Chemical ionisation
CLND	Chemiluminescent nitrogen detector
DART-MS	Direct analysis in real time mass spectrometry
DESI-MS	Desorption electrospray ionisation mass spectrometry
DR-FTIR	Diffuse-reflectance Fourier transform infrared
EASY-MS	Easy ambient sonic-spray ionisation mass spectrometry
EC	Electrochemistry
ELDI	Electrospray-assisted laser desorption/ionisation
ESI	Electrospray ionisation
ESR	Electron spin resonance
Far-IR	Far infrared
FL	Fluorescence
FTIR	Fourier transform infrared (often used interchangeably with mid-IR)
GC	Gas chromatography
GC-MS	Gas chromatography mass spectrometry
HPLC	High-performance (or high pressure) liquid chromatography
HPLC-MS	High-performance liquid chromatography-mass spectrometry
LC	Liquid chromatography
LC-MS	Liquid chromatography mass spectrometry
LOD	Limit of detection
LOQ	Limit of quantification

LSD	Light scattering detector
LTP-MS	Low-temperature plasma mass spectrometry
MALDI	Matrix-assisted laser desorption/ionisation
Mid-IR	Mid-infrared (often referred to as FTIR)
MS	Mass spectrometry
N-4-MP-1-4-NPM	N-(4-methoxyphenyl)-1-(4-nitrophenyl) methanimine
Nano ESI-MS	Nano electrospray mass spectrometry
NIR	Near infrared
NIRS	Near-infrared spectroscopy
NMR	Nuclear magnetic resonance
NP-HPLC	Normal phase high-performance liquid chromatography
NTP	Non-thermal plasma
PADI-MS	Plasma-assisted desorption ionisation-mass spectrometry
PAHs	Polycyclic aromatic hydrocarbons
PAT	Process analytical technology
PTR-MS	Proton transfer reaction mass spectrometry
R _f	Retention factor
RF	Radio frequency
RI	Refractive index
RP-HPLC	Reverse phase high-performance liquid chromatography
S/N	Signal-to-noise ratio
STEYX	Standard deviation of the y-value and x-value
TFC-MS-MS	Turbulent flow liquid chromatography tandem mass spectrometry
TLC	Thin layer chromatography
TOFMS	Time-of-flight mass spectrometry
UPLC	Ultra performance liquid chromatography
UV/Vis	Ultraviolet-visible

Publications and presentations

Publications

- Frank J.M. Rutten*, Jasim M.S. Jamur and Paul Roach (2015)
'Fast and versatile ambient surface analysis by plasma-assisted desorption/ionisation mass spectrometry', Spectroscopy Europe, 27 (6) 1.
- In preparation:
 - 1) Jasim M.S. Jamur*, Paul Roach and Frank J.M. Rutten
'Rapid identification and quantification of pharmaceutically relevant mixtures on TLC plates with PADI mass spectrometry.'
 - 2) Jasim M.S. Jamur*, Paul Roach and Frank J.M. Rutten
'Analysis of pharmaceutical solids and liquids from glass slides and cotton swabs with PADI mass spectrometry.'

Oral presentations

- *Developing a novel ambient mass spectrometry technique for rapid reaction monitoring in pharmaceuticals production*, ISTM Postgraduate Symposium 2015, Keele University.
- Submission in preparation: *Plasma-assisted desorption ionisation mass spectrometry – PADI-MS for the analysis of pharmaceutical solids and liquids from glass slides and cotton swabs*, British Mass Spectrometry Society Annual Meeting 2018, Churchill College, Cambridge.

Posters

- Separation and analysis techniques for the monitoring of pharmaceutical reaction mixtures, Institute for Science and Technology in Medicine (ISTM) Postgraduate Symposium 2014, Keele University.
- Direct analysis of pharmaceutical mixtures from thin layer chromatography plates by plasma-assisted desorption ionisation mass spectrometry – PADI-MS, ISTM Postgraduate Symposium 2016, Keele University.
- Direct analysis of pharmaceutical mixtures from thin layer chromatography plates by plasma-assisted desorption ionisation mass spectrometry – PADI-MS, British Mass Spectrometry Society - Ambient Ionisation Special Interest Group international meeting 2017, Keele Hall.
- In preparation: Mass spectrometry for the monitoring of imine (Schiff Base) formation as a model of pharmaceutical reaction mixtures, British Mass Spectrometry Society - Ambient Ionisation Special Interest Group international meeting, 2018, Syngenta, Jealott's Hill, Berkshire.

Acknowledgements

Firstly, I gratefully acknowledge my country Iraq and financial support by Ministry of Higher Education and Scientific Research. I would like to thank Ibn Al-Haitham college of Education for Pure Sciences and University of Baghdad.

I would like to thank my supervisor Dr Frank Rutten who has supported me during my research. I would not be able to complete the lab work and thesis writing without his assistance and his encouragement. I would also like to thank my co-supervisor Dr Paul Roach and my advisor Dr Anthony Curtis who have contributed to finish my work.

At the same time, I would like to extend my thanks to the staff and students at Keele University and school of pharmacy for their advice along the way.

I would like to offer many thanks to my mother, brothers, sisters, and my special family my wife Sanaa and my sons Mohammed and Ahmed. I would never have been able to finish my PhD study without their support and encouragement.

This thesis is dedicated to my late father. He was the main source of inspiration. Dad, thank you very much for everything.

CHAPTER 1: Introduction

1.1. General introduction

The pharmaceutical industry is an essential component of healthcare systems around the world. It includes many public and private organizations which discover, develop, manufacture and market pharmaceuticals for human and animal health. Pharmaceutical companies have competed on the basis of innovation through new drugs to meet developing medical needs. There are challenges within the pharmaceutical industry revolving around novel drug formulation and new synthetic routes to reduce costs and increase the safety standard for manufacturer employees and patients. Therefore, companies innovate continuously to maximise benefit from a limited patent life. According to a recent review, developing drugs to marketing approval costs an estimated \$802 million for each new drug (1). Research and development (R&D) costs are expected to remain at current levels or slightly increase in the future. When combined with other factors, such as increase in competition, opening new markets and lower uptake, there is a need for the industry to find ways to reduce costs. Similar cost and quality drivers which have affected other industries are forcing the pharmaceutical industry to find ways to improve quality while maintaining or reducing manufacturing costs, which today represent 36% of the industry's cost (2). For example, the annual report of pharmaceutical company AstraZeneca for 2013 indicated that sales declined in the United States by 9% to 9.691 billion from \$10,655 million and \$13,426 million in 2010 and 2011 respectively (3), in a European pharmaceutical market worth \$205 billion.

The pharmaceutical industry at present predominantly uses batch production processes, involving the synthesis of unique compounds from organic and/or inorganic starting material, often involving several reaction steps. Reactants react with each other after being mixed in a reaction vessel: while the desired substance is formed, the original reactants are consumed. It is desirable to produce a batch as rapidly as possible. Therefore, it is desired

to determine when the reaction is completed, i.e. the reactants are no longer present and the desired product(s) formed. In addition, undesired products can be formed in the reaction vessel and require detection and characterisation, enforced by regulatory authorities. A common method for determining when the reaction is completed is to measure the concentration of the product molecule. This is often combined with a measurement of the concentration of one or more of the reactants. The active pharmaceutical ingredients produced can be formulated into a range of pharmaceutical products, including solids (tablets and capsules), liquids, creams and gases (4). A crucial product analysis concerns pharmaceutical tablets which may contain several active pharmaceutical ingredients (APIs). Identification and distribution of these APIs in tablets is particularly important (5). Therefore, testing of the pharmaceutical product to certify the quality includes chemical and physical analysis.

1.2. Reaction monitoring

Reaction monitoring ideally provides information about the conversion rate and the formation of impurities as well as products. In addition, it can be used to develop and validate continuous manufacturing based on the customers' requirements such as lowest cost and highest yield. Therefore, development of a novel, fast and sensitive method to use for monitoring of pharmaceutical synthesis reactions is required in order to avoid the problems of traditional techniques, which can be time-consuming, lack sensitivity and require sample pre-treatment. Reaction times depend on reaction type and can be completed in minutes, hours or days (6), so a fast analytical method is desirable. Companies spend considerable resources on new methods and equipment to perform this task. Chemical reactions must be monitored by analytical methods to determine their kinetics, completion time, purity, quantity and product yield. Spectroscopic techniques, in particular ultraviolet (UV) and infrared (IR), are used for this purpose (7).

A wide range of process analytical technology (PAT) approaches have been developed for monitoring of chemical reactions (7). There has been increasing interest in the use of PAT to follow the process of reactions in pharmaceutical and chemical industries and for quality confirmation of final products (7). Monitoring of quality in the pharmaceutical industry includes several steps starting from the analysis of raw materials to final products. Analysis methods should be accurate and ideally require little or no sample pre-treatment (8). Manufacturing of traditional pharmaceuticals is achieved using batch processing with laboratory screening conducted on samples collected to appraise the quality (7). Detection and identification of substances in a mixture are important aspects for the development and production of pharmaceutical compounds, including analysis of reactants, intermediates and final products (8). To assess compounds in mixtures (including quantity if necessary) chromatography is often employed to separate individual components prior to chemical analysis.

Several separation and analysis techniques including chromatography, spectroscopy and ambient mass spectrometry were used in this study for identification and monitoring of pharmaceutical reactions.

1.3. Pharmaceutical applications of separation techniques

1.3.1. Chromatography

Chromatography is a separation technique for mixtures exploiting the distribution of analytes between two phases: the stationary and mobile phase. The chromatographic separation is based on differential partitioning between these phases. For example, analytes partitioning between stationary and mobile phase take longer to pass through a HPLC system based on the relative affinity for mobile and stationary phase. These phases could be liquid-liquid, solid-liquid or gas-liquid. Chromatography plays a critical role in the

separation, identification and quantification of mixture components. Chromatography is a powerful technique that is extensively used to analyse different kinds of samples (solid, liquid or gaseous) (9, 10). Chromatographic separation techniques have been used for separation of compounds of various polarities (hydrophilic and hydrophobic). These techniques can be used to separate volatile compounds such as polycyclic aromatic hydrocarbons (PAHs), alcohol, epoxides, aromatic amines, aromatic esters, nitriles and volatile carboxylic acids. They can also be used to separate non-volatile compounds such as amino acids, sugars, phospholipids, glyphosate, antibiotics, synthetic food dyes, enzymes and phenols.

1.3.1.1. Thin layer chromatography (TLC)

Thin layer chromatography is a simple and inexpensive separation method routinely used to separate and identify substances. Although several materials are used as stationary phases for TLC plates such as silica gel, alumina, zirconium oxide, florisil and ion exchanger, silica gel is still the most commonly used. Chemically bonded is also another type of stationary phase which is formed by combining silica gel and transitional ions and use to detect and separate organic mixtures on TLC plate (11).

TLC is a solid-liquid chromatography technique in which the stationary phase is a polar absorbent and the mobile phase is normally a mixture of solvents. The equilibrium of molecules between the stationary phase and mobile phase for different analytes is not the same. This equilibrium depends on the polarity of the analyte molecules, the stationary phase and the mobile phase. Molecules that strongly interact with the stationary phase will spend more time in the stationary phase, and conversely, molecules that weakly interact with the stationary phase will spend more time in the mobile phase and hence progress across the stationary phase faster. For the qualitative analysis, each separate spot on TLC

plate will be identified by using retention factor (R_f), because each spot has a different R_f . The equation of retention factor is that dividing the distance travelled by sample on distance travelled by solvent:

$$R_f = \frac{\text{distance travelled by sample}}{\text{distance travelled by solvent}}$$

There are four essential aspects to optimise TLC separation: sample preparation, sample application, chromatogram development and qualitative and quantitative analysis. In the sample preparation step, to obtain good results, samples must meet requirements such as filtration, extraction and clean-up to remove contaminants and it sometimes also necessary to increase concentration. The stationary phase must contact the solvent in the bottle and capped with a cover and then leave the TLC plate until the solvent moves and spots rise and reaches the end of the TLC plate. The next procedure step is leaving the TLC plate for drying (evaporation of solvent) for few minutes and circle the spots by pencil after marking their location under UV light. In the quantitative analysis, spots can be determined by direct and indirect quantification. In the direct method, sample spots can be determined, and spot area is measured directly from the TLC plate by measuring the calibration. In indirect quantification, sample spots must be transferred from a TLC plate for analysis by another technique such as mass spectrometry. The modification of silica stationary phase with polar and non-polar ligands is important for a wide range of scientific and industrial processes (12). A balanced force of molecules depends on the polarity of stationary phase of TLC plate, the polarity of mobile phase and the polarity of components in the solution to be analysed. The main disadvantage of silica gel bonded is that a high concentration highly acidic free silanol groups increases the retention time with basic compounds and this will lead to occurrence of some of the chromatographic problems such as broad peak tailing for these compounds. Alumina is the second most commonly used absorbent for TLC plate

after silica gel. Alumina is prepared by calcination from aluminium hydroxide. Aluminium oxide (Al_2O_3) is the most widely used type and the functional groups on the alumina surface are oxide ions, a hydroxyl group and aluminium cation (13). Compared to silica gel, anhydrous alumina is stronger to adsorb analytes particularly for nonpolar compounds such as ethers, hydrocarbons, aldehydes and ketones, while to separate polar compounds such as amines, alcohols and carboxylic acids, silica gel is more used. When combining TLC with diffuse-reflectance Fourier transform infrared (DR-FTIR), zirconium oxide has used as stationary phase in the detection of unknown samples (14). In comparison with silica gel and alumina, zirconium oxide is higher infrared (IR) reflectivity. Ion exchanger plays a crucial role in separating of positive and negative ions (cations and anions) from a mixture of metallic ions. The silica gel surface is modified with positive materials to separate the cations and modified with negative materials to separate anions.

Even though a number of more advanced analytical methods have been developed, TLC is still widely used in the food and pharmaceutical industries (15). TLC can be used for monitoring of synthesis reactions but without providing the information about structural information on the molecules (16). TLC is combined with spectroscopic detection methods such as UV/Vis, Fourier transform infrared (FTIR) and nuclear magnetic resonance (NMR) to use for qualitative and quantitative analysis of the separated compounds (17). However, limitations of TLC are: the position of the spot gives limited information on the nature and quantity of molecules unless used with advanced analytical techniques such as mass spectrometry (MS). The time delay is another limitation due to having to wait for the TLC plate to develop. TLC is most commonly used combined with a broad-band UV/VIS source to identify analytes and this is quite a limited technique, hence the drive to use alternatives and in particular (ambient) MS. Due to these practical constraints, TLC method cannot provide enough structure details of chemical compounds (15). TLC-MS is

used to identify and quantify small and large molecules such as peptides, proteins and amino acids (18). To improve the detection of spots on TLC plates, several mass spectrometric techniques have been combined with TLC such as electrospray-assisted laser desorption/ionisation (ELDI) MS, DESI, DART or matrix-assisted laser desorption/ionisation (MALDI) (12). In a study by Van Berkel, electrospray mass spectrometry has been used to monitor a dyes mixture consisting of crystal violet, rhodamine and methylene after separation on a TLC plate (19). TLC and easy ambient sonic-spray ionisation mass spectrometry (TLC- EASY-MS) has been applied in qualitative monitoring of drugs and synthesis chemistry (20). The mixture spots of allyl phenylamine, phenyl amine and ethyl pyridine on the TLC plate were detected by EASY-MS after developing the TLC plate. TLC- EASY-MS has been used to analyse tablets of propranolol and amlodipine after dissolving them in water, and monitor the synthesis of oxazoline-5-carboxylic ester (20). A TLC plate coupled with desorption electrospray ionisation mass spectrometry (DESI-MS) has been used to monitor rhodamine and the mixture solution of aspirin, caffeine and acetaminophen after separation on a silica gel plate (21). Several organic compounds including starting materials and reaction mixtures of glycopeptides, peptides and carbohydrate reactions were monitored by matrix-assisted laser desorption/ionisation time-of-flight mass spectrometry (MALDI-TOFMS) after separation on TLC plate (22). Danigel and co-workers have shown that TLC coupled with TOFMS was used for monitoring and quantification of etoposide (23). Analysis of organic compounds including amines using ELDI/MS technique after separation on a TLC plates was successfully carried out by Lin *et al.* (24). TLC also coupled to mass ionisation techniques such as matrix-assisted laser desorption and ionisation (MALDI) to analyse glycolipids and phospholipids. In a study conducted by Van Berkel *et al.*, it was shown that the DESI-MS method can be used directly to analyse the spots of goldenseal alkaloids on

TLC plates (25). Planar chromatography has been coupled with real time-of-flight mass spectrometry (DART-TOF-MS) and used for direct analysis of pharmaceutical mixtures including caffeine (26).

1.3.1.2. High-performance liquid chromatography (HPLC)

Liquid chromatography (LC) is a chromatographic separation technique important for a wide range of scientific and industrial applications. In LC, the sample and mobile phases are liquid, and the stationary phase is solid. A small volume (20 μ L) of liquid sample is required to penetrate the porous stationary phase. The individual components of the sample are transferred to the column by liquid mobile phase and then separated, collected and identified by a spectrometric technique, most commonly UV/VIS spectrophotometry. The past century has seen the rapid development of liquid chromatography in many fields.

High-performance liquid chromatography or high-pressure liquid chromatography (HPLC) is a further development of LC, which is now widely used to separate, identify and quantify compounds in solution. The history of HPLC started in 1960. After that and especially from 1970, the technique including column and other instrumentations has improved significantly and became widely known as high-performance liquid chromatography. Several further developments have been introduced since 2006, in particular Ultra performance liquid chromatography (UPLC) which uses even higher pressures. Compared to HPLC, UPLC is faster, has better resolution and separation and reduced solvent consumption. However, in UPLC, increased pressure reduces the average life of columns (27). HPLC is still the standard technique, with increasing use of UPLC in industrial applications. HPLC is widely used for qualitative and quantitative analysis in the pharmaceutical industry (28), including R&D applications to discover, develop and manufacture novel pharmaceutical compounds (29-32).

The HPLC instrument consists of the column which holds the stationary phase, a pump to move the mobile phase through this column and a detector to measure the retention times of the compounds in a mixture (33). The retention time of compounds on HPLC columns, as for the stationary phase in TLC, varies based on their polarity and on the chemical or physical interactions between the mobile phase and stationary phase. Methanol and acetonitrile are the most common solvents used as an organic mobile phase in HPLC and water as aqueous mobile phase (34, 35). Data collection on HPLC provides important information about the qualitative and quantitative analysis of molecules. Identification of components can be achieved by measuring their retention times, their quantities by measuring the peak area or peak height.

1.3.1.2.1. HPLC components

HPLC consists of five main components as shown in Figure 1.1.

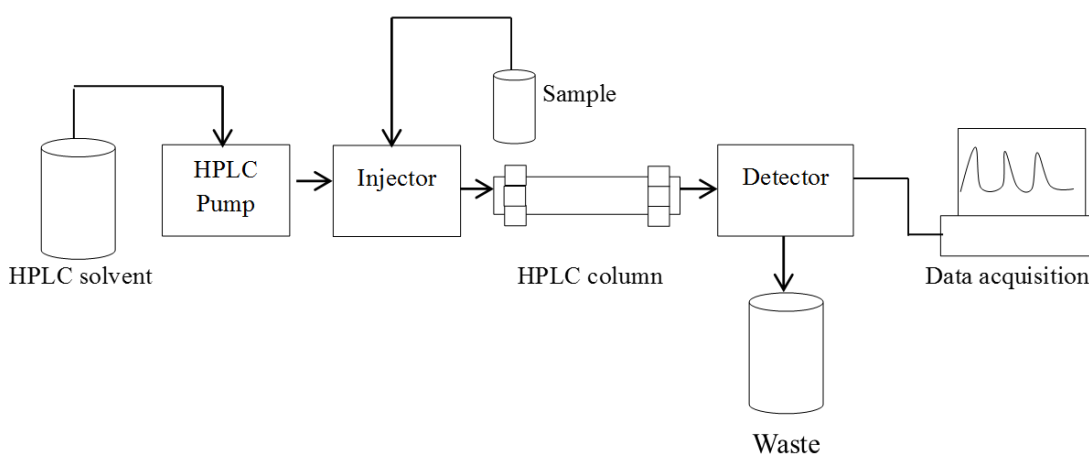


Figure 1. 1. Schematic diagram of high-pressure liquid chromatography (HPLC).

1-Pump

A pump pushes the liquid (mobile phase and sample) through the column at an accurate flow rate usually of the order of 1-2 mL/min for HPLC. In isocratic chromatography, a constant mobile phase composition is passing through the column.

2-Injector

The injector is used to introduce liquid samples into the mobile phase flow stream. Normal volumes of the liquid sample are between 5 and 20 μL . The injector has to withstand the high pressures of the chromatographic system, in particular when using UPLC.

3- Column

The column is the component in HPLC in which the analyte mixture is separated into its constituent components. Because of its small particle size, the stationary phase can separate the analyte by the interaction between the analyte, the stationary phase and the mobile phase.

4- Detector

The detector in HPLC detects and quantifies the individual components which elute from the column. The first detector for HPLC was ultraviolet (UV) and introduced in the 1960s. After that, other detectors have been developed for a wide range of scientific and industrial HPLC applications (36).

5- Data acquisition system

Database comparison allows identification of molecules by retention time (qualitative analysis) and determination of the amount present (quantitative analysis) by peak height or area.

1.3.1.2.2. Types of columns in HPLC

Types of column based on internal diameter and length-

- Preparative column: i.d. > 4.6 mm; length 50- 250 mm and the flow rate is 1 mL/min. This type of column is used for purification of a sample. Therefore, the peak shape and injected amount are not important.
- Analytical column: i.d. 1.0- 4.6 mm; length 15-250 mm.
- Capillary column: i.d. 0.1- 1.0; various lengths.
- Nano column; < 0.1 mm.

Types of column based on the construction materials for the tubing-

- Stainless steel: the most used because it gives high-pressure ability.
- Glass: used for biomolecules.
- Polymer: used for biocompatible.

Types of column based on separation method-

- Normal phase column: The packing of the column consists of a polar material, usually silica. Because water is more polar than silica, it cannot be used as a mobile phase, therefore hexane and methylene chloride are often used as mobile phase.
- Reverse phase column: A polar solvent mixture such as water-acetonitrile or water-methanol is used as mobile phase.
- Ion exchange column: in this type of column, the stationary phase must be acidic or basic and has positive or negative charge. The mobile phase is a polar liquid. Separation of molecules will occur by exchange of sample ions with the ions of the stationary phase.

- Size exclusion column: molecules in these columns will separate according to their size. The stationary phase in these columns is a polymer. Small molecules will infiltrate into the pores of the stationary phase while the large molecules will infiltrate partially into the pores. In this case, larger molecules will elute first from the column, before smaller molecules.

1.3.1.2.3. Types of HPLC detectors

- Ultraviolet-visible (UV-Vis) absorbance detectors: because most compounds absorb in the ultraviolet or visible region of 190-600 nm, UV-Vis detection is still commonly used for HPLC. UV should have a chromophore, and the solvents must be transported.
- Fluorescence (FL) detector: solute samples are excited at higher energy wavelength and fluorescent emission is detected (37). The sensitivity of FL detector can be 100X better than a UV detector, for samples with low analyte concentrations. FL detectors have some limitations such as cost, and they are suitable for analysis of fluorescing compounds only.
- Electrochemical (EC) detector: because the EC detector is a very sensitive and selective HPLC detector, it can be used to detect oxidising or reducing compounds (38, 39).
- Radioactivity detector: it is also named radio flow detector which is used to analyse radioactive samples that flow from the HPLC column. These detectors are very sensitive and can be used to detect the radiolabelled compounds in metabolism or toxicological studies (36). The limitation of radioactivity detectors is that using large flow cell volumes leads to decreased resolution and increase peak broadening.

- Conductivity detector: it is one of the most widely used detectors for HPLC and measures the conductivity of the mobile phase. They are used for ion exchange chromatography particularly for detection of molecules that do not have a UV chromophore (40, 41). However, the limitation of conductivity detectors is that not all compounds can be analysed by these detectors. They also require a dedicated HPLC column.
- Chemiluminescent nitrogen detector (CLND): it is also called a gas phase detector and is used particularly for nitrogen-containing compounds when the column outflowing with oxygen and transporters gas like helium or argon. CLND is sensitive and it can be used to analyse petroleum and food flavour samples (42-44).
- Chiral detector (CD): these detectors are used to analyse the absorbance difference of right and left polarised light.
- Refractive index (RI) detector: it is the oldest detector for liquid chromatography. RI has been extensively used for measuring the difference in optical refractive index between the analyte and mobile phase. However, RI detectors have limited sensitivity.
- Light scattering detector (LSD): Evaporative light scattering detector (ELSD) is one of the most popular detectors of LSD and can be used with gradients. However, limitation of the LSD is that buffers must be volatile.
- Corona discharge detector (CDD): it is an important detector in the liquid chromatography technologies. CDD is highly sensitive, simple and easy to use (10). CDD has been used for a wide range of analysis such as drug discovery (45), impurities (46), and natural product isolation (47). On the other hand, limitation of CDD is that the volatile buffers are required to use.

1.3.1.2.4. Types of HPLC

A) Normal phase HPLC

In this method, the retention times of the compounds on HPLC column depends on their polarity. Normal phase HPLC (NP-HPLC) often called normal phase chromatography uses nonpolar mobile phases such as hexane, ethyl acetate and methylene chloride and polar stationary phases such as silica gel. NP-HPLC is used to separate and analyse water sensitive molecules, cis-trans isomers and chiral compounds.

B) Reverse phase HPLC

Reverse phase high-performance liquid chromatography (RP-HPLC) was developed at the end of the 1970s for separation of small organic compounds (31). The RP-HPLC method uses a polar mobile phase and a non-polar stationary phase. Reverse phase is more popularly used than normal phase due to the hydrophobic interaction between the stationary phase and analytes, it suitable to use for separation of organic compounds. In reverse phase, separation of the analytes can be improved by optimising the pH and using several solvents mixed. In addition, the RP-HPLC method can also be used to analyse polar, nonpolar and ionic compounds and this makes the method very versatile.

HPLC is used to isolate and purify compounds, including combinatorial synthesis (48). HPLC is one of the most widely used techniques in the analysis of complex mixtures containing biomolecules (49, 50). HPLC is used to ensure the quality and quantity of a drug and other potentially harmful molecules and it also can be used for monitoring progress of disease treatment. Applications can be in R&D to develop new medicines; in research to monitor the effectiveness of such medicines; in a more routine production of medicines and in more routine monitoring of patients. HPLC has been developed and used

in multiple reaction monitoring for describing many fatty aldehydes including 4-hydroxy nominal and acrolein in plasma and brain samples of animals (51). The reaction between aniline and 4-fluoro benzaldehyde was monitored over time using online HPLC-UV method (52). A reversed-phase high-performance liquid chromatographic (RP-HPLC) method has been developed to monitor the synthesis of 4-amino-2-chloro-6,7-dimethoxyquinazoline during reaction time (53). The reaction mixtures (cationic) of cisplatin with methionine and nucleotides were monitored using a RP-HPLC method (54). Online reaction monitoring is important and has been one of the most widely used methods for a wide range of scientific and industrial processes. These methods are developed to provide information and understand the mechanism of organic reactions. On-line HPLC has been used to monitor the reaction of DMAP catalysed acylation of phenols and acetic anhydride (55). Online HPLC has also been used with multivariate statistical process control for monitoring of a steady state reaction (56). There are crucial limitations in terms of necessary sample preparation, solution only sampling, the length of time needed for sampling, lack of inherent molecular information and the need for trained laboratory staff for HPLC sampling.

1.4. Pharmaceutical applications of spectroscopic techniques

1.4.1. Spectrophotometry

1.4.1.1. Ultraviolet-visible (UV/Vis) spectroscopy

UV/Vis is very common spectroscopy method and widely used to measure the spectral absorption of molecules in the regions between 200 and 800 nm (57). UV/Vis light can excite the electrons in an analyte to higher energy states upon absorbing photons of a specific wavelength. The Beer-Lambert law applies for concentrations in the linear range for specific spectrophotometers ($A = a \cdot b \cdot c$).

Where A is the measured absorbance of the sample, at a specific wavelength, usually that of maximum absorbance $a(\lambda_{\max})$, b is the path length, c is the concentration of the sample. When using molarity concentration, the law above is written as $A = \epsilon \cdot b \cdot c$. In the quantitative analysis of the individual compounds, the selection of wavelength in the derivative spectra is difficult compared to absorbance spectra. Although UV/Vis spectroscopy is simple and cheap, it suffers from limited sensitivity. The main problem is mixture analysis, in particular when several components absorb at the same or similar wavelength, which occurs readily given the inherently broad peaks. UV/Vis spectroscopy indicates the presence and nature of unadded functional groups. Conversely, molecules which only have electron bonding s orbitals ($s \rightarrow s^*$ transition) are difficult to detect by UV-Vis. For example, methane only has C-H bonds and hence cannot be observed in the range of UV-Vis. Organic compounds that have more conjugated bonds will shift to longer wavelengths. For instance, the peak of anthracene (three aromatic rings) in the spectrum shifts toward longer wavelengths than benzene (one aromatic ring). UV detection is commonly used in HPLC instrumentation.

1.4.1.1.1. UV/Vis instrumentation

1- Light source such as deuterium or tungsten lamp to produce the radiation at a suitable wavelength. However, a xenon flash lamp was used in this study.

2- A monochromator is the most common selector that filters used as a wavelength selector in the UV/Vis due to its ability for scanning broad ranges of wavelengths with good resolution.

3- Quartz or fused silica is used as a sample cuvette in the UV region, whereas quartz or glass is used in the visible region. In this study, quartz was used in the UV region.

4- The detector of UV is like that used by Vis.

5- A PC to record the signal. A schematic illustration of a UV/Vis spectrophotometer is shown in Figure 1.2.

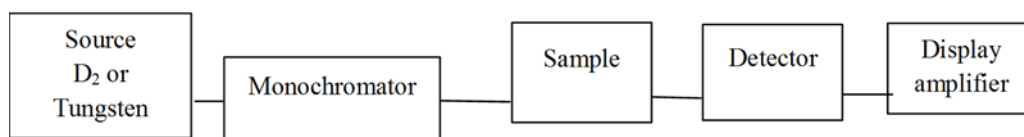


Figure 1. 2. Schematic diagram of a UV/Vis Spectrophotometer.

UV/Vis can be used for qualitative and quantitative analysis of molecules. UV-Vis spectroscopy is used in the pharmaceutical industry to monitor the manufacturing process and product quality of drugs. UV-Vis has several important applications in the biochemical and the environment areas. Recently, UV-Vis spectroscopy has been used as a quantitative analysis method in the study of breast and cervix cancers (58). UV method has been developed for the determination of didanosine and gliclazide in a pure and tablet formulation (59, 60). Wang and co-workers have shown that UV-Vis method was applied for online monitoring of photochemical reactions including methylene blue and methyl orange (57). In a study by Berg *et al.*, UV-Vis spectroscopy has been successfully used as an online method to monitor the cleaning in place of membrane plants in water. The results showed that UV-Vis is a stable, suitable and fast method for this application and saves time, energy and chemicals compared to alternatives (61). UV-Vis spectroscopy has been used for the monitoring of imine (Schiff Base) formation between the carbonyl group of 4-nitrobenzaldehyde and amine group of ethylenediamine (62).

The UV-Vis method was also applied to monitor the extent of 5-hydroxymethylfurfural by reaction between glucose and cellulose (solid-liquid reaction) at high temperature using hydrothermal conditions (63). UV-Vis absorbance has been used to monitor the reaction of polyvinyl chloride with methyl piperazine over time. The product (aminated polyvinyl chloride) was formed at 90 C° for 6 hours (64). Three types of contaminations such as polycyclic aromatic, monocyclic aromatic and organic acids compounds were detected and monitored in water using UV-Vis spectroscopy method (65).

1.4.2. Vibrational spectroscopies

1.4.2.1. Infrared spectroscopy (IR)

Infrared spectroscopy (IR) is an analytical technique used to identify and study organic and inorganic compounds. The main aim of IR is to identify the functional groups of molecules. The most widely used spectral range for chemical analysis is in the mid-IR. Most organic compounds absorb IR radiation within this range (4000 cm⁻¹ to 400 cm⁻¹). The regions > 1650 cm⁻¹ are the most important widely used of the IR spectrum. To explain and understand the IR spectra it should first understand the essential principles of IR spectroscopy. The IR spectrum is divided into three regions; near infrared (NIR), mid-infrared (MID-IR, often referred to as Fourier-transform IR or FTIR) and far infrared (FAR-IR). Mid-IR can detect functional groups for the biological and organic compounds through vibrating dipoles. Far-IR, although promising for some aspects, is yet to be widely used in the pharmaceutical industry. The NIR region covers 14000-4000 cm⁻¹ wavenumbers, the MID-IR region covers 4000-400 cm⁻¹ and the FAR-IR region covers 400-10 cm⁻¹. Near-infrared spectroscopy (NIRS) is the first non-visible region in the infrared spectrum introduced by Herschel in 1800 (66). Since 1960 NIR spectroscopy has improved rapidly and there have been many publications for identification of unknown

compounds using this method (66). NIRS has become most widely used for direct analysis of pharmaceutical compounds without sample treatment (67). NIRS is used as a process analytical technology (PAT) method in the pharmaceutical industry to monitor the quality or process of drug manufacturing including tablet manufacture, freeze drying and pellet formation (68-70). Reich has shown that NIRS can be applied to study the physical and chemical characterization of different dosage forms such as tablets, capsules and implants (71).

MID-IR can be used to analyse various types of samples such as solids, liquids and gas, and it is not only used for identification analysis, but also for quantification. It is an important method for a wide range of scientific and industrial processes. Fourier transform infrared spectroscopy (FTIR) is one of the vibrational techniques and has been extensively used to identify the functional groups of molecules. It also can be used for qualitative and quantitative analysis of mixture components. FTIR is simple and inexpensive instrumentation and plays an important role in a wide range of applications (72). In FTIR spectroscopy, a little amount of sample is required to give a good spectrum in a short time. FTIR spectroscopy coupled to partial least squares has been used to analyse paracetamol and caffeine in pharmaceutical mixtures (73).

FTIR also plays a critical role to keep the pharmaceutical characteristics of peptides and nucleotides and there are several efforts have been made on the synthesis of small organic compounds. The FTIR method has been applied as a powerful tool to monitor solid-phase reactions. FTIR spectra showed that all starting materials were converted to product (74). It has also been used to monitor the reaction of alkoxysilane-terminated polybutadiene polymer over time, and this study showed that the monitoring was limited to qualitative analysis (75). FTIR has been successfully used for monitoring of enaminones synthesis by reaction between aniline and 3-butyln-2-one using ethanol as solvent (76). However, FTIR

provides limited structural information, and it is not a suitable method for all types of compounds especially for complex systems due to its difficulty to identify these compounds (77). In addition, FTIR is not playing a major role in the quantification analysis of vibration groups of the surfaces (62).

1.4.1.2.1. Basic principles of IR spectroscopy

In order to calculate the vibrational frequencies, the period r is given by $r = 2\pi \sqrt{\frac{\mu}{k}}$.

- 1- The force constant (k): this constant is proportional to bond strength. For example, in mid-IR the stretching frequency, and hence absorbance wavelength, of the carbonyl group (C=O) is higher than carbon-oxygen bond group (C-O).
- 2- The reduced mass (μ): in general, heavier atoms will have slower vibration and lower energy (wavelength). For example, in mid-IR compare C-O versus H-O.
- 3- Overtone peaks: For organic compounds that have not C=O or C-H bonds, it can see a small peak at 3450 cm^{-1} and this due to the overtone peak of C=O is lower twice than normal C=O frequency. This is commonly studied in NIR spectroscopy.
- 4- Dipole moment: it is a selection rule that a change in dipole is required for a vibration to generate a peak in the IR spectrum. Because carbonyl group is strongly polar, it has intensive bands, due to the higher electronegativity of oxygen compared to carbon. However, if a vibration is symmetrical, it will not cause any change in dipole moment and not be visible in the IR spectrum.
- 5- Vibrational modes: there two types of the molecular vibrations in IR: stretching and bending. In stretching vibrations, the bond length is changed, these occur at higher energy. Stretching vibrations can be divided into symmetrical and asymmetrical. Bending vibrations, also named deformations, occur at low energy. Bending vibrations

can be divided into in-plane (scissoring and rocking) and out-of-plane (wagging and twisting).

An FTIR spectrometer consists of light source, interferometer, sample compartment and detector. The light source emits radial light within the mid-IR range and going directly to the beam splitter. The interferometer contains two mirrors, one moving and one fixed. The beam splitter reflects half of light beam to the fixed mirror, while the other half is transmitted to the moving mirror. The mirrors reflect both light beams and return them to the beam splitter. After recombination of these beams, the Fourier-transformed light travels to the detector after interaction with the sample, Figure 1.3. After mathematical deconvolution of the detected light a spectrum is constructed. For the work presented here an Attenuated Total Reflection (ATR) accessory was used for sampling.

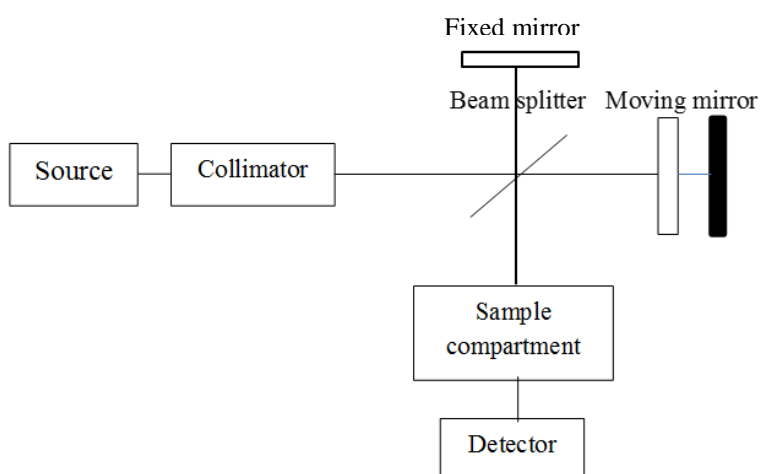


Figure 1. 3. Schematic diagram of an FT spectrometer.

1.4.1.2.2. Steps of generating the FTIR spectrum

- 1- Fourier transform is used to calculate the frequency versus intensity plot: the spectrum.
- 2- All frequencies can be seen by the detector at the same time, making FT more efficient than dispersive IR and hence the standard method.

3- Because FTIR spectroscopy is a single beam technique, background spectra should be recorded.

1.4.2.2. Raman spectroscopy

Raman spectroscopy is a vibrational technique that can be used for identification and quantification of molecules and can provide structural information on the molecules. Raman spectroscopy detects different vibrations in which polar disability rather than dipole changes. Raman spectroscopy can be applied in several areas including pharmaceutical and biomedical analysis because it allows a view of the chemical distribution using optical microscopy. Because Raman spectroscopy covers a wide spectral range from 3500 cm^{-1} to 50 cm^{-1} and the bands are sharper than for mid-IR, it can more often than that technique be used for both qualitative and quantitative analysis.

1.4.2.2.1. Basic principles of Raman spectroscopy

Raman spectroscopy depends on the scattering of radiation by interaction with molecular vibrations (78). When monochromatic laser light interacts with vibrating molecules, the laser photon energy is shifted up or down and this shift can provide information about those vibrations. If the laser photons scatter from the sample in standard Raman spectroscopy this will mostly be elastic in which case the scattered photons have the same energy and wavelength as the incoming ones. This is known as Rayleigh scattering and carries no chemical information, Figure 2.4 (79). Non-elastic scattering can involve loss or increase of energy of the scattered photons.

Very few photons can excite a vibration to a higher energy virtual state, from which it can drop back to a real excited state, leaving the scattered photon with a decreased energy. This is known as Stokes or Raman scattering. This can be analysed by measuring the energy of

the scattered light (80). The scattered photon shifts away from the excitation wavelength by an amount equal to the vibration wavelength, comparable to an IR absorption. Anti-Stokes scattering involves scattering photons gaining energy from a vibration dropping from an excited state into the ground state, Figure 1.4. This very weak effect is not normally used in Raman spectroscopy (81-83).

To observe the scattered photons, the light is collected at an angle and the excitation wavelength filtered out. While Raman scattering depends on it (84), the Raman shift is not depending on the wavelength of radiation obtained (81), and can be directly linked to a vibration. The Raman effect depends on vibrations with changes in polarizability, in contrast to IR where dipole changes are observed. Hence different vibrations will be detected with these complementary techniques. Symmetric vibrations can be detected strongly by Raman, while asymmetric vibrations can be detected strongly by IR. Vibration polar bonds such C-O, N-O and O-H have weak Raman scatters, whereas neutral bonds such as C-C, C-H and C=C have strong Raman scatters, but weak IR absorption.

Raman spectroscopy can be more specific than FTIR due to narrow bands (85). Raman spectroscopy is still limited for quantitative reaction monitoring due to limited sensitivity or non-resonant Raman, instability of laser systems, equipment costs and fluorescence effects.

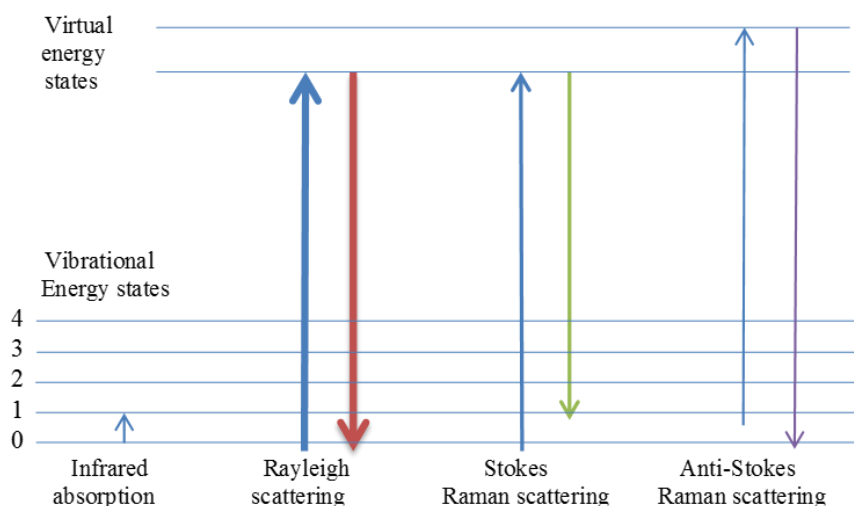


Figure 1. 4. Schematic illustration of excitation states of molecules via Rayleigh, Stokes and anti-Stokes Raman scattering.

Raman spectroscopy has several useful applications in the pharmaceutical analysis such as quantification of tablets, qualitative analysis of polymorphs, monitoring of production, in-line quantitative monitoring of active coating and monitoring of process induced transformations in pharmaceutical manufacturing (86-90). Raman spectroscopy can also be used for monitoring of pharmaceutical synthesis of chemical reactions and crystallisation of solid state (91). Raman spectroscopy is also a sensitive technique to monitor impurities within the reaction (92). Raman spectroscopy has been used for quantitative in-line monitoring of the crystallisation process of flufenamic acid as a function of time and temperature (93). Raman spectroscopy has also been used for online monitoring of different semi-continuous emulsions such as homo and copolymerization reactions (94). Raman spectroscopy has been successfully used to monitor the reaction of α -bromo-*o*-toluic acid in 80% aqueous ethanol. The results showed that the C-Br stretching peak for the starting material (α -bromo-*o*-toluic acid) decreases in intensity with time, while they show an increase in intensity for the vibrational peak of the product (phthalide) (95). Raman spectroscopy was combined with micro TOF mass spectrometry and used as an

online technique for monitoring of 1,3-diamino propane and benzaldehyde reactions using tissue paper as a substrate, and the reactants materials and product were identified (96).

There are a number of important differences between these techniques including separation and spectroscopic techniques. UV-Vis spectroscopy has crucial limitations, in particular, difficult interpretation because of interfering absorption bands. Compared to IR, the UV-Vis development studies are slower due to its methodological difficulties and this lead to far-UV bands for most organic compounds. UV-Vis provides limited structural information on the molecules (97). Compared to other techniques such as GC, HPLC and NMR, FTIR is a fast, cheap and accurate method particularly for monitoring of fast reversible reactions (98). Mid-IR can detect functional groups through vibrating dipoles. A limitation is that only such functional groups are detected and as the same ones may occur in different molecules in a mixture, or indeed in different places in the same molecule, IR is of limited value when analysing complex molecules or mixtures. Compared to FTIR methods, Raman spectroscopy is more expensive and more specific than FTIR, but it is less sensitive unless in resonant mode or under surface-enhanced conditions. However, Raman spectroscopy is still limited for quantitative reaction monitoring due to the instability of the laser and shows sometimes narrow bands (99).

1.5. Mass spectrometry (MS)

Mass spectrometry is a powerful, accurate and sensitive analytical method that can be used to analyse mixtures by detecting the mass to charge ratio of gas phase ions without the need for separation of components (100). It has unique abilities to detect a wide range of chemical species at low concentrations and small sample amounts, and directly measure their molecular weight as well as determine molecular structure through analysis of fragmentation patterns. MS is widely used for qualitative and quantitative analysis (101).

MS provides critical information for a wide range of applications such as environmental, geological, biotechnology and pharmaceutical including drug discovery, combinatorial chemistry, pharmacokinetics and drug metabolism studies. MS has been extensively used for qualitative and quantitative analysis of large molecules such as biomolecules and small organic molecules. MS can provide useful information about the structure of the molecules during the fragmentation process. Compared to other techniques such as FTIR, Raman microscope and HPLC-UV/Vis, MS is highly sensitive, specific, requires little or no sample preparation and provides structural information for the analyte molecules. Separation is sometimes crucial because it is difficult to distinguish the molecules without separating them, hence techniques coupled to chromatography.

In mass spectrometry (MS), chemical compounds are ionised to produce charged fragments and molecules which are then analysed according to their mass to charge ratio (m/z). The first step in MS analysis is the generation of gas-phase ions. These ions are then separated and detected after passing through an electromagnetic field (102). Mass spectrometers consist of three basic parts: a source region in which ionization takes place, a mass-selective analyser and an ion detector. Analytes are submitted to a series of steps (102): ionisation, acceleration, separation and detection. In the mass analysis, the sample could be solid, liquid or gas. The type of mass spectrometry used depends on the sample phase. Solid phase samples can be ionised using a plasma-desorption method. Liquid or solution samples can be analysed using electrospray ionisation (ESI) and matrix-assisted laser desorption/ionisation (MALDI). Chemical ionisation (CI) and electron ionisation (EI) can be used to ionise gas or volatile samples.

MS instruments consist of three main components: an ion source, analyser and detector as shown in Figure 1.5: ion source to produce ions from the molecule after transfer into the gaseous state, the analyser to separate the ions according to their mass to charge ratio and

detector to detect and record the separated ions. An MS spectrum provides highly detailed information about the chemical structure of compounds through interpretation of molecular ion and fragmentation pattern.

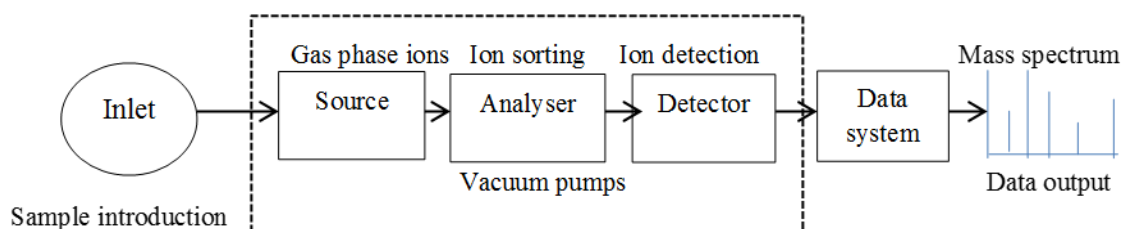


Figure 1. 5. Components of a mass spectrometer.

1.5.1. Practical steps in mass spectrometry

1-Ionise the sample in the ionisation chamber ion source after evaporation. In the ionisation chamber, the ions are produced by shelling the vapour compounds by electrons.

2- In the ionisation chamber, the positive ions are accelerated into an analyse tube and produce radical cations.

3- Separate the produced ions in the analyser using quadrupole and then identify based on their mass to charge ratio.

4- Fragment and analyse these ions in the second analyser. After ionising the molecule, the radical ions which are produced will have enough energy to break the bonds to give fragment ions. These radical ions can also give radical new cations and neutral molecules during the fragmentation process.

5- Detect and measure the ions and then convert them into a spectrum of intensity versus m/z .

Mass spectrometers have become key tools in of the pharmaceutical industry, including for drug discovery, combinatorial chemistry, pharmacokinetics and drug metabolism investigations. Mass spectrometry has a pivotal role in reaction monitoring in various areas due to its high specificity (103). Because MS is rapid, highly sensitive and specific, it can overcome limitations of spectroscopic reaction monitoring techniques such as UV/Vis, IR and electron spin resonance (ESR), to detect reactants, intermediates and products and fully characterise a reaction mixture (104, 105). Mass spectrometry plays a critical role in reaction monitoring and there have been several studies that have reported using mass spectrometry techniques in this field (104).

In recent years, there has been an increasing interest in on-line monitoring of trace compounds in industrial and environmental applications. Electrochemistry (EC) coupled with mass spectrometry was found to be a very sensitive online technique for identification of reactants and products of chemical reactions for non- polar compound detection (106-109). Proton transfer reaction mass spectrometry (PTR-MS) has been used as on-line monitoring technique to measure the trace concentrations of volatile organic compounds such as benzene and acetonitrile in human breath (110). The PTR-MS technique has also been used as a tool for on-line monitoring of 2-propenamide (acrylamide) in the headspace of food products samples (111).

Electrospray ionisation (ESI) is a soft ionisation technique that can be used to ionise small and large molecules at atmospheric pressure. Compared to other ionisation techniques, ESI adds multiple charges to large molecules, and this can increase with molecular weight. ESI-MS is important for a wide range of pharmaceutical and biological compounds (112). ESI-MS is applied to monitor synthetic chemical reactions and study the intermediate compounds and mechanisms. ESI-MS spectra provide clear signals about the structure information on the molecules (113). Nanoelectrospray mass spectrometry (nano ESI) is

one of the ionisation techniques and has been developed for monitoring of chemical reaction of proteins and peptides in humans and animals such as cytochrome, angiotensin and pepsin (114).

1.5.2. Hyphenated techniques using mass spectrometry

Mass spectrometry combined with chromatographic or spectroscopic techniques plays an important role in the pharmaceutical analysis including monitoring and identification of impurities. Hyphenated techniques have a pivotal role in identification and quantification of unknown chemical components in complex mixtures. The past decades have seen a growing trend towards hyphenated techniques in many (pharmaceutical) applications (115). Studies have shown the beneficial effect of these hyphenated techniques (116, 117), in practical applications to ensure the quality and safety of pharmaceuticals. The main advantage of these combined techniques is to increase the sensitivity and selectivity of qualitative and quantitative analysis, particularly for unknown chemical components, in a mixture. Other advantages of using hyphenated techniques are a very low limit of detection and limit of quantification and high precision in the determination (118). There are several types of hyphenated techniques such as LC-MS (119, 120), GC-MS (117, 121), LC-FTIR (122) and LC-NMR (123). LC- (and HPLC)-MS are the most in use in the pharmaceutical industry. The most explored/used hyphenated techniques combine chromatographic separation, principally using gas chromatography (GC) and (HPLC)LC, with mass spectrometry. HPLC (125, 126), GC (127, 128) and LC (117, 129) have been combined with mass spectrometry for qualitative and quantitative analysis of mixtures (130). Different approaches based on mass spectrometry were applied to develop a simple method that can be used to monitor chemical reactions to save time, sample and solvents and to provide structural information on the analytes (130). HPLC is developing by connection with mass spectrometry (HPLC-MS) as a hyphenated method to use in pharmaceutical

analysis for monitoring of drug substances and dosage forms. HPLC-MS-MS has been used to monitor the reaction of the oxidation of isothiazolium salt by investigation of the intermediates and products over time (131). LC-MS and capillary electrophoresis mass spectrometry (CE-MS) have been used for monitoring of anticancer drugs such as tamoxifen (for breast cancer treatment) and oxazaphosphorines (for solid malignancies treatment) (132). Turbulent flow liquid chromatography was coupled with tandem mass spectrometry (TFC-MS-MS) and used to monitor antidepressant drugs in human serum, including citalopram, doxepin and imipramine (133). There is increasing concern that some of these techniques are being limited and disadvantaged for pharmaceutical analysis. For example, the procedures of LC-MS including sample pre-treatment such as extraction, filtration, and separation are required and they are also time consuming. Another problem of LC-MS is the use of short columns and this might be that chromatographic separation is likely to be incomplete (116). GC-MS and LC-MS were used as monitoring methods for chemical reactions, but chromatographic fractionation of reaction mixtures can be before the analysis (131). Ion mobility mass spectrometry (IM-MS) has been successfully applied as a fast and sensitive technique for identification and quantification monitoring of biocatalytic reactions (134). Limitations of standard MS are: it is not a direct analysis of the sample and a sample preparation is required (pre-concentration and extraction).

1.5.2.1. LC/MS instrumentation

A schematic diagram of a mass spectrometer linked to LC is shown in Figure 1.6. Mixtures are separated in the LC system, and for each component, a mass spectrum is generated. LC combined with MS is a powerful analytical technique that can be used to separate and identify compounds. Electrospray ionisation (ESI) is the most widely used ionisation method in LC/MS due to it being most suitable for polar compounds and readily coupled to LC instrumentation. However, limitation of combined LC/MS with ionisation methods

gives little fragmentation which is not useful for providing information about the molecule structure.

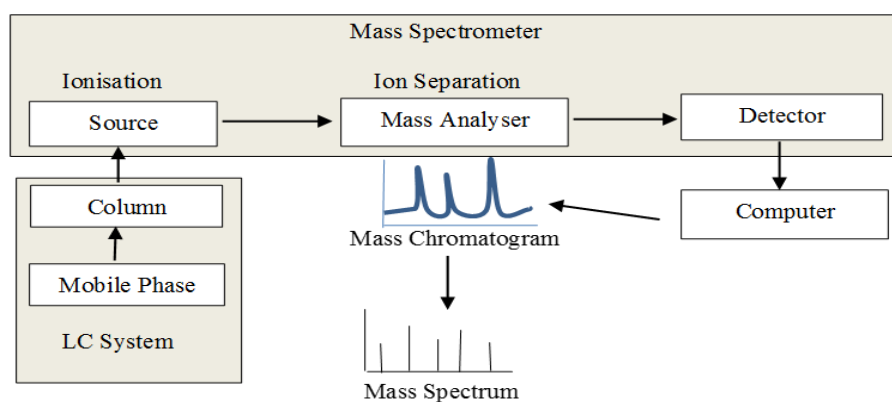


Figure 1. 6. Schematic diagram of mass spectrometer linked to LC.

1.5.3. Ambient mass spectrometry (AMS)

Recently, researchers have shown an increased interest in directly analysing samples under atmospheric conditions using the relatively new range of ambient mass spectrometric (AMS) techniques. Since they were reported in the last two decades, they have attracted a lot of interest. AMS has important advantages over other traditional mass techniques: as it is a direct ionisation of the sample at ambient conditions, little or no sample preparation is generally required, and it can readily be interfaced with a diversity of mass spectrometers. Ambient ionisation mass spectrometric methods have been applied for a wide range of fields such as pharmaceuticals (quality control of pharmaceutical products and drug packaging materials), biomedicine and environmental pollution (135).

MS requires molecules in the vapour phase and this is not the case for ambient ionisation approaches to MS. In the ambient ionisation methods of the mass spectrometry, there is no sample preparation and ion formation in ambient conditions. Several important stages of direct ionisation methods have been developed to analyse the sample and these make

ambient ionisation methods powerful techniques that can be used for rapid analysis of complex mixtures (136). Different kinds of samples such as solid, liquid, gas, cream and gel can be analysed by these techniques.

Several traditional ionisation techniques have been used for analysis of samples such as matrix-assisted laser desorption (MALDI) and chemical ionisation (CI). However, limitations of these techniques are the ionisation of a sample is completed in a closed device like a capillary and sample pre-treatment is required, Figure 1.7.

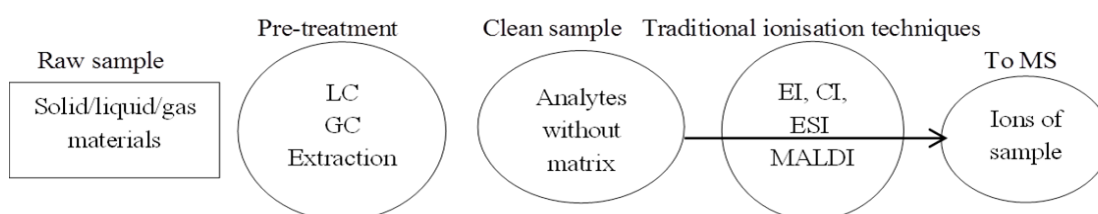


Figure 1. 7. Components of traditional ways to produce ions of samples.

In the ambient ionisation techniques, the energy is generated from the source and it interacts with analytes to produce ions and these ions are moved to the MS for detection. Desorption electrospray ionisation (DESI) is an example of the ambient ionisation techniques that use a solvent as a source. It uses an electrical source of charged aqueous spray that interacts with samples on the solid surface. The charged droplets will dissolve all chemicals in the samples during the reaction. Furthermore, the small droplets that are produced from the sample surface lead to rapid evaporation of the solvent (136, 137).

Several ambient desorption/ionisation techniques were introduced at the inception of the field, notably desorption electrospray ionisation (DESI), direct analysis in real time (DART) and plasma-assisted desorption ionisation (PADI) (138). Studies over the past

years using ambient ionisation mass spectrometric techniques have provided important information on the chemical composition of compounds. A rapid development of new ambient ionisation techniques with mass spectrometry has been seen in several areas, which has led to shortening analysis time and extended the sample formats that can be analysed (135). DESI and DART are still the AMS techniques most frequently used for identification of chemical compounds including polar compounds such as peptides and proteins and non-polar analytes such as coniceine and lycopene (139), DESI and DART have been used to identify molecules in organic synthesis, human skin and food (140).

1.5.3.1. Plasma-based ambient mass spectrometry

A number of ambient MS techniques use different types of plasma for the ionisation and desorption of analytes, prior to analysis in the mass spectrometer. Here only two will be discussed in some detail: DART as the most frequently used and commercially available technique and PADI, which is used throughout the investigation reported on in this thesis. Plasma is considered to be the fourth state of matter in addition to solid, liquid and gas. Plasmas can be divided into two groups depending on the type and amount of energy: the excited species (ions, electrons, photons, neutrals) can be at high or low temperature. Low temperature plasmas can be sub-divided into two main classifications; thermal and non-thermal (cold) plasmas. In thermal plasmas, molecules are fully ionised, while they are partly ionised in non-thermal plasmas (141). The plasma, often He-based and containing He*, can upon interaction with the ambient atmosphere, as is the case in ambient MS applications, form a range of reactive species, including $(\text{H}_2\text{O})_n \text{H}^+$, e^- , UV, N_2^+ (142). Any of these excited species can in principle ionise and volatilise analyte molecules so they can be detected by mass spectrometry (143). A plasma forms can be electrons, positive and negative ions, atoms, free radicals and photons. Plasma is generated at low pressure or atmospheric pressure by a combination of energy to gas by various ways

including mechanical, voltage and radio frequency (144-146). In general, the activity of plasmas depends on the generation source of temperature and this may help to use plasma technologies for a wide range of applications including gas treatment and chemical synthesis (144). PADI plasma is generated by a radio frequency field using helium gas, while DART plasma is generated by discharge gas (helium or nitrogen). Characteristics and parameters of PADI and DART are different. PADI uses low voltage (hundreds of volts) to drive the electrical discharge compared to that used by DART (kV). PADI uses non-thermal plasma, while DART uses thermal plasma and the temperature must be between 150 °C and 250 °C.

Plasma can play an important role in addressing the issue of growth of bacteria and can reduce the number of bacteria in the human body in a few seconds (147). Plasma sources are essential for a wide range of applications such as spectroscopic analysis, gas treatment, material processing and lamps. The last decades have seen a growing trend towards the use of atmospheric plasma sources in atomic and mass spectrometry. Microwave plasma sources have been used as detectors in atomic emission and gas chromatographic techniques to produce surface wave plasma using mixture gases such as helium, nitrogen and argon. The results showed that the use of a mixed of these gases can improve the method sensitivity (148). Plasma needle is a type of atmospheric plasma technologies that operate at room temperature, and it was developed to remove cancer cells and can also use as a treatment for wound healing and bacterial infections (142).

In recent years, there has been an increasing interest in applications of non-thermal atmospheric pressure plasmas (149). Because of the rapid development of non-thermal atmospheric pressure plasmas at low temperature, it plays an important role for treatment of infected or chronic wounds (150). Biomaterials treatment has been studied by many researchers using non-thermal plasmas (NTP) with various techniques (143). NTP is not

only used in the medical applications for sterilization, but it also can be used as a key tool in several medical treatments such as corneal infections, dental diseases, cancers leishmaniasis and blood coagulation (151). Non-thermal atmospheric plasma plays a critical role in the maintenance of the characteristics of the substance such as molecular weight and volume, and this can impact on the substance composition of devices (152, 153). It can also play an important role by addressing the heat issue, because some of the sterilization technologies need 120°C and this causes degradation of medical devices, and vacuum chambers are required. However, non-thermal atmospheric plasma needs below 40°C and without the need for vacuum chambers (152). A novel method of NTP has been developed for skin cleansing by killing pathogens of skin infections such as bacteria and fungus (154). NTP also plays an important role in the treatment of atmospheric pollution by removal of volatile organic compounds (VOC) using chemical reaction engineering. This action occurs by reacting reactive species produced by NTP with pollutant compounds. In this case, the atomic oxygen produced by plasma will oxidise the volatile organic compounds and produce CO or CO₂ (155). NTP has also been developed and used to remove non-catalytic and catalytic VOC abatement and nitrogen oxide (NO_x) as atmospheric pollutants from exhaust gases (156, 157). NTP is important for a wide range of scientific and industrial processes such as antiseptic of cell surfaces damage (158), accelerate wound healing (159) and for cancer treatment due to its ability to stop tumour cells growing (160, 151). Although both thermal and non-thermal plasmas are beneficial, there are little differences between them. In thermal plasma, the energy from electrons to heavy particles equals the energy from heavy particles to the environment and the temperature is the same for both. However, in non-thermal plasma, the energy transfer is not so effective, and the gas temperature is low. Non-thermal plasmas are also named non-equilibrium plasmas (151).

1.5.3.2. Ambient mass spectrometry techniques

1.5.3.2.1. Desorption electrospray ionisation (DESI)

DESI is the first AMS technique for MS and was introduced by the Cooks group in 2004. It uses a solvent as a source to ionise the molecule at ambient conditions. The mechanism of ionisation is that the electrical source sprays the droplets of solvent to produce the ions from the surface of the molecule (161). The produced ions are detected, separated and identified using the suitable mass spectrometer. ESI is a standard ionisation technique in MS and LC-MS. The electrospray part of ESI-MS aimed at a sample surface, generating ions from it by solution phase ionisation which are propelled into the MS inlet by the impact of subsequent droplets. Compared to electrospray ionisation (ESI), a lot of fragmentation can be gained from DESI. In DESI, the molecules can be ionised at atmospheric pressure with little sample preparation. DESI has a wide range of applications and it can be used for direct analysis of different types of samples as it is highly sensitive and fast. DESI-MS has been used as an on-line monitoring method for investigation of pharmaceutical ingredients such as tablets (aspirin, folic acid and acetaminophen), salve and liquids as samples (162).

1.5.3.2.2. Direct analysis in real time (DART)

DART was introduced by Laramee and Cody in 2005. In DART, the atoms and ions are excited from a gas using the plasma at atmospheric pressure. All charged species are filtered out so that the sample is only exposed to excited neutrals. Positive or negative ions even electrons can be produced in DART ionisation. In DART, a stream of gas (helium or nitrogen), but helium is mostly used with an electric discharge uses to produce electrons, ions and excited state gas. With using helium, the excited-state helium reacts with water in the air to produce protonated water, after which the proton is transferred to the molecule

(ionisation). Another ionisation mechanism is that the excited-state helium reacts with a neutral to produce a radical cation and electron (163). In DART, the only helium can interact with the sample when the plasma is filtered, while in PADI and LTP the plasma reacts with the analyte (164).

DART was applied successfully for quality assurance in pharmaceutical manufacturing. Direct analysis in real time (DART) coupled to mass spectrometry and has been used for monitoring of pesticides in the agricultural products such as tomatoes and apples (165), for a quality monitor of olive oil (166) and for reaction monitoring of indolin-2, 3-dione Schiff bases (167). DART was developed to analyse liquids and solids samples without the need for extraction (141) and for analysis of non-polar compounds (168).

1.5.3.2.3. Low-temperature plasma probe (LTP)

LTP was introduced after PADI. In LTP, the plasma interacts with the sample on the probe, and then ions are produced from the surface (169). Numerous micro-discharges produce streamer like jets, a voltage is applied to cylindrical electrode outside of the discharge chamber with a grounded needle inside. Compared to DESI, the investigation LTP does not need to spray solvent and it has a simple construction. Compared to DART, LTP uses non-thermal plasma. In LTP, the non-thermal plasma is generated at atmospheric pressure like PADI. LTP has been developed as cheap and easy AMS method when coupled to mass spectrometry (103). Low-temperature plasma mass spectrometry (LTP-MS) has been successfully applied to monitor several reactions including ethylenediamine with acetic anhydride and methanol with acetic anhydride (135).

1.5.3.2.4. Plasma assisted desorption ionisation-mass spectrometry (PADI-MS)

PADI-MS was introduced after DESI and DART in 2007. It uses plasma for direct analysis of analytes on a surface. PADI-MS employs non-thermal plasma generated by a radio frequency field using helium (170, 136). Compared to DESI, PADI utilises non-thermal plasma gas as a source, while DESI uses the solvent spray to analyse samples (171). Compared to DART, the PADI source is a cold atmospheric glow discharge that is differentiated by low voltage and power (170). There are some of the similarities between PADI and other ambient ionisation techniques. The plasma source for PADI is similar to that used for DART and dielectric barrier discharge ionisation (DBDI). PADI and LTP are used non-thermal plasma without the need for heating the sample (135).

PADI has also some advantages over spectroscopic methods such as UV/Vis, IR, and NMR, and chromatographic methods such HPLC, LC-MS and GC-MS. PADI is easy to set up, little or no sample preparation is required, it has short analysing time and can be applied for direct analysis of various compounds such as solids, creams and liquids (170). In addition, PADI-MS provides information about chemical speciation, whilst also allowing spatial localisation of sampling onto individual glass slides and cotton swabs.

Several applications of PADI have been used for direct analysis of mixture components in various pharmaceutical compounds (170), and it can be used for analysis of polar and non-polar analytes (172). Salter and co-workers have shown the effect and optimisation of analytical parameters of PADI such as the distance between the plasma flame and sample surface, radio frequency power and surface temperature for some polymers on signal intensities (164). In a study by Bowfield *et al.*, two different sources of PADI such as micro-PADI and needle PADI have been used to analyse several species of

pharmaceuticals including paracetamol and ibuprofen tablets from the surfaces after optimising the parameters (173).

A more versatile, faster and more sensitive method is needed in the pharmaceutical industry to use for rapid, affordable characterisation of the pharmaceutical mixtures. This would give rise to better and lower cost, and could have a significant impact on the analysis of chemical compounds in other areas. Therefore, the aim of the study was to develop a novel method for detailed and rapid monitoring of pharmaceutically relevant reactions with a little or no sample preparation. A novel analytical approach for monitoring pharmaceutically relevant reactions is reported in this thesis using plasma assisted desorption ionisation mass spectrometry (PADI-MS). Ambient mass spectrometry in the form of plasma assisted desorption ionisation mass spectrometry (PADI-MS) has the potential to fill this important gap in the pharmaceutical industry's analytical arsenal.

This thesis has been divided into four parts. The first part deals with plasma-substrate interaction studied by PADI-MS and Raman microscopy using paracetamol tablets as a model system. This was achieved by the surface characterisation of tablets by Raman microscopy after exposure to the non-thermal PADI plasma flame. This was compared with time-resolved PADI-MS experiments. The second part was concerned with PADI mass spectrometry analysis of mixtures from TLC plates. This involved analysis of mixture solutions of paracetamol and caffeine after deposition on TLC plates, both with and without the separation of spots. Part three of the study presented PADI-MS for the analysis of pharmaceutical solids and liquids from glass slides and cotton swabs as convenient and cost-effective substrates. This was achieved by analysing solid and liquid samples of paracetamol, caffeine and Panadol using PADI-MS from glass slides and cotton swabs. The fourth section presented PADI-MS for the monitoring of imine (Schiff Base) formation as a model pharmaceutical reaction. This was achieved by comparing the

findings of PADI-MS with other analytical techniques: TLC, HPLC and FTIR using cotton swabs as a substrate.

References

1. DiMasi, J.A. Hansen, R.W. and Grabowski, H.G. (2003) 'The price of innovation: new estimates of drug development costs', *Journal of Health Economics*, 22, p.p.151–185.
2. Mollan Jr., M.J. Ph.D. and Lodaya, M. Ph.D., 'Continuous processing in pharmaceutical manufacturing', Pfizer Inc.
3. Pioneering science, life-changing medicines, 2013, AstraZeneca annual report and form 20-F information.
4. Fung, K. Y. and Ng, K. M. (2003) 'Product-centered processing: pharmaceutical tablets and capsules', *AIChE Journal*, 49 (5), p.p. 1193–1215.
5. Earnshaw, C. J. Carolan, V. K. Richards, D. S. and Clench, M. R. (2010) 'Direct analysis of pharmaceutical tablet formulations using matrix-assisted laser desorption/ionisation mass spectrometry imaging', *Rapid Communications in Mass Spectrometry.*, 24, p.p. 1665–1672.
6. Meher, A.K. and Chen, Y-C. (2016) 'Online monitoring of chemical reactions by polarization-induced electrospray ionization', *Analytica Chimica Acta*, 937, p.p. 106–112.
7. Elipe, M.V.S. and Milburn, R.R. (2016) 'Monitoring chemical reactions by low-field benchtop NMR at 45MHz: pros and cons', *Magnetic Resonance in Chemistry.*, 54, p.p. 437–443.
8. Blanco, M. Eustaquio, A. Gonza'lez, J. M. Serrano, D. (2000) 'Identification and quantitation assays for intact tablets of two related pharmaceutical preparations by reflectance near-infrared spectroscopy: validation of the procedure', *Journal of Pharmaceutical and Biomedical Analysis*, 22, p.p. 139–148.
9. Prathap, B. Dey, A. Srinivasa rao, G. H. Johnson, P. and Arthanariswaran, P. (2013) 'A review - importance of RP-HPLC in analytical method development', 3 (1), p.p. 15–23.

10. Scott, R.P.W. (2003) 'Principles and practice of chromatography', Chrom-Ed Book Series, p.p. 1–100.
11. Gocan, S. (2002) 'Stationary phases for thin-layer chromatography', *Journal of Chromatographic Science*, 40, p.p. 1–12.
12. Köhler, J. Chase, D.B. Farlee, R.D. Vega, A.J. Kirkland, J.J. (1986) 'Comprehensive characterization of some silica-based stationary phase for high-performance chromatography', *Journal of Chromatography*, 352, p.p. 275–305.
13. Gocan, S. (1990) 'Stationary phase in thin-layer chromatography in modern thin-layer chromatography', N. Grinberg, Ed. Marcel Dekker, New York, NY, p. p. 5–137.
14. Danielson, N.D. Katon, J.E. Bouffard, S.P. and Zhu, Z.H. (1992) 'Zirconium oxide stationary phase for thin-layer chromatography with diffuse reflectance Fourier transform infra-red detection', *Analytical Chemistry*, 64, p.p. 2183–2186.
15. Himmelsbach, M. Waser. M. and Klampfl, C. W. (2014) 'Thin layer chromatography–spray mass spectrometry: a method for easy identification of synthesis products and UV filters from TLC aluminium foils', *Analytical and Bioanalytical Chemistry.*, 406, p.p. 3647–3656.
16. Lee, P.J. Murphy, B.P. Balogh, M.P. and Burgess, J.A. (2010) 'Improving organic synthesis reaction monitoring with rapid ambient sampling mass spectrometry', Waters Corporation, Milford, MA, USA.
17. Sherma, J. (2014) 'Biennial review of planar chromatography: 2011-2013', *Cent. Eur. Journal of Chemistry*, 12(4), p.p. 427–452.
18. Tuzimski, T. (2011) 'Application of different modes of thin-layer chromatography and mass spectrometry for the separation and detection of large and small biomolecules', *Journal of Chromatography A*, 1218, p.p. 8799–8812.

19. Van Berkel, G. J. (2002) 'Thin-layer chromatography and electrospray mass spectrometry coupled using a surface sampling probe', *Analytical Chemistry*, 74, p.p. 6216–6223.
20. Haddad, R. Milagre, H. M. S. Catharino, R. R. and Eberlin, M. N. (2008) 'Easy ambient sonic-spray ionization mass spectrometry combined with thin-layer chromatography', *Analytical Chemistry*, 80, p.p. 2744–2750.
21. Van Berkel, G. J. Ford, M. J. and Deibel, M. A. (2005) 'Thin-layer chromatography and mass spectrometry coupled using desorption electrospray ionization', *Analytical Chemistry*, 77, p.p. 1207–1215.
22. Hilaire, P. M. S. Cipolla, L. Tedebark, U. and Meldal, M. (1998) 'Analysis of organic reactions by thin layer chromatography combined with matrix-assisted laser desorption/ionization time-of-flight mass spectrometry', *Rapid Communications in Mass Spectrometry*, 12, p.p. 1475–1484.
23. Danigel, H. Schmidt, L. and Jungclas, H. (1985) 'Combined thin layer chromatography/mass spectrometry: an application of ^{252}Cf plasma desorption mass spectrometry for drug monitoring' *Biomedical Mass Spectrometry*, 12, (9), p.p. 542–544.
24. Lin, S-Y. Huang, M-Z. Chang, H-C. and Shiea, J. (2007) 'Using electrospray-assisted laser desorption/ionization mass spectrometry to characterize organic compounds separated on thin-layer chromatography plates', *Analytical Chemistry*, 79(22), p.p. 8789–8795.
25. Van Berkel, G.J. Tomkins, B.A. and Kertesz, V. (2007) 'Thin-layer chromatography/desorption electrospray ionization mass spectrometry: investigation of goldenseal alkaloids', *Analytical Chemistry*, 79(7), p.p. 2778–2789.

26. Morlock, G. and Ueda, Y. (2007) 'New coupling of planar chromatography with direct analysis in real time mass spectrometry', *Journal of Chromatography A.*, 1143, (1–2), p.p. 243–251.
27. Taleuzzaman, M. Ali, S. Gilani, S.J. Imam, S.S. and Hafeez, A. (2015) 'Ultra performance liquid chromatography (UPLC) - A Review', *Austin Journal of Analytical and Pharmaceutical Chemistry*, 2 (6), p.p. 1056–1061.
28. Kupiec, T. (2004) 'Quality-Control Analytical Methods: High-Performance Liquid Chromatography', *International Journal of Pharmaceutical Compounding*, 8, (3), p.p. 223–227.
29. Lunn, G. and Wiley, J. (2005) 'HPLC methods for recently approved pharmaceuticals', Wiley-Interscience.
30. Gorog, S. (2006) 'The importance and the challenges of impurity profiling in modern pharmaceutical analysis', *Trends in Analytical Chemistry*, 25, p.p. 755–757.
31. Gorog, S. (2007) 'The changing face of pharmaceutical analysis', *Trends in Analytical Chemistry*, 26, p.p.12–17.
32. Kazakevich, Y. V. and LoBrutto, R. (2007) 'HPLC for pharmaceutical scientists', Wiley-Interscience.
33. Vikrant, V. (2014) 'A review on HPLC and RP-HPLC analysis method', *International Journal of Institutional Pharmacy and Life Sciences*, 4(4), p.p. 50–64.
34. Martin, M. and Guiochon, G. (2005) 'Effects of high pressures in liquid chromatography', *Journal of Chromatography A*, 7, (1-2), p.p. 16–38.
35. Liu, Y. and Lee, M.L. (2006) 'Ultrahigh-pressure liquid chromatography using elevated temperature. *Journal of Chromatography*', 1104 (1-2), p.p. 198–202.
36. Swartz, M. (2010) 'HPLC detectors: a brief review', *Journal of Liquid Chromatography & Related Technologies*, 33, p.p. 1130–1150.

37. Blau, K. and Halket, J.M. (1993) 'Handbook of derivatives for chromatography', 2nd ed., Wiley: New York.
38. Kissinger, P.T. and Heineman, W.R. (1984) 'Laboratory techniques in electroanalytical chemistry', Marcel Dekker, New York.
39. Ackworth, I.N. (1997) 'Coulometric electrode array detectors for HPLC', (Progress in HPLC-HPCE, Vol. 6). Brill Academic: Boston.
40. Fritz, J.S. and Gjerde, D.T. (2009) 'Ion Chromatography, 4th, Completely Revised and Enlarged Edition', Wiley: New York.
41. Weiss, J. 'Handbook of Ion Chromatography', (2005) Wiley: New York.
42. Model 8060 Nitrogen Specific HPLC Detector, brochure A-8060-99-25M, Aantek Instruments: Houston, TX, 1999.
43. Petritis, K. Elfakir, C. and Dreux, M. (2001) 'HPLC-CLND for the analysis of underivatized amino-acids', LC-GC Europe, 14, p.p. 389–395.
44. Shi, H. (1997) 'Supercritical fluid chromatography with chemiluminescent nitrogen and sulphur detection', Blacksburg, Virginia.
45. Reilly, J. Everatt, B. and Aldcroft, C. (2008) 'Implementation of charged aerosol detection in routine reversed-phase liquid chromatography methods', Journal of Liquid Chromatography & Related Technologies, 31 (20), p.p. 3132–3142.
46. Asa, D. (2005) 'Impurity testing with a universal HPLC detector', Genetic Engineering News., 25 (19), p.p. 33–34.
47. Lisa, M. Lynen, F. Holcapek, M. and Sandra, P. (2007) 'Quantitation of triacylglycerols from plant oils using charged aerosol detection with gradient compensation', Journal of Chromatography A., 1176(1–2), p.p. 135–142.
48. McPolin, O. (2009) 'An introduction to HPLC for pharmaceutical analysis', Warrenpoint, Mourn Training Services.

49. Jadaun, G. P. S. Dixit, S. Saklani, V. Mendiratta, S. Jain, R. and Singh, S. (2017) 'HPLC for peptides and proteins: principles, methods and applications', *Pharm Methods*, 8(1), p.p. 139–144.
50. Malviya, R. Bansal, V. Pal, O.P. and Sharma, P.K. (2010) 'High-performance liquid chromatography: a short review', *Journal of Global Pharmacy Technology.*, 2(5), p.p. 22–26.
51. Tie, C. Hu, T. Jia, Z-X. and Zhang, J-L. (2016) 'Derivatization strategy for the comprehensive characterization of endogenous fatty aldehydes using HPLC-multiple reaction monitoring', *Analytical Chemistry*, 88, p.p. 7762–7768.
52. Foley, D. A. Wang, J. Maranzano, B. Zell, M. T. Marquez, B. L. Xiang, Y. and Reid, G. L. (2013) 'Online NMR and HPLC as a Reaction Monitoring Platform for Pharmaceutical Process Development', *Analytical Chemistry*, 85, p.p. 8928–8932.
53. Rao, R.N. Nagaraju, D. Jena, N. and Kumaraswamy, G. (2006) 'Development and validation of a reversed-phase HPLC method for monitoring of synthetic reactions during the manufacture of a key intermediate of an anti-hypertensive drug', *Journal of Separation Science*, 29(15), p.p. 2303–2309.
54. Riley, C. M. Sternson, L. A. Repta, A. J. and Slyter, S. A. (1983) 'Monitoring the reactions of cisplatin with nucleotides and methionine by reversed-phase high-performance liquid chromatography using cationic and anionic pairing ions', 130, p.p. 203–214.
55. Schafer, W. A. Hobbs, S. Rehm, J. Rakestraw, D. A. Orella, C. McLaughlin, M. Ge, Z. and Welch, C. J. (2007) 'Mobile tool for HPLC reaction monitoring', *Organic Process Research & Development*, 11, p.p. 870–876.

56. Zhu, L. Brereton, R. G. Thompson, D. R. Hopkins, P. L. and Escott, R. E. A. (2007) 'On-line HPLC combined with multivariate statistical process control for the monitoring of reactions', *Analytica Chimica Acta*, 584, p.p. 370–378.
57. Wang, N. Tan, F. Zhao, Y. Tsoi, C. C. Fan, X. Yu, W. and Zhang, X. (2016) 'Optofluidic UV-Vis spectrophotometer for online monitoring of photocatalytic reactions', *Scientific Reports*, p.p. 1–8.
58. Brown, J. Q. Vishwanath, K. Palmer, G. P. and Ramanujam, N. (2009) 'Advances in quantitative UV–visible spectroscopy for clinical and pre-clinical application in cancer', *Current Opinion in Biotechnology*, 20, p.p. 119–131.
59. Ahmed, Md. S. M. and Chakravarethy, I. E. (2016) 'Development and validation of UV spectroscopic method for the determination of didanosine in pharmaceutical dosage forms', *World Journal of Pharmacy and Pharmaceutical Sciences*, 5, 6, p.p. 2008–2012.
60. Jamadar, S. A. Mulye, S. P. Karekar, P. S. Pore, Y. V. and Burade, K. B. (2011) 'Development and validation of UV spectrophotometric method for the determination of Gliclazide in tablet dosage form', *Der Pharma Chemica*, 3 (4), p.p. 338–343.
61. Berg, T. H. A. Ottosen, N. van den Berg, F. and Ipsen, R. (2017) "Inline UV-Vis spectroscopy to monitor and optimize cleaning-in-place (CIP) of whey filtration plants", *Food Science and Technology*, 75, p.p. 164–170.
62. Kim, J. Jung, D. Park, Y. Kim, Y. Moon, D. W. and Lee, T. G. (2007) 'Quantitative analysis of surface amine groups on plasma-polymerized ethylenediamine films using UV–visible spectroscopy compared to chemical derivatization with FT-IR spectroscopy, XPS and TOF-SIMS', *Applied Surface Science*, 253, p.p. 4112–4118.
63. Kawamura, K. Yasuda, T. Hatanaka, T. Hamahiga, K. Matsuda, N. Michio Ueshima, M. and Nakai, K. (2017) 'In situ UV-VIS spectrophotometry within the second time scale as a research tool for solid-state catalyst and liquid-phase reactions at high

- temperatures: Its application to the formation of HMF from glucose and cellulose', *Chemical Engineering Journal*, 307, p.p. 1066–1075.
64. Roudman, A. R. and Kusy, R. P. (1998) 'UV-visible spectroscopic study of the reaction kinetics of methyl piperazine-modified poly (vinyl chloride)s for use as fixed-state proton carrier membranes', *Polymer*, 39, (16) p.p. 3641–3649.
65. Hu, Y. and Wang, X. (2017) 'Application of surrogate parameters in characteristic UV–vis absorption bands for rapid analysis of water contaminants', *Sensors and Actuators, B* 239 p.p. 718–726.
66. Blanco, M. Coello, J. Iturriaga, H. Maspoch, S. and de la Pezuela, C. (1998) 'Near-infrared spectroscopy in the pharmaceutical industry', *Analyst*, p.p. 123–135.
67. Siddiqui, M.R. AlOthman, Z.A. and Rahman, N. (2013) 'Analytical techniques in pharmaceutical analysis: A review', *Arabian Journal of Chemistry*, p.p. 1–13.
68. Maurer, L. and Leuenberger, H. (2009) 'Applications of near-infrared spectroscopy in the full-scale manufacturing of pharmaceutical solid dosage forms', *Pharmazeutische Industrie*, 71, p.p. 672–674.
69. De Beer, T.R.M. Verduyck, P. Burggraeve, A. Quinten, T. Ouyang, J. Zhang, X. Vervaet, C. Remon, J.P. and Baeyens, W.R.G. (2009) 'In-line and real-time process monitoring of a freeze-drying process using Raman and NIR spectroscopy as complementary process analytical technology (PAT) tools', *Journal of Pharmaceutical Sciences*, 98, p.p. 3430–3446.
70. Mantanus, J. Ziemons, E. Lebrun, P. Rozet, E. Klinkenberg, R. Streel, B. Evrard, B. and Hubert, Ph. (2009) 'Moisture content determination of pharmaceutical pellets by near-infrared spectroscopy: method development and validation', *Analytica Chimica Acta*, 642, p.p. 186–192.

71. Reich, G. (2005) 'Near-infrared spectroscopy and imaging: basic principles and pharmaceutical applications', *Advanced Drug Delivery Reviews*, 57, p.p. 1109–1143.
72. Jackson, M. and Mantsch, H. H. (1995) 'The use and misuse of FTIR spectroscopy in the determination of protein structure', *Critical Reviews in Biochemistry and Molecular Biology*, 30(2), p.p. 95–120
73. Bouhsain, Z. Garrigues, S. and Guardia, M. de la. (1996) 'Simultaneous stopped-flow determination of paracetamol, acetylsalicylic acid and caffeine in pharmaceutical formulations by Fourier transform infrared spectrometry with partial least-squares data treatment', *Analyst*, 121, pp. 1935–1938.
74. Yan, B. Kumaravel, G. Anjaria, H. Wu, A. Petter, R. C. Jewell, C. F. and Wareing, J. R. (1995) 'Infrared Spectrum of a Single Resin Bead for Real-Time Monitoring of Solid-Phase reactions', *J. Org. Chem.*, 60, p.p. 5736–5738.
75. Huber, M. P. Kelch, S. and Berke, H. (2016) 'FTIR investigations on hydrolysis and condensation reactions of alkoxy silane-terminated polymers for use in adhesives and sealants', *International Journal of Adhesion & Adhesives*, 64, p.p. 153–162.
76. Chisholm, D. R. Valentine, R. Pohl, E. and Whiting, A. (2016) 'Conjugate addition of 3-butyne-2-one to anilines in ethanol: alkene geometric insights through in situ FTIR monitoring', *The Journal of Organic Chemistry*, 81 (17), p.p. 7557–7565.
77. Wenning, M. and Scherer, S. (2013) 'Identification of microorganisms by FTIR spectroscopy: perspectives and limitations of the method', *Applied Microbiology and Biotechnology*, 97, p.p. 7111–7120.
78. Bumbrah, G. S. and Sharma, R. M. (2016) 'Raman spectroscopy–Basic principle, instrumentation and selected applications for the characterization of drugs of abuse', *Egyptian Journal of Forensic Sciences*, 6, p.p. 209–215.

79. Smith, W.E. and Dent, G. (2005) 'Introduction, basic theory and principles', Modern Raman Spectroscopy – A Practical Approach, John Wiley & Sons, Ltd.
80. Mariani, M. M. and Deckert, V. (2012) 'Raman spectroscopy: principles, benefits, and applications', Methods in Physical Chemistry, Wiley Online Library.
81. Skoog, D.A. Holler, F.J. and Crouch, S.R. (2006) 'Principles of instrumental analysis', 6th ed. Cengage Learning.
82. Willard, H.H. Meritt Jr, L.L. Dean, J.J. and Settle Jr, F.A. (1988) 'Instrumental methods of analysis', 7th ed. New Delhi: CBS Publisher & Distributors.
83. Smith, E. and Dent, G. (2005) 'Modern Raman spectroscopy: a practical approach', England, Chichester: John Wiley & Sons.
84. Settle, F.A. (1997) 'Handbook of instrumental techniques for analytical chemistry', New Jersey: Prentice, Inc.
85. Aarnoutse, P.J. and Westerhuis, J.A. (2005) 'Quantitative Raman reaction monitoring using the solvent as internal standard', *Anal. Chem.*, 77(5), p.p. 1228–1236.
86. Strachan, C.J. Rades, T. Gordon, K.C. and Rantanen, J. (2007) 'Raman spectroscopy for quantitative analysis of pharmaceutical solids', *Journal of Pharmacy and Pharmacology*, 59 (2), p.p. 179–192.
87. Hédoux, A. Guinet, Y. and Descamps, M. (2011) 'The contribution of Raman spectroscopy to the analysis of phase transformations in pharmaceutical compounds', *International Journal of Pharmaceutics*, 417 (1/2), p.p. 17–31.
88. De Beer, T. Burggraeve, A. Fonteyne, M. Saerens, L. Remon, J.P. and Vervaet, C. (2011) 'Near-infrared and Raman spectroscopy for the in-process monitoring of pharmaceutical production processes', *International Journal of Pharmaceutics*, 417 (1/2), p.p. 32–47.

89. Müller, J. Knop, K. Wirges, M. and Kleinebudde, P. (2010) 'Validation of Raman spectroscopic procedures in agreement with ICH guideline Q2 with considering the transfer to real-time monitoring of an active coating process', *Journal of Pharmaceutical and Biomedical Analysis*, 53 (4), p.p. 884–894.
90. Wikström H, Marsac PJ, Taylor LS. (2005) 'In-line monitoring of hydrate formation during wet granulation using Raman spectroscopy', *J Pharm Sci.*, 94 (1), p.p. 209–219.
91. Rantanen, J. (2007) 'Process analytical applications of Raman spectroscopy', *Journal of Pharmacy and Pharmacology*, 59, p.p. 171–177.
92. Shackman, J. G. Giles, J. H. and Denton, M. D. (2000) 'Pharmaceutical reaction monitoring by Raman spectroscopy', In further developments in scientific optical imaging; special publication 254; Denton, M. B., Ed.; Royal Society of Chemistry: London, p.p. 186–201.
93. Hu, Y. Liang, J. K. Myerson, A. S. and Taylor, L. S. (2005) 'Crystallization monitoring by Raman spectroscopy: simultaneous measurement of desupersaturation profile and polymorphic form in flufenamic acid systems', *Industrial & Engineering Chemistry Research*, 44 (5), p.p. 1233-1240.
94. Marlon M. Reis, M. M. Araújo, P. H.H. Sayer, C. and Giudici, R. (2004) 'Comparing near-infrared and Raman spectroscopy for on-line monitoring of emulsion copolymerization reactions', *Macromolecular Symposia*, 206, p.p. 165–178.
95. Jeon, S. Woo, J. Kyong, J-B. and Choo, J. (2001) 'Kinetic study of α -Bromo-o-toluic acid using Raman spectroscopy', *Bull. Korean Chem. Soc.*, 22 (11), p.p. 1264–1266.
96. Meher, A. K. and Chen, Y-C. (2016) 'Combination of Raman spectroscopy and mass spectrometry for online chemical analysis', *Analytical Chemistry*.
97. Förster, H. (2004) 'UV/VIS Spectroscopy', *Mol. Sieves*, 4, p.p. 337–426.

98. Zagonel, G. F. Peralta-Zamora, P. and Ramos, L. P. (2004) 'Multivariate monitoring of soybean oil ethanolysis by FTIR', *Talanta*, 63, p.p. 1021–1025.
99. Aarnoutse, P.J. and Westerhuis, J.A. (2005) 'Quantitative Raman reaction monitoring using the solvent as internal standard', *Analytical Chemistry*, 77 (5), p.p. 1228–1236.
100. Sparkman, O. D. (2000) 'Mass spectrometry desk reference', Pittsburgh: Global View Pub.
101. El-Aneed, A. Cohen, A. and Banoub, J. (2009) 'Mass spectrometry, review of the Basics: electrospray, MALDI, and commonly used mass analysers', *Applied Spectroscopy Reviews*, 44, p.p. 210–230.
102. Rouessac, F. and Rouessac, A. (2007) 'Chemical analysis: modern instrumentation methods and techniques', France: John Wiley and Sons.
103. Ma, X. Zhang, S. Lin, Z. Liu, Y. Xing, Z. Yang, C. and Zhang, X. (2009) 'Real-time monitoring of chemical reactions by mass spectrometry utilizing a low-temperature plasma probe', *Analyst*, 134, p.p. 1863–1867.
104. Ma, X. Zhang, S. and Zhang, X. (2012) 'An instrumentation perspective on reaction monitoring by ambient mass spectrometry', *Trends in Analytical Chemistry*, 35, p.p. 50–66.
105. Cheng, S. Wu, Q. Dewald, H. D. and Chen, H. (2016) 'Online monitoring of methanol electro-oxidation reactions by ambient mass spectrometry', *J. Am. Soc. Mass Spectrum*.
106. Liu, P. Lanekoff, I.T. Laskin, J. Dewald, H.D. and Chen, H. (2012) 'Study of electrochemical reactions using nanospray desorption electrospray ionization mass spectrometry', *Analytical Chemistry*, 84, p.p. 5737–5743.
107. Diehl, G. Liesener, A. and Karst, U. (2001) 'Liquid chromatography with postcolumn electrochemical treatment and mass spectrometric detection of non-polar compounds', *Analyst*. 126, p.p. 288–290.

108. Kertesz, V. and Van Berkel, G.J. (2002) 'Surface-assisted reduction of aniline oligomers, N-phenyl-1,4-phenylenediamine and thionin in atmospheric pressure chemical ionization and atmospheric pressure photoionization', *Journal of the American Society for Mass Spectrometry*, 13, p.p. 109–117.
109. Brown, T.A. Chen, H. and Zare, R.N. (2015) 'Identification of fleeting electrochemical reaction intermediates using desorption electrospray ionization mass spectrometry', *Journal of the American Society*, 137, p.p. 7274–7277.
110. Lindinger, W. Hansel, A. and Jordan, A. (1998) 'Proton-transfer-reaction mass spectrometry (PTR-MS): on-line monitoring of volatile organic compounds at pptv levels', *Chemical Society Reviews*, 27, p.p. 347–354.
111. Pollien, P. Lindinger, C. Yeretjian, C. and Blank, I. (2003) 'Proton transfer reaction mass spectrometry, a tool for on-line monitoring of acrylamide formation in the headspace of maillard reaction systems and processed food', *Analytical Chemistry*, 75, p.p. 5488–5494.
112. Hofstadler, S.A. Bakhtiar, R. and Smith, R.D. (1996) 'Electrospray ionization mass spectrometry', *Journal of Chemical Education*, 73 (4), p.p. 1–7.
113. Banerjee, S. and Mazumdar, Sh. (2012) 'Electrospray ionization mass spectrometry: A technique to access the information beyond the molecular weight of the analyte', *International Journal of Analytical Chemistry*, p.p. 1–40.
114. Fligge, T. A. Kast, J. Bruns, K. and Przybylski, M. (1999) 'Direct monitoring of protein–chemical reactions utilising nanoelectrospray mass spectrometry', *Journal of the American Society for Mass Spectrometry*, 10, p.p. 112–118.
115. Patel, K. N. Patel, J. K. Patel, M. P. Rajput, G. C. and Patel, H. A. (2010) 'Introduction to hyphenated techniques and their applications in pharmacy', *Pharmaceutical Methods.*, 1(1), p.p. 2–13.

116. Lim, C.K. and Lord, G. (2002) 'Current developments in LC-MS for pharmaceutical analysis', *Biological and Pharmaceutical Bulletin*, 25(5), pp. 547–557.
117. De Lima Gomes, P.C. Barletta, J.Y. Nazario, C.E. Santos-Neto, A.J. Von Wolff, M.A. Coneglian, C.M. Umbuzeiro, G.A. and Lancas, F.M. (2011) 'Optimisation of in situ derivatization SPME by experimental design for GC-MS multi-residue analysis of pharmaceutical drugs in wastewater', *J. Sep. Sci.*, 34(4), p.p. 436–445.
118. Rajmund, M. Sebastian, S. Magdalena J. and Aleksandra L. (2012) 'Application of hyphenated techniques in speciation analysis of arsenic, antimony, and thallium', *The Scientific World Journal*, p.p. 1–17.
119. Wang, X.M. Zhang, Q.Z. Yang, J. Zhu, R.H. Zhang, J. Cai, L.J. and Peng, W.X. (2012) 'Validated HPLC-MS/MS method for simultaneous determination of curcumin and piperine in human plasma', *Tropical Journal of Pharmaceutical Research* ., 11(4), p.p.621–629.
120. Nandakumar, S. Menon, S. and Shailajan, S. (2012) 'A rapid HPLC-ESI-MS/MS method for determination of β -asarone, a potential anti-epileptic agent, in plasma after oral administration of *Acorus calamus* extract to rats', *Biomedical Chromatography*., 27(3), p.p. 318–326.
121. Wollein, U. and Schramek, N. (2012) 'Simultaneous determination of alkyl mesilates and alkyl besilates in finished drug products by direct injection GC/MS', *European Journal of Pharmaceutical Sciences*, 45(1-2), p.p. 201–204.
122. Patel, K. N. Patel, J. K. Patel, M. P. Rajput, G. C. and Patel, H. A. (2010) 'Introduction to hyphenated techniques and their applications in pharmacy', *Pharmaceutical Methods*, 1 (1), p.p. 2–13.

123. Lindon, J.C. Nicholson, J.K. and Wilson, I.D. (2000) 'Directly coupled HPLC-NMR and HPLC-NMR-MS in pharmaceutical research and development', *Journal of Chromatography B: Biomedical Sciences and Applications*, 748(1), p.p. 233–258.
124. Rajmund, M. Sebastian, S. Magdalena J. and Aleksandra L. (2012) 'Application of hyphenated techniques in speciation analysis of arsenic, antimony, and thallium', *The Scientific World Journal*, p.p. 1–17.
125. Wang, X.M. Zhang, Q.Z. Yang, J. Zhu, R.H. Zhang, J. Cai, L.J. and Peng, W.X. (2012) 'Validated HPLC-MS/MS method for simultaneous determination of curcumin and piperine in human plasma', *Tropical Journal of Pharmaceutical Research*, 11(4), p.p.621–629.
126. Nandakumar, S. Menon, S. and Shailajan, S. (2012) 'A rapid HPLC-ESI-MS/MS method for determination of β -asarone, a potential anti-epileptic agent, in plasma after oral administration of *Acorus calamus* extract to rats', *Biomedical Chromatograph*, 27(3), p.p.318–326.
127. De Lima Gomes, P.C. Barletta, J.Y. Nazario, C.E. Santos-Neto, A.J. Von Wolff, M.A. Coneglian, C.M. Umbuzeiro, G.A. and Lancas, F.M. (2011) 'Optimization of in situ derivatization SPME by experimental design for GC-MS multi-residue analysis of pharmaceutical drugs in wastewater', *Journal of Separation Science*, 34(4), p.p. 436–445.
128. Wollein, U. and Schramek, N. (2012) 'Simultaneous determination of alkyl mesitates and alkyl besitates in finished drug products by direct injection GC/MS', *European Journal of Pharmaceutical Sciences*, 45(1-2), p.p. 201–204.
129. Wu, J. Jia, L.-T. Shao, L.-M.Chen, J.-M.Zhong, D.-D.Xu, S. and Cai, J.-T. (2013) 'Drug-drug interaction of rabeprazole and clopidogrel in healthy Chinese volunteers', *European Journal of Clinical Pharmacology*, 69 (2), p.p.179–187.

130. Zhang, W. and Huang, G. (2015) 'Fast screening of analytes for chemical reactions by reactive low-temperature plasma ionization mass spectrometry', *Rapid Communications in Mass Spectrometry*, 29, p.p.1947–1953.
131. Baumann, S. Moder, M. Herzsuh, R. and Schulze, B. (2003) 'Reaction kinetic monitoring by high-performance liquid chromatography coupled to mass spectrometry: Oxidation processes of selected isothiazoles', *Chromatographia*, 57(1), p.p. 147–152.
132. Guetens, G. De Boeck, G. Highley, M.S. Wood, M. Maes, R.A.A. Eggermont, A.A.M. Hanauske, A. de Bruijn, E.A. and Tjaden, U.R. (2002) 'Hyphenated techniques in anticancer drug monitoring II. Liquid chromatography-mass spectrometry and capillary electrophoresis-mass spectrometry', *Journal of Chromatography A*, 976, p.p. 239–247.
133. Sauvage, F. L. Gaulier, J. M. Lachâtre, G. and Marquet, P. (2006) 'A fully automated turbulent-flow liquid chromatography-tandem mass spectrometry technique for monitoring antidepressants in human serum', *Therapeutic Drug Monitoring*, 28, p.p. 123–130.
134. Yan, C. Schmidberger, J. W. Parmeggiani, F. Hussain, S. A. Turner, N. J. Flitsch, S. L. and Barran, P. (2016) 'Rapid and sensitive monitoring of biocatalytic reactions using ion mobility mass spectrometry', *Analyst*, 141, p.p. 2351–2355.
135. Huang, M.Z. Yuan, C.H. Cheng, S.C. Cho, Y.T. and Shiea, J. (2010) 'Ambient ionisation mass spectrometry', *Annual Review of Analytical Chemistry*, 3, p.p. 43–65.
136. Huan-Wen, C. Bin, H. U. and Xie, Z. (2010) 'Principle and application of ambient mass spectrometry for direct analysis of complex samples', *Chinese Journal of Analytical Chemistry*, 38(8), p.p. 1069–1088.
137. Cooks, R.G. Ouyang, Z. Takats, Z. and Wiseman, J. (2006) 'Ambient mass spectrometry', *Science*, 311(5767), p.p.1566–1570.

138. Venter, A. Nefliu, M. and Cooks, R. G. (2008) 'Ambient desorption ionization mass spectrometry', *Trends in Analytical Chemistry*, 27, (4), p.p. 284–290.
139. Takats, Z. Wiseman, J.M. Gologan, B. and Cooks, R.G. (2004) 'Mass spectrometry sampling under ambient conditions with desorption electrospray ionization', *Science*, 306, p.p. 471–473.
140. Cody, R.B. Laramee, J.A. and Durst, H.D. (2005) 'Versatile new ion source for the analysis of materials in open air under ambient conditions', *Analytical Chemistry*, 77(8), p.p. 2297–2302.
141. Haertel, B. von Woedtke, T. Weltmann, K-D. and Lindequist, U. (2014) 'Non-thermal atmospheric-pressure plasma possible application in wound healing', *Search Results Biomolecules & Therapeutics.*, 22(6), p.p. 477-490.
142. Stoffels, E. Kieft, I. E. and Sladek, R. E. J. (2003) 'Superficial treatment of mammalian cells using plasma needle', *Journal of Physics D: Applied Physics*, 36, p.p. 2908–2913.
143. Yonson, S. Coulombe, S. L'éveillé, V. and Leask, R. L. (2006) 'Cell treatment and surface functionalization using a miniature atmospheric pressure glow discharge plasma torch', *Journal of Physics D: Applied Physics*, 39, p.p. 3508–3513.
144. Tendero, C. Tixier, C. Tristant, P. Desmaison, J. Leprince, P. (2006) 'Atmospheric pressure plasmas: A review', *Spectrochimica Acta Part B* 61, p.p. 2–30.
145. Conrads, H. and Schmidt, M. (2000) 'Plasma generation and plasma sources', *Plasma Sources Science Technology*, 9 p.p. 441–454.
146. Nehra, V. Kumar, A. and Dwivedi, H. K. (2008) 'Atmospheric Non-Thermal Plasma Sources', *International Journal of Engineering*, 2, p.p. 53– 68.

147. Kong, M. G. Kroesen, G. Morfill, G. Nosenko, T. Shimizu, T. van Dijk, J. and Zimmermann J. L. (2009) 'Plasma medicine: an introductory review', *New Journal of Physics*, 11, p.p. 1–35.
148. Hubert, J. Bordeleau, S. Tran, K. C. Michaud, S. Millette, B. Sing, R. Jalbert, J. Boudreau, D. Moisan, M. and Margot, J (1996) 'Atomic spectroscopy with surface wave plasmas', *Fresenius' Journal of Analytical Chemistry*, 355, p.p. 494– 500.
149. Korolov, I. Fazekas, B. Széll, M. Kemény, L. and Kutasi, K. (2016) 'The effect of the plasma needle on the human keratinocytes related to the wound healing process', *Journal of Physics D: Applied Physics.*, 49, p.p. 1–12.
150. Reuter, S. Winter, J. Schmidt-Bleker, A. Schroeder, D. Lange, H. Knake, N. Schulz-von der Gathen, V. and K-D Weltmann, K. D. (2012) 'Atomic oxygen in a cold argon plasma jet: TALIF spectroscopy in ambient air with modelling and measurements of ambient species diffusion', *Plasma Sources Science and Technology*, 21, p.p. 1–7.
151. Fridman, G. Friedman, G. Gutsol, A. Shekhter, A. B. Vasilets, V. N. and Fridman, A. (2008) 'Applied plasma medicine', *Plasma Process. Polym.*, 5, p.p. 503–533.
152. Klämpfl, T. G. Isbary, G. Shimizu, T. Li, Y-F Zimmermann, J. L. Stolz, W. Schlegel, J. Morfill, G. E. and Schmidt, H-U. (2012) 'Cold atmospheric air plasma sterilization against spores and other microorganisms of clinical interest', *Applied and Environmental Microbiology*, 78 (15), p.p. 5077–5082.
153. Matthews, I.P. Gibson, C. and Samuel, A.H. (1994) 'Sterilisation of implantable devices', *Clin. Mater.* 15 (3), p.p. 191–215.
154. Xiong, Z. and Graves, D. B. (2017) 'A novel cupping-assisted plasma treatment for skin disinfection', *Journal of Physics D: Applied Physics*, 50, p.p. 1–6.
155. Nobrega, P. A. Rohani, V. Cauneau, F. and Fulcheri, L. (2017) 'Chemical engineering approach applied to non-thermal plasma reactors', France.

156. Vandenbroucke, A. M. Morent, R. De Geyter N. and Leys. C. (2011) 'Non-thermal plasmas for non-catalytic and catalytic VOC abatement', *Journal of Hazardous Materials*, 195, p.p. 30–54.
157. Talebizadeh, P. Babaie, M. Brown, R. Rahimzadeh, H. Ristovski, Z. and Arai, M. (2014) 'The role of non-thermal plasma technique in NO_x treatment: A review', *Renewable and Sustainable Energy Reviews*, 40, p.p. 886–901.
158. Kvam, E. Davis, B. Mondello, F. and Garner, AL. (2012) 'Nonthermal atmospheric plasma rapidly disinfects multidrug-resistant microbes by inducing cell surface damage', *Antimicrob Agents Chemother.*, 56, p.p. 2028–2036.
159. Arjunan, K.P. and Clyne, A.M. (2011) 'A nitric oxide producing pin-to-hole spark discharge plasma enhances endothelial cell proliferation and migration', *Plasma Med.*, 1, p.p. 279–293.
160. Schlegel, J. Körtzer, J. and Boxhammer, V. (2013) 'Plasma in cancer treatment', *Clinical Plasma Medicine*, 1 (2), p.p. 2–7.
161. Takats, Z. Wiseman, J. M. Gologan, B. and Cooks, R.G. (2004) 'Mass spectrometry sampling under ambient conditions with desorption electrospray ionization', *science*, 306, p.p. 471–473.
162. Chen, H. Talaty, N. N. Takats, Z. and Cooks, R. G. (2005) 'Desorption electrospray ionization mass spectrometry for high-throughput analysis of pharmaceutical samples in the ambient environment', *Analytical Chemistry*, 77, p.p. 6915–6927.
163. Petucci, C. Diffendal, J. Kaufman, D. Mekonnen, B. Terefenko, G. and Musselman, B. (2007) 'Direct analysis in real time for reaction monitoring in drug discovery', *Analytical Chemistry*, 79(13), p.p. 5064–5070.
164. Salter, T. L. Gilmore, I. S. Bowfield, A. Olabanji, O. T. and Bradley, J. W. (2013) 'Ambient surface mass spectrometry using plasma-assisted desorption ionization:

- effects and optimization of analytical parameters for signal intensities of molecules and polymers', *Analytical Chemistry*, 85, p.p. 1675–1682.
165. Edison, S.E. Lin, L.A. and Parrales, L. (2011) 'Practical considerations for the rapid screening for pesticides using ambient pressure desorption ionisation with high-resolution mass spectrometry', *Food Additives and Contaminants*, 28 (10), p.p. 1393–1404.
166. Vaclavik, L. Cajka, T. Hrbek, V. and Hajslova, J. (2009) 'Ambient mass spectrometry employing direct analysis in real time (DART) ion source for olive oil quality and authenticity assessment', *Analytica Chimica Acta*, 645, p.p. 56–63.
167. Aboul-Fadl, T. Abdel-Aziz, H. A. Kadi, A. Ahmad, P. Elsaman, T. Attwa, M. W. and Darwish, I. A. (2011) 'Microwave-assisted solution-phase synthesis and DART-mass spectrometric monitoring of a combinatorial library of indolin-2,3-dione Schiff bases with potential antimycobacterial activity', 16, p.p. 5194–5206.
168. Cody, R. B. (2009) 'Observation of molecular ions and analysis of nonpolar compounds with the direct analysis in real time ion source', *Analytical Chemistry*, 81(3), p.p.1101–1107.
169. Harper, J.D. Charipar, N.A. Mulligan, C.C. Zhang, X. Cooks, R.G. and Ouyang, Z. (2008) 'Low-temperature plasma probe for ambient desorption ionization', *Analytical Chemistry*, 80(23), pp. 9097-9104.
170. Ratcliffe, L.V. Rutten, F.J.M. Barrett, D.A. Terry Whitmore, T. Seymour, D. Greenwood, C. Gonzalvo, Y. A. Robinson, S. and McCoustra, M. (2007) 'Surface analysis under ambient conditions using plasma-assisted desorption/ ionisation mass spectrometry', *Analytical Chemistry*, 79 (16), p.p. 6094–6101.

171. Ding, X. and Duan, Y. (2015) 'Plasma-based ambient mass spectrometry techniques: the current status and future prospective', *Mass Spectrometry Reviews*, 34, p.p. 449–473.
172. Huang, M-Z. Cheng, S-C. Cho, Y-T. and Shiea, J. (2011) 'Ambient ionisation mass spectrometry: A tutorial', *Analytica Chimica Acta.*, 702, p.p. 1–15.
173. Bowfield, Barrett, D.A. Alexander, M.R. Ortori, C.A. Rutten, F.M. Salter, T.L. Gilmore, I.S. and Bradley, J.W. (2012) 'Surface analysis using a new plasma assisted desorption/ionisation source for mass spectrometry in ambient air', *Review of Scientific Instruments*, 83, p.p. 1–7.

CHAPTER 2: Experimental details

2.1. Chemicals

All chemicals were used without any further purification.

2.2. Standard and Sample Preparation

Fresh samples of paracetamol, caffeine and Panadol were used for most analysis using PADI-MS without the need for preparation and that only for Raman sample preparation was required (for more information see Chapter 3 and Chapter 5). Pure compounds and sample solutions which are described and used in this thesis including individual and mixtures of paracetamol, caffeine and Panadol were prepared in high purity deionised water (details can be found in Chapter 4 and Chapter 5). In addition, solutions of para-anisidine and 4-nitrobenzaldehyde were prepared in dichloromethane for imine formation purpose (for more details see Chapter 6).

2.3. Experimental techniques

2.3.1. Chromatographic techniques

2.3.1.1. Thin layer chromatography (TLC)

TLC plates consisting of silica gel 60 F254, 25 on aluminium sheets of size 20 × 20 cm were supplied by Merck KGaA, Darmstadt, Germany. TLC spots were visualised by means of a handheld UV lamp (Upland CA, City, U.S.A).

2.3.1.2. High-performance liquid chromatography (HPLC)

HPLC was carried out using a Perkin Elmer system consisting of a Flexar LC Autosampler, a Flexar LC Detector, Flexar Quaternary LC pump and ODS-C₁₈ column 150 mm × 4.6 mm (Matlab, UK). HPLC experiments were performed in the isocratic mode.

2.3.2. Spectroscopic techniques

2.3.2.1. Ultraviolet-visible (UV/Vis) spectrophotometer

A UV-Vis spectrophotometer, model Cary 50 Bio, Varian, UK was used in this work. Absorbance spectra of blank (solvent) and samples were recorded using quartz cells. To ensure a linear response, a maximum absorbance of 3 was used, using dilutions as required.

2.3.3. Vibrations spectroscopy techniques

2.3.3.1. Fourier transform infrared spectroscopy (FTIR)

FTIR spectrometry was carried out using a Thermo Fisher Scientific iS10 instrument (Hemel Hempstead, UK) fitted with a DTGS detector and a single bounce germanium ATR smart accessory.

2.3.3.2. Raman spectroscopy

A Thermo FT DXR Raman microscope (Thermo Fisher, Hemel Hempstead, UK) with spectral range $3500\text{-}50\text{ cm}^{-1}$ was used in this study.

2.3.4. Plasma-assisted desorption ionisation-Mass spectrometry (PADI-MS)

The PADI-MS instrumentation used here was built in-house following a previous design by Ratcliffe et al. (1). A single quadrupole (Waters Micromass ZQ, Manchester, UK) was used with the ESI front-end removed to accept a modified Stoffels-design plasma pencil ionisation source (2). The plasma pencil was fabricated to provide coaxial dual gas flow; an inner ceramic tube (outer diameter $\sim 2\text{ mm}$) was encompassed within a quartz glass tube (outer diameter $\sim 5\text{ mm}$). Helium gas was flowed through both tubes controlled using separate flow meters, the flow inside the ceramic tube will in this work be referred to as

inner flow, the flow between the ceramic and quartz tubes as outer flow. A thickness tungsten filament provided the connection of the RF. 5-15 W was used for all experiments as reported. A non-thermal plasma was generated using a 13.56 MHz RF power source (Kurt J. Lesker, USA) and a matching network (1).

The PADI-MS technique has been divided into two main parts: PADI source and MS instrument. The PADI source consists of non-thermal (cold) plasma, radio frequency (RF), inflow gas such as helium, argon or nitrogen. The main advantage of non-thermal plasma in the field of applications such as organic compounds and the aqueous environment is that it does not cause any thermal or electric damage to the sample surface. Outer flow is possible to obtain high intensity and stable signals of molecules and extra peaks can be detected. Compared to the traditional mass spectrometers, the sample in the PADI-MS system is ionised outside the vacuum chamber. The basic principles of PADI-MS work are: a non-thermal plasma “needle” operates by RF using specific plasma power inflow gas under atmospheric pressure conditions at low voltages. The plasma visible flame interacts with the sample surface and then the volatile ions are produced from the surface.

The schematic of the PADI source including a pencil without the outer quartz tube is shown in Figure 2.1, while the end of the plasma pencil, sample and mass spectrometer inlet geometry is shown in Figure 2.3. The visible non-thermal plasma plume emerging from a coaxial helium gas flow 13.65 MHz RF plasma pen was near-contact (5 mm separation) with the sample under investigation, using optimised PADI-MS acquisition settings of 8 W and a carrier gas flow of 224 mL/min (inner flow) and (224 mL/min outer flow). Sample ions were directed into a single quadrupole MS by use of a sniffer tube, each acquisition being 1 minute.

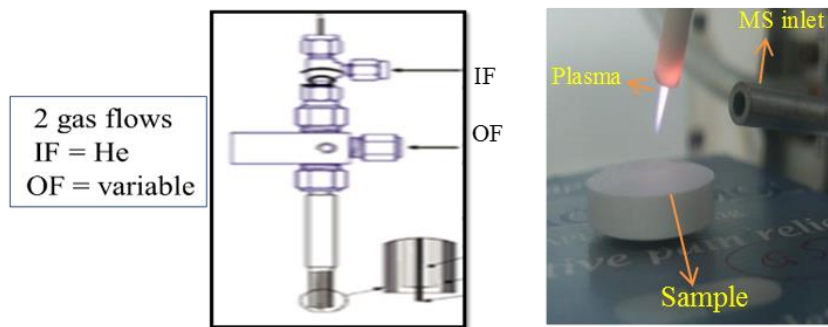


Figure 2. 1. Schematic of the PADI probe and source in operation.

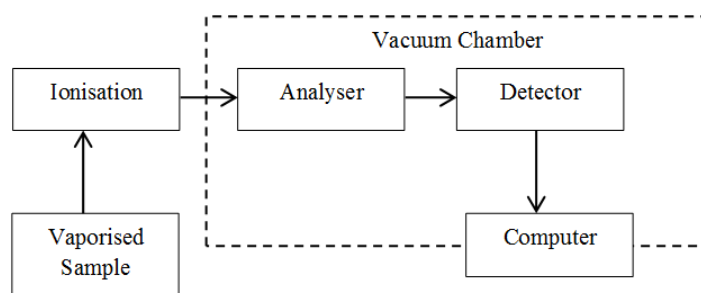


Figure 2. 2. Schematic diagram of PADI-MS instrument.

References

1. Ratcliffe, L.V. Rutten, F.J.M. Barrett, D.A. Terry Whitmore, T. Seymour, D. Greenwood, C. Gonzalvo, Y.A. Robinson, S. and McCoustra, M. (2007) 'Surface analysis under ambient conditions using plasma-assisted desorption/ ionisation mass spectrometry', *Analytical Chemistry*, 79 (16), p.p. 6094–6101.
2. Stoffels, E. Flikweert, A. J. Stoffels, W. W. and Kroesen, G. M. W. (2002) 'Plasma needle: a nondestructive atmospheric plasma source for fine surface treatment of (bio) materials', *Plasma Sources Science and Technology.*, 11, p.p. 383-388

**CHAPTER 3: PADI Plasma-substrate interaction
studied by PADI-MS and Raman spectroscopy using
paracetamol tablets as a model system**

Abstract

PADI-MS and Raman spectroscopy were used in this chapter as different analytical techniques to yield complementary information. Raman microscopy is a scattering vibrational spectroscopic method that can yield spectra without the need for sample preparation. Raman samples the chemical composition of the top layer of the tablet through the laser approximately 1 μm into a sample. Complementary to these features, PADI-MS is able to produce positive and negative ions from a substantially thinner layer and it can detect molecules in seconds. Raman microscopy has been used to examine the chemical changes in the surface layer of paracetamol tablets due to interaction with a low temperature helium to plasma flame. Raman microscopy conditions were optimised of 532 nm laser wavelength, 5.0 mW laser power and a 10x objective with a 2.0 seconds collection time. PADI-MS used helium with flow rate of 224 mL/min, and the distance between the plasma flame and sample was 5 mm. Sample ions were directed into a single quadrupole MS through a sniffer tube, each acquisition being 1 minute. Pure and paracetamol tablets were analysed directly after exposure to the room temperature non-thermal plasma flame up to a specific time. The results showed that the chemistry of paracetamol was affected after exposure to non-thermal plasma due to the changes in intensities of the diagnostic, adduct and fragment peaks. PADI-MS can be applied for direct analysis of pure and pharmaceutical tablets with little or no sample preparation required, and it also provides information about chemical speciation in seconds. The results of this study indicate that the PADI-MS technique is suitable for analysis of pharmaceutical tablets directly. However, the measurement time until the onset of damage to a sample is 50 seconds.

3.1. Introduction

Plasma is the fourth state of matter in addition to solid, liquid and gas. Plasmas are important for a wide range of scientific and industrial processes. The plasma used in this work, upon interaction with the ambient atmosphere, contains a range of reactive species, including $(\text{H}_2\text{O})_n$, H^+ , He^* , e^- , UV, N_2^+ . These species react with atoms from the sample surface (1). It would be interesting to study the effect of plasma on the chemical composition of compounds using one of the ambient mass spectrometry (AMS) techniques because no previous study has investigated this effect. Plasma technologies can be divided into two parts: thermal and non-thermal plasma (NTP). In thermal plasma, molecules are fully ionised, while in NTP, they are partly ionised (2). In recent years, researchers have shown an increased interest in using NTP at atmospheric conditions in medical applications (3-7).

One of the main advantages of the NTP under atmospheric pressure is the ability for desorption of molecules from a surface without the need for elevated temperatures (8). This has led to the wide use of NTP in applications which need low temperature such as biomedical and materials processing applications (9-12). Non-thermal atmospheric plasma plays a critical role in the maintenance of the substances characteristics such as molecular weight and volume, and this can impact on the substance composition of devices (13, 14). It can also play an important role by addressing the heat issue because some of the sterilization technologies need 120°C that causes degradation of medical devices and need vacuum chambers, while non-thermal atmospheric plasma needs below 40°C without using vacuum chambers (13). Recent trends in the treatment of environmental pollution have led to a proliferation of studies that use plasma technologies to remove pharmaceutical compounds from surface and ground water. Degradation and removal of pharmaceutical pollutants such as ibuprofen and diclofenac from aqueous solutions have been studied by

several research groups using nonthermal plasmas (13, 14). Recently, NTP has been also developed and used as cleaning technologies to remove multi-pollutants such as SO₂, NO_x and Hg from coal (15). Because NTP is increasingly important in the industrial applications especially in medicine and biology, generation of NTP at atmospheric pressure has been studied using innovative technologies covering a wide range of areas (12). In addition, NTP is important for a wide range of scientific and industrial processes such as antiseptic of cell surfaces damage (16), accelerate wound healing (17) and for cancer treatment due to its ability to stop tumour cells growing (18, 19).

Several analytical methods including spectroscopic techniques such as nuclear magnetic resonance (NMR), near infrared (NIR), Fourier transformed infrared (FTIR) and Raman spectroscopy, and chromatographic techniques such as HPLC have been used in the analysis of pharmaceutical solids (20). Limitations of FTIR are: it has a single beam in comparison with MS and cannot provide details about the structure of compounds; not a suitable method for all types of compounds; not playing a major role in the quantification analysis of vibration groups of the surfaces (21). HPLC is expensive, chemicals, time and solvent consuming and sample preparation is required. Compared to spectroscopic and chromatographic techniques, mass spectrometry is more sensitive, faster, small sample amounts are required, and ability to directly measure molecular weight. Hyphenated mass techniques such as liquid chromatography-mass spectrometry (LC-MS) (22) and gas chromatography-mass spectrometry (GC-MS) (23, 24) were developed to support and ensure the quality and safety of pharmaceuticals. However, workup procedures such as extraction, filtration, and separation are required when using these techniques (25).

Ambient mass spectrometry (AMS) has some advantages over spectroscopic, chromatographic and hyphenated mass techniques which are that samples are desorbed and ionised directly from surfaces at atmosphere pressure with little or no sample preparation.

Desorption electrospray ionisation (DESI) and direct analysis in real time (DART) are the most common techniques of AMS. The detection of produced ions is the same for both methods, but DESI uses a solvent as a source to ionise the molecule, while DART uses a stream of gas (helium or nitrogen) (for more details see Chapter 2). However, the spray solvents in DESI make this method a bit messy (26), and the spectra need more investigation. DART is an expensive technique and has lower detection selectivity and this due to the lack of a separation, and is not suitable method for all kinds of compounds such as the analysis of polymers (27).

The work presented here investigates the use of direct PADI-MS and Raman analysis for paracetamol tablets as a model for pharmaceutically relevant solids. PADI-MS and Raman microscopy methods can give good signals without the need for sample preparation. In addition, they are able to show the chemical composition of the top layer of a tablet. Paracetamol tablet was selected in this study as model drug due to its being small molecule and most drugs are still in this category. The specific objective of this study was in three stages: 1) many samples of the paracetamol tablets were exposed to visible plasma from 0 seconds to 5 minutes; 2) Raman microscopy was used to know the chemical composition of the top layer of the exposed tablets; 3) changes and behaviours of intensity for the adduct and fragment peaks of these exposed tablets were seen using PADI-MS. In this study, these methods were successfully used to analyse the paracetamol tablets using the optimal conditions. Raman microscopy showed that the differences between the peak area of vibrations and exposure times to plasma flame were significant and changed after 20 seconds. However, no significant changes were found between the shape and position of vibration peaks. Further analysis using PADI-MS showed that the changes in intensity of the signals were observed during the exposure time to plasma flame. These changes may be due to damage to the sample after exposure to the plasma flame. The analysis of these

methods provided an important opportunity to advance the understanding of the behaviour of molecules with time after exposure to the NTP. The main aim of this study was to develop a novel simple, fast, sensitive and cost-effective method, that can be used to show the chemical composition of the top layer of the paracetamol tablets after exposure to the plasma flame. This study also aims to compare PADI-MS (ambient mass spectrometry) with Raman microscopy (vibrational technique) for this type of analysis. In this Chapter, the objectives used to reach some conclusions about this sampling method were:

- 1- Sample paracetamol (tablet) as model for pharmaceutically relevant solids.
- 2- Investigation of the chemical composition of the top layers for tablets by Raman microscopy after exposure to non-thermal plasma flame.
- 3- Use direct non-thermal plasma interaction to analyse the tablet without any preparation by PADI-MS.

3.2. Materials and methods

3.2.1. Apparatus:

In the PADI-MS instrumentation, a single quadrupole (Waters Micromass ZQ, Manchester, UK) was used with a Stoffels-design source (28). The flow helium measurement was calibrated and found to be 224 mL/min through flow tube, and a distance between the visible plasma flame and sample of 5 mm. The effect of water vapour on ionisation efficiency was investigated by flowing the He through a water vapour added environment before the plasma pencil being directed to the plasma pen outflow (for more information see Chapter 2). A Thermo DXR Raman microscope with spectral range 3500-50 cm⁻¹ was used in this study. The conditions for Raman spectroscopy were optimised for all samples in this study and found to be: laser wavelength 532 nm, laser power 5.0 mW,

10x objective, collect exposure time 2.0 sec, sample exposure 2 and aperture 25 μm pinhole.

3.2.2. Chemicals:

Pure paracetamol was manufactured by Alfa Aesar, UK (purity 98%). Paracetamol tablets containing 500 mg paracetamol per tablet were supplied by Galpharm International Ltd, UK. Helium gas was supplied by British Oxygen Company (BOC) gases, UK (purity 99%). Deionised water was provided through a Pure Lab Option ELGA, with the resistivity 18 M Ω , Model Ultra Clear TWF UV.

3.2.3. Preparation of samples:

The samples of paracetamol tablets were analysed directly by PADI-MS without any preparation and the spectra were recorded as a function of time, while they were prepared by exposing to the PADI plasma for set times before using Raman microscopy.

3.2.4. Procedure:

Method development for plasma effect on paracetamol tablets over time by Raman microscopy and PADI-MS:

- 1- Pure paracetamol and several samples of paracetamol tablets were exposed to PADI plasma under atmospheric pressure during different times: 10 secs, 20 secs, 30 secs, 50 secs, 1 min, 2 min, 3 min and 5 min. Plasma spot size which focused into the sample was approximately 1020 μm , 1080 μm , 1200 μm , 1500 μm , 1800 μm , 2100 μm , 2400 μm and 3000 μm respectively. Nine sample of paracetamol tablets was analysed directly by Raman microscopy using the optimal conditions. Laser spot size which focused into the sample was approximately 2 μm .

- 2- A sample of paracetamol tablet was analysed directly by PADI-MS using the optimal conditions with a total acquisition time of 5 minutes.

Although the type of plasma used is often termed as a 'cold plasma', there is some degree of localised heating near the plasma plume. To investigate the potential effects that such heating causes on the sample during the analysis, and indeed the quality of mass spectral data obtained, thermal imaging was conducted, Figure 3.1. This allowed observation of the spatial and temperature changes associated with plasma-sample interaction.

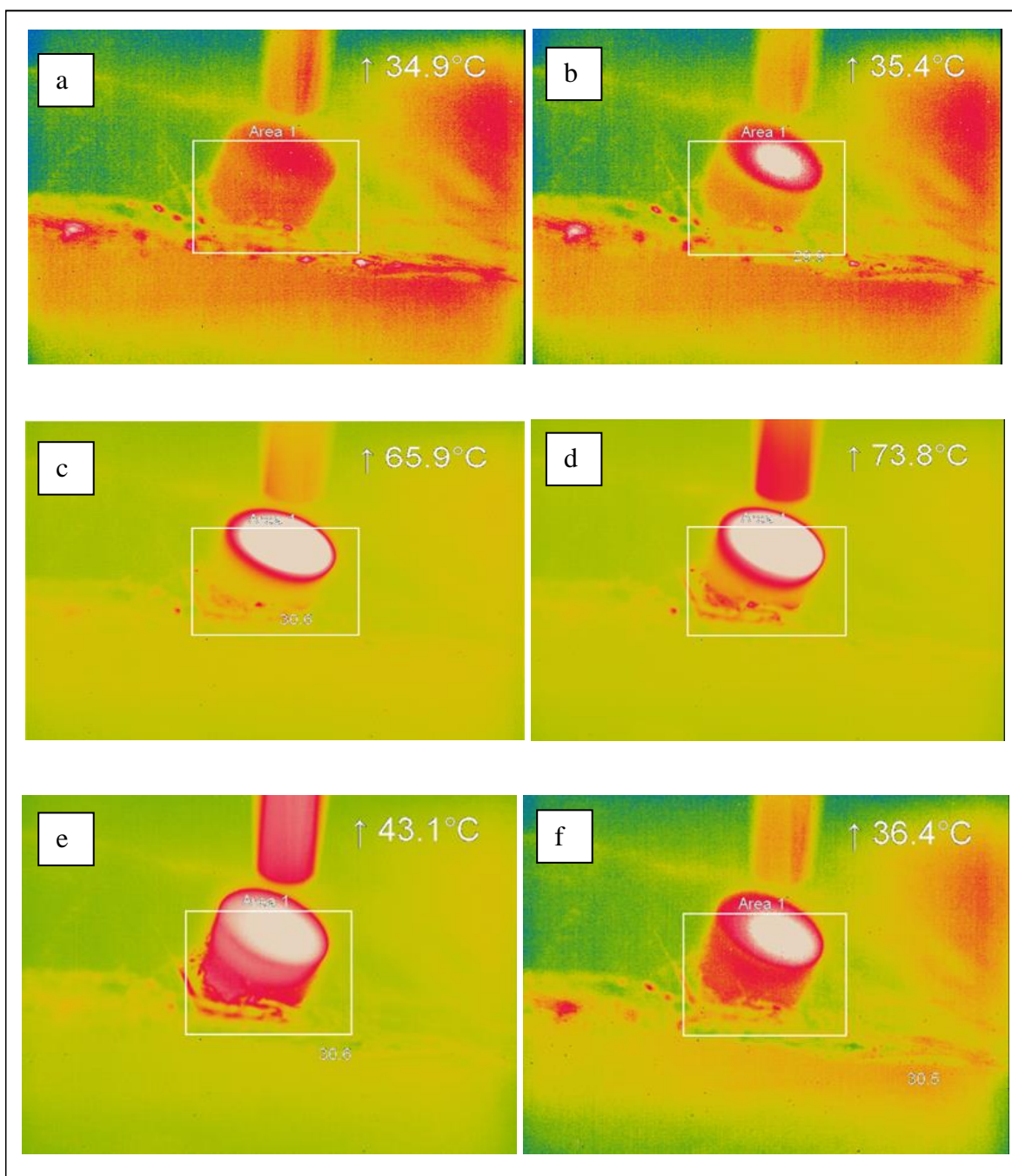


Figure 3. 1. Thermal camera images of a sample of paracetamol tablet during exposure to the plasma at different times: a 5 secs; b 15 secs; c 35 secs; d 1 min; e 3 min and f 5 min.

3.3. Results and discussion

3.3.1. Method development and optimisation of PADI-MS and Raman spectroscopy conditions

Paracetamol tablets were used to optimise the methodology by maximising the protonated peaks for the compound. PADI-MS conditions of interest were plasma power, helium carrier gas flow rate and the distance between the visible plasma and sample surface. Dry helium delivery adjacent to the needle-tip was used following optimisation of a coaxially arranged delivery of inner flow rate of 224 mL/min, and the distance between the visible plasma flame and sample was 5 mm. These conditions gave the highest signal-to-noise ratio of the sample main ions and this was found to be optimum for all solid samples. With shorter plasma pencil to sample distance (< 5 mm), as expected, the noise was increased. A possible explanation for this is that the sample is damaged more during exposure to the reactive species associated with the plasma, while both sample damage and intensities of ions were minimised when using longer plasma pencil to sample distance (> 5 mm), a distance of 5 mm being an optimal balance between damage and ion generation. Raman microscopy conditions following optimisation comprised: 532 nm laser wavelength, 5.0 mW laser power and a 10x objective with a 2.0 second collection time.

3.3.2. Exposure of sample to plasma flame

This section deals with the difference between the qualitative analysis method using Raman microscopy and PADI-MS. This is achieved by comparing the results of Raman microscopy with that used in PADI-MS. Both methods have been developed in this investigation. Paracetamol samples were prepared by contact to visible plasma by different interaction times before analysis. The PADI-MS plasma was used as a source to expose the whole sample of paracetamol tablets at 0 secs, 10 secs, 20 secs, 30 secs, 50 secs, 1 min, 2

min, 3 min and 5 min using the optimal conditions. Photos of the PADI-MS source set-up and paracetamol tablets after exposure to NTP are shown in Figures 3.2 and 3.3.

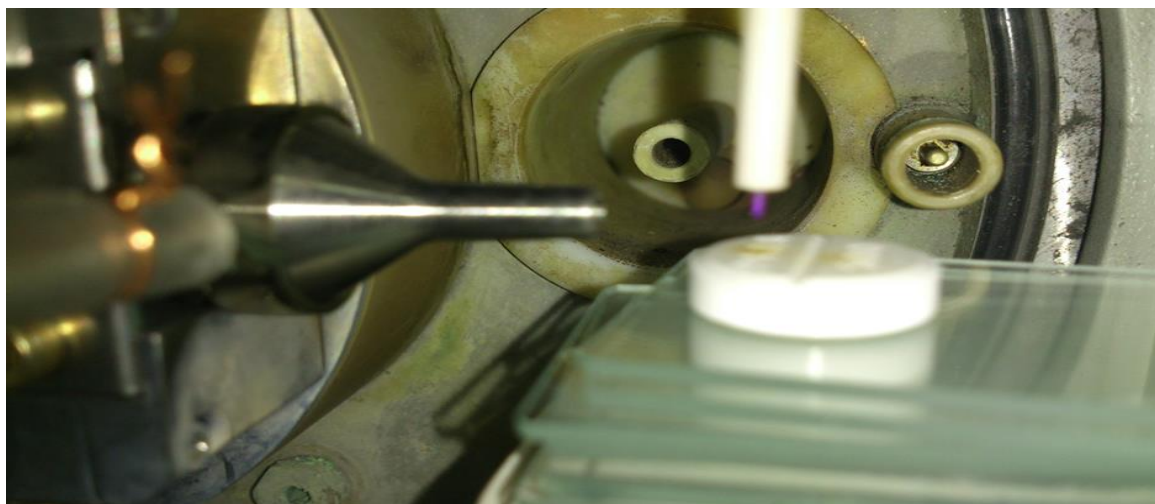


Figure 3. 2. Photo of the PADI source in operation using helium directly from a cylinder with flow rate of 224 mL/min, and the distance between the plasma flame and sample was 5 mm.

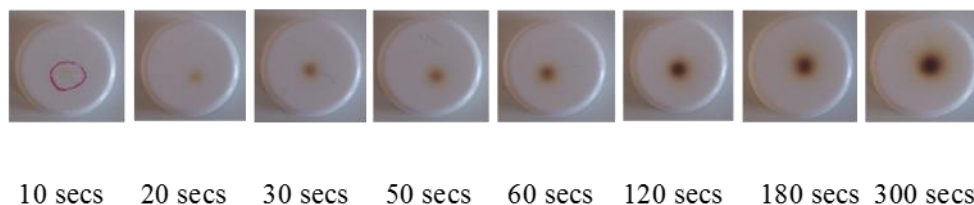


Figure 3. 3. Photos of paracetamol tablets after exposure to room temperature non-thermal plasma flame (from 10 secs to 300 secs) at 7W.

Visual inspection indicates cumulative discolouration of the samples as a function of plasma exposure time. The red circle in the first exposure sample (10 seconds) shows the place of the exposed area, Figure 3.3. The experimental data of the visible damage spot

size due to the PADI plasma for each sample as a function of time is shown in Figure 3.4. There was an increase in damage spot size to 30 seconds by 1.2x, after which this further increased to the end of data acquisition of 5 minutes by 2.5x, Figure 3.3. Clearly there are reactive species outside the visible flame. Damage increased during exposure to the plasma flame, in particular after 30 seconds. Therefore, chemical analysis is required to investigate if there is a limit to get good results without significant change of the surface chemistry.

The first phase of chemical analysis examined the impact of NTP interaction with paracetamol tablets at different exposure times using Raman microscopy. The molecular structure of paracetamol is shown in Figure 3.5. The vibrations of paracetamol in the Raman spectra were identified successfully.

In the second phase of chemical analysis, a paracetamol tablet was analysed directly using PADI-MS with a total acquisition time of 5 minutes without the need for preparation. Adduct and fragment peaks of paracetamol in the PADI-MS spectra were detected and identified as a function of time. Data were collected and then compared with the results of Raman microscopy.

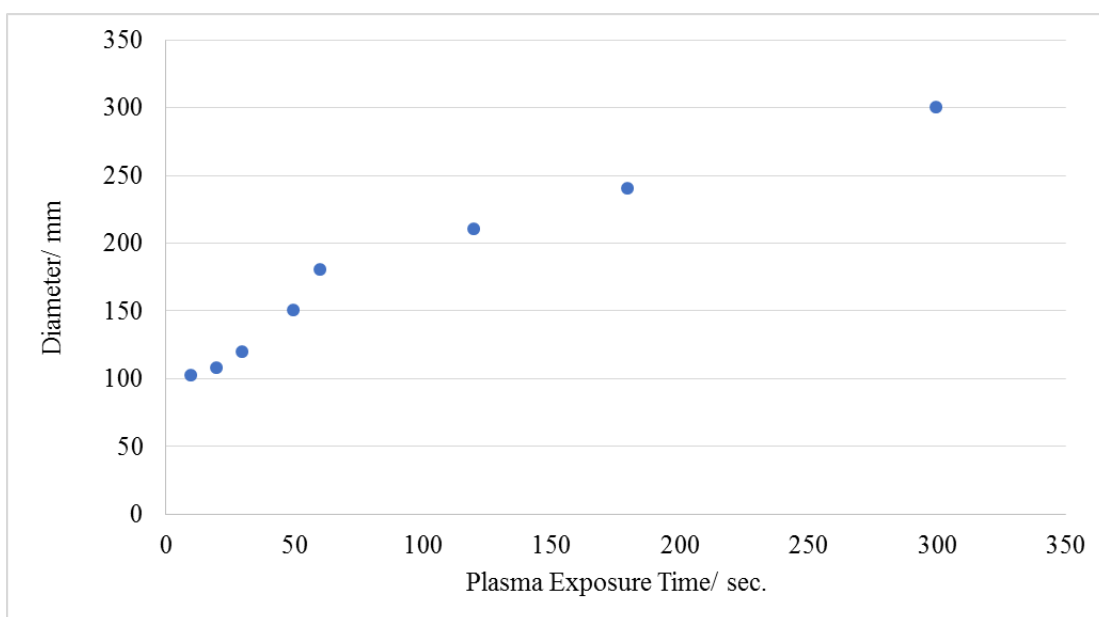


Figure 3. 4. Spot size of PADI plasma as a function of plasma exposure time.

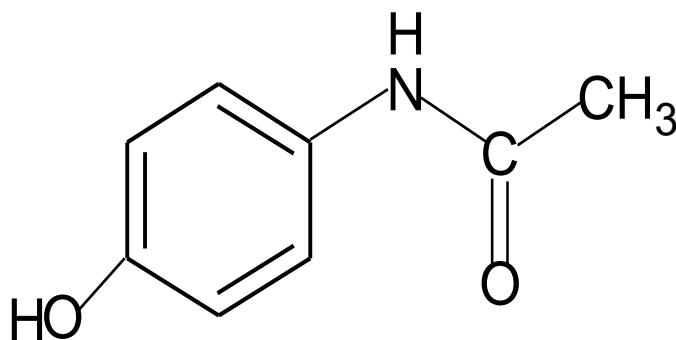


Figure 3. 5. Molecular structure for paracetamol.

3.3.3. Raman microscopy

3.3.3.1. Identification of functional groups of paracetamol

The first part of analysis studied the detection and identification of pharmaceutical tablets using the optimised conditions for Raman microscopy as outlined in Section 3.4.1. Changes in signal intensity of the sample tablets after interaction to plasma flame were compared to that measured in the 0-second sample. Paracetamol tablets were used as pharmaceutically relevant models. Paracetamol (500 mg) tablets were analysed directly using Raman microscopy. A 0-second paracetamol tablet was analysed as a control sample before analysis of exposed tablets using Raman microscopy. The vibrational peaks of paracetamol in the Raman spectrum were observed and identified as listed in Table 1 using the optimal conditions. Changes in the chemistry of the samples that were exposed to the cold plasma over time were identified by comparison with a 0-second exposure plasma. The Raman spectrum shows a clear signal intensity of vibrations for 0-second tablet plasma, Figure 3.6. The carbonyl group (C=O) has stretching vibration at 1648 cm^{-1} . The vibration stretches involve C-NH open, C-NH bend and Aryl C-C were observed at

1323.24 cm^{-1} , 1559.62 cm^{-1} and 1609.387 cm^{-1} respectively. Other vibrations such as C-O-H, Aryl CH bend, Aryl CH wag and ring deformation are shown in Table 3.1. Most of these vibrations have linked to the molecular structure for paracetamol, Figure 3.5. Manadanol tablet contains paracetamol 500 mg, maize starch, colloidal anhydrous silica, magnesium stearate and potassium sorbent. The percentage of concentration (w/w) for paracetamol in the paracetamol tablet is 87 % by dividing the content of paracetamol in the tablet by the weight of tablet (500 mg/570 mg). Changes in intensity with time may, in principle, be attributed to either thermal desorption of analytes from the surface, degradation or continued excitation of analytes on the surface or in the gas phase.

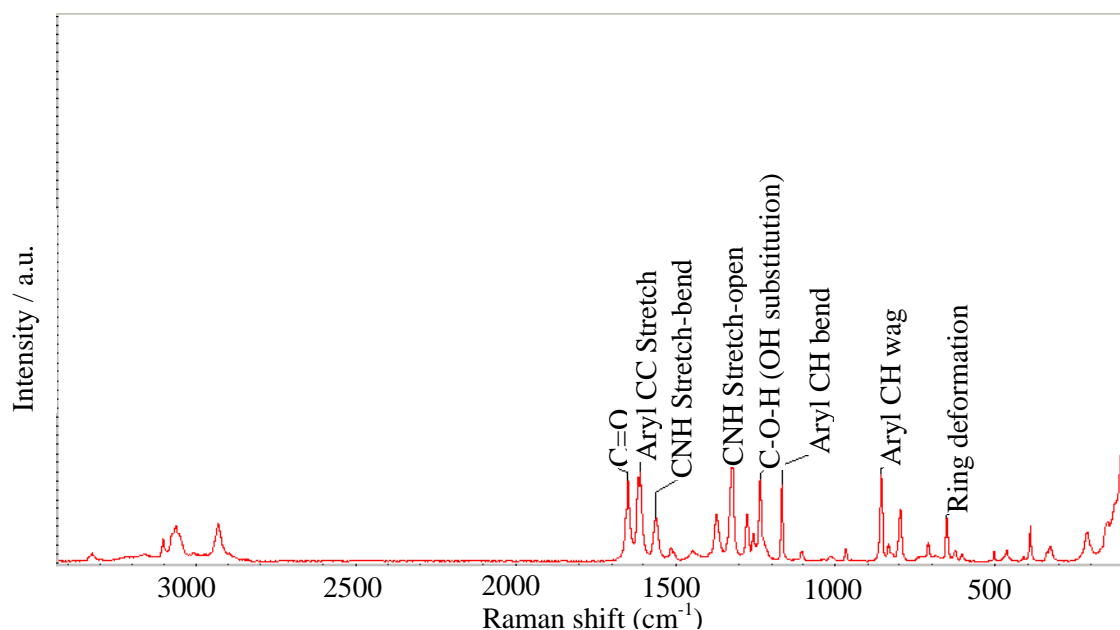


Figure 3. 6. Raman spectrum of 500 mg 0-seconds paracetamol tablet (without exposure to plasma).

Table 3. 1. Vibrations of paracetamol molecule in Raman spectrum Figure 3.5.

Peak position cm^{-1}	Vibration
651.52	Ring deformation
856.43	Aryl CH wag (Para Sub)
1167.55	Aryl CH bend
1236.56	C-O-H (OH substitution)
1323.24	CNH Stretch-open
1559.62	CNH Stretch-bend
1609.39	Aryl CC Stretch
1647.90	(C=O) Stretch

3.3.3.2. Effect of visible plasma on the chemistry of paracetamol tablets

The analysis in this section examined the impact of plasma flame on the paracetamol chemistry. This was achieved by comparing the peak positions and peak heights between 0- second exposure to plasma and exposed samples. This examination also provides information about the behaviour of the intensity of vibration peaks over time. The Raman spectra present an overview of vibration peaks of paracetamol tablets after exposure to NTP at different times: 10 secs, 20 secs, 30 secs, 50 secs, 1 min, 2 min, 3 min and 5 min, Figure 3.7, 3.8, and 3.9. The vibration peaks of exposed samples that observed in all spectra including aryl CH, COH, CNH, carbonyl group (C=O) and aryl CC stretch are different to that used by the 0-seconds time sample. A negative correlation was found between signal intensity of vibration peaks and plasma exposure. It can be seen from Figure 3.6, 3.7, and 3.8 that the intensity signal of vibration peaks decreases from 10 seconds until the end of acquisition time of 5 minutes. In addition, the results showed some changes that happened in the shape of vibration peaks for aryl CC stretch and CNH stretch-bend during the exposure time to plasma, in particular for exposure samples between 10 seconds and 5 minutes. However, the Raman spectra did not show any important shift for any peak. These findings may help us to understand that the positions of vibrations were not affected by exposure to visible plasma. However, the chemistry of paracetamol tablets

can be affected when interacting with NTP as a function of time. This can be proved by looking to visual inspection of exposed tablets in Figure 3.3. It can be seen from the photos in this Figure that the size of the burned area increased as a function of time, hence the chemical structure of tablet changed. Data from these Figures can be compared with the data in Figure 3.6 which show there is difference in the signal intensity between 0-seconds exposure to plasma and exposure tablets.

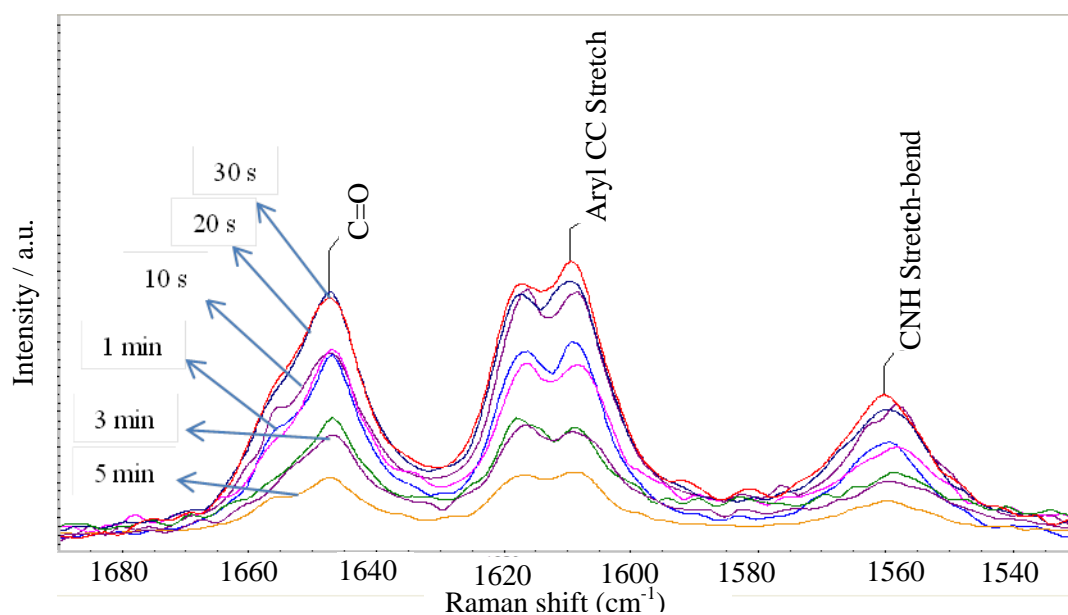


Figure 3. 7. Raman spectra of C=O, aryl CC and CNH stretch-bend of paracetamol tablets after exposure to NTP at different times: 10 secs, 20 secs, 30 secs, 50 secs, 1 min, 2 min, 3 min and 5 min.

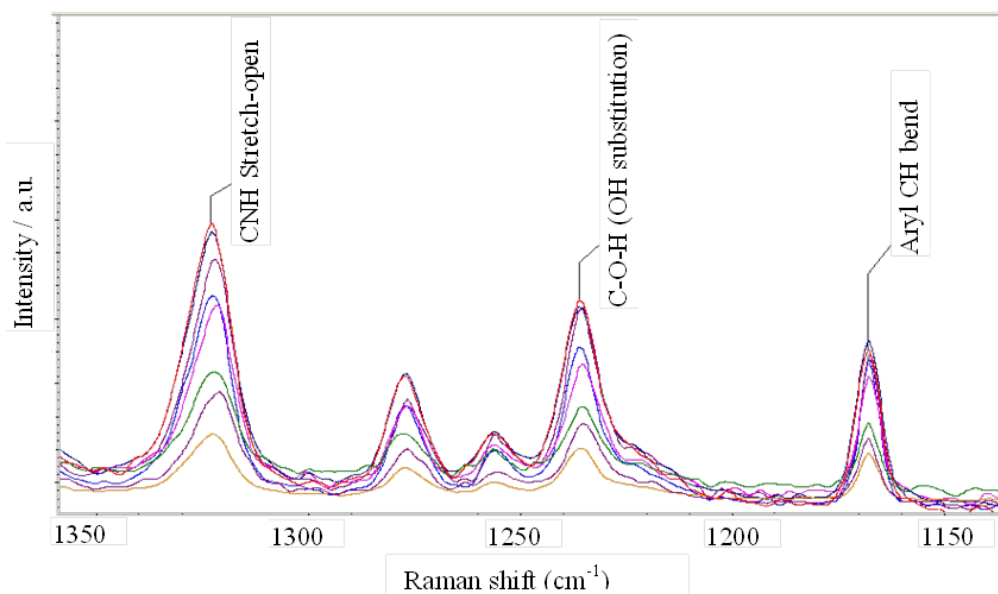


Figure 3. 8. Raman spectra of CNH stretch-open, C-O-H (OH substitution) and aryl CH bend of paracetamol tablets after exposure to NTP at different times: 10 secs, 20 secs, 30 secs, 50 secs, 1 min, 2 min, 3 min and 5 min.

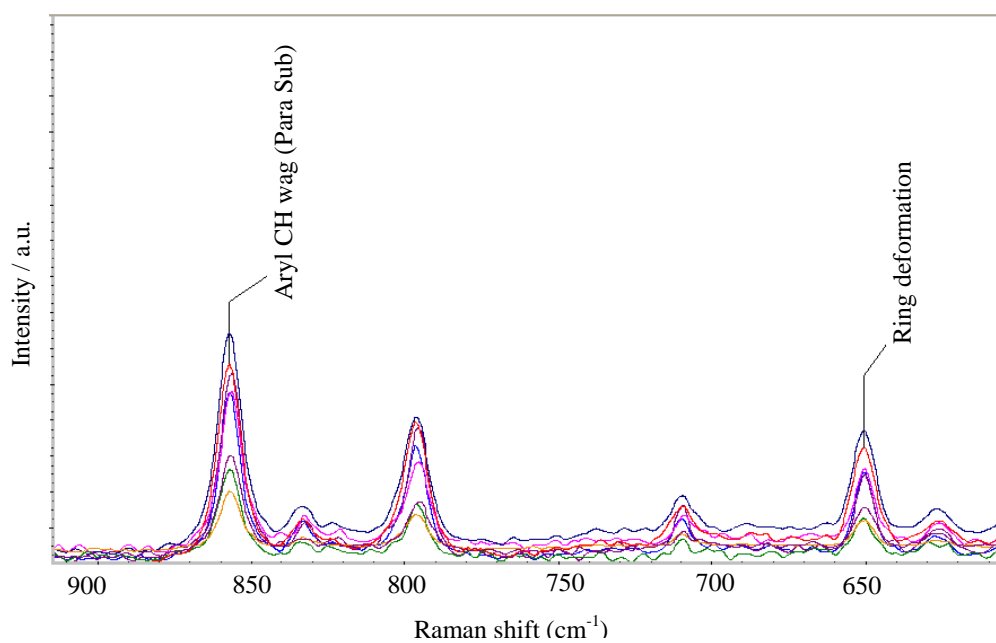


Figure 3. 9. Raman spectra of aryl CH wag and ring deformation of paracetamol tablets after exposure to NTP at different times: 10 secs, 20 secs, 30 secs, 50 secs, 1 min, 2 min, 3 min and 5 min.

The results also show there is a clear difference between the signal intensity of the vibration peaks for paracetamol tablet such as CH, COH, CNH and C=O, and exposure time to NTP up to 5 minutes, Figure 3.10. The signal intensity of C=O, CNH and C-O-H stretches increased up to ~ 30 seconds, after which they decrease to 5 minutes. This due to that the chemistry was not affect by plasma flame and there is no damage in the tablet until 30 seconds of analysis time. Taken together, these results suggest that there is an association between the exposure time to NTP and the intensity signal of each vibration peak of paracetamol.

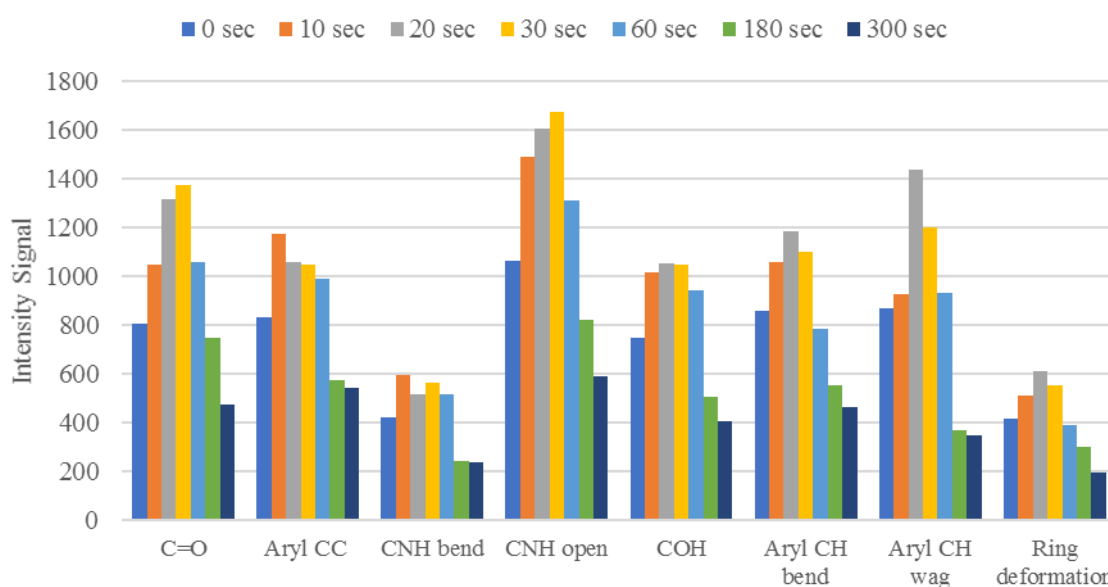


Figure 3. 10. Peak height measurements of the vibration peaks for paracetamol tablet with a total acquisition time of 5 minutes using Raman microscopy.

Further analysis showed that there was also a positive relationship between the ratio of signal intensity for vibration peaks of paracetamol and exposure plasma time. Data were collected by determining the ratios of the intensity of vibrations peaks versus analysis time. The intensity of vibrations for paracetamol was normalised in order to show the plasma effect on the behaviour of intensities over interaction time. There was a clear trend of

increasing in the ratios of intensity signal for C=O/aryl CH bend and C=O/CNH stretch open, reaching a peak between 120 seconds and 180 seconds respectively, after which they decrease until the end of data acquisition of 5 minutes, Figures 3.11 and 3.12. The reason of increasing the intensity for C=O due to oxidising the hydroxyl group generating carboxylic acid. The chemical composition of paracetamol was affected and changed after 120 seconds exposure to plasma. These experiments results confirmed that the paracetamol tablet was damaged more at and after 120 seconds exposure to plasma, Figure 3.2.

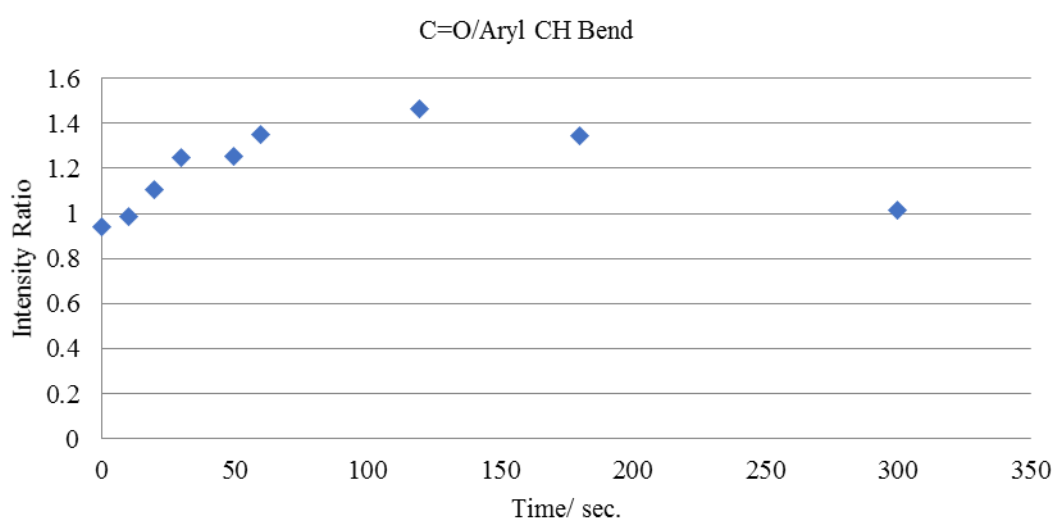


Figure 3. 11. Intensity ratios measurement of C=O/aryl CH bend of paracetamol tablet (500 mg) with an acquisition time of 5 minutes using Raman microscopy.

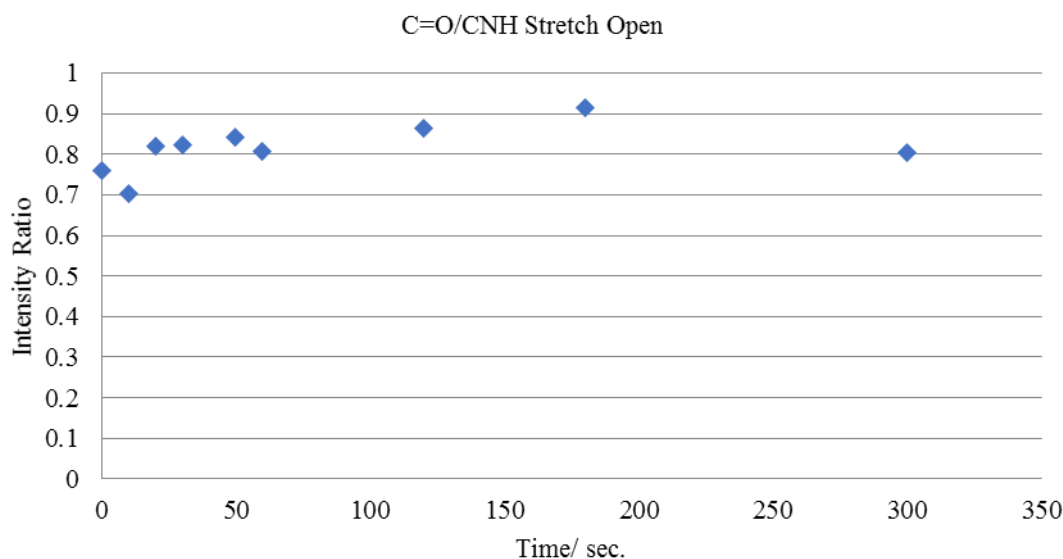


Figure 3. 12. Intensity ratios measurement of C=O/CNH stretch open of paracetamol tablet (500 mg) with an acquisition time of 5 minutes using Raman microscopy.

3.3.4. Plasma-assisted desorption ionisation mass spectrometry (PADI-MS)

3.3.4.1. Identification of fragment and adduct peaks of paracetamol

Following additional analysis of paracetamol tablets using Raman microscopy, PADI-MS was used to get maximum and different information about the effect of visible plasma on the chemistry of paracetamol. Another primary aim of this study is to exploit these techniques to learn more about the plasma-tablet interaction and to show if there are any differences between Raman microscopy and PADI-MS for analysing paracetamol tablets. In this part of the analysis, the detection and identification of pharmaceutical tablets were studied using the optimised conditions for PADI-MS as outlined in Section 3.1.1. Pure paracetamol and tablet were analysed directly using PADI-MS. Although the paracetamol molecular ion M^+ m/z 151 was detected, protonated paracetamol $[M+H]^+$ at m/z 152 was more abundant and easy to see in all spectra. This could be attributed to a pK_a effect. The pK_a for paracetamol is 9.5, so it is a basic compound. Therefore, paracetamol would be

expected to gain a proton and give the high-intensity signal for 152 in comparison with 151.

This analysis showed the effect of NTP with paracetamol tablets over time using PADI-MS. PADI-MS spectrum of pure paracetamol is shown in Figure 3.13. One sample of 500 mg paracetamol tablet was exposed and analysed directly at the same time by PADI-MS using helium directly from a cylinder with flow rate of 224 mL/min, and the distance between the plasma flame and sample was 5 mm with an acquisition time of 5 minutes. Several PADI-MS spectra of the paracetamol tablet using different times of exposing to NTP up to 5 minutes are shown in Figure 3.14. There are clear intensity signals of adduct and fragment peaks observed in the spectrum. These ions were analysed and identified according to their mass to charge ratios. Two diagnostic peaks relating to paracetamol's molecular ion were observed for $[M+H]^+$ at m/z 152 and $[2M+H]^+$ at m/z 303, with a hydrated peak presented at m/z 320 for $[2M+H_2O]^+$, Figure 3.13. We can see that the signal intensity of the protonated paracetamol peak ($[M+H]^+$ m/z 152) increased up to ~ 1 minute, after which it decreased to the end of data acquisition at 5 minutes. The changes in intensity in particular after 1 minute may be due to the sample being affected and damaged during exposure to plasma at more than this time. The percentage of concentration (w/w) for paracetamol in the paracetamol tablet is 87 %. Therefore, the signal intensity of 152 is expected to be higher than others, but it is lower than $M+H_2O$ m/z 169. This will be improved in the next experimental chapters by using carrier gas additives such as outer helium flow added with water vapour prior to interacting with the plasma plume. Further adduct and fragment peaks can be identified as listed in Table 3.2.

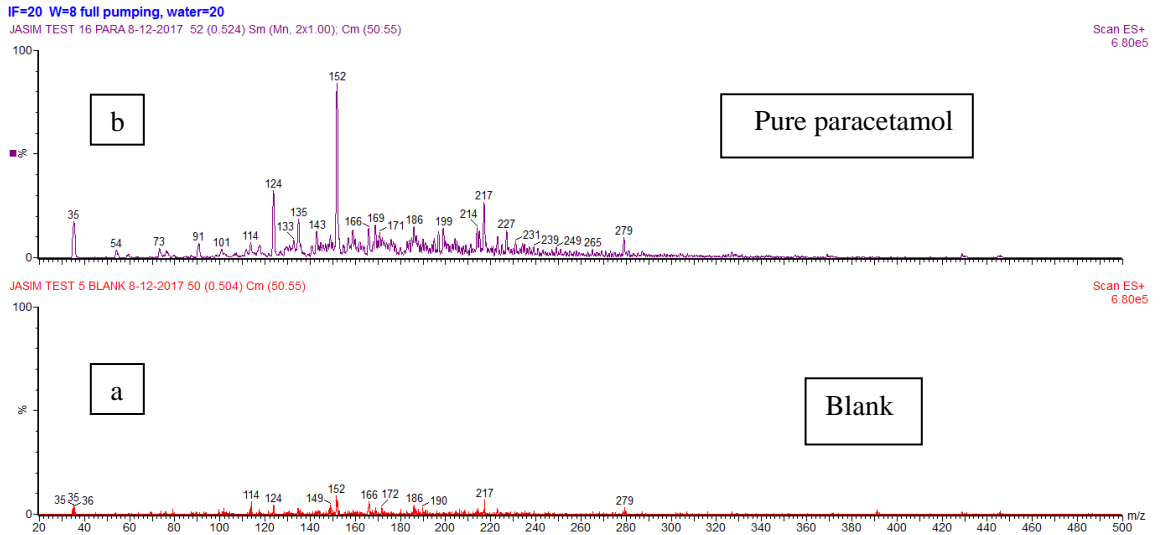


Figure 3. 13. PADI-MS spectra of background and pure paracetamol at exposure time to plasma with an acquisition time of 1 minute.

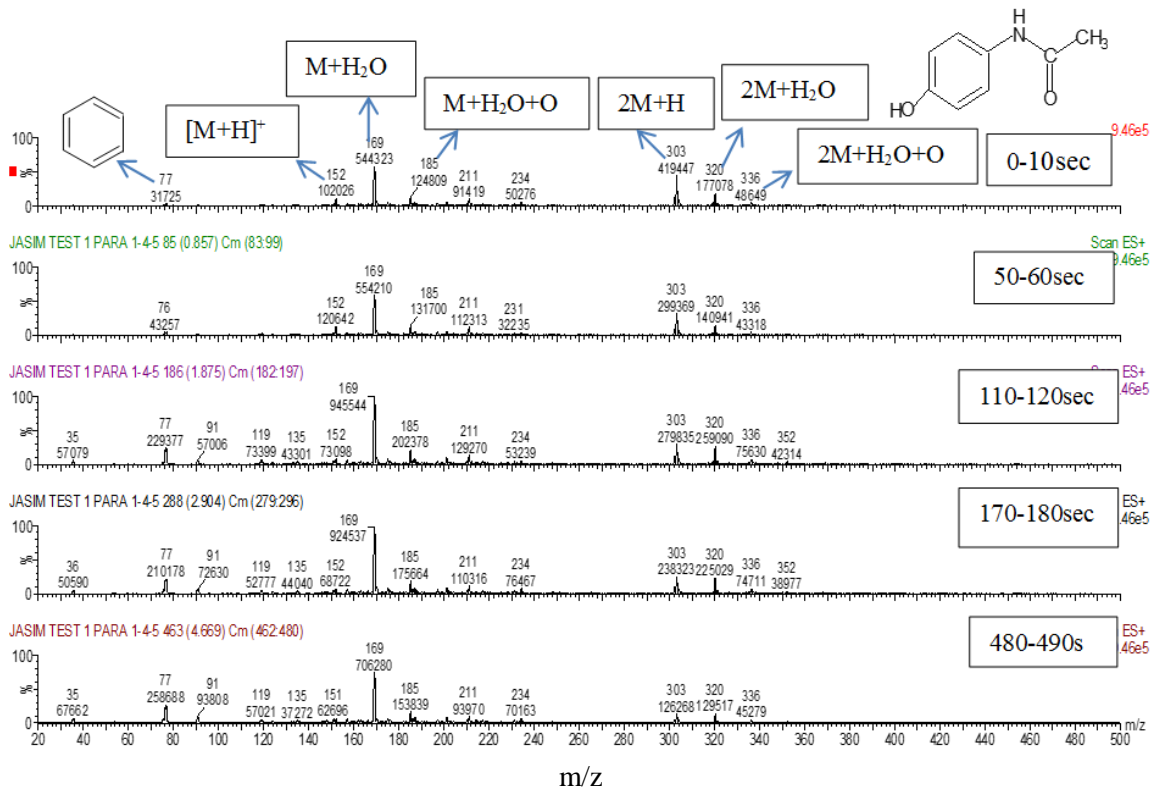


Figure 3. 14. PADI-MS spectra of paracetamol tablet at different exposure times to plasma with an acquisition time of 5 minutes.

Table 3. 2. Diagnostic, adduct and fragment peaks of paracetamol.

Diagnostic peaks for paracetamol	m/z
Aromatic ring (C ₆ H ₅)	77
[M+H] ⁺	152
[M+H ₂ O] ⁺	169
M+H ₂ O+O	185
[2M] ⁺²	302
[2M+H] ⁺²	303
2[M+H ₂ O] ⁺²	320
2M+H ₂ O+O	336

3.3.4.2. Effect of plasma flame on paracetamol tablet chemistry using PADI-MS

In this section, the impact of plasma on the paracetamol chemistry was examined by PADI-MS using the optimal conditions, Figures 3.15 and 3.16. Both pure and tablet showed the same behaviour of intensity during the exposure time to plasma. The intensity of protonated paracetamol [M+H]⁺ increased and reached a peak at 45 seconds, after which it reduced to 5 minutes. This could be attributed to degradation or excitation of analytes on the surface or in the gas phase.

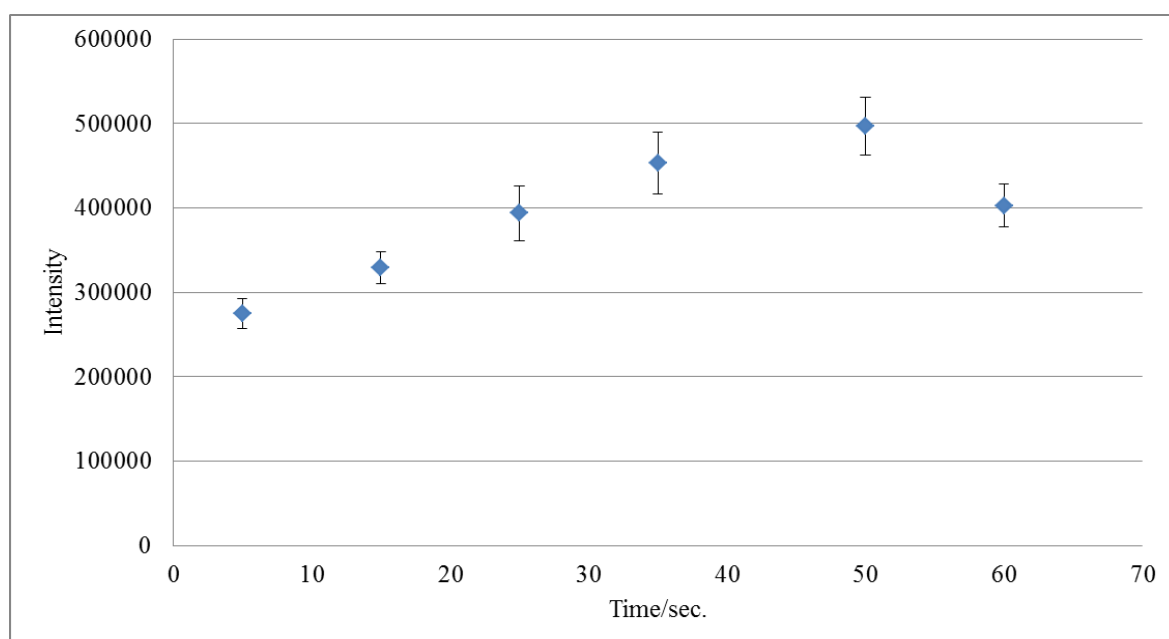


Figure 3. 15. PADI-MS signal intensity for [M+H]⁺ in pure paracetamol.

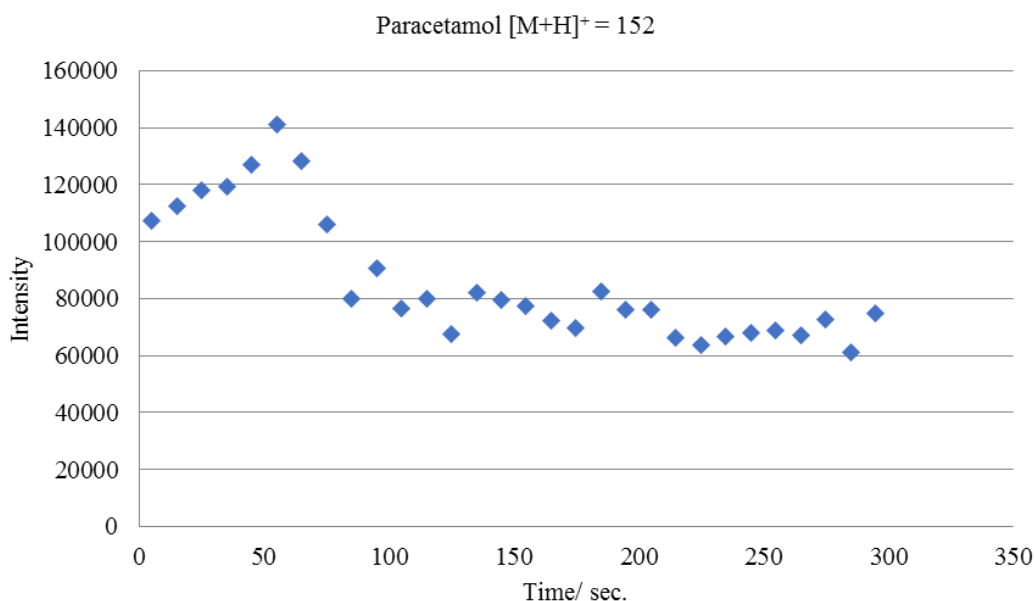


Figure 3. 16. PADI-MS signal intensity for $[M+H]^+$ in paracetamol tablet with a total acquisition time of 5 minutes.

To investigate the heating causes on the sample during the analysis, The temperature was measured using the exact same PADI parameters using a thermal camera by interacting the visible plasma with a tablet (29). The temperature increased dramatically to 75 °C at 45 seconds, after which it increased slowly to 80 °C at 1 minute, and then dropped to 36 °C until 5 minutes. This indicated why the $[M+H]^+$ peak for paracetamol increase in intensity up to ~ 45 seconds, after which they decrease up to 1 minute (for more details see Chapter 3). Some of the main intensities of the adduct and fragment peaks of exposed samples for paracetamol tablets over time are shown in Figure 3.17. There is a general decrease in intensities of $[M+H]^+$ at m/z 152, 2M at m/z 302 and 2M+H at m/z 303 after 45 seconds. This observed decrease in intensity with time may, in principle, be attributed to damage the sample after exposure to plasma flame. However, there is a clear increase in the intensity of aromatic ring (C_6H_5) at m/z 77 until the end of data acquisition and this may be due to losing the oxygen from the molecule. The intensities of the $M+H_2O$ at m/z 169 and

2M+H₂O at m/z 320 were also decreased after 2 minutes, Figure 3.16. From the data in this Figure, it is apparent that the length of analysis time is important to obtain more information about the structure compound of paracetamol. This result indicates that the analysis time up to ~ 50 seconds is enough mostly to detect and identify the molecule.

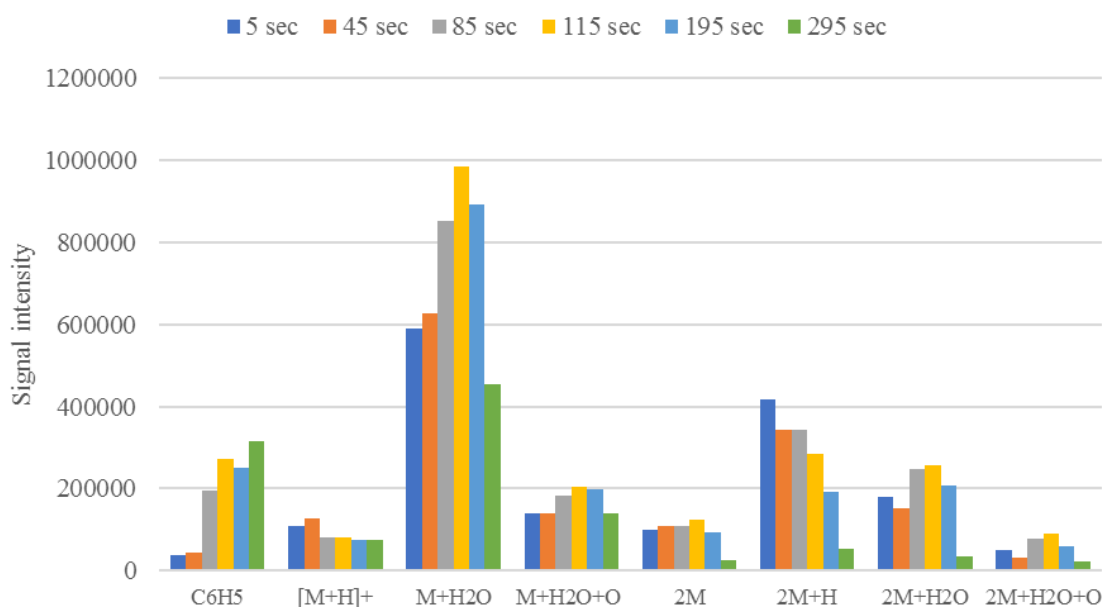


Figure 3. 17. Signal intensity of adduct and fragment peaks for each sample of paracetamol tablet against acquisition time up to 5 minutes in 5 seconds intervals 5, 45, 85, 115, 195 and 295 seconds.

The ratios of intensity between adduct peaks of paracetamol and aromatic ring were calculated. The results showed that the behaviour of the intensity of ratios for [M+H]⁺ m/z 152/C₆H₅ m/z 77, 2M m/z 302/77 and M+H₂O m/z 169/77 over time are similar, Figure 3.18. However, as can be seen from this Figure, the ratio of intensity by a factor of 169/77 is higher than that used by 152/77, 302/77. The reason of this is the intensity of M+H₂O m/z 169 was higher than that used of 152 and 302. These results show that the differences between the intensity of [M+H]⁺, 2M, M+H₂O and C₆H₅ decreased after 50 seconds. They

also show that the intensity of $[M+H]^+$, 2M and M+H₂O are higher than C₆H₅. As shown in this Figure, the ratios of these factors are almost constant up to ~50 seconds, after which they reduced until the end of data acquisition. These results indicate that the paracetamol tablet can be damaged after exposing to plasma after 50 seconds. Therefore, it suggests that the analysis can be stopped after 30 seconds without the need to wait until the end of acquisition time.

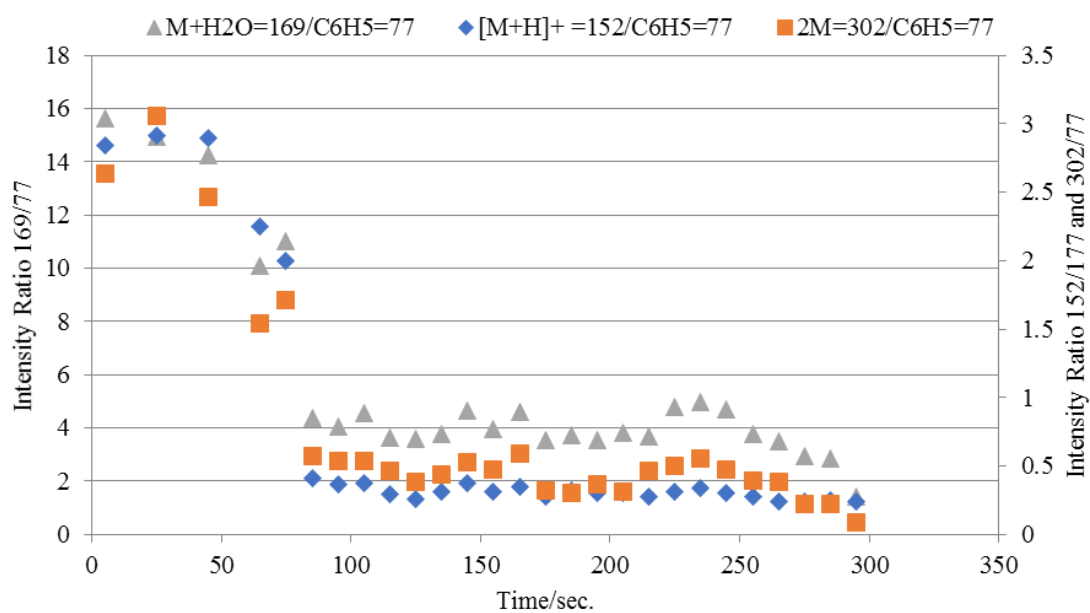


Figure 3. 18. Signal intensity ratios of adduct and fragment peaks of paracetamol tablet by a factor of 152/77, 302/77 and 169/77 with acquisition time up to 5 minutes using PADI-MS.

3.4. Conclusions

The study has focused on the development of a novel method for use in the study of the effect of non-thermal plasma on the chemical structure of pharmaceutical samples. The present study was designed to investigate the effect of PADI plasma under atmospheric pressure on the chemistry of paracetamol tablets as a model system. In this work, PADI-MS and Raman microscopy have been successfully used to analyse the tablets after exposure to the plasma flame. Both methods are simple, fast and can give informative data without the need for sample preparation. In addition, they were used directly to show the chemical composition of the tablet. This study has shown that paracetamol in the tablet can be detected and identified directly by PADI-MS and Raman microscopy without separation from the components. Comparison of both proposed methods has shown that the PADI-MS is better than Raman microscopy due to its ability to produce the ions from the surface of the sample and detect them in seconds. PADI-MS can provide much information on chemical structures for pharmaceutical molecules. Therefore, the PADI-MS method is more suitable for pharmaceutical sample analysis.

This study has found generally the chemistry of paracetamol-containing tablets was affected by exposure to the non-thermal plasma. The visible spot size after PADI plasma exposure was substantial, growing to a dark, circular area of 3000 μm diameter after 5 min exposure. Discolouration of the samples indicated that the chemical composition was changed. The Raman spectra show changes in the shape of some peaks of the functional groups for paracetamol, but the heights are more strongly affected. It did not show any important shift for any peak. The top layer of the tablet showed clear signs of oxidation, whilst the blackening also suggests carbonisation, which however could not be unequivocally determined from the spectra.

The experiments of PADI-MS showed that there are differences in intensity of the diagnostic, adduct and fragment peaks. The results indicate that a significant proportion of the paracetamol molecules in the tablet were damaged after exposing to plasma beyond 30-45 seconds. However, until 45 seconds there are no discernible differences in the PADI spectra, making 30s the optimal data acquisition time. The PADI-MS spectra showed that the signal intensity of 152, which was expected to be higher than others, but it is lower than $[M+H_2O]^+$ m/z 169. This result may be explained by the fact the conditions need to be improved using carrier gas additives such as outer helium flow added with water vapour prior to interacting with the plasma plume.

This is the first study to investigate the effect of NTP on a pharmaceutical tablet. It would be interesting to compare the analysis of this study including solid samples to those used by liquid samples in Chapter 4 and Chapter 5. The analysis of these samples undertaken here has extended our knowledge by providing a new understanding of the plasma interaction with samples and inform further investigations of chemical ionisation methods. The methods used for this study may be applied to other pharmaceuticals such as solids or creams. The findings of this study have a number of important implications for future practice and they also provide insights for future research. Determining strategies to reduce the damage caused by the PADI plasma, including potential temperature effects, whilst further increasing the intensity of diagnostic ions is a priority.

Overall, the results of this study indicate that PADI-MS is fast, highly sensitive and specific, allowing direct analysis in seconds, providing detailed information about the chemical structure of pharmaceutical samples when operating below the observed damage threshold time of 30 seconds.

References

1. Yonson, S. Coulombe, S. Léveillé, V. and Leask, R. L. (2006) 'Cell treatment and surface functionalization using a miniature atmospheric pressure glow discharge plasma torch', *Journal of Physics D: Applied Physics*, 39, p.p. 3508–3513.
2. Haertel, B. von Woedtke, T. Weltmann, K-D. and Lindequist, U. (2014) 'Non-thermal atmospheric-pressure plasma possible application in wound healing', *Biomolecules & Therapeutics*, 22(6), p.p. 477-490.
3. Kong, M. G. Kroesen, G. Morfill, G. Nosenko, T. Shimizu, T. van Dijk, J. and Zimmermann J. L. (2009) 'Plasma medicine: an introductory review', *New Journal of Physics*, 11, p.p. 1–35.
4. Laroussi, M. (2009) 'Low-Temperature Plasmas for Medicine', *IEEE Trans. Plasma Science*, 37 (6), p.p. 714–725.
5. Fridman, G. Friedman, G. Gutsol, A. Shekhter, A. B. Vasilets, V. N. and Fridman, A. (2008) 'Applied plasma medicine', *Plasma Process. Polym.*, 5, p.p. 503–533.
6. Stoffels, E. Kieft, I.E. Sladek, R.E. van der Laan, E.P. and Slaaf, D.W. (2004) 'Gas plasma treatment: a new approach to surgery', *Critical Reviews in Biomedical Engineering*, 32 (5-6), p.p. 427–460.
7. Stoffels, E. (2007) 'Tissue processing with atmospheric plasmas', *Contrib. Plasma Physics*, 47 (1-2), p.p. 40–48.
8. Laroussi, M. and Akan, T. (2007) 'Arc-Free Atmospheric Pressure Cold Plasma Jets: A Review', *Plasma Processes. Polymers*, 4, p.p. 777–788.
9. Eliasson, B. and Kogelschatz, U. (1991) 'Modelling and applications of silent discharge plasmas IEEE trans', *Plasma Science*, 19 (2), p.p. 309–323.

10. Dorai, R. and Kushner, M. J. (2003) 'A model for plasma modification of polypropylene using atmospheric pressure discharges', *Journal of Physics D: Applied Physics*, 36, p.p. 666–685.
11. Laroussi, M. (1996) 'Sterilisation of contaminated matter with an atmospheric pressure plasma', *IEEE Trans. Plasma Science*, 24 (3), p.p. 1188–1191.
12. Laroussi, M. (2005) 'Low-Temperature Plasma-Based Sterilisation: Overview and State-of-the-Art', *Plasma Proc. Polym.*, 2 (5), p.p. 391–400.
13. Klämpfl, T. G. Isbary, G. Shimizu, T. Li, Y-F Zimmermann, J. L. Stolz, W. Schlegel, J. Morfill, G. E. and Schmidt, H-U. (2012) 'Cold atmospheric air plasma sterilization against spores and other microorganisms of clinical interest', *Applied and Environmental Microbiology*, 78 (15), p.p. 5077–5082.
14. Matthews, I.P. Gibson, C. and Samuel, A.H. (1994) 'Sterilisation of implantable devices', *Clin. Mater.* 15 (3), p.p. 191–215.
15. Aziz, K. H. H. Miessner, H. Mueller, S. Kalass, D. Moeller, D. Ibrahim Khorshid, I. and Rashid, M. A. M. (2017) 'Degradation of pharmaceutical diclofenac and ibuprofen in aqueous solution, a direct comparison of ozonation, photocatalysis, and non-thermal plasma', *Chemical Engineering Journal*, 313, p.p. 1033–1041.
16. Kvam, E. Davis, B. Mondello, F. and Garner, AL. (2012) 'Nonthermal atmospheric plasma rapidly disinfects multidrug-resistant microbes by inducing cell surface damage', *Antimicrob Agents Chemother.*, 56, p.p. 2028–2036.
17. Arjunan, K.P. and Clyne, A.M. (2011) 'A nitric oxide producing pin-to-hole spark discharge plasma enhances endothelial cell proliferation and migration', *Plasma Med.*, 1, p.p. 279–293.
18. Schlegel, J. Köritzer, J. and Boxhammer, V. (2013) 'Plasma in cancer treatment', *Clinical Plasma Medicine*, 1 (2), p.p. 2–7.

19. Fridman, G. Friedman, G. Gutsol, A. Shekhter, A. B. Vasilets, V. N. and Fridman, A. (2008) 'Applied plasma medicine', *Plasma Process. Polym.*, 5, p.p. 503–533.
20. Chieng, N. Rades, T. and Aaltonen, J. (2011) 'An overview of recent studies on the analysis of pharmaceutical polymorphs', *Journal of Pharmaceutical and Biomedical Analysis*, 55, pp. 618–644.
21. Kim, J. Jung, D. Park, Y. Kim, Y. Moon, D. W. and Lee, T. G. (2007) 'Quantitative analysis of surface amine groups on plasma-polymerized ethylenediamine films using UV–visible spectroscopy compared to chemical derivatization with FT-IR spectroscopy, XPS and TOF-SIMS', *Applied Surface Science*, 253, p.p. 4112–4118.
22. Lim, C.K. and Lord, G. (2002) 'Current developments in LC-MS for pharmaceutical analysis', *Biol Pharm Bull.*, 25(5), p.p. 547–557.
23. De Lima Gomes, P.C. Barletta, J.Y. Nazario, C.E. Santos-Neto, A.J. Von Wolff, M.A. Coneglian, C.M. Umbuzeiro, G.A. and Lancas, F.M. (2011) 'Optimisation of in situ derivatization SPME by experimental design for GC-MS multi-residue analysis of pharmaceutical drugs in wastewater', *Journal of Separation Science*, 34(4), p.p. 436–445.
24. Wollein, U. and Schramek, N. (2012) 'Simultaneous determination of alkyl mesitates and alkyl besitates in finished drug products by direct injection GC/MS', *European Journal of Pharmaceutical Sciences*, 45(1-2), p.p. 201–204.
25. Lee, P.J. Murphy, B.P. Balogh, M.P. and Burgess, J.A. (2010) 'Improving organic synthesis reaction monitoring with rapid ambient sampling mass spectrometry', Waters Corporation, Milford, MA, USA.

26. Madhusudanan, K. P. (2007) 'Direct analysis in real time (DART) – a new ionization technique', 12th ISMAS Symposium cum, Workshop on Mass Spectrometry, p.p. 25–30.
27. Bridoux, M.C. and Machuron-Mandard, X. (2013) 'Capabilities and limitations of direct analysis in real time orbitrap mass spectrometry and tandem mass spectrometry for the analysis of synthetic and natural polymers', 27(18), p.p. 2057–2070.
28. Ratcliffe, L.V. Rutten, F.J.M. Barrett, D.A. Terry Whitmore, T. Seymour, D. Greenwood, C. Gonzalvo, Y.A. Robinson, S. and McCoustra, M. (2007) 'Surface analysis under ambient conditions using plasma-assisted desorption/ ionisation mass spectrometry' Anal. Chem., 79 (16), p.p. 6094–6101.
29. P. Roach and F.J.M. Rutten, to be publishe

CHAPTER 4: PADI Mass spectrometry analysis of mixtures from TLC plates

Abstract

In this chapter, a novel analytical approach was developed for identification of chemical components in aqueous mixtures of pharmaceutically relevant compounds using a TLC plate as a substrate. PADI-MS has been applied for direct analysis of solutions of paracetamol and caffeine in pure and mixed form on TLC plates. Samples of paracetamol and caffeine were analysed as aqueous solutions applied to TLC plate substrates. PADI-MS acquisition settings were optimised at 8 W and a helium carrier gas flow of 224 mL/min (inner flow) and (224 mL/min outer flow). Sample ions were directed into a single quadrupole MS by use of a sniffer tube, each acquisition being 1 minute. The sample spots on the TLC plate substrate were analysed directly by PADI-MS with and without developing the TLC plate, using ethyl acetate as mobile phase. The LOD and LOQ were determined for paracetamol and caffeine in a 1:1 mixture solution. The LOD for paracetamol and caffeine without developing the TLC plate was found to be 0.14 mg/mL and 0.16 mg/mL respectively. This improved to 15 µg/mL and 49 µg/mL, and respectively after separation of the spots. The LOQ for paracetamol and caffeine without developing the TLC plate was found to be 0.48 mg/mL and 0.54 mg/mL respectively. This improves to 50 µg/mL and 165 µg/mL respectively after separation of the spots. The LOD and LOQ for paracetamol after separation were 10 times lower, while for caffeine the improvement was a factor of 3. Therefore, the separation is not always necessary, and spots can be identified on TLC plates using PADI-MS without separation. However, the separation of the spots can give higher signal-to-noise ratio (S/N) of molecules, and hence the sensitivity of diagnostic adduct and fragment peaks can be improved. Therefore, separation was better due to no interference was found between compounds.

4.1. Introduction

Analysis of complex reaction mixtures can play an important role in understanding mechanisms of reaction pathways and improving products (1). The reason of using a mixture of compounds in this study is to identify mixture ingredients and this can help to confirm the quality and safety of drugs by determining the presence and quantity of components in a mixture. This study aims to establish whether PADI-MS is able to analyse mixtures and what are the limitations of the method. Paracetamol and caffeine are two important pharmaceutical compounds, used individually or together for treatment. Paracetamol is used as an analgesic and antipyretic drug that inhibits the cyclooxygenase enzyme (2,3). Caffeine is used to promote the analgesic effect of paracetamol when combined (4). Paracetamol is extensively used to reduce a headache, general pain including chronic pain and reduce temperature particularly that associated with bacterial and viral infection (5-8). Caffeine is a much consumed compound by humans via its presence in drinks such as coffee (9, 10). As well as in pharmaceutical formulations, caffeine can be extremely harmful to human beings. Excessive consuming of caffeine can lead to anxiety and nervousness (11), raised blood pressure and heart disease (12). Paracetamol and caffeine are one of the most widely used combinations of pharmaceuticals (13).

Several analytical methods have been reported in the analysis of paracetamol and caffeine in the various pharmaceutical mixtures, such as spectroscopic, chromatographic and spectrophotometric techniques (14). High-performance liquid chromatography (HPLC) has been the most widely used method to analyse the pharmaceutical mixtures. HPLC is also the most used of the liquid chromatographic methods for separating the complex mixture of compounds (15). HPLC method has been used to analyse a mixture of paracetamol, caffeine and chlorphenamine using a C₁₈ column and a mobile phase consisting of

methanol and potassium phosphate (45:55 v/v) (16). A RP-HPLC method has been successfully applied to analyse the pharmaceutical mixture including paracetamol and caffeine using Brownlee Bio C₁₈ column and isocratic mobile phase of water-acetonitrile (85:15 v/v) at room temperature, and the analysis time per sample was 6 minutes (17). This is because the quantification analysis and the limit of detection is very good. However, the disadvantages of HPLC are that it is relatively expensive, chemicals, time-consuming and sometimes extensive sample preparation required. HPLC also gives one peak for each compound and this may not always be specific enough to tell us whether a component is present in the sample or not.

Mass spectrometry is a sensitive and fast analytical method and it can be used to detect and monitor a wide range of compounds. In addition, MS methods can measure molecular weight directly with small sample amounts. Mass spectrometry techniques are combined with chromatography such as gas chromatography-mass spectrometry (GC-MS) (18, 19), high-performance liquid chromatography connected with a tandem mass spectrometry (HPLC-MS/MS) (20, 21) and liquid chromatography-mass spectrometry (LC-MS) (22) to provide more information about the chemical structure of compounds. On the other hand, pre-concentration and sample preparation are still required in these techniques (23).

In recent years, there has been an increasing interest in ambient mass spectrometry (AMS). In the AMS techniques, samples are desorbed and ionised directly from surfaces under atmosphere pressure (for more information see Chapter 2). Desorption electrospray ionisation (DESI) and direct analysis in real time (DART) are the most common techniques of AMS, but the type of source is different. DESI uses a solvent to ionise the sample, while DART uses a plasma.

In this study, a very simple and rapid analysis of (individual and mixture) solutions from TLC plates using PADI-MS has been explored in a variety of ways. PADI is another type of the modern ambient ionisation techniques that uses non-thermal visible plasma as a source to produce ions from the surfaces of molecules. Compared to DESI and DART, PADI uses different plasma (non-thermal visible plasma) that does not cause any thermal or electric damage to the sample surface. The present study explores, for the first time, the effect of type of substrate on identification of paracetamol and caffeine in the mixture solutions using a novel method of PADI-MS. This study therefore sets out to assess the effect of water vapour, temperature and the effect of matrix on signal intensities of these samples. A qualitative analysis method was used in these investigations. The study offers important insights on how to develop a new method that can be used to detect and identify the pharmaceutical compounds from other substrates. This study can also provide new insight into applying this novel method to analyse unknown chemical compounds in many fields not only in pharmaceutical analysis. A major advantage of the mixture analysis using this method is that it avoids the problems of other analytical methods such as time-consuming, sensitivity and sample pre-treatment. This method is particularly useful in studying of pharmaceutical production. Many researchers have utilized several techniques to measure the chemical compounds in the mixture solutions, but the problem with the experimental methods is that sample preparation, filtration and extraction are required.

An objective of this study was to detect and identify paracetamol and caffeine as a mixture from a TLC plate before and after the separation of spots. TLC plates as substrate are low cost, convenient, good dimensional stability, fast, easier to interpret spectra particularly for complex mixtures and they are heat resistant and this makes the spots on the TLC plate and the method easy to develop and this also allows the possibility of using strong solvents. TLC plates are faster than paper chromatography because the stationary phase of TLC is a

thin layer of inert material supported on a flat surface like a glass plate and this allows the solvent to move quickly through the stationary phase. The main aim of this study was to develop a novel fast, sensitive and cost-effective method that can be used for identification of unknown components in pharmaceutically relevant solutions from TLC plates. PADI-MS provides information about chemical speciation, whilst also allowing spatial localisation by sampling individual TLC spots. This study used a qualitative case study approach to investigate the measurement of paracetamol and caffeine in single component and mixture solutions from TLC plates. The benefit of this approach is that it allows qualitative methods analysis to be more useful for identifying and characterising. The purpose of using paracetamol and caffeine as model drugs in this study is that they are small molecule drugs and most drugs are still in this category. The work presented here investigates the use of PADI analysis directly from a TLC plate, using paracetamol and caffeine as models for pharmaceutically relevant mixtures. Mixed standard solutions and off-the-shelf pain relief pharmaceuticals, Panadol and paracetamol, and caffeine were used. The analysis was compared pre- and post TLC- separation.

The analysis of samples using PADI-MS is divided into two sections. The first section of this study shows that PADI-MS has been used to analyse the mixture of paracetamol and caffeine directly from TLC plates without separation of spots. In the second section, the study set out to detect these compounds using this technique after the separation of spots from TLC plates using ethyl acetate as a solvent. This study used qualitative analysis of paracetamol and caffeine by placing one drop of the mixture on TLC plate and then analysing directly using PADI-MS without any separation to save time and solvents. This study was also designed to develop the TLC plate after separation of the spots by improving the limit of detection and limit of quantification for these compounds. However,

to get an optimal limit of detection is necessary to separate the spots of paracetamol and caffeine on the TLC plate prior to PADI-MS analysis.

Matrix effect is important for the quality of the results particularly for solid samples and this might impact on the sensitivity of the analytical response either positively or negatively (24). This study attempts to show that matrix of analytes (paracetamol and caffeine) did not affect on the results and this will be discussed in details in the results and discussion section.

Understanding the link between the behaviour of peak intensity and analysis time will attempt to improve the measurement of samples by the length of analysis time. This is also important to explain the experimental data which are collected by PADI-MS spectra. The experiments of this work were examined to show how the best way of pharmaceutical mixtures analysis can be chosen. For PADI, the temperature is important for desorption of samples. For AMS techniques including PADI, the temperature is important and can play a vital role in desorption of samples (25). Therefore, in order to increase the signal intensity of the analysis, the temperature of the sample must be increased. Plasma interacts with both sample and TLC plates at the same time. Plasma heats the sample to generate the gas phase of the molecules then the ions are produced (positive and negative ions) from surfaces. After that, MS separates and detects ions. On the other hand, this chapter includes the identification of paracetamol and caffeine in the mixture solution from dry TLC plates and this will be discussed in detail in the practical evaluation part. In this Chapter, the objectives used to reach some conclusions about this sampling method were:

- 1) Sample paracetamol and caffeine directly as model for pharmaceutically relevant solutions.
- 2) Use a TLC plate to present solution samples to PADI-MS.

- 3) Use direct non-thermal plasma interaction to analyse the solution without any preparation by PADI-MS.
- 4) Compare the PADI-MS results before separation of spots with after separation of the spots.
- 5) Assess limits of detection and quantification for each combination of the above.

4.2. Materials and methods

4.2.1. Apparatus:

In the PADI-MS instrumentation, a single quadrupole (Waters Micromass ZQ, Manchester, UK) was used with the front end removed to accept a Stoffels-design plasma pen ionisation source using a 13.56 MHz RF power source (26). The plasma pencil was fabricated to provide coaxial dual gas flow; an inner ceramic tube was encompassed within a quartz glass tube. The helium gas flow through both tubes was controlled using separate flow meters, the flow inside the ceramic tube will henceforth be referred to as inner flow, the flow between the ceramic and quartz tube as outer flow. Mass conditions including inflow gas, out flow vapour and plasma power were set up for all experiments. The conditions of PADI-MS were optimised and set up for all samples in this study using preliminary analysis and found to be plasma power of 8 W, He inflow of 224 mL/min and the distance between the plasma flame and sample of 5 mm. The effect of water vapour on ionisation efficiency was investigated by flowing the He through a water vapour added environment before the plasma pencil (for more information see Chapter 2).

4.2.2. Chemicals:

Panadol ExtraTM tablets containing 500 mg paracetamol and 65 mg caffeine per tablet were used as obtained from an over the counter pharmacy. Pure paracetamol was purchased

from Alfa Aesar, UK (purity 98%), and pure caffeine was purchased from Organics, China (purity 98%). Helium gas was supplied by British Oxygen Company (BOC) gases, UK (purity 99%). Ethyl acetate was supplied by Fisher Scientific, UK with high purity laboratory reagent grade (Assay (GLC) > 99%). Deionised water was provided through a Pure Lab Option (ELGA) with a conductivity of 0.067 MS/cm.

4.2.3. Preparation of sample solutions:

Panadol solutions were prepared by dissolving 1 Panadol Extra tablet in 10 mL deionised water. A range of high purity paracetamol and caffeine solution concentrations of 0.02 - 5 µg/µL were prepared by dissolving the solutes in deionised water. Paracetamol and caffeine mixtures were prepared by mixing 2 mL of equally concentrated solutions. These were all freshly made prior to use.

4.2.4. Standard TLC plates:

Standard TLC plates consisting of Silica gel 60 F254, 25 on aluminum sheets of size 20 × 20 cm were supplied by Merck KGaA, Darmstadt, Germany.

4.2.5. Procedure:

A. Sample substrates without separation:

1. Squares of 2 x 2 cm TLC plate were cut and used for all analysis in method A.
2. One drop of single paracetamol and single caffeine (both 5 µg/µL) and Panadol tablet solution (50 mg/mL paracetamol+6.5 mg/mL caffeine) were deposited on the TLC plate using a Pasteur pipette. The droplet size was 32.4 µL allowing deposition of 162 µg API. Other serial dilutions of 1:1 (w/w) mixtures of paracetamol and caffeine were also deposited on TLC

plate as shown in Table 4.1. For each measurement of a single drop of solution with a volume of 32.4 μL (the weight of one drop was 0.032 g) was deposited. These droplets contained the following amounts of API / paracetamol and caffeine as listed in Table 4.2.

3. The deposition spot of individual and paracetamol/caffeine mixtures on the TLC plate was analysed immediately without drying by PADI-MS with a total acquisition time of 1 minute.

B. Sample substrates with separation:

1. A large TLC sheet was cut horizontally into plates 6.5 cm by 2.5 cm and used for all analysis in method B.
2. Small spots of single paracetamol and single caffeine (both 5 mg/mL) and 1:1 (w:w) mixtures were deposited using a spotter tube on TLC plates. The droplet size was 0.8 μL (the weight of one spot was 0.0008 g). Further details are shown in Table 4.1.
3. The separation on TLC plates was developed using ethyl acetate as solvent.
4. Spots were seen and circled using pencil under UV light and were identified.
5. Each spot was analysed immediately without drying by PADI-MS with a total acquisition time of 1 minute.

To investigate the potential effects that such heating causes on the sample during the analysis, and indeed the quality of mass spectral data obtained, the temperature was measured using the exact same PADI parameters using a thermocouple (chromel-alumel type) by contact the visible plasma with TLC plate without a sample.

Table 4. 1. Concentrations and amounts of paracetamol and caffeine in the mixtures used for methods A and B.

Concentration of each analyte (mg/mL)	2.5	0.5	0.1	0.01
Amount of each analyte per droplet (μg)				
Method A: Analysis without separation	81	16.5	3.24	0.324
Method B: Analysis after separation	2	0.4	0.08	0.008

Table 4. 2. The amount of molecule per mole in the solution of an individual and a mixture of paracetamol/caffeine.

Solution	Paracetamol $\mu\text{g}/\mu\text{mole}$	Caffeine $\mu\text{g}/\mu\text{mole}$
Paracetamol 5 $\mu\text{g}/\mu\text{L}$	162 / 1.07	
Caffeine 5 $\mu\text{g}/\mu\text{L}$		162 / 0.83
Mixture: both 2.5 $\mu\text{g}/\mu\text{L}$	81 / 0.53	81 / 0.41
Mixture: both 0.5 $\mu\text{g}/\mu\text{L}$	16.5 / 0.11	16.5 / 0.08
Mixture: both 0.1 $\mu\text{g}/\mu\text{L}$	3.24 / 0.02	3.24 / 0.016
Mixture: both 0.01 $\mu\text{g}/\mu\text{L}$	0.324 / 0.002	1.324 0.0016

4.3. Results and discussion

4.3.1. Optimised conditions used for all following experiments

Solids and solutions of highly pure compounds were used as a control to identify and optimise methodology. Paracetamol and caffeine solutions at a range of concentrations (Table 4.1) were deposited on TLC plates using procedure A and analysed by PADI-MS. To get the best conditions to analyse samples on PADI-MS, repeated measures of the single component were used. PADI-MS conditions of interest were plasma power, helium carrier gas flow rate and the distance between the visible plasma and sample surface.

4.3.1.1. Plasma Power

Plasma power of 8W was found to give the highest intensity of the sample main ions (or less noise). This was found to be optimum for all pure samples and also gave good results when applied to mixtures of controls in varying ratios, Figure 4.1. The stability of spectrum observed with respect to the time of plasma-sample interaction was seen to vary somewhat in relation to the intensity of ions observed rather than varying ion composition. With higher plasma powers ($> 8W$), as expected, the noise was increased. The reason for this is the sample can be damaged more during exposure to high plasma flame in particular more than 8 W. At the same time, intensities of molecules were minimised when using lower plasma powers ($< 8W$).

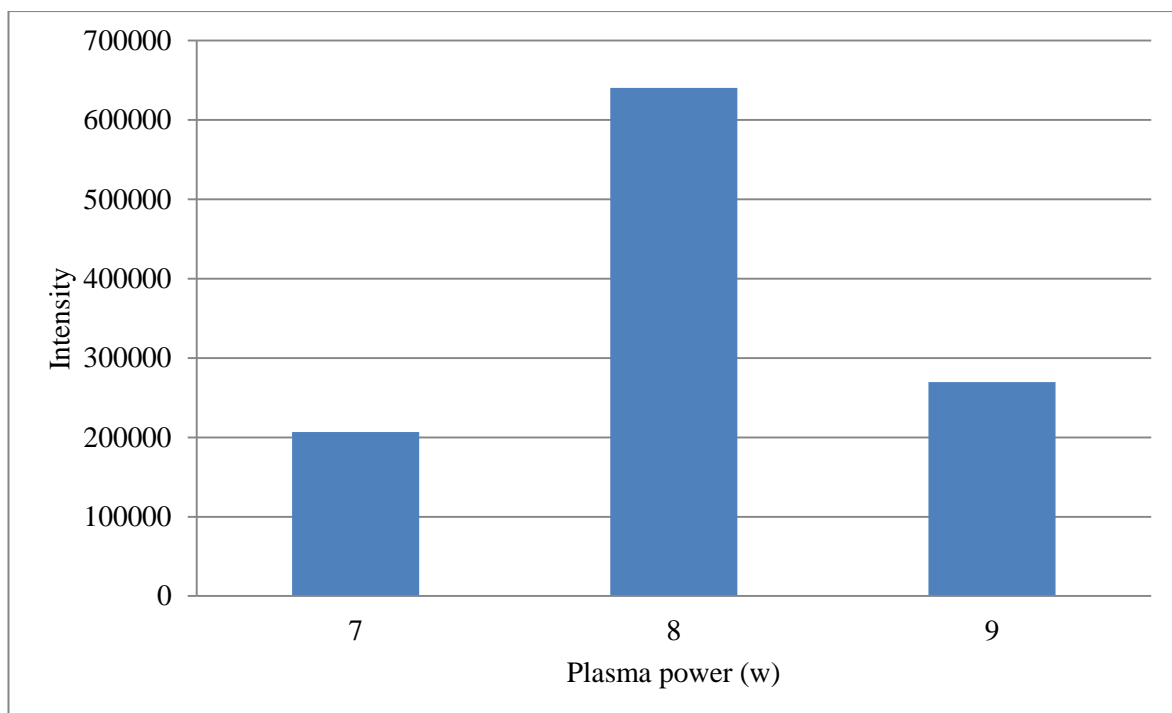


Figure 4. 1. Signal intensity of $[M+H]^+$ in paracetamol tablet against different plasma power using helium added with a total acquisition time of 1 minute.

4.3.1.2. Plasma pencil to sample distance

The distance between the plasma flame and sample of 5 mm was also found to give the highest intensity of the sample, Figure 4.2. The same problems that were mentioned before can happen when the plasma pencil to sample distance was higher or less than 5 mm.

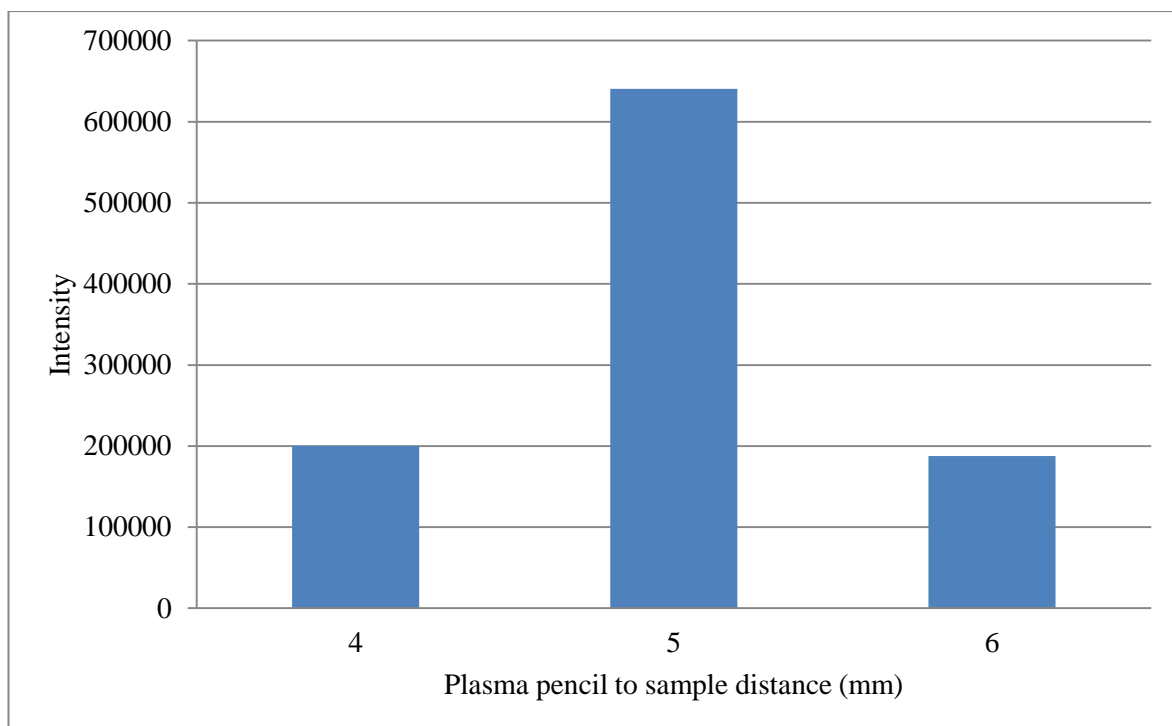


Figure 4. 2. Signal intensity of $[M+H]^+$ in paracetamol tablet against different plasma pencil to sample distance using helium added with a total acquisition time of 1 minute.

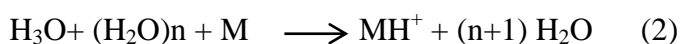
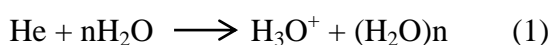
4.3.1.3. Carrier gas flow rate

A carrier gas flow of 224 mL/min (inner flow) and (224 mL/min outer flow) was also found to give the highest intensity of the sample ions.

4.3.1.4. Carrier gas additives

Spectral differences were observed when the outer He flow was added with water vapour prior to interacting with the plasma plume. This was investigated in order to study possible effects of chemical ionisation, with anticipated protonated water being formed within the water vapour infused plasma. Results suggest that the analysis of paracetamol and caffeine mixture using helium added with water vapour as gas flow is better than using dry helium; the signal intensity of diagnostic molecular and fragment ions was significantly improved, aiding determination of the chemical composition of dilute mixtures, Figure 4.3.

Several solvents including methanol, ethanol, hexane, petroleum spirit, dichloromethane and ethyl acetate were trialled as mobile phase to separate the spots of pure paracetamol and caffeine in the mixture solution on TLC plates. Ethyl acetate was found to be the most suitable solvent for this purpose. Carrier gas additive was investigated to improve the signal intensity of diagnostic molecular and fragment peaks of paracetamol and caffeine molecules. Results suggest that the analysis of paracetamol and caffeine mixture using helium added with water vapour as gas flow is better than using dry helium, Figure 4.3. Spectral differences were observed when flowing the outer He flows through added water vapour environment prior to reaching the plasma flame. As expected, the gas phase ions are formed by the reaction between the helium and water which then produce H_3O^+ , and then H_3O^+ reacts with a molecule (M) to form protonated molecule (MH^+) according to equations below (35):



As an analog to electrospray ionisation mass spectrometry (ESI-MS) that uses any polar solvent such as H_2O , ACN and THF for proton donation, here H_2O vapour was used to achieve a similar effect.

The results showed that signal intensity of diagnostic molecular and fragment peaks was significantly improved when using helium added with water vapour, this aiding determination of the chemical composition of dilute mixtures. There is the higher signal intensity of protonated paracetamol $[\text{M}+\text{H}]^+$ m/z 152 when using helium added with water vapour as gas flow, Figure 4.3. Diagnostic peaks relating to paracetamol molecular ion were observed an m/z 152 for $[\text{M}+\text{H}]^+$ and m/z 304 for $[2\text{M}+2\text{H}]^+$, with a hydrated peak presented at m/z 320 $[2\text{M}+\text{H}_2\text{O}]^+$, Figure 4.3. The diagnostic peak m/z 166 could be

assigned either to $[M+O-H]^+$ or to $[M+NH]^+$ (with nitrogen reacting from the air during plasma treatment), but it is most likely identified as M+O-H due to the paracetamol molecule gaining the hydroxyl group from the water vapour. Further adduct and fragment peaks can be identified as listed in Table 4.3. There was also a clear trend of increasing the intensity and stable signals of protonated paracetamol when using helium added with water vapour, Figure 4.4. The protonated caffeine peak $[M+H]^+$ at m/z 195 could not be detected using dry helium (Figure 4.5). The data in Figures 4.4 and 4.5 is that 15 seconds indicate enough to see all diagnostic peaks relating to paracetamol and caffeine with stable signals without the need to wait until 60 seconds. The diagnostic peak of caffeine was detected $[M+H]^+$ at m/z 195 when using helium with added water vapour. However, this protonated peak was not detected when using dry helium, Figure 4.5. This maybe due to the pK_a effect. The pK_a for caffeine is 14 (basic compound), therefore, it can gain protons from water easily.

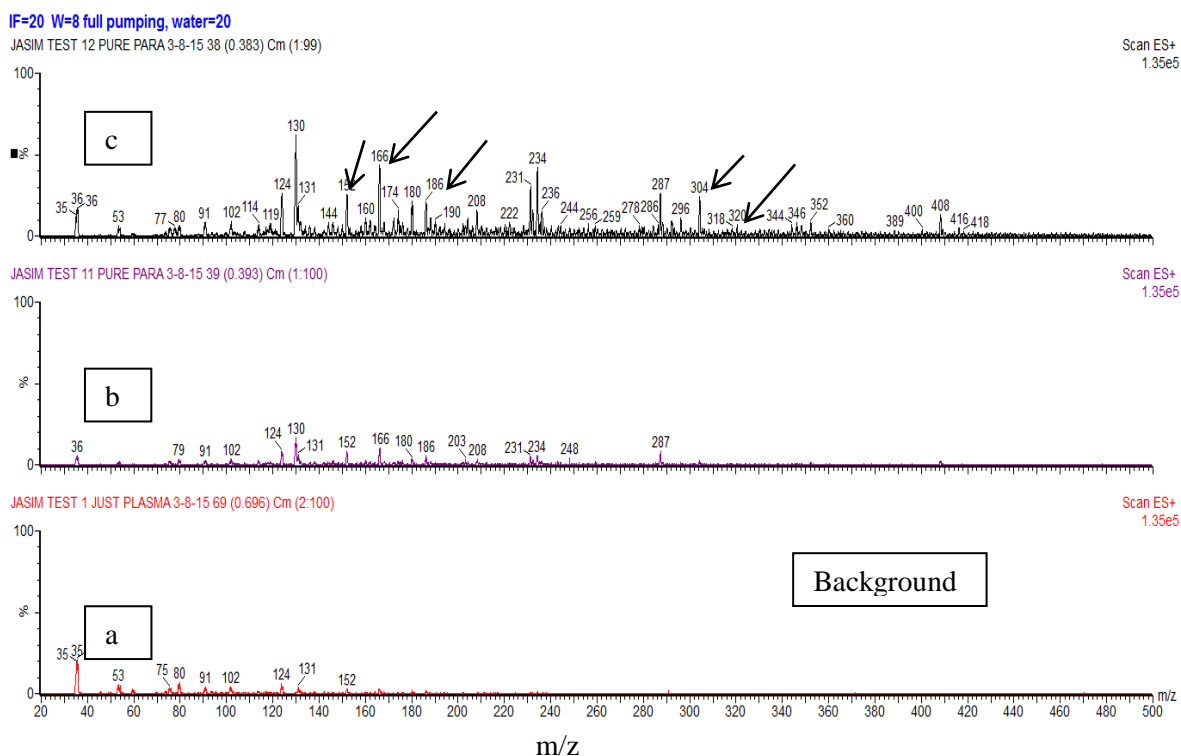


Figure 4. 3. PADI-MS spectra of single paracetamol ($5 \mu\text{g}/\mu\text{L}$) using dry helium (b) and helium added with water vapour (c) with a total acquisition time of 1 minute. Arrows indicate diagnostic peaks that link to paracetamol.

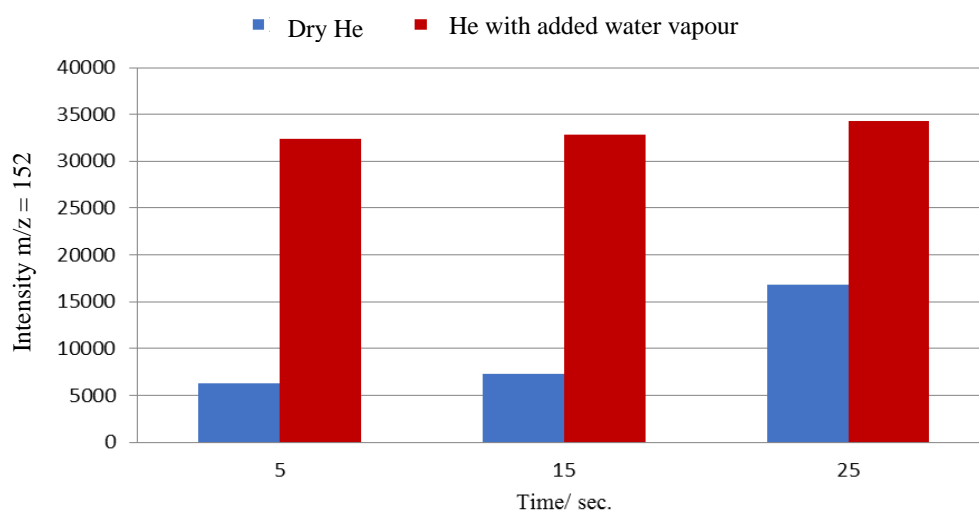


Figure 4. 4. Signal intensity of protonated paracetamol $m/z = 152$ ($5 \mu\text{g}/\mu\text{L}$) against time using dry helium and added with water vapour in 5 seconds intervals 0-5, 10-15 and 20-25 seconds.

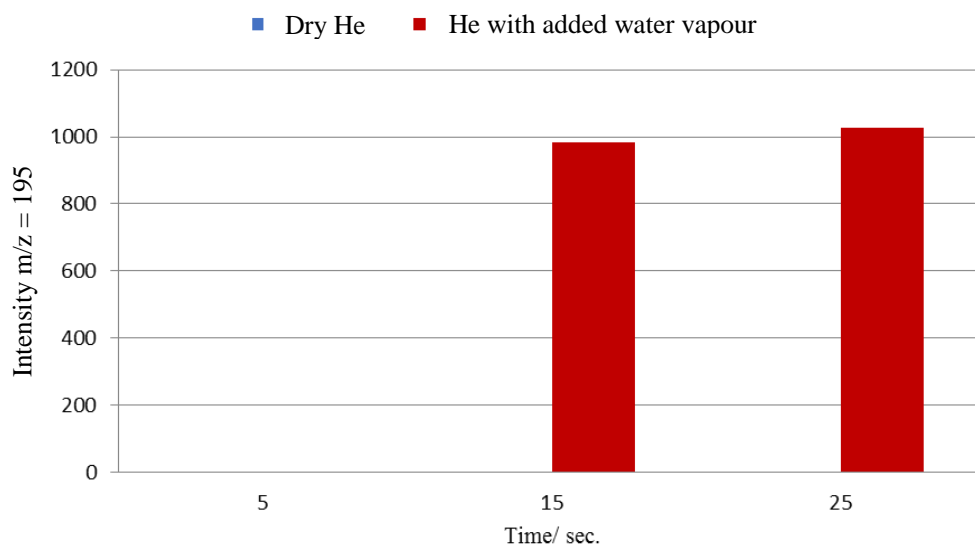


Figure 4. 5. Signal intensity of protonated caffeine $m/z = 195$ ($5 \mu\text{g}/\mu\text{L}$) against time using dry helium and added with water vapour in 5 seconds intervals 0-5, 10-15 and 20-25 seconds.

Table 4. 3. Diagnostic, adduct and fragment peaks of paracetamol and caffeine.

Diagnostic peaks for paracetamol	m/z	Diagnostic peaks for caffeine	m/z
$[\text{M}+\text{H}]^+ + 2\text{H}_2\text{O}-\text{COCH}_3\text{NH}$	130	M^+	194
$[\text{M}+\text{H}]^+$	152	$[\text{M}+\text{H}]^+$	195
$\text{M}+\text{O}-\text{H}$ or $\text{M}+\text{NH}$	166		
$[\text{M}+\text{H}]^+ + 2\text{H}_2\text{O}-\text{N}$	174		
$[\text{M}+\text{H}]^+ + \text{CO}$	180		
$\text{M}-\text{H}+2\text{H}_2\text{O}$	186		
$2\text{M}-\text{CH}_3$	287		
$[2\text{M}+2\text{H}]^{+2}$	304		
$[2\text{M}+\text{H}_2\text{O}]^+$	320		
$3\text{M}-\text{CH}_3\text{COH}_2$	408		

4.3.2. Time dependence of plasma interaction

Continuous sampling of the same area with the visible part of the plasma flame in touch with the sample surface gives rise to spectral changes observed over time using helium added with water vapour. Changes in intensity with time were compared using initial analysis of pure paracetamol and caffeine solutions (both 5 $\mu\text{g}/\mu\text{L}$) which were measured separately, Figure 4.6. The plasma exposure has an effect on signal intensity. Notably, a similar behaviour was observed between the behaviour of the two compounds tested (paracetamol and caffeine) over time. There were also significant differences observed in the signal intensity of protonated paracetamol and caffeine ions. They showed that $[\text{M}+\text{H}]^+$ m/z 152 is 4x more abundant than M^+ m/z 194.

To investigate potential heating of the sample during the analysis, the temperature was measured using the exact same PADI parameters using a thermocouple (chromel-alumel type) under a TLC plate, Figure 4.6. The temperature was also measured using a thermal camera focused at the top of a TLC plate. In both experiments the visible plasma was held at the optimised 5 mm distance from the top of the TLC plate (27). During this acquisition period, the temperature rose to 45 $^{\circ}\text{C}$ in 60 seconds in the thermocouple measurements. The thermal camera measured an increase to 60 $^{\circ}\text{C}$ in 60 seconds, while it was below 60 $^{\circ}\text{C}$ when the previously discussed analysis time threshold was reached after 45 seconds. The $[\text{M}+\text{H}]^+$ peaks of both paracetamol and caffeine increase in intensity up to ~ 45 seconds, after which they decrease up to 1 minute. It seems unlikely that the limited temperature increase is the (sole) cause for this. Changes in intensity with time may, in principle, also be attributed to loss of analyte due to removal or degradation or continued excitation of analytes on the surface or in the gas phase. The porosity of the TLC plate may also have a role to play. Although the ratios by a factor of 152/194 and 152/195 are enough to investigate the level of fragmentation with time. Data acquisition for 35 seconds was

decided as the optimal time for the high-intensity signal of protonated paracetamol and the analysis can be stopped at that time in order to avoid any damage to the sample by the plasma.

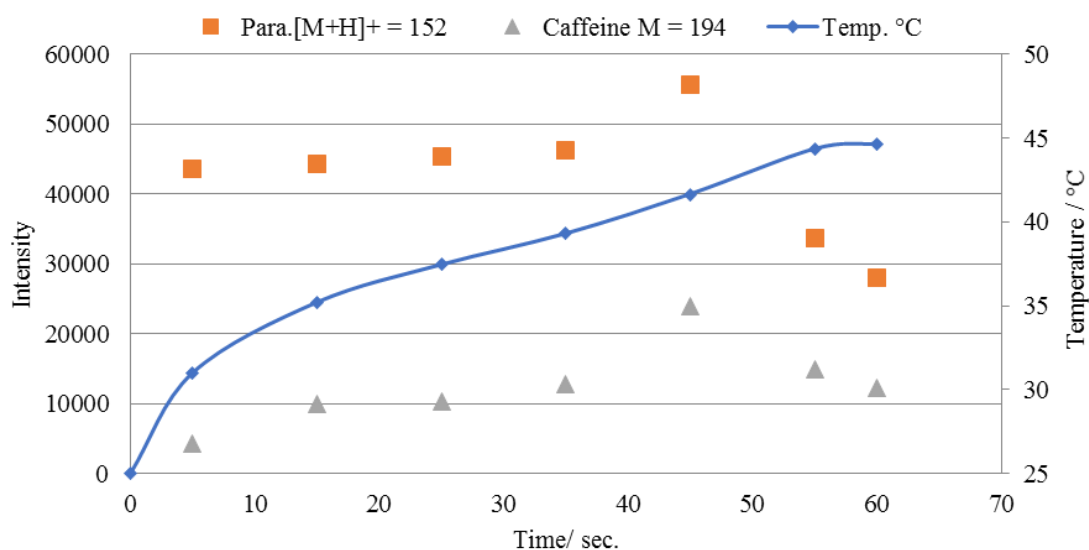


Figure 4. 6. The signal intensity of pure paracetamol and caffeine solutions (both 5 $\mu\text{g}/\mu\text{L}$) deposited on a TLC plate using helium added with water vapour in 5 seconds intervals 0-5, 10-15, 20-25, 30-35, 40-45 and 55-60 seconds using thermal couple.

The intensity of protonated paracetamol was also normalised to that of the caffeine molecular ion and protonated caffeine. The intensity ratios of 152/194 and 152/195 remained steady over the first 25 seconds, after which they decreased to 45 seconds, and then settle at a constant value up to 1 minute, Figure 4.7 and Figure 4.8. The results also showed that the intensity behaviour by a factor of 195/194 was similar to that of 152/194 and 152/195, Figure 4.9. According to these data, we can infer that PADI-MS is limited by analysis after 30 seconds due to it gives unstable signals after this time. It also found that the signal intensity of protonated paracetamol was higher than that used of caffeine

molecular ion and protonated caffeine over time, and this may be attributed to the same reasons as mentioned before.

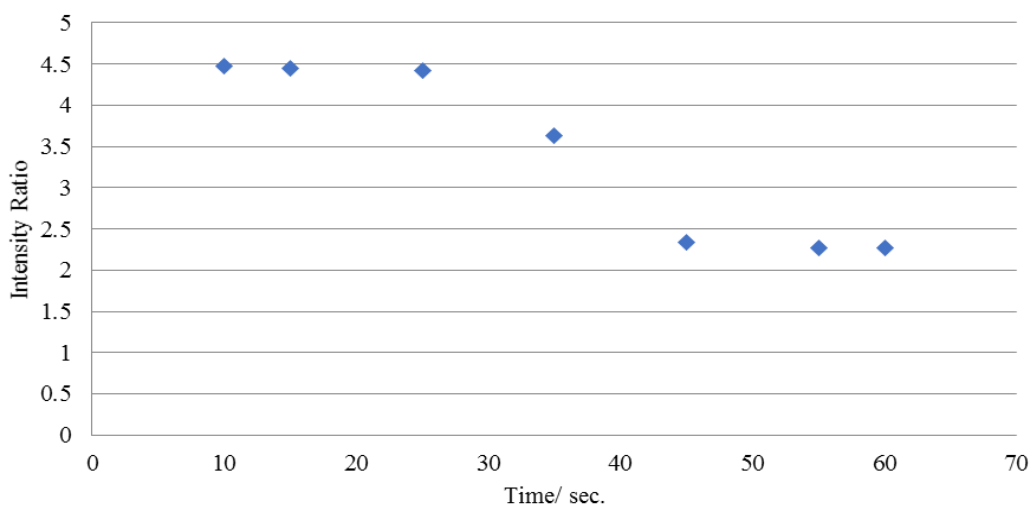


Figure 4. 7. Intensity ratios for paracetamol and caffeine by a factor of 152/194 (both 5 $\mu\text{g}/\mu\text{L}$) applied and measured separately using helium added with water vapour in 5 seconds intervals 0-5, 10-15, 20-25, 30-35, 40-45 and 55-60 seconds.

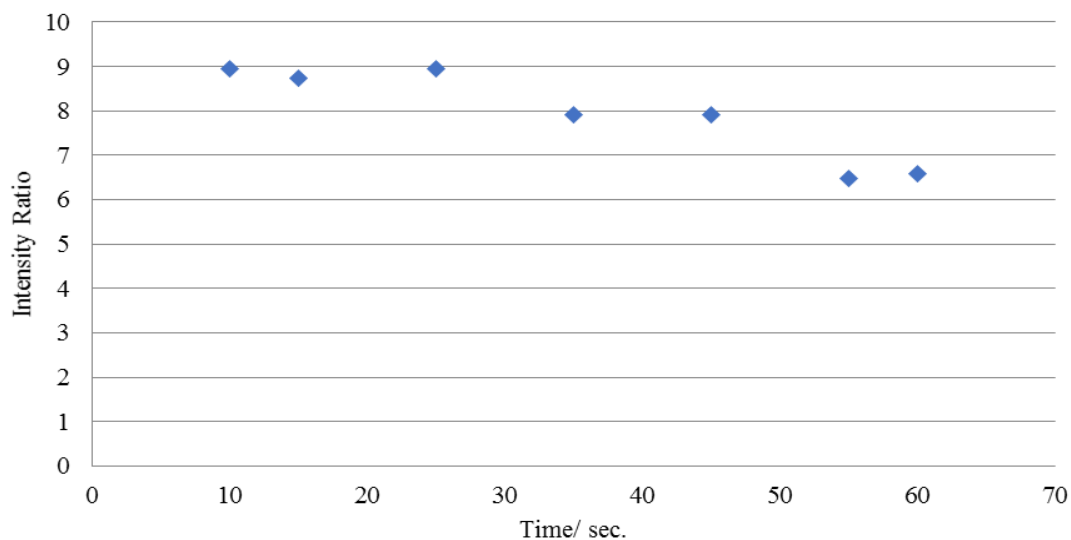


Figure 4. 8. Intensity ratios for paracetamol and caffeine by a factor of 152/195 (both 5 $\mu\text{g}/\mu\text{L}$) applied and measured separately using helium added with water vapour in 5 seconds intervals 0-5, 10-15, 20-25, 30-35, 40-45 and 55-60 seconds.

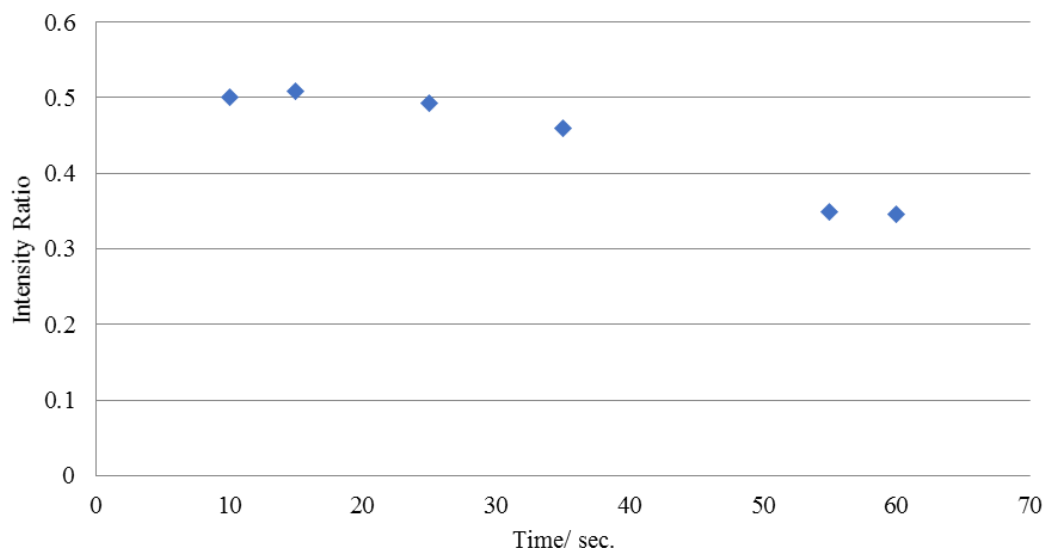


Figure 4. 9. Intensity ratios for caffeine by a factor of 195/194 ($5 \mu\text{g}/\mu\text{L}$) measured using helium added with water vapour in 5 seconds intervals 0-5, 10-15, 20-25, 30-35, 40-45 and 55-60 seconds.

4.3.3. Analysis of Mixtures

Various mixtures of paracetamol and caffeine were analysed as control samples before analysis of an off-the-shelf pharmaceutical mixture, Panadol ExtraTM. In all experiments, the same concentrations of 1:1 (w/w) mixed solutions of paracetamol and caffeine were used to analyse the mixtures except the Panadol tablet solution as shown in method A and B.

4.3.3.1. Method A: Analysis without separation of spots

The first set of mixture analysis aimed to identify paracetamol and caffeine spots on TLC plates using PADI-MS without separation. Changes in intensity as a function of time were compared using dry helium only and helium added with water vapour in the outer flow.

The results were compared to 'no sample' which was taken before sampling to spectra taken 'with sample' in the plasma plume (Figure 4.10). No sample spectrum shows a little of the sample but this fairly low level, and this may be due to contamination of the sniffer tube. The sniffer tube was cleaned several times to minimise contamination effects. The analysis presented here demonstrates the use of PADI analysis directly from TLC plates, using the mixtures of paracetamol/caffeine as models for pharmaceutically relevant mixtures. Paracetamol and caffeine aqueous solutions over a range of concentrations were deposited on a TLC plate and analysed immediately (without the need to dry) by PADI-MS using the optimal conditions as described in Section 4.3.1. High purity mixed solutions (1:1) were used as a standard to optimise conditions, Figure 4.10. Changes in intensity with time were compared using initial analysis of mixed solutions of paracetamol and caffeine (2.5 $\mu\text{g}/\mu\text{L}$) which were measured from TLC plates without separation of spots using helium added with water vapour and dry helium in time upon binning of data in 5 seconds intervals. The intensities for most diagnostic, adduct and fragment peaks of paracetamol using helium added with water vapour are higher than that used by dry helium, Figure 4.10. This agrees with the previous results for the separate molecules and again shows that using helium added with water vapour for sample analysis can improve peak intensities for all diagnostic ions. Protonated peaks of paracetamol and caffeine were used to measure the extent of the effect of using helium added with water vapour on mixture analysis.

The results found increases in the intensity of protonated paracetamol when using helium added with water vapour to be 2x higher to that used by dry helium, Figure 4.11. The results also showed that the protonated caffeine ($[\text{M}+\text{H}]^+$ m/z 195) is difficult to detect when using dry helium, Figure 4.12. This may be due to the caffeine molecule gaining a proton easier when using helium added with water vapour. Similar to that mentioned

before, 15 seconds is enough time to detect all diagnostic peaks relating to paracetamol and caffeine with good signals.

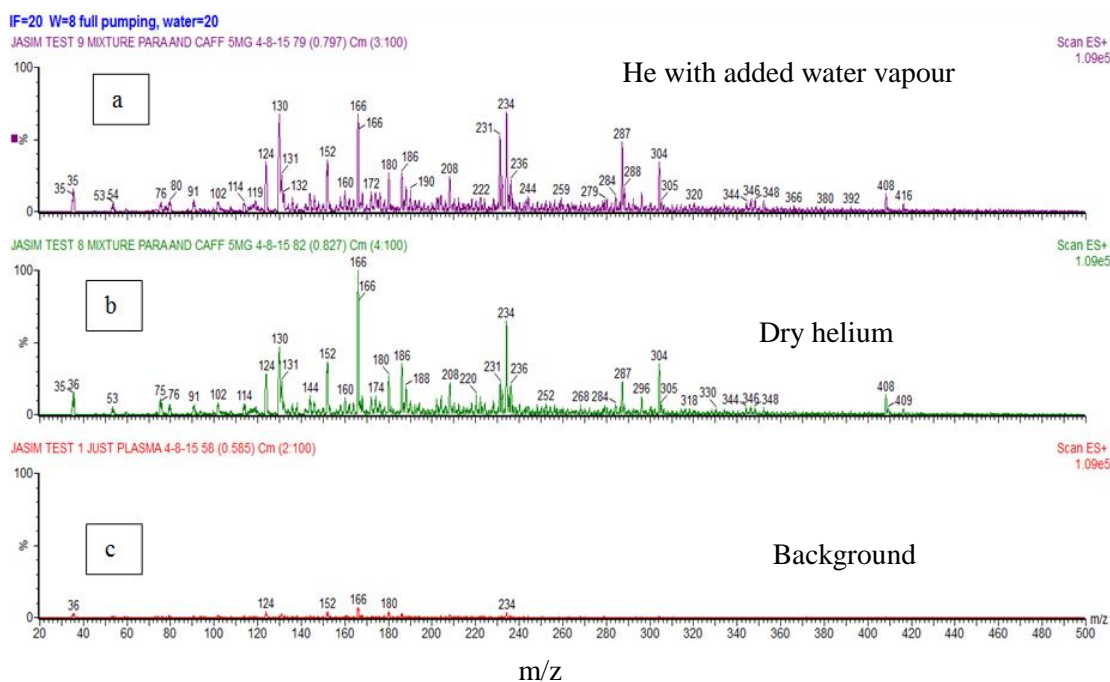


Figure 4. 10. PADI-MS spectra for the mixture solution of paracetamol and caffeine (both 2.5 $\mu\text{g}/\mu\text{L}$) from TLC plates using helium added with water vapour (a), dry helium (b) and background (c) with acquisition time of 1 minute.

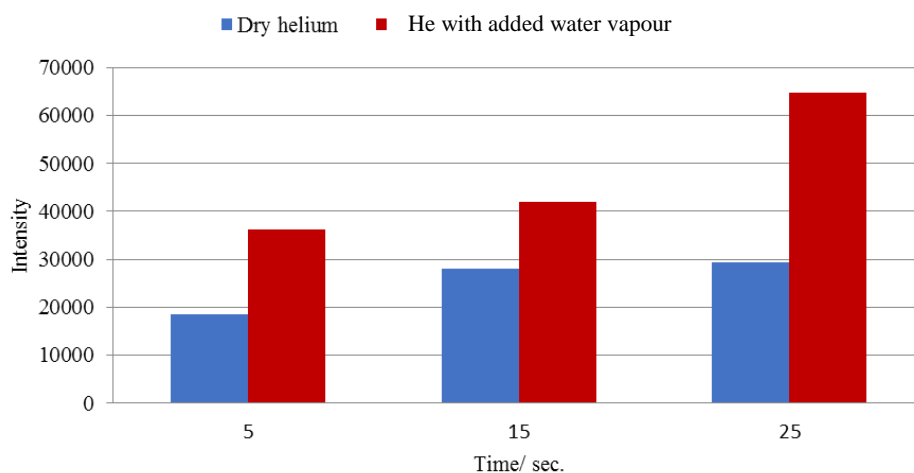


Figure 4. 11. Signal intensity of protonated paracetamol ($[\text{M}+\text{H}]^+$ m/z 152) (2.5 $\mu\text{g}/\mu\text{L}$) in the mixture solution from TLC plate using dry helium and added with water vapour in 5 seconds intervals 0-5, 10-15 and 20-25 seconds.

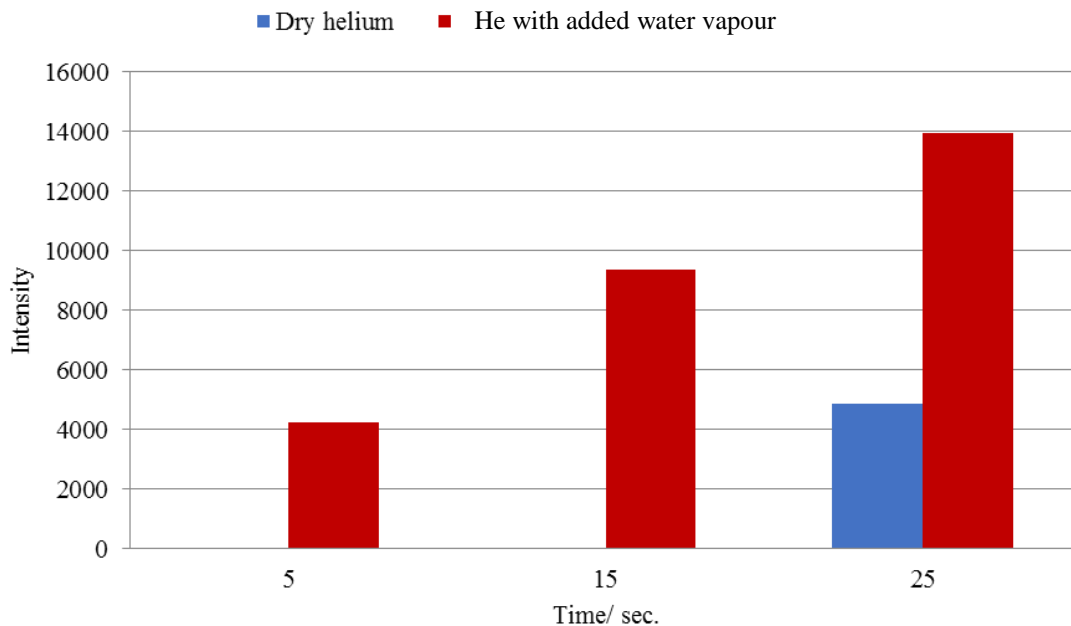


Figure 4. 12. Signal intensity of protonated caffeine ($[M+H]^+$ m/z 195) ($2.5 \mu\text{g}/\mu\text{L}$) in the mixture solution from TLC plate using dry helium and added with water vapour in 5 seconds intervals 0-5, 10-15 and 20-25 seconds.

The PADI-MS intensities of molecular ions / protonated ions of 1:1 mixed solutions onto a TLC plate are shown in Figure 4.13. As with the pure species, paracetamol gives rise to a strong singly charged species $[M+H]^+$ at m/z 152, with the presence of caffeine identified by M^+ at m/z 194. Time-dependent analysis of the main identifying peaks shows a similar profile as was observed for the pure compound analysis. There is a general increase in all peak intensities over the first ~35 seconds, after which the intensity of all peaks reduces. Different profiles are observed when using helium alone or when using an outer He flow added with water vapour such as sensitivity, with the additional $[M+H]^+$ peak of caffeine as discussed above and this gives more confirmation of the presence of caffeine in the solution. As can be seen from the Figure 4.13 there is more intense signal of protonated paracetamol in comparison with intensities of caffeine molecular ion and protonated

caffeine. The intensity of $[M+H]^+$ m/z 152 for paracetamol was higher $\sim 5x$ compared to that of M^+ m/z 194 for the caffeine molecular ion. The observed increase in the intensity of paracetamol in pure and mixture solutions could be explored by considering their respective pK_a values. The pK_a for paracetamol and caffeine are 9.5 and 14 respectively, therefore, caffeine is more basic (strong basic) than paracetamol (weak basic), hence caffeine molecular ion (M^+ m/z 194) could be expected to give small signal intensity. Another contributing factor might be related to the molecular mass of each compound. The molecular mass for paracetamol is 151 g/mol while for caffeine is 194, so, each 1 g of paracetamol contains 0.0066 moles whereas each 1 g of caffeine contains 0.0051 moles. Hence a 1/1 weight ratio means a molar ratio of (66/51). The results, as shown in all figures, also indicate that intensity of caffeine molecular is bigger than protonated caffeine. This means paracetamol accepts proton easier than caffeine. There are several possible explanations for these results. The first reason for this may be related to pK_a as mentioned before. The second reason could be attributed to the solubility of paracetamol and caffeine in the solvent. Because paracetamol is less polar than caffeine, paracetamol moves long with ethyl acetate on TLC plate compared to caffeine which interacts with silica gel (polar stationary phase) more than paracetamol. Another reason could be attributed to the amount of molecules per droplet in the solution of an individual and the mixtures of paracetamol/caffeine. The number of moles of paracetamol in the individual and mixtures is higher than caffeine. For example, paracetamol 5 $\mu\text{g}/\mu\text{L}$ contains 162 μg / 1.07 μmole , while caffeine 5 $\mu\text{g}/\mu\text{L}$ contains 162 μg / 0.83 μmole . Other amounts of paracetamol/caffeine mixtures are presented in Table 4.2.

These findings may help us to understand that the samples can be analysed easily by PADI-MS, with rapid analysis of less than 30 seconds giving molecular ion information without strongly affecting the sample due to plasma interaction until 30 seconds. For

example, the sample measurement can be repeated using specific time by heating the TLC plate to 45 °C and then put the sample immediately on TLC plate and measured directly by PADI-MS. The temperature was measured using the exact same PADI parameters using a thermocouple (chromel-alumel type). The results showed that the time is likely not a major effect as the temperature increase is so limited, Figures 4.6 and 4.13. Thermal desorption requires higher temperatures to become significant, considering that neither molecule evaporates very easily.

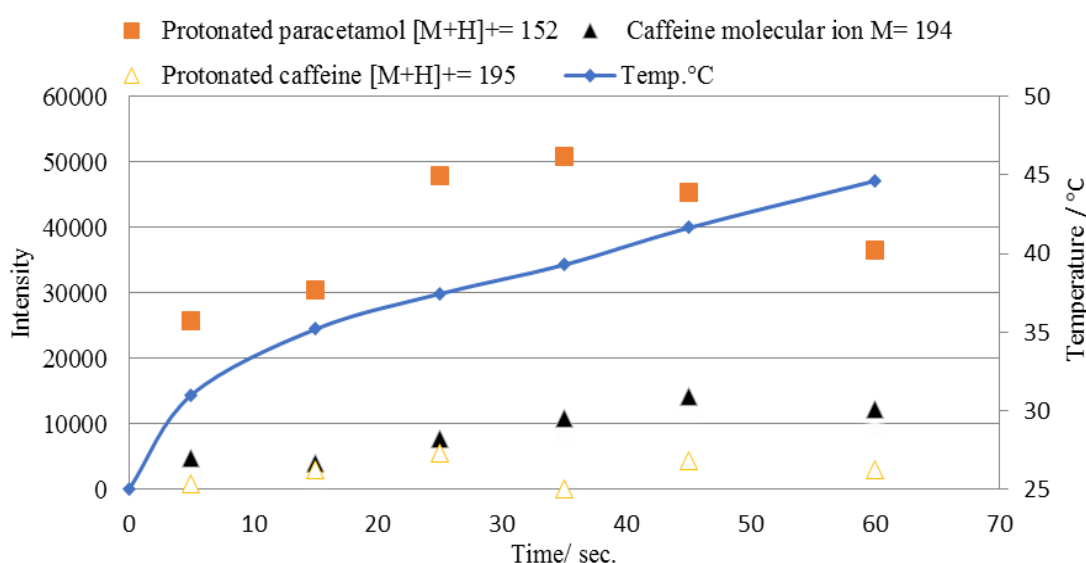


Figure 4. 13. Signal intensity of mixed solutions (1:1) paracetamol and caffeine (both 2.5 µg/µL) using helium added with water vapour in 5 seconds intervals 0-5, 10-15, 20-25, 30-35, 40-45 and 55-60 seconds.

The pure and mixture solutions of paracetamol and caffeine were compared in order to indicate whether a matrix effect occurs. The results of this study did not show any significant differences in intensities for paracetamol between pure and mixture spectra, Figure 4.14. Although the caffeine molecular ion peak cannot be seen at m/z 194 in the spectra, it also did not show changes in intensities between pure and mixture solutions.

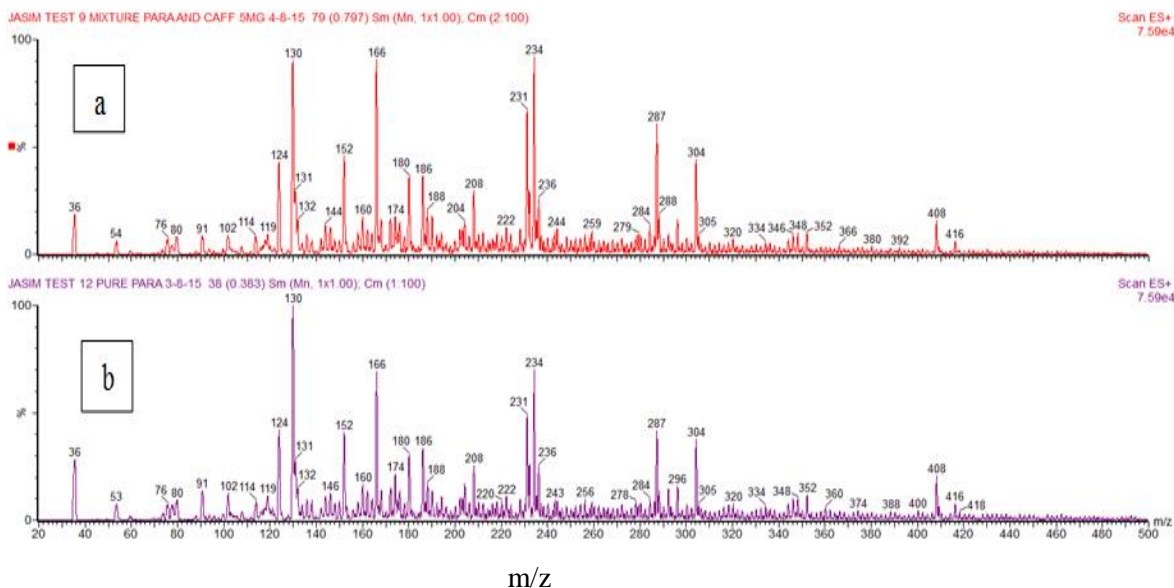
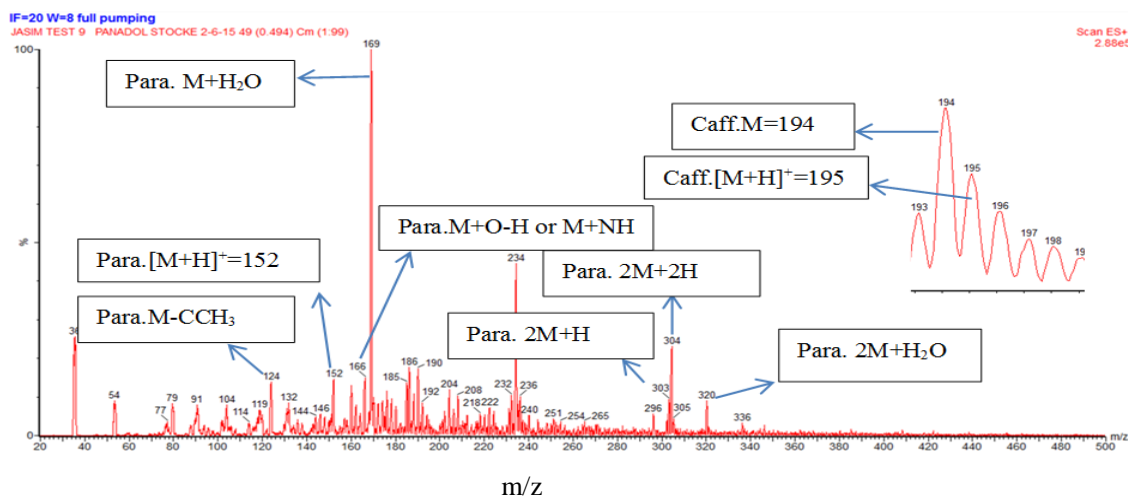


Figure 4. 14. PADI-MS spectra (20-500 m/z) of mixed solutions (1:1) paracetamol and caffeine (both 2.5 $\mu\text{g}/\mu\text{L}$) (a) and single paracetamol (5 $\mu\text{g}/\mu\text{L}$) from TLC plates using helium added with water vapour before separation of spots with a total acquisition time of 1 minute.

The results obtained from the analysis of paracetamol and caffeine in the mixture solution of Panadol are shown in Figure 4.15 a total acquisition time of 1 minute. Diagnostic peaks of caffeine were observed at m/z 194 for M^+ and m/z 195 for $[\text{M}+\text{H}]^+$. From the same PADI-MS spectrum, it can see that adduct ions of paracetamol: at m/z 152 for $[\text{M}+\text{H}]^+$, at m/z 169 for $[\text{M}+\text{H}_2\text{O}]^+$, at m/z 303 for $[2\text{M}+\text{H}]^+$, at m/z 304 for $[2\text{M}+2\text{H}]^{+2}$ and at m/z 320 for $[2\text{M}+\text{H}_2\text{O}]^+$. Other adduct and fragment peaks can be identified as listed in Table 4.3. This results indicate that the main identifying peaks here are similar to that observed of the pure compounds and mixture analysis, Figure 4.15. What stands out in the this Figure is that the ratio of components of paracetamol and caffeine in the mixture not affected on the identification. Mixture of paracetamol and caffeine in Panadol solution were compared with mixed solutions (1:1) paracetamol and caffeine, with a total acquisition time of 1 minute, Figure 4.16. There were also big differences observed in the signal intensity of

protonated paracetamol and caffeine ions. They showed that $[M+H]^+$ m/z 152 is 3x more abundant than M^+ m/z 194. The signal intensity of both 152 and 194 increased and reached a peak during ~35 seconds, after which they decreased until the end of data acquisition at 1 minute. This is indeed similar to that used by mixed solutions (1:1) of paracetamol and caffeine.



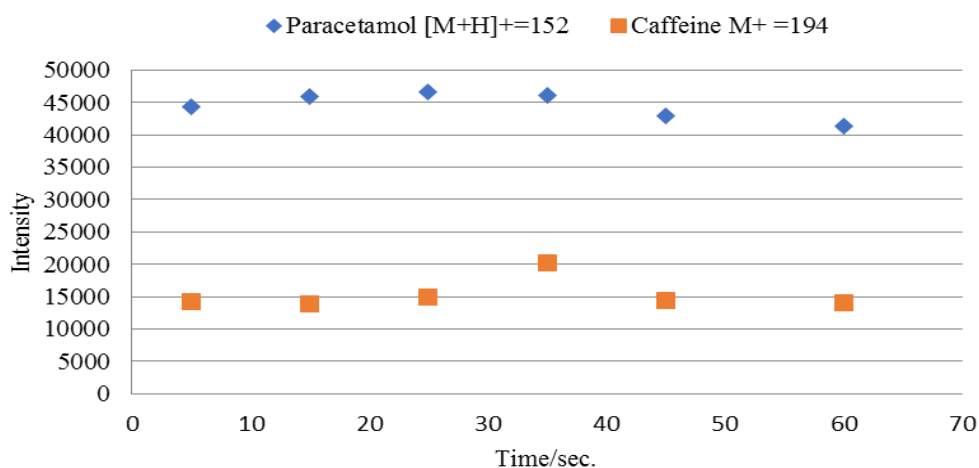


Figure 4. 16. PADI-MS data of Panadol solution containing 50 mg/mL paracetamol and 6.5 mg/mL of caffeine deposited on the TLC plate using helium added with water vapour before separation of spots with a total acquisition time of 1 minute.

4.3.3.2. Method B: Analysis after separation of spots

To compare the analysis with another method for detection and identification of pharmaceutical solutions, mixtures of paracetamol and caffeine were developed on the TLC plates using ethyl acetate as a solvent to obtain a better signal using the same optimal conditions. The second section of the analysis was concerned with depositing spots of paracetamol and caffeine on TLC plates and then separating these spots using ethyl acetate as solvent. The PADI-MS analysis was successful as it was able to identify the individual spots of paracetamol and caffeine which are separated on TLC plates. An increase in intensity was detected for pure paracetamol and caffeine solutions (both 5 $\mu\text{g}/\mu\text{L}$). A clear hydrated peak of solvent (ethyl acetate) was observed in the spectra of paracetamol and caffeine at m/z 106 $[\text{M}+\text{H}_2\text{O}]^+$, Figure 4.17. This refers to the immediate analysis of TLC plate after separation of spots while this peak (106) reduces on drying the TLC plate. Analyte spots were separated from TLC plates using ethyl acetate and then analysed immediately without drying by PADI-MS with, as previously an acquisition time of 1

minute. Diagnostic peaks for paracetamol such as $[M+H]^+$ m/z 152 and $[2M+H]^+$ m/z 304 were detected, the caffeine molecular ion was also observed at m/z 194, and other peaks can be identified as listed in Table 4.3. However, no extra peaks for caffeine were detected. For example, caffeine is expected to give a fragment peak at m/z 109 $M-CH_3N(CO)_2$. Identification of paracetamol and caffeine spots in the mixture solutions (both $2.5 \mu\text{g}/\mu\text{L}$) from TLC plate using PADI-MS with a total acquisition time of 1 minute is shown in Figure 4.18. It can be seen that a very small peak of protonated paracetamol is presented in the spectrum of before sampling and caffeine which we assign to contamination inside the mass spectrometer inlet, Figure 4.18. However, high signal intensities of protonated, fragment and adduct peaks of paracetamol and caffeine molecules were observed in the spectra after separation of spots from the same TLC plate. The results showed that identification of molecules' spots was improved after separation of spots on TLC plate with higher signals and lower noise. The results obtained from the different analysis times of paracetamol in the mixed solution (1:1) are shown in Figure 4.19. There has been a rise in the signal intensity of time up to ~ 35 seconds. These results suggest that in 5 seconds intervals 30-35 seconds was decided as the optimal time for the high-intensity signal of protonated paracetamol and the analysis can be stopped at that time. Changes in intensity in particular after 35 seconds may be due to that the sample can be affected by the plasma after this time. Changes in signal intensity of paracetamol in the mixed solutions (1:1) with the range of 0.01 - $2.5 \mu\text{g}/\mu\text{L}$ are presented in Figure 4.20. An increase in signal intensity of $[M+H]^+$ m/z 152 was observed up to ~ 35 seconds when using $2.5 \mu\text{g}/\mu\text{L}$ which was 14x more abundant than using $0.01 \mu\text{g}/\mu\text{L}$, after which they decreased by 8x up to 1 minute. However, with using higher concentration $> 2.5 \mu\text{g}/\mu\text{L}$, no increases in intensity can be observed.

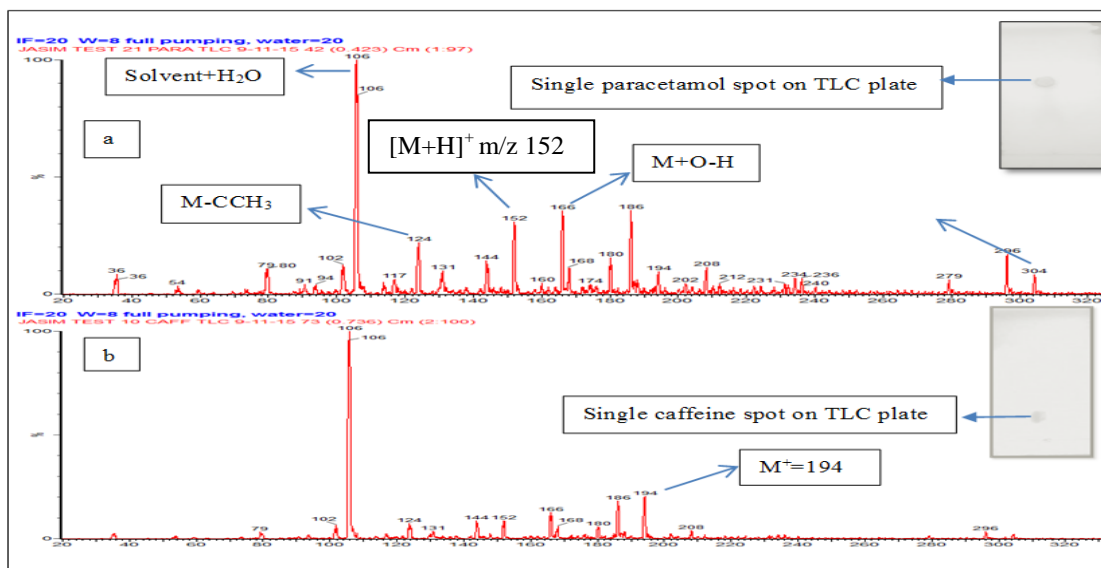


Figure 4. 17. PADI-MS spectra of individual spots of paracetamol (a) and caffeine (b) (both 5 $\mu\text{g}/\mu\text{L}$) on the TLC plate after separation of spots with a total acquisition time of 1 minute.

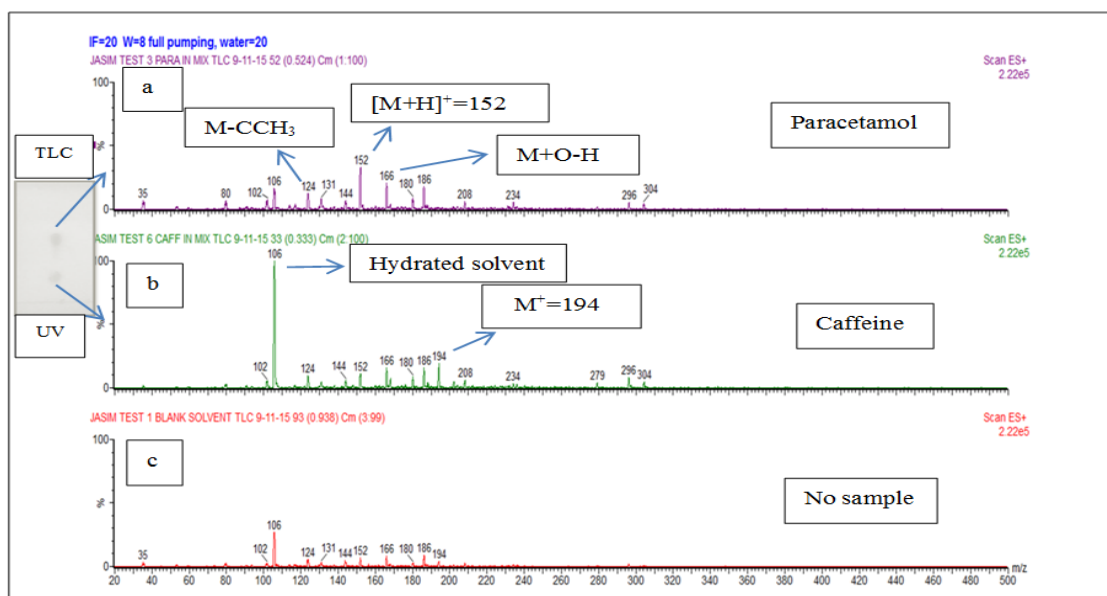


Figure 4. 18. PADI-MS spectra of paracetamol and caffeine spots (a and b respectively) (both 2.5 $\mu\text{g}/\mu\text{L}$) on the TLC plate after separation of spots with a total acquisition time of 1 minute.

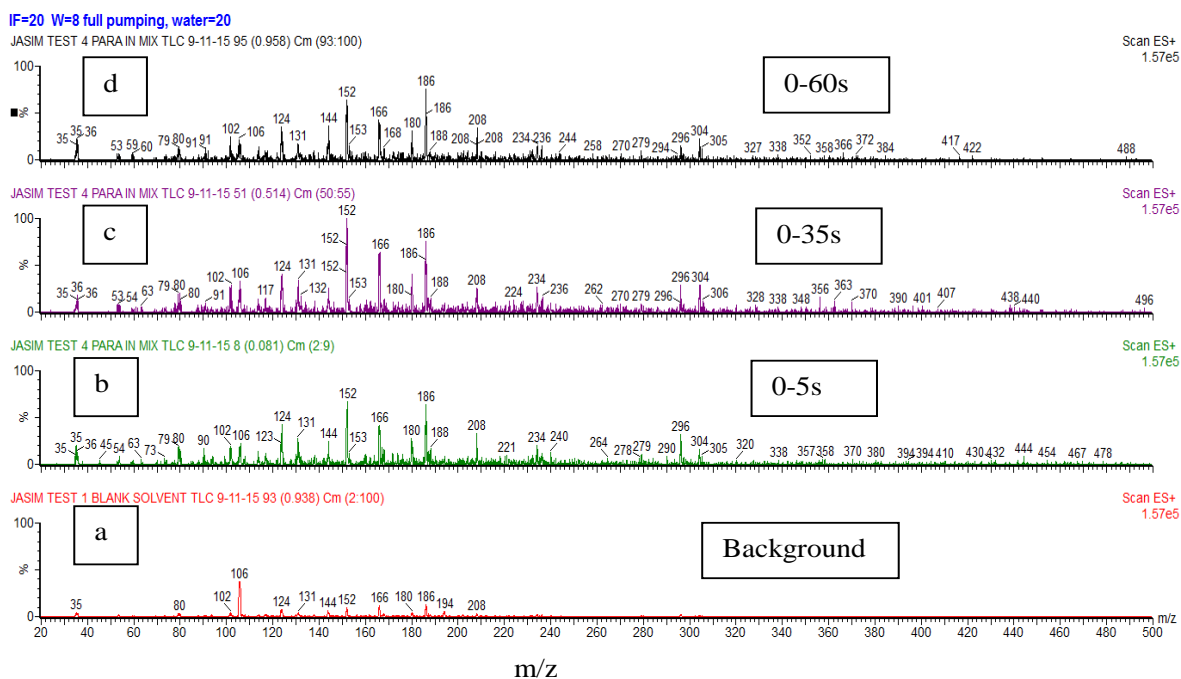


Figure 4. 19. PADI-MS spectra of paracetamol spot in the mixture solution (2.5 $\mu\text{g}/\mu\text{L}$) on the TLC plate in 5 seconds intervals 0-5 (b), 30-35 (c) and 55-60 seconds (d) after separation of spots with a total acquisition time of 1 minute.

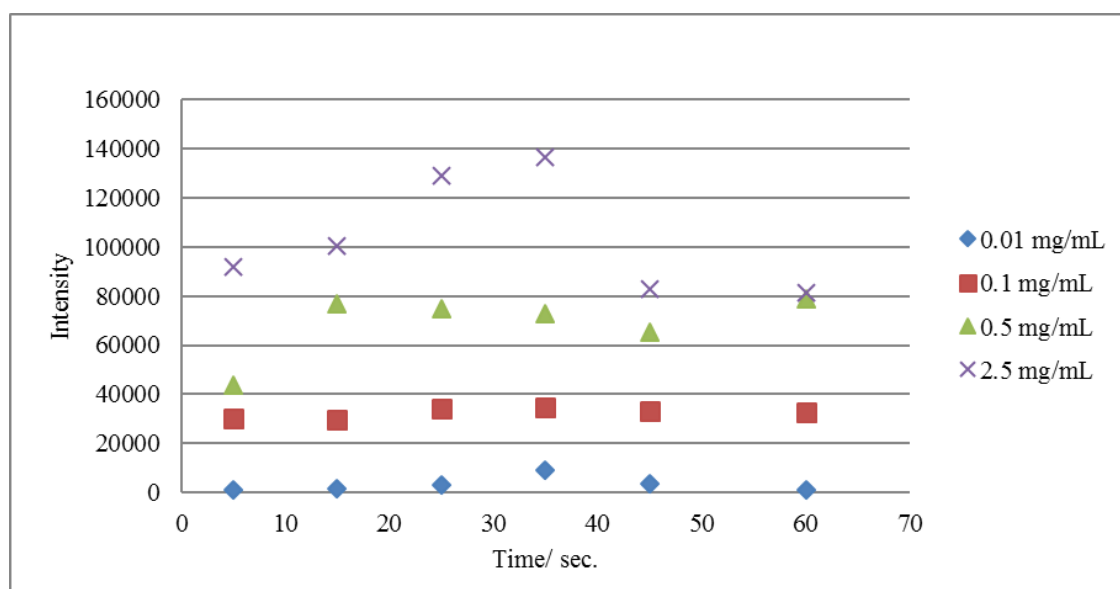


Figure 4. 20. Signal intensity of different mixture concentrations of protonated paracetamol $m/z = 152$ measured from TLC plates after separation of spots with a total acquisition time of 1 minute.

The intensity ratio of m/z 152/195 of 1:1 mixed of paracetamol and caffeine (both 2.5 $\mu\text{g}/\mu\text{L}$) was stable over the first 35 seconds, after which it decreases up to 1 minute, Figure 4.21. It is possible, therefore, that can measure these samples using this time to get a good correlation without any damage of the sample. There was also an increase in signal intensity of diagnostic peaks of paracetamol in the mixture solution on the TLC plates after separation of spots up to ~ 35 seconds, after which they decrease up to 1 minute, Figure 4.22. No differences between the behaviour of the intensity of paracetamol peaks and caffeine peaks have found before and after separation of spots on TLC plates.

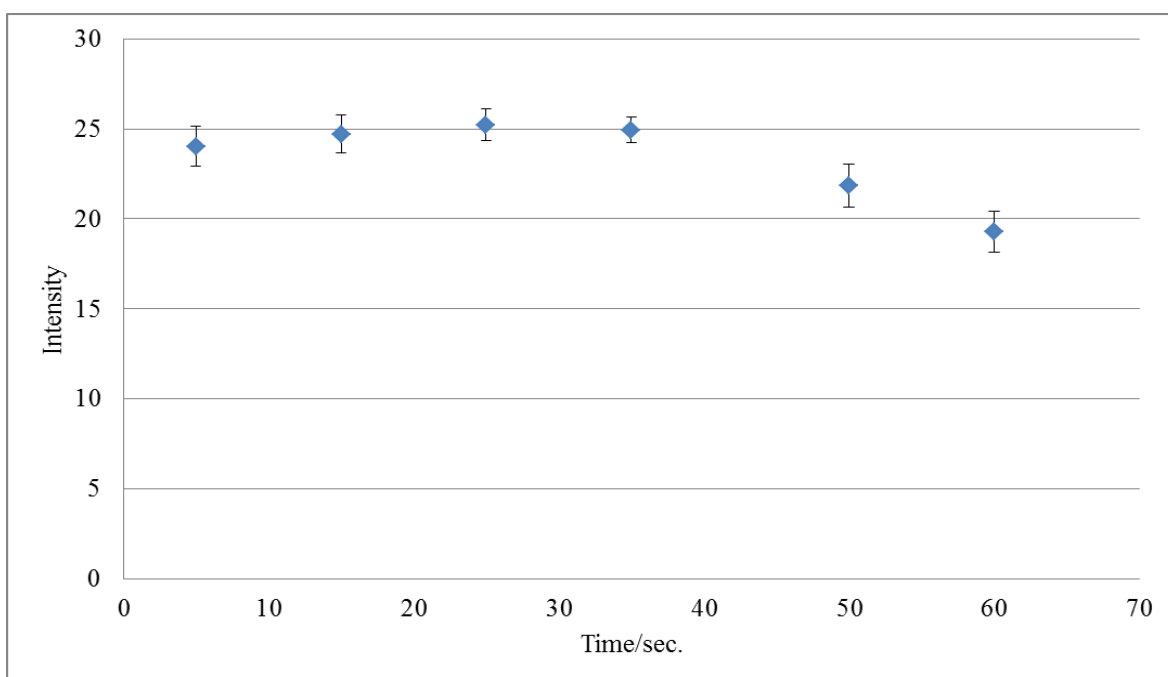


Figure 4. 21. Intensity ratios by a ratio of 152/195 of 1:1 mixed of paracetamol and caffeine (both 2.5 $\mu\text{g}/\mu\text{L}$) applied using TLC plate after separation of spots with a total acquisition time of 1 minute.

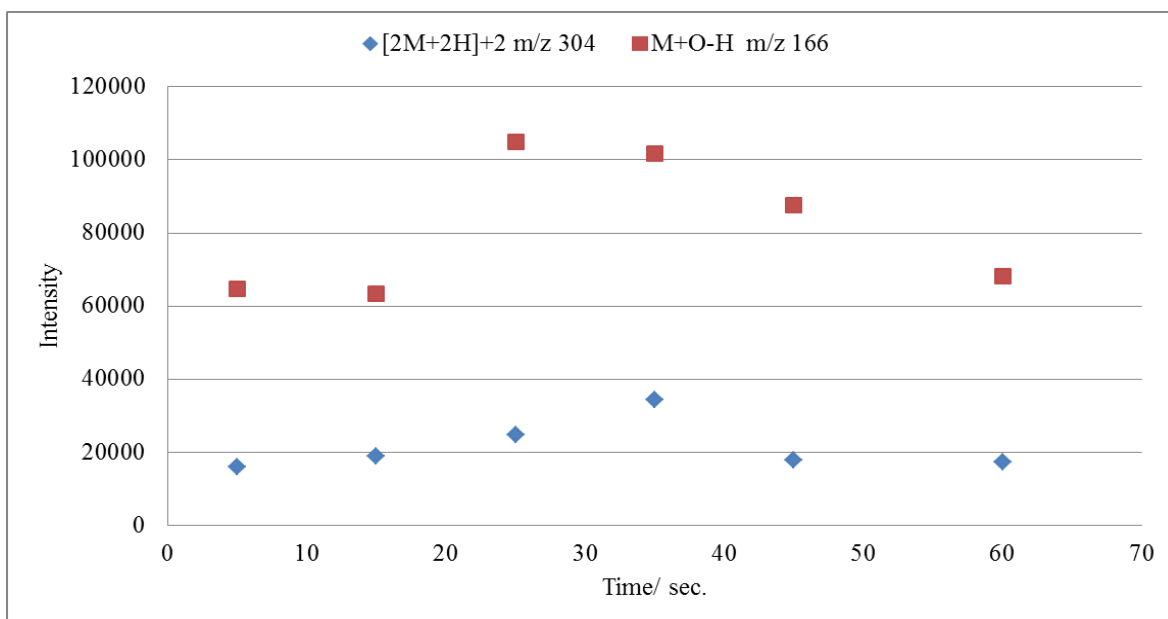


Figure 4. 22. Signal intensity of 1:1 mixture of [2M+2H]⁺2 m/z 304 and M+O-H m/z 166 for paracetamol (2.5 µg/µL) using TLC plate after separation of spots with a total acquisition time of 1 minute.

4.3.4. Quantification

Further experiments of the mixture solutions at lower concentrations of paracetamol and caffeine from TLC plates were analysed by PADI-MS. The correlation between signal intensity and concentration of paracetamol and caffeine was determined for the concentration range of 0.01 to 0.1 µg/µL in 5 seconds intervals 30-35 seconds. The calibration curves between peak intensity and concentrations of protonated paracetamol and caffeine molecular ions in the mixture solution without and after separation of spots are presented in Figure 4.23 and Figure 4.24. There was a positive correlation between signal intensity and concentrations of the mixture solutions with a very good linear relationship after separation of spots.

The correlation coefficients (R^2) values of paracetamol and the caffeine were found to be 0.972 and 0.966 without separation of spots (Figure 4.23), 0.999 and 0.996 respectively

after separation of spots (Figure 4.24). The limit of detection (LOD) and limit of quantification (LOQ) were also determined by considering standard deviation to the slope:

$$LOD = \frac{STEYX}{Slope} \times 3$$

$$LOQ = \frac{STEYX}{Slope} \times 10$$

STEYX means the standard deviation of the y-value and x-value.

Very promisingly, when a 1:1 mixed solution of lower concentration (both 0.01 $\mu\text{g}/\mu\text{L}$) were spotted on the TLC plate, it was not possible to identify the spot under UV light. Therefore, the spot was assumed to be in the same location as after higher concentration experiments, and that area was analysed directly by PADI-MS. Diagnostic peaks of paracetamol and caffeine were detected in the 0.01 $\mu\text{g}/\mu\text{L}$ mixture solution. This confirms that PADI-MS is more sensitive than UVspectroscopy as expected.

The comparison showed significant differences between the LOD and LOQ before and after separation of the spots. The limits of detection for paracetamol before and after separation of spots were found to be 0.14 mg/mL and 15 $\mu\text{g}/\text{mL}$ respectively, while for caffeine were 0.16 mg/mL and 49 $\mu\text{g}/\text{mL}$ respectively. The limits of quantification (LOQ) for paracetamol before and after separation of spots were found to be 0.48 mg/mL and 50 $\mu\text{g}/\text{mL}$ respectively, while for caffeine were 0.54 mg/mL and 165 $\mu\text{g}/\text{mL}$ respectively. These results indicate that the LOD and LOQ for paracetamol and caffeine can be improved when the TLC is developed by separating the spots. However, the linearity is limited using high concentrations of the mixture ($> 0.5 \mu\text{g}/\mu\text{L}$) for both before and after separation of spots because it causes nonlinearity including deviation in the calibration curve.

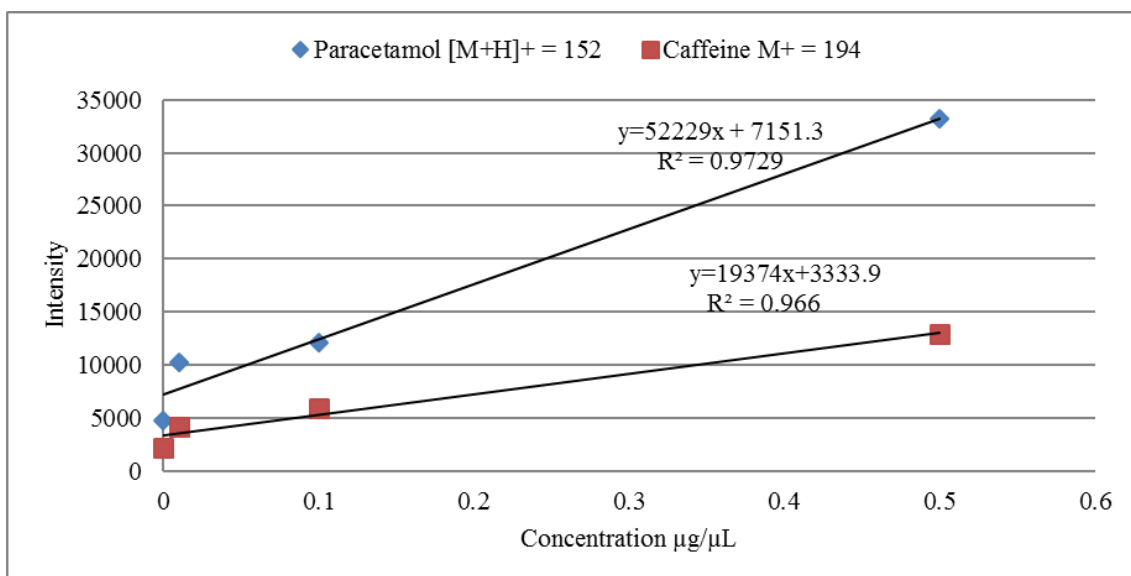


Figure 4. 23. Plot of mass spectrum intensity versus concentrations of aqueous 1:1 paracetamol and caffeine without separation of the spots with a total acquisition time of 30-35 seconds.

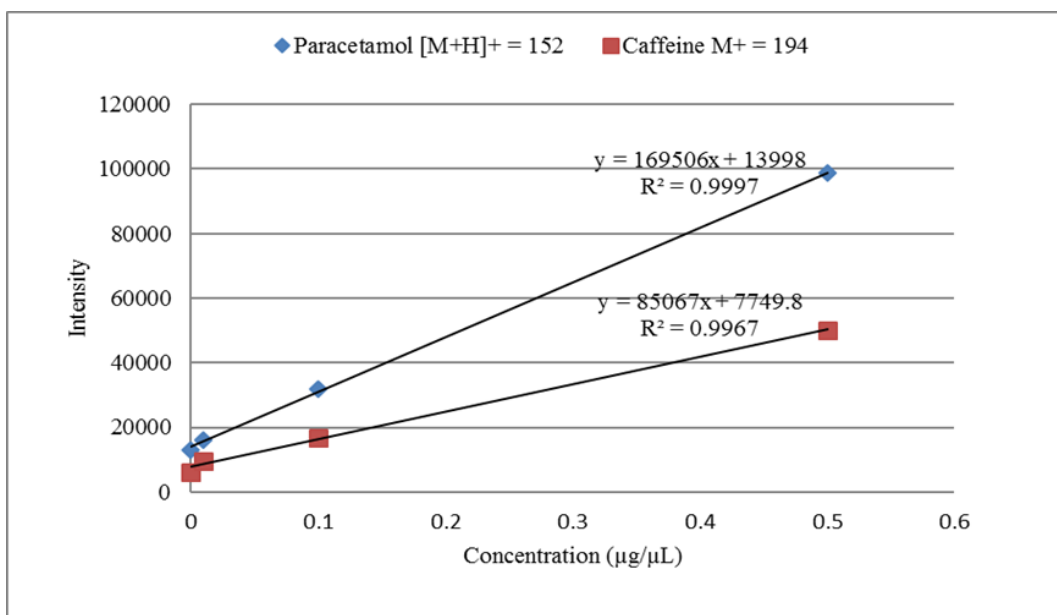


Figure 4. 24. Plot of mass spectrum intensity versus concentrations of aqueous 1:1 paracetamol and caffeine after separation of spots with a total acquisition time of 30-35 seconds.

4.3.4.1. Practical evaluation

There were differences between the results of mixture analysis using dry and wet TLC plates. Mixture spots of paracetamol and caffeine were deposited on TLC plates and then separated using ethyl acetate as a solvent and allowed to dry for more than 30 minutes, prior to analysis by PADI-MS with an acquisition time of 1 minute. The results were inferior: the caffeine spot could not be identified in this analysis and it was also difficult to see all adduct and fragment peaks of paracetamol in the PADI-MS spectra. A possible explanation for this might be that solutions were absorbed into the porous alumino-silicate layer of the TLC plates during the drying. The results showed that the paracetamol spectrum is similar to the caffeine spectrum and no difference was observed, Figure 4.25. This may be due to the solubility of paracetamol and caffeine in the solvent. Paracetamol moves long with ethyl acetate on TLC plate compared to caffeine which interacts with silica gel (polar stationary phase) more than paracetamol. Changes in signal intensity of paracetamol in the mixed solutions (1:1) with the range of 0.02-2.5 $\mu\text{g}/\mu\text{L}$ are presented in Figure 4.26.

There were several important differences between the results when using dry TLC plates and wet TLC plates to analyse a mixture of paracetamol and caffeine after separation of spots. With using wet TLC plates there has been a regular increase in the intensity of protonated paracetamol at all concentrations over interaction time up to ~35 seconds, after which it decreases up to 1 minute, Figure 4.20. However, an irregular behaviour of intensities was found with using dry TLC plates, Figure 4.26. There was a positive correlation between signal intensity and concentrations of the mixture solutions with a very good linear relationship when using wet TLC plates, Figure 4.24, while not good correlation between signal intensity and concentrations was found when using dry TLC

plates, Figure 4.27. The correlation coefficients (R^2) values of paracetamol and the caffeine were found to be 0.8256 and 0.7083 respectively using dry TLC plates (Figure 4.27).

The comparison showed differences between the LOD and LOQ using wet and dry TLC plates. The limits of detection using wet TLC plates were found to be 15 $\mu\text{g/mL}$ for paracetamol and 49 $\mu\text{g/mL}$ for caffeine, whereas they were 395 $\mu\text{g/mL}$ and 551 $\mu\text{g/mL}$ respectively using dry TLC plates. The limits of quantification using wet TLC plates were found to be 50 $\mu\text{g/mL}$ for paracetamol and 165 $\mu\text{g/mL}$ for caffeine, while they were 1317 $\mu\text{g/mL}$ and 1839 $\mu\text{g/mL}$ respectively using dry TLC plates. That is a positive result that drying is not required which saves a lot of time.

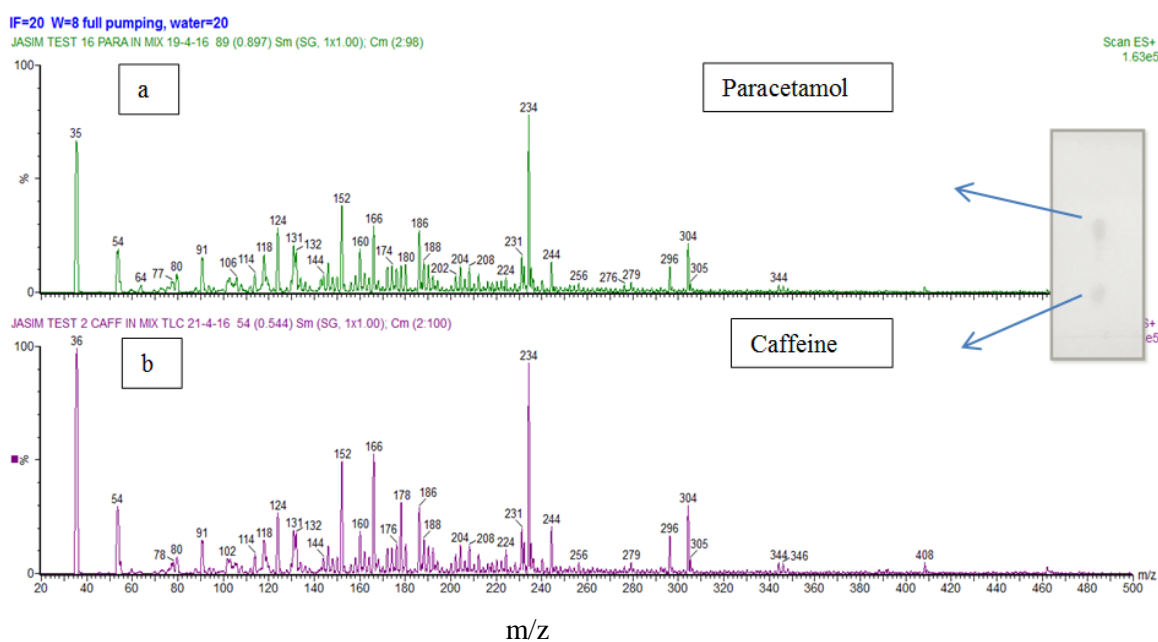


Figure 4. 25. PADI-MS spectra of aqueous 1:1 paracetamol and caffeine using dry TLC plate (both 2.5 $\mu\text{g}/\mu\text{L}$) after separation of spots with a total acquisition time of 1 minute.

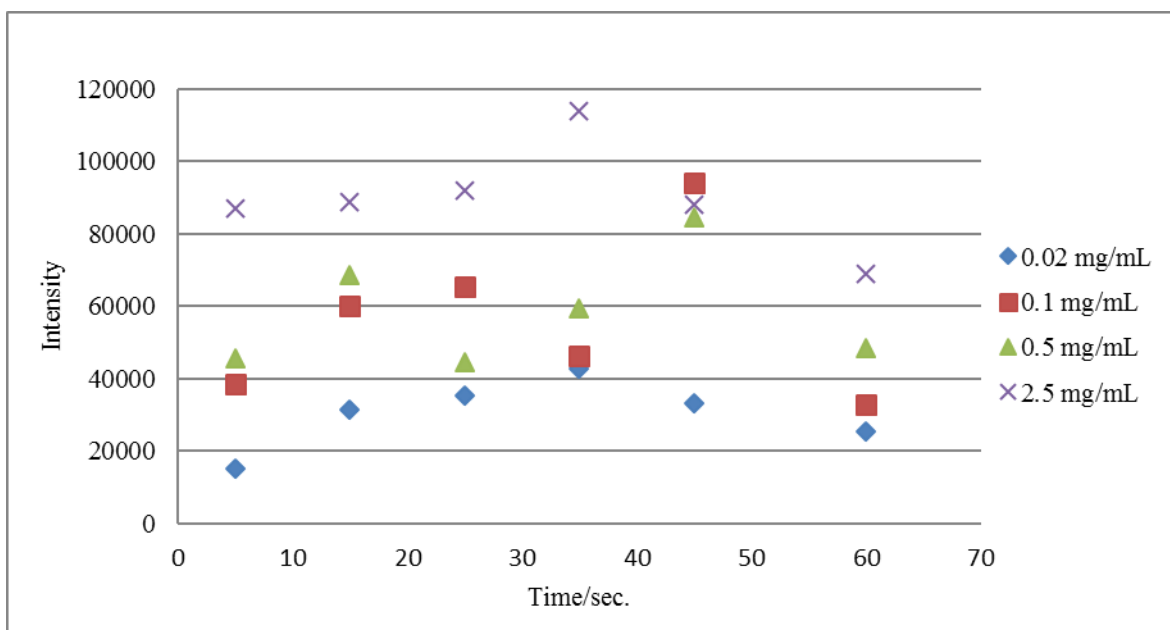


Figure 4. 26. Signal intensity of different mixture concentrations of paracetamol in aqueous 1:1 solution measured from dry TLC plates after separation of spots with a total acquisition time of 1 minute.

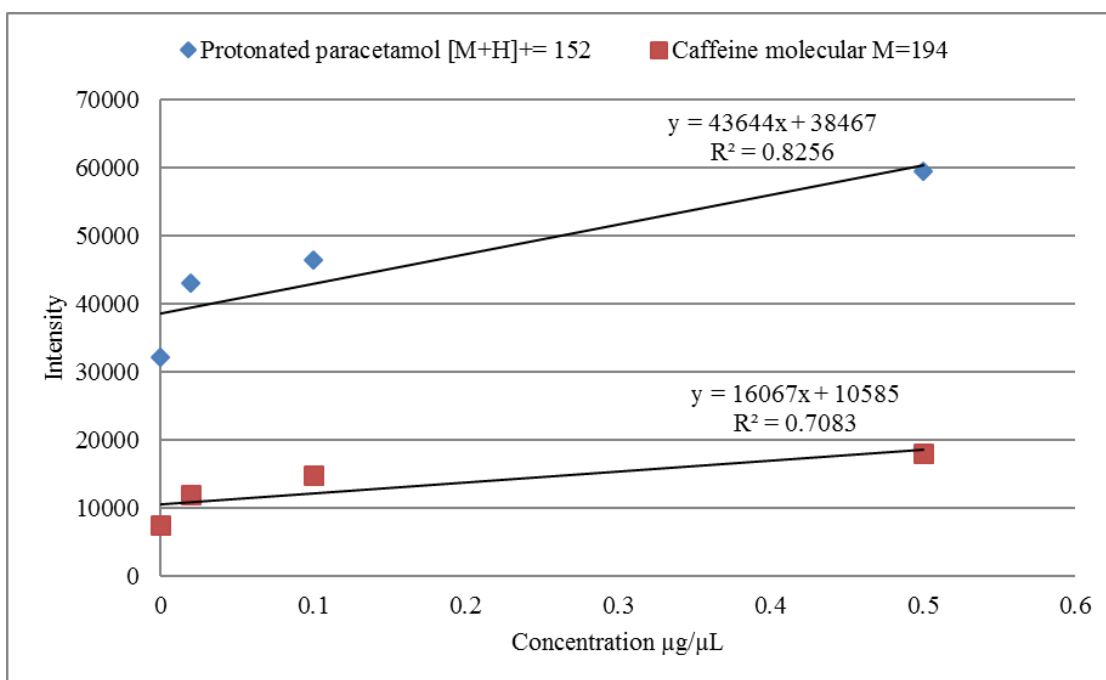


Figure 4. 27. Plot of mass spectrum intensity versus concentrations of aqueous 1:1 paracetamol and caffeine solution after separation of spots using dry TLC plate with a total acquisition time of 30-35 seconds.

4.4. Conclusions

PADI-MS was used in this study due to it being a sensitive technique, allowing direct analysis in seconds, its ease of use and in order to avoid limitations of techniques currently used for the analysis of mixtures in the pharmaceutical industry. This study set out to identify chemical components in mixture solutions of pharmaceutically relevant compounds on TLC plates. Paracetamol and caffeine were used as model compounds. This study has indicated that the PADI-MS technique is able to be used for direct analysis of pharmaceutical liquids using this simple substrate. The results showed that the method is simple, sensitive, fast and has good linearity. Small amounts of samples are required for analysis compared to other methods.

The study showed that small spots containing low amounts of compounds (4 μ L, which contained 8 ng of analyte) could easily be analysed from a TLC plate by PADI-MS without sample preparation in 35 seconds. Best results were achieved when immediately analysing the TLC plates without prior drying. In addition, the study showed that the limit of detection of paracetamol and caffeine using PADI detection was at least 10x better than using UV detection. This study has shown that a 35s acquisition was the optimal time for the high-intensity signal of adduct and fragment peaks for paracetamol and caffeine in the liquid sample. However, significantly shorter acquisition provided sufficient signal to identify these compounds. The results showed that identification of spots was improved after separation of spots on the TLC plate with higher signals and lower background. The intensity of protonated paracetamol (152) is 5x more abundant than caffeine molecular ion (194) in the mixture solution. Positive correlation was found between signal intensity and concentrations of the mixture solutions when measuring immediately after deposition or developing, but not after drying TLC plates. This might be related to the absorption of solution compounds into the porous alumina layer on the TLC plates.

The main goal of the current study was to develop a novel method that can be used for identification of components in complex mixtures that cannot be (conveniently) resolved by other methods such as chromatographic and spectroscopic techniques. Considerably more work needs to be carried out to detect and identify the components in mixture solutions from other substrates. The results of this study can be applied for identification of other pharmaceutical mixture solutions using TLC plates, and it also may well have a bearing on quantitative analysis. One of the greatest challenges for future research is the quantitative analysis of mixture solutions from TLC plates using this method.

Overall, this study has found that generally, the components in a mixture can be identified directly from a TLC plate by PADI-MS without separation of spots (method A), and this can save time and solvents. However, for low concentrations of caffeine, in particular, it is recommended to achieve the optimal limit of detection by first separating the spots on the TLC plate using ethyl acetate as a solvent and then analysing the individual spots of paracetamol and caffeine by PADI-MS (Method B). In the experiments of this study, the same concentrations of 1:1 (w/w) mixed solutions of paracetamol and caffeine were used in the mixtures solutions. In future investigations, different concentrations and ratios of these mixtures should be explored in order to further investigate potential and suppression effects. Comparing the effect of added water vapour to the He flow, important differences were found. Intensities of paracetamol and caffeine in the mixture solution were noticeably improved using this simple modification.

References

1. Chanchala, D. K. Rachel, V. B. Martin, R. L. P. Mitchel, D. B. Arthur, L. W. Facundo, M. F. and May, D. W. (2016) 'Detect TLC: Automated reaction mixture screening utilizing quantitative mass spectrometry image features', *Journal of the American Society for Mass Spectrometry*, 27, p.p. 359–365.
2. Boutaud, O. Aronoff, D. M. Richardson, J. H. Marnett, L. J. and Oates, J. A. (2002) 'Determinants of the cellular specificity of acetaminophen as an inhibitor of prostaglandin H₂ synthases', *Proceedings of the National Academy of Sciences of the United States of America*, 99 (10), p.p. 7130–7135.
3. Chandrasekharan, N. V. Dai, H. Roos, K. L. T. Evanson, N. K. Tomsik, J. Elton, T. S. and Simmons, D. L. (2002) 'COX-3, a cyclooxygenase-1 variant inhibited by acetaminophen and other analgesic/antipyretic drugs: Cloning, structure, and expression', *Proceedings of the National Academy of Sciences of the United States of America*, 99 (21), p.p. 13926–13931.
4. Laska, E. M. Sunshine, A. Zigelboim, I. Roure, C. Marrero, I. Wanderling, J. and Olson, N. (1983) 'Effect of caffeine on acetaminophen analgesia', *Clinical Pharmacology & Therapeutics*, 33 (4), p.p. 498–509.
5. Wang, S.F., Xie, F. and Hu, R.F. (2007) 'Carbon-coated nickel magnetic nanoparticles modified electrodes as a sensor for determination of acetaminophen', *Sensors and Actuators B* 123, p.p. 495–500.
6. Koch-Weser, J. (1976) 'Medical intelligence. Drug therapy: acetaminophen', *The New England Journal of Medicine*, 295 (23), p.p. 1297–1300.
7. Clissold, S.P. (1986) 'Paracetamol and phenacetin', *Drugs*, 32, p.p. 46–159.

8. Nikles, C.J. Yelland, M. Marc, C.D. and Wilkinson, D. (2005) 'The role of paracetamol in chronic pain: an evidence-based approach', *American Journal of Therapeutics*, 12(1), p.p. 80–91.
9. Bhawani, S. A. Fong, S. S. and Ibrahim, M. N. M. (2015) 'Review Article: Spectrophotometric analysis of caffeine', *International Journal of Analytical Chemistry*, pp. 1–7.
10. Wanyika, H. N. Gatebe, E. G. Gitu, L. M. Ngumba, E. K. and Maritim, C. W. (2010) 'Determination of caffeine content of tea and instant coffee brands found in the Kenyan market', *African Journal of Food Science*, 4(6), p.p. 353 – 358.
11. Neal, L. and Benowitz, M.D. (1990) 'Clinical pharmacology of caffeine', *Annual Review of Medicine*, 41, pp. 277–288.
12. Sand, B. Kudrow, L. and Haghighi, A. (2002) 'Analysis of caffeine', p.p. 1–5.
13. Christena, V. Hickmann, S. Rechenberg, B. and Fent, K. (2010) 'Highly active human pharmaceuticals in aquatic systems: A concept for their identification based on their mode of action', *Aquatic Toxicology*, 96, p.p. 167–181.
14. Franeta, J.T. Agbaba, D. Eric, S. Pavkov, S. Aleksic, M. and Vladimirov, S. (2002) 'HPLC assay of acetylsalicylic acid, paracetamol, caffeine and phenobarbital in tablets', *Il Farmaco*, 57 (9), p.p. 709–713.
15. Siddiqui, M. R. AlOthman, Z. A. and Rahman, N. (2017) 'Analytical techniques in pharmaceutical analysis: A review', *Arabian Journal of Chemistry*, 10, p.p. 1409–1421.
16. Sun, S. F. Lui, G. R. and Wang, Y. H. (2006) 'Simultaneous determination of acetaminophen, caffeine, and chlorphenamine maleate in paracetamol and chlorphenamine maleate granules', *Chromatographia*, 64 (11–12), p.p. 719–724.

17. Adress Hasan, H. M. Habib, I. H. and Khatab, A. A. (2017) 'RP-HPLC Determination of Paracetamol-Containing Components in Quaternary and Binary Mixtures', *European Chemical Bulletin*, 6(7), p.p. 330–335.
18. De Lima Gomes, P.C. Barletta, J.Y., Nazario, C.E., Santos-Neto, A.J., Von Wolff, M.A. Coneglian, C.M. Umbuzeiro, G.A. and Lancas, F.M. (2011) 'Optimisation of in situ derivatization SPME by experimental design for GC-MS multi-residue analysis of pharmaceutical drugs in wastewater', *Journal of Separation Science*, 34(4), p.p. 436–445.
19. Wollein, U. and Schramek, N. (2012) 'Simultaneous determination of alkyl mesitates and alkyl besitates in finished drug products by direct injection GC/MS', *European Journal of Pharmaceutical Sciences*, 45(1-2), p.p. 201–204.
20. Wang, X.M. Zhang, Q.Z. Yang, J. Zhu, R.H. Zhang, J., Cai, L.J. and Peng, W.X. (2012) 'Validated HPLC-MS/MS method for simultaneous determination of curcumin and piperine in human plasma', *Tropical Journal of Pharmaceutical Research*, 11(4), p.p. 621–629.
21. Nandakumar, S. Menon, S. and Shailajan, S. (2012) 'A rapid HPLC-ESI-MS/MS method for determination of β -asarone, a potential anti-epileptic agent, in plasma after oral administration of *Acorus calamus* extract to rats', *Biomedical Chromatography*, 27(3), p.p. 318–326.
22. Lim, C.K. and Lord, G. (2002) 'Current developments in LC-MS for pharmaceutical analysis', *Biological and Pharmaceutical Bulletin*, 25(5), p.p. 547–557.
23. Lee, P.J. Murphy, B.P. Balogh, M.P. and Burgess, J.A. (2010) 'Improving organic synthesis reaction monitoring with rapid ambient sampling mass spectrometry', Waters Corporation, Milford, MA, USA.

24. Santiago da Silva, C.M. Habermann, G. Marchi, M.R.R. and Zocolo, G. J. (2012) 'The role of matrix effects on the quantification of abscisic acid and its metabolites in the leaves of *Bauhinia variegata* L. using liquid chromatography combined with tandem mass spectrometry', *Brazilian Journal of Plant Physiology*, 24(3), p.p. 223–232.
25. Salter, T.L.R. Bunch, J. and Gilmore, I.S. (2014) 'Importance of sample form and surface temperature for analysis by ambient plasma mass spectrometry (PADI)' *Analytical Chemistry*, 86, p.p. 9264–9270.
26. Ratcliffe, L.V. Rutten, F.J.M. Barrett, D.A. Terry Whitmore, T. Seymour, D. Greenwood, C. Gonzalvo, Y.A. Robinson, S. and McCoustra, M. (2007) 'Surface analysis under ambient conditions using plasma-assisted desorption/ ionisation mass spectrometry' *Analytical Chemistry*, 79 (16), p.p. 6094–6101.
27. P. Roach and F.J.M. Rutten, to be publish

**CHAPTER 5: Plasma-assisted desorption ionisation
mass spectrometry – PADI-MS for the analysis of
pharmaceutical solids and liquids from glass slides and
cotton swabs**

Abstract

Compared to chapter 4, this study has identified different pharmaceutical forms (solids and liquids) using different substrates such as glass slides and cotton swabs. The direct mass spectrometric analysis of pharmaceutically relevant compounds is reported in this chapter using PADI-MS. Samples of paracetamol, caffeine and Panadol tablets were either analysed as solid clinical grade tablets, or as aqueous solutions applied to glass substrates or taken as swabs and analysed directly from the cotton tip. Mixtures of compounds have also been analysed to assess the ability of this method to provide qualitative and (semi-) quantitative information. The results of this study indicate that the PADI-MS technique is simple, sensitive, fast and suitable for analysis of pharmaceutical tablets and solutions, either directly from solid samples or via cotton swabs in the case of aqueous solutions. Calibration curves of paracetamol and caffeine were linear in the range of 10- 100 $\mu\text{g/mL}$. The LOD and LOQ were determined for paracetamol and caffeine in a 1:1 mixture solution. The LOD for paracetamol using glass slides and cotton swabs was found to be 6 $\mu\text{g/mL}$ and 5 $\mu\text{g/mL}$, while for caffeine it was found to be 22 $\mu\text{g/mL}$ and 18 $\mu\text{g/mL}$ respectively. The LOQ for paracetamol using glass slides and cotton swabs found to be 29 $\mu\text{g/mL}$ and 12 $\mu\text{g/mL}$, while for caffeine was found to be 96 $\mu\text{g/mL}$ and 42 $\mu\text{g/mL}$ respectively. Results highlight difference between the use of glass slides and cotton swabs as substrates for analysis of these compounds by PADI-MS. The signal intensity of paracetamol analysed directly from cotton swabs was higher than that found when using glass slides, although the opposite case was found for caffeine indicating a substrate dependence on sampling. Cotton swabs have been found to be more practical than glass slides due to being easiest in use. Both substrates are inexpensive, with the method being demonstrated as a rapid means to easily analyse samples with no need for any sample preparation.

5.1. Introduction:

Direct and rapid analysis of compounds giving chemical information would be of major benefit in the preparation of samples where reaction mixtures need to be process monitored. This is particularly interesting for the pharmaceutical industry during synthesis, as well as in forensics for investigation of unknown samples. Real-time analysis giving molecular data, e.g. by mass spectrometry, without the need for any sample preparation and which can be carried out by a non-expert would be a major addition in key industrial processes. For example, paracetamol tablets containing 500 mg paracetamol per tablet must be monitored to ensure raw material quality and quantity, that of intermediates found in reaction and product mixtures. Qualitative analysis of paracetamol in the tablets is necessary to confirm that the tablets contain the same correct component, while a quantitative analysis is important to determine the content of paracetamol (1). Paracetamol and caffeine, as mentioned in Chapter 4, are amongst widely used groups of analgesic drugs by humans.

Over the past years, there has been a dramatic increase in the analysis of pharmaceutical solids using analytical techniques such as nuclear magnetic resonance (NMR), near infrared (NIR), Fourier transformed infrared (FTIR) and Raman spectroscopy (2). As mentioned in the previous chapter, high-performance liquid chromatography (HPLC) is still the most used method in pharmaceutical analysis. A HPLC method has been developed for separation and quantification of a mixture of paracetamol, caffeine and chlorphenamine using a C₁₈ column and the mobile phase consists of methanol and potassium phosphate (45:55 v/v) (3). HPLC has also been used to separate and determine a multi mixture components of pharmaceuticals including dextromethorphan and diphenhydramine hydrochloride on an ODS column using an isocratic method (4). HPLC using a gradient method has been developed for measurement of dextro-propoxyphene

with other combination components such as paracetamol, caffeine and aspirin in tablet and capsule formulations with a run time of 23 minutes (5). A HPLC method was described to determine three pharmaceutical compounds (paracetamol, caffeine and chlorpheniramine) in a tablet formation using on a Hypersil CN column and the mobile phase was a mixture of acetonitrile, an ion-pair solution and tetrahydrofuran (13:14:87 v/v) (6). In the study by Franeta *et al.*, and Sawyer *et al.*, HPLC has also been used to determine the mixture components including paracetamol, caffeine and aspirin in tablet formulations and effervescent tablets on a C₁₈ column using a mixture of acetonitrile-water (25:75 v/v) and water-methanol-acetic acid respectively as a mobile phase (7, 8). However, there are obvious limitations in terms of necessary sample preparation, solution only sampling, the length of time needed for sampling, lack of inherent molecular information and the need for trained laboratory staff for HPLC sampling. Although HPLC is an important analysis technique with good limits of detection for compounds such as paracetamol and caffeine, these drawbacks accumulate to make this method very costly.

Mass spectrometry is an analytical method which has unique abilities to detect a wide range of chemical species at low concentrations, reaching to 10⁻¹² g. Due to its high sensitivity, rapid analysis, the need for small sample amounts, and ability to directly measure molecular weight hyphenated mass techniques such as liquid chromatography-mass spectrometry (LC-MS) (9), gas chromatography-mass spectrometry (GC-MS) (10, 11) and high-performance liquid chromatography connected with a tandem mass spectrometry (HPLC-MS/MS) (12, 13) are fast becoming key tools in pharmaceutical analysis. These hyphenated techniques support pharmaceutical development and ensure the quality and safety of pharmaceuticals. They have also been used for isolating and screening of new natural compounds for pharmaceutical application (14). However, work-up procedures such as extraction, filtration, and separation are required when using these

techniques (15). There have been several mass techniques used for online monitoring of compounds in many fields including biological and environmental such as proton transfer reaction mass spectrometry (PTR-MS) (for more details see Chapter 1).

Recently, there has been renewed interest in ambient mass spectrometry (AMS) for chemical qualitative analysis. In the AMS techniques, samples are desorbed and ionised directly from sample surfaces under atmosphere pressure, with the ions being directly generated outside the necessary vacuum of the MS itself. Methods of AMS have been divided into three categories based on ionisation mechanisms (16): spray methods such as DESI, EASI, EESI and PS; plasma methods such as DART, LTP and PADI and laser methods such as ELDI and LAESI. Desorption and ionisation can occur for all these methods. The detection of produced ions using DESI is similar to that used by DART, but DESI uses a solvent as a source to ionise the molecule, while DART uses a stream of gas (helium or nitrogen) (for more details see Chapter 2). However, these methods have some limitations. For example, the spray solvents in DESI make this method a bit chaotic (17), and DESI spectra need more investigation to draw the right analytical conclusions. The lack of a separation in DART causes lower detection selectivity and this makes this technique more vulnerable to false finding (18), and it is an expensive technique. In addition, the analysis of polymers is still not well known using DART (19). Analysing compounds using DESI and DART mostly depends on the matrix and this yields a lack of quantification abilities.

The work presented here demonstrates the use of PADI analysis directly from glass slides and cotton swabs, using paracetamol and caffeine as models for pharmaceutically relevant mixtures. Mixed standard solutions and off-the-shelf pain relief pharmaceuticals were investigated as test samples, Panadol and paracetamol, along with caffeine which is often used as an additive to increase pharmaceutical delivery in the body. Paracetamol and

caffeine were used as model drugs in this study due to their direct clinical relevance as small drug molecules. This study has been divided into three parts: the first part deals with the direct analysis of paracetamol, caffeine and Panadol tablets using PADI-MS and the second part examines the identification of individual and mixture solutions of paracetamol and caffeine from glass slides. The remaining part of the study shows the identification of these compounds using cotton swabs as a different substrate, with the intention that this sampling method will be relevant as a common sampling method.

The specific aim of this study was to develop a novel, simple, fast, sensitive and cost-effective analytical method that can be used for identification of unknown components in pharmaceutically relevant tablets and solutions using different types of substrates. This will help to avoid the potential problems of using the traditional methods for pharmaceutical analysis. In this Chapter, the objectives used to reach some conclusions about this sampling method were:

- 1) Use glass slides and cotton swabs to present solution samples to PADI-MS.
- 2) Assess limits of detection and quantification for each combination of above.

5.2. Materials and methods

5.2.1. Apparatus:

In the PADI-MS instrumentation, a single quadrupole (Waters Micromass ZQ, Manchester, UK) was used with the front end removed to accept an in-house built Stoffels-design plasma pencil as ionisation source using a 13.56 MHz RF power supply (20). The plasma pencil was fabricated to provide coaxial dual gas flow: an inner ceramic tube was encompassed within a quartz glass tube. Helium gas was flown through both tubes controlled using separate flow meters. The schematic diagram of the PADI probe and

source in operation is shown in Figure 8 in Chapter 1. The flow inside the ceramic tube will henceforth be referred to as ‘inner flow’, the flow between the ceramic and quartz tube as ‘outer flow’. The measurement conditions of plasma were optimised for all samples in this study and using water (for more information see Chapter 3). The effect of water on ionisation efficiency was investigated by flowing the helium through a water vapour added environment before the plasma pencil being directed to the plasma pencil outflow (for more information see Chapter 2).

5.2.2. Chemicals and materials:

Panadol ExtraTM tablets containing 500 mg paracetamol and 65 mg caffeine per tablets were used as obtained from an over the counter pharmacy. Paracetamol tablets containing 500 mg paracetamol per tablet and Pro Plus tablets containing 50 mg caffeine were purchased from the Body Care shop. The paracetamol tablets containing 500 mg paracetamol per tablet were manufactured by Galpharm International Ltd, UK. Pro Plus tablet containing 50 mg caffeine is a registered trademark. Pure paracetamol was manufactured by Alfa Aesar, UK (purity 98%), and pure caffeine was manufactured by Acros Organics, China (purity 98%). Helium gas was supplied by British Oxygen Company (BOC) gases, UK (purity 99%). Deionised water was provided through a Pure Lab Option ELGA, with the resistivity 18 M Ω , Model Ultra Clear TWF UV. Standard glass microscope slides and cotton swabs were supplied by Fisher Scientific, UK.

5.2.3. Preparation of sample solutions:

Panadol solutions were prepared by dissolving 1 Panadol Extra tablet in 10 mL deionised water. A range of high purity paracetamol and caffeine solution concentrations of 0.02 - 5 $\mu\text{g}/\mu\text{L}$ were prepared by dissolving the solutes in deionised water. Paracetamol and

caffeine mixtures were prepared by mixing 2 mL of equally concentrated solutions. These were all freshly made prior to use.

5.2.4. Procedure:

- 1- Pure paracetamol, pure caffeine, paracetamol tablet (500 mg), Pro Plus tablet containing 50 mg caffeine and Panadol tablets were analysed directly by PADI-MS.
- 2- Standard microscope glass slides were used for all analysis.
- 3- One drop of single paracetamol and single caffeine (both 5 $\mu\text{g}/\mu\text{L}$) and Panadol tablet solutions (50 mg/mL paracetamol+6.5 mg/mL caffeine) were deposited on the glass slide using a Pasteur pipette (for more details see Chapter 4). The deposition spot of individual and paracetamol/caffeine mixtures on the glass slide was analysed immediately by PADI-MS with a total acquisition time of 1 minute.
- 4- Samples analysed using cotton swabs were taken by dipping the cotton tip into a solution of an individual solutions and paracetamol/caffeine mixtures and analysed immediately by PADI-MS with a total acquisition time of 1 minute using the same conditions above.

To investigate the potential effects that such heating causes on the sample during the analysis, and indeed the quality of mass spectral data obtained, thermal imaging was conducted (for more details see Chapter 3).

5.3. Results and discussion:

5.3.1. Method development and optimisation of PADI-MS conditions

Sampling using the PADI probe was optimised for each type of sample and substrate combination. Optimised conditions used to analyse all samples (individual and paracetamol /caffeine mixtures in liquid) are presented in Table 5.1.

Table 5. 1. The optimal conditions of PADI probe for analysing of individual and paracetamol /caffeine mixtures in liquid.

PADI parameters	Optimised conditions
Plasma power	8W
Inner flow rate (He)	224 mL/min
Sample – plasma distance	5 mm
Outer flow composition	He with water vapour
Outer flow rate	224 mL/min

The gas phase is formed by the reaction between the helium and water and then produce H_3O^+ , and then H_3O^+ reacts with a molecule (M) to form protonated molecular (MH^+) (20) (for more details see Chapter 4).

5.3.2. Analysis of pure and tablets

The first part of analysis studied the detection and identification of pure and pharmaceutical tablets using the optimised conditions for PADI-MS as outlined in Section 5.4.1. Changes in signal intensity of the sample tablets with time were compared to that measured in the sample solutions. Pure paracetamol and pure caffeine were analysed directly using PADI-MS.

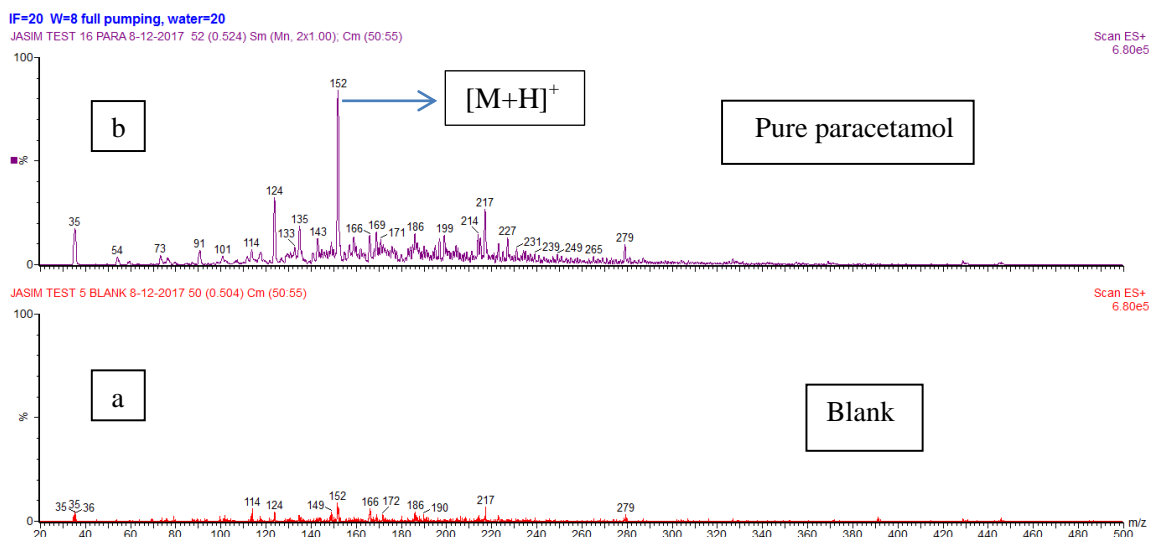


Figure 5. 1. PADI-MS spectra of background (a) and pure paracetamol (b) with a total acquisition time of 1 minute.

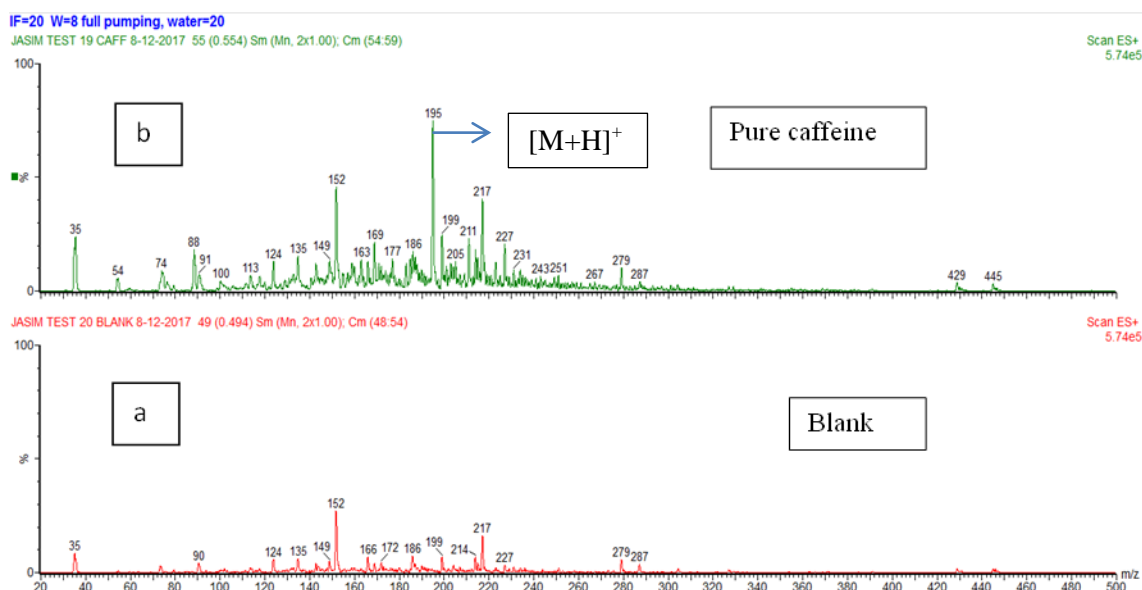


Figure 5. 2. PADI-MS spectra of background (a) and pure caffeine (b) with a total acquisition time of 1 minute.

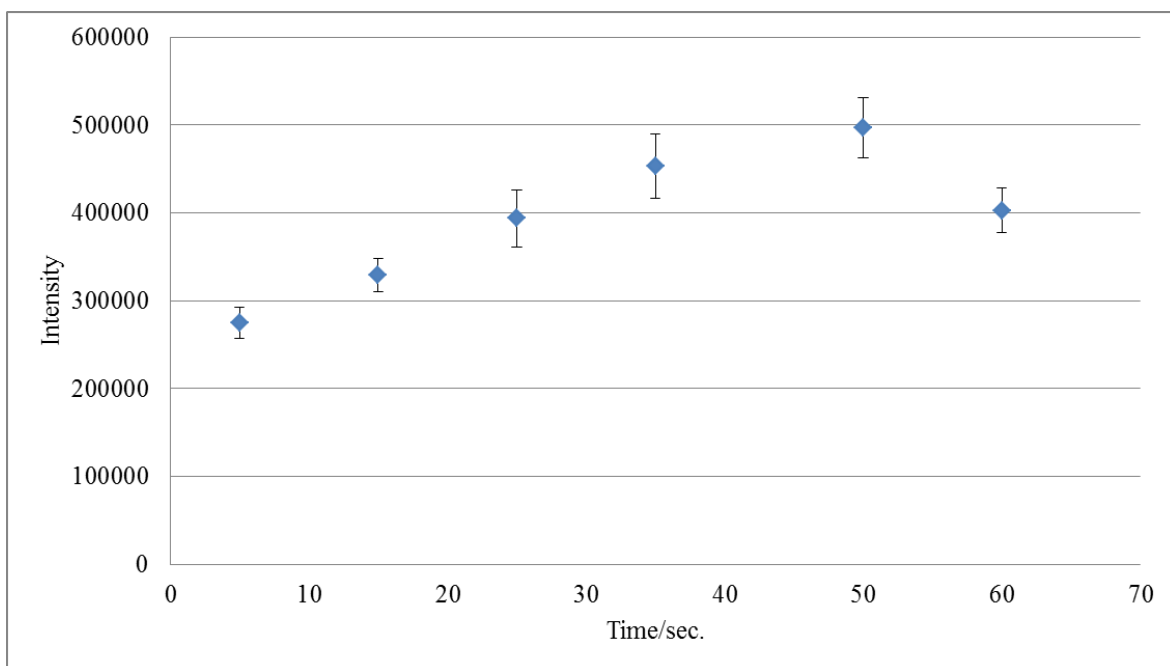


Figure 5. 3. PADI-MS signal intensity for [M+H]⁺ in pure paracetamol.

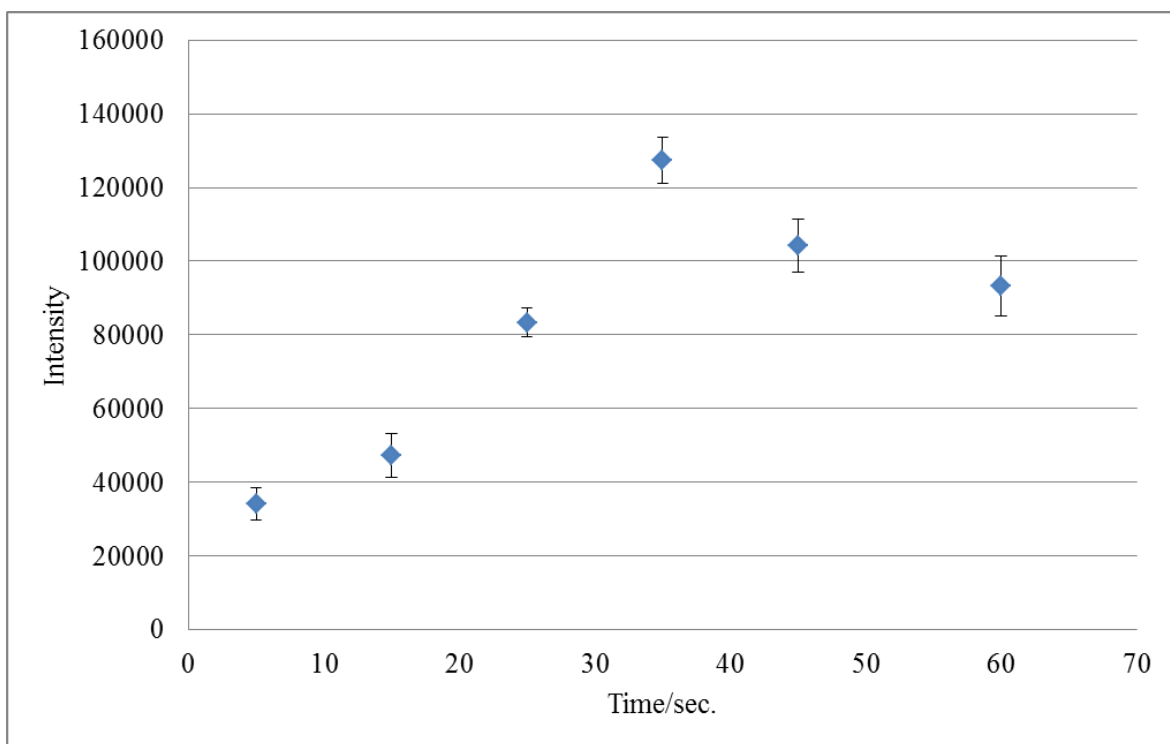


Figure 5. 4. PADI-MS signal intensity for [M+H]⁺ in pure caffeine.

Paracetamol, caffeine and Panadol tablets were used as pharmaceutically relevant models. Paracetamol (500 mg) and Panadol (500 mg paracetamol and 65 mg caffeine) tablets were analysed directly using PADI-MS. Even though the paracetamol molecular ion M^+ m/z 151 was detected, protonated paracetamol $[M+H]^+$ at m/z 152 was more abundant and easy to see in all spectra. As can be seen, from Figure 5.5, stable and high signal intensity of protonated paracetamol in both paracetamol and Panadol tablets were observed at $[M+H]^+$ m/z 152 (spectrum a and spectrum b). Another diagnostic spectral feature relating to the paracetamol molecular ion was observed at $[2M+2H]^+$ m/z 304. The diagnostic peak $M+O-H$ m/z 166 could be assigned either to $M+O-H$ or to $M+NH$ (with nitrogen reacting from the air during plasma treatment), but it is most likely identified as $M+O-H$ due to the paracetamol molecule gaining the hydroxyl group from the water vapour. Higher mass accuracy would be required to further interrogate this. Small diagnostic peaks were also observed relating to the caffeine molecular ion at M^+ m/z 194, $M^+ - CN$ m/z and $M^+ + H_2O$ m/z 212. Further diagnostic peaks of paracetamol and caffeine were identified as listed in Table 5.2. The results have compared 'no sample' which was taken before sampling to spectra taken 'with sample' in the plasma plume (Figure 5.5). No sample spectrum shows a little of the sample but this is fairly low level, and this may be due to contamination of the sniffer tube. To resolve this problem, the sniffer tube was cleaned several times to minimise contamination effects.

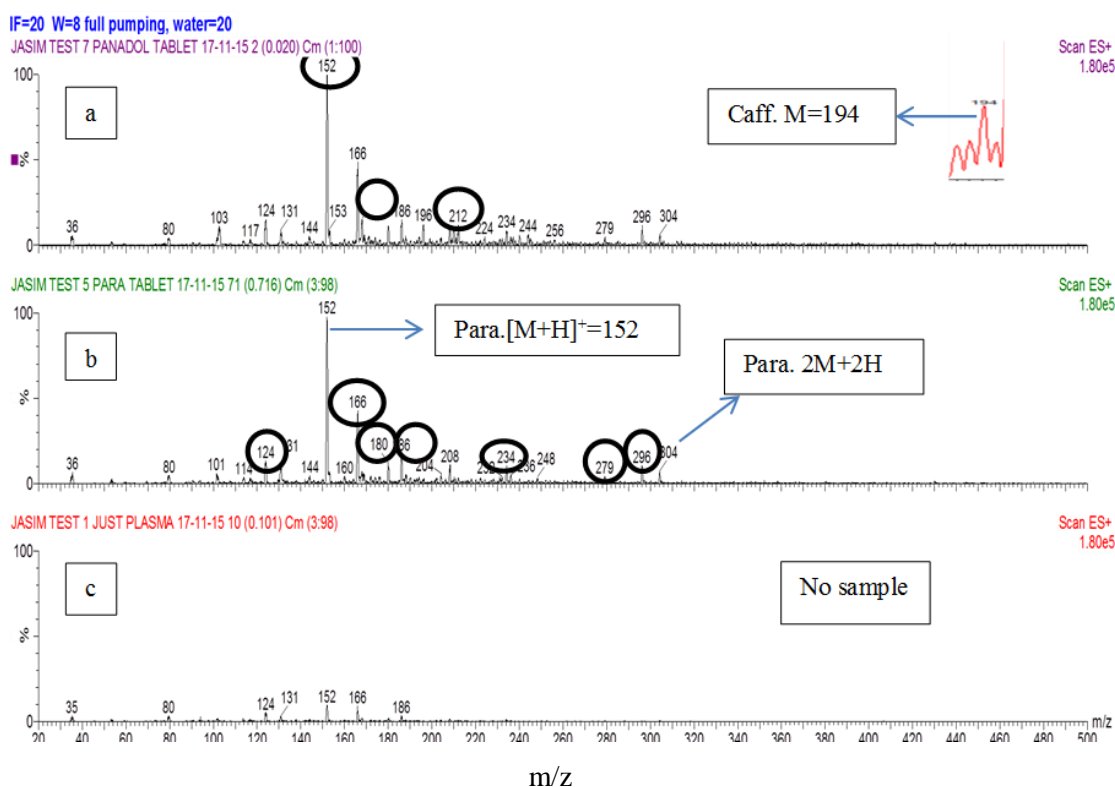


Figure 5. 5. PADI-MS spectra of (a) Panadol tablet containing 500 mg paracetamol and 65 mg caffeine; (b) paracetamol tablet containing 500 mg paracetamol; (c) no sample with a total acquisition time of 1 minute.

Table 5. 2. Diagnostic peaks for paracetamol and caffeine.

Diagnostic peaks for paracetamol	m/z	Diagnostic peaks for caffeine	m/z
$[M+H]^+$	152	M^+	194
$M+O-H$ or $M+NH$	166	$[M + H_2O]^+$	212
$CO + [M+H]^+$	180		
$[2M+H_2O]^+ - (COCH_3)_2$	234		
$[2M+H_2O]^+ - COCH$	279		
$[2M+2H_2O]^+ - COCH_2$	296		
$[2M+2H]^+$	304		

5.3.2.1. Plasma-sample interaction time

The length of interaction time between the visible plasma and sample is important in order to get a good signal and more information on molecules. Figure 5.6 shows the experimental data of intensity signal versus time in 5 seconds intervals (0-5 sec, 0-15 sec, 0-25 sec, 0-35 sec, 0-45 sec, 0-60 sec) of 500 mg protonated paracetamol in a paracetamol tablet. It can be seen from the data in Figure 5.6 that the $[M+H]^+$ of paracetamol increases in intensity over an interaction time up to ~35 seconds, after which it decreases up to 1 minute. As shown in Figure 5.6, 5 seconds intervals at 30-35 seconds was decided as the optimal time for the high-intensity signal of protonated paracetamol and the analysis can be stopped after that time.

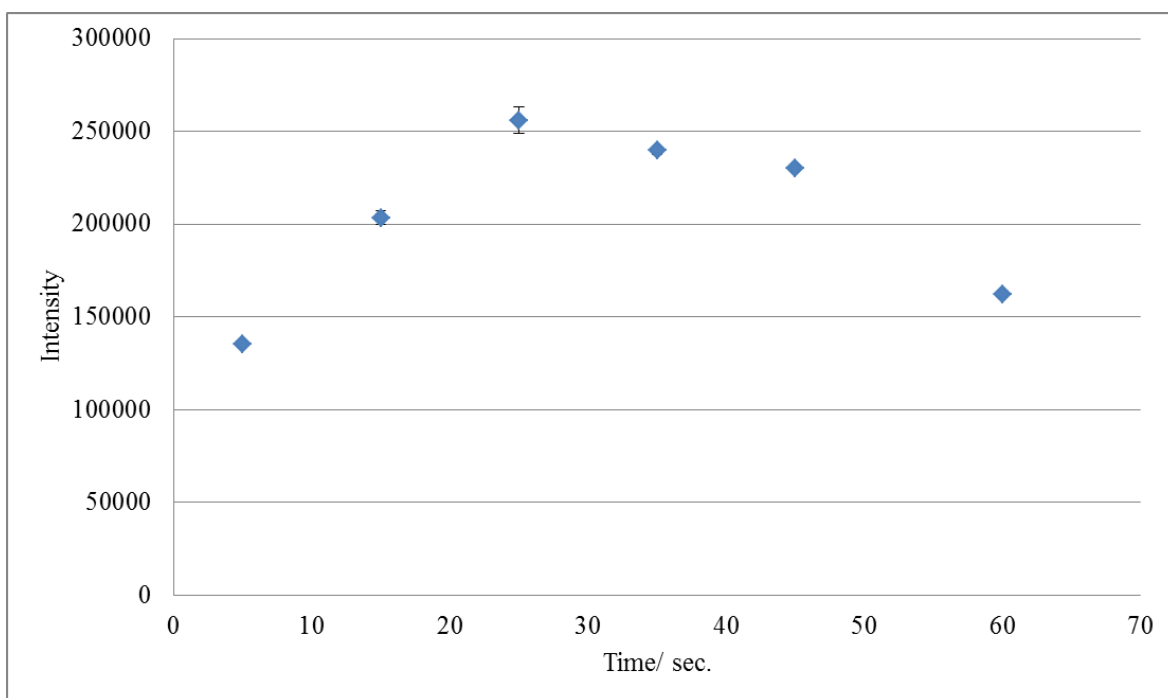


Figure 5. 6. Signal intensity of $[H+M]^+$ in paracetamol tablet versus time upon binning of data in 5 seconds intervals up to a total acquisition time of 60 seconds.

To investigate the heating causes on the sample during the analysis, the temperature was measured using the exact same PADI parameters using a thermal camera by interacting the visible plasma with a tablet (21). The temperature in the middle of the paracetamol tablet was measured for 5 minutes. The temperature increased dramatically to 75 °C at 45 seconds, after which it increased slowly to 80 °C at 1 minute, and then dropped to 36 °C until 5 minutes. This indicated why the $[M+H]^+$ peak for paracetamol increased in intensity up to ~ 45 seconds, after which it decreased up to 1 minute. Little thermal changes could be detected within the area of the substrate exposed to the plasma, although sample heating does occur slowly up to a maximum of ~45 °C after ~30 seconds interaction. The behaviour of other fragments and adduct peaks of paracetamol with interaction time were also investigated. According to these data, we can see that all intensity signals have the same behaviour during analysis time. Diagnostic peaks relating to caffeine molecular ion were observed at M^+ m/z 194, and $[M+H_2O]^+$ m/z 212 (Figure 5.5). Figure 5.7 provides the experimental data of both protonated paracetamol and caffeine molecules in a Panadol tablet.

Results demonstrate that $[M+H]^+$ m/z 152 and M^+ m/z 194 peaks both increase in intensity over the first 25 seconds of plasma-sample interaction, after which they decrease; here we recorded up to 60 seconds. These results match those observed in earlier experiments of the paracetamol tablet (Figure 5.6), and there is no difference between the measurement of paracetamol presented in a tablet (with formulation compounds) and in when presented in a mixture of caffeine in a Panadol tablet (Figure 5.7). The reason for this is that the percentage of concentration (w/w) for paracetamol in the paracetamol tablet is 87 % by dividing the content of paracetamol in the tablet on the weight of tablet (500 mg/570 mg), while it is 77 % for paracetamol in the Panadol tablet by dividing 500 mg/694 mg. There were also big differences observed in the signal intensity of protonated paracetamol and

caffeine ions. They showed that $[M+H]^+$ m/z 152 is 7x more abundant than M^+ m/z 194. As shown in Figure 5.7, the behaviour of the intensity of $[M+H]^+$ m/z 152 in Panadol tablet over time is similar to that of caffeine molecular ion. Data collected suggests that a minimum time of plasma interaction for good ion signal to be collected is only ~15 seconds, with an only limited change in intensity up to 30 seconds. The results from the data in Figure 5.7 suggest that 15 seconds is enough to see these molecules without the need to wait until 1 minute.

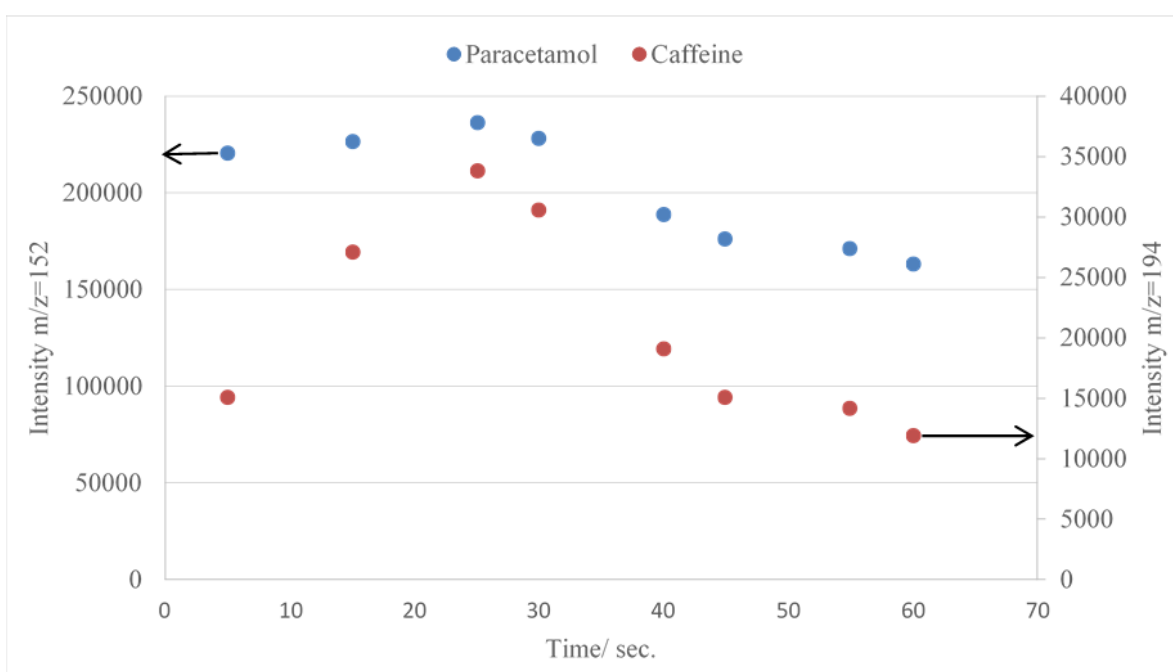


Figure 5. 7. Signal intensity of $[H+M]^+$ ($m/z = 152$; left y-axis) and caffeine ions ($m/z = 194$; right y-axis) in a Panadol tablet versus time with a total acquisition time of 1 minute.

Optimised PADI-MS conditions were used for the analysis of a ProPlus tablet containing 50 mg caffeine with no paracetamol (Figure 5.8). Findings are similar to Figure 5.6 (up to 30 seconds ion intensity not much change - which is good). The percentage of concentration (w/w) for caffeine in Pro Plus tablet is 30 % by divided the content of

caffeine in the tablet on the weight of tablet (50 mg/164 mg), while it is 10 % for caffeine in the Panadol tablet by dividing 65 mg/694 mg. Therefore, the intensity signal of caffeine in the Pro Plus tablet expected to be 3x higher than that in Panadol tablet, but they are similar as shown in Figures 5.7 and 5.8. This may be due to caffeine amount distributed as an active ingredient in the sample, making the actual sampled volume of caffeine small in relation to previous tests, or that the Panadol tablet can be measured easier than the Pro Plus tablet and this can be related to the physics natural of Pro Plus tablet. On the other hand, additional to the caffeine molecular ion peak at M^+ m/z 194, protonated caffeine $[M+H]^+$ was observed at m/z 195 in the Pro Plus tablet (Figure 5.8).

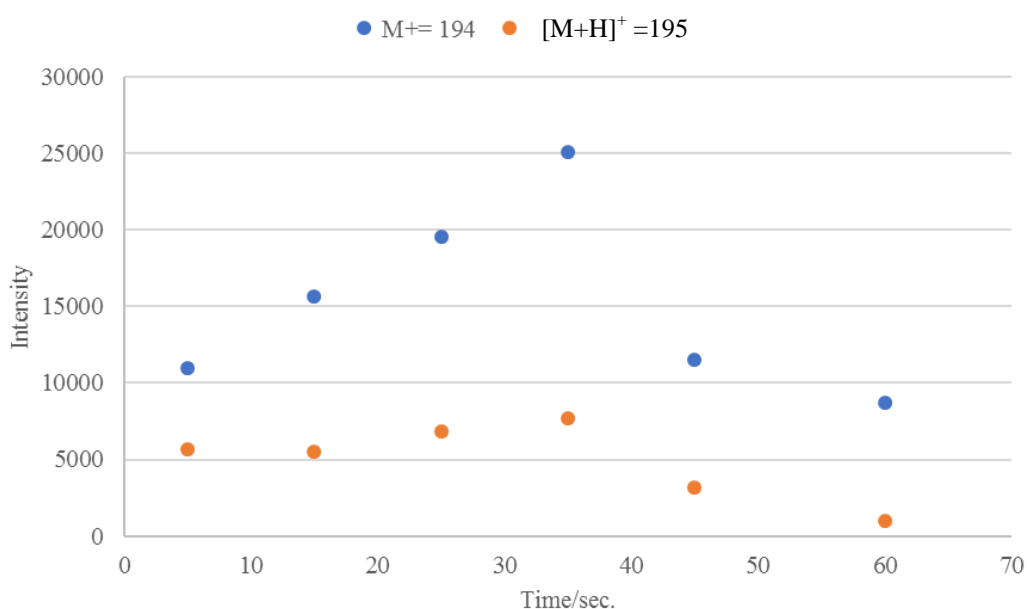


Figure 5. 8. Signal intensity of caffeine molecular ion in Pro Plus tablet contains 50 mg versus time caffeine with a total acquisition time of 1 minute.

The results obtained from the different measurements of paracetamol in the Panadol tablet are shown in Figures 5.9 and 5.10. Comparing the two results, it can be seen that the analysis of protonated paracetamol in 5 second intervals (Figure 5.9) is in agreement with

that used by accumulated seconds (Figure 5.10). There has been a rise in the signal intensity of protonated paracetamol linearly over accumulated time up to ~35 seconds, after which they deviate slightly up to 1 minute, Figure 5.10. These results provide further support for the intensity behaviour of molecules that increase up to ~35 seconds.

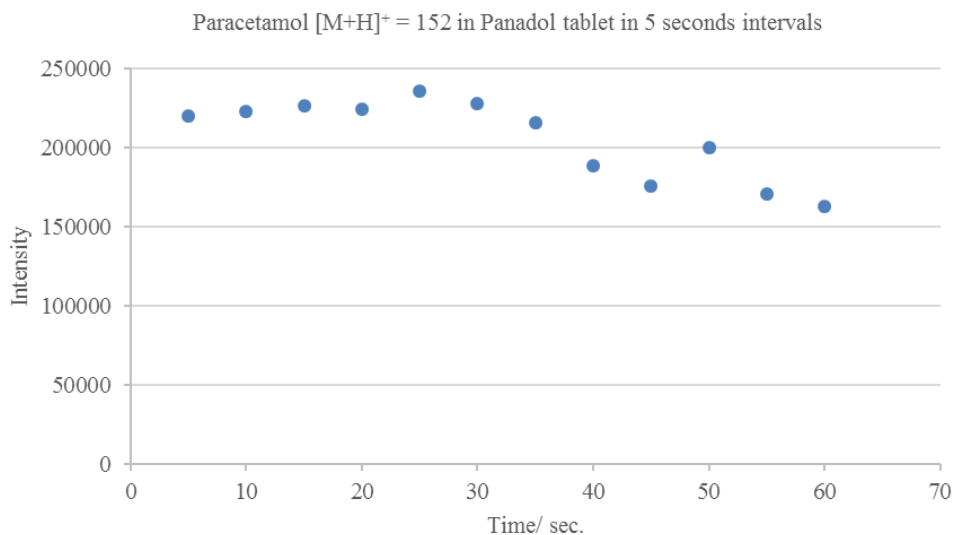


Figure 5. 9. Signal intensity of protonated paracetamol in Panadol tablet in 5 seconds intervals 0-5, 5-10, 10-15, 15-20, 20-25, 25-30, 30-35, 35-40, 40-45, 45-50, 50-55 and 55-60 seconds.

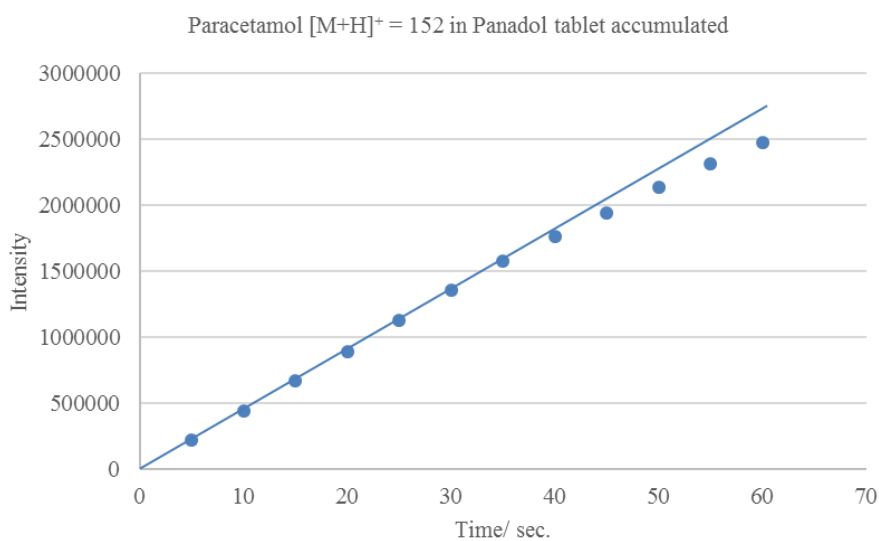


Figure 5. 10. Signal intensity of protonated paracetamol in Panadol tablet in accumulated seconds 0-5, 0-10, 0-15, 0-20, 0-25, 0-30, 0-35, 0-40, 0-45, 0-50, 0-55 and 0-60 seconds.

5.3.3. Analysis of individual compounds/mixtures from glass slides

The analysis presented here demonstrates the use of PADI analysis directly from glass slides, using individual compounds and mixtures of paracetamol/caffeine as models for pharmaceutically relevant mixtures. Paracetamol, caffeine and Panadol aqueous solutions over a range of concentrations were deposited on a glass slide and analysed immediately (without the need to dry) by PADI-MS using the optimal conditions as described in Section 5.3.1. High purity single component and mixed solutions (1:1) were used as a standard to optimise conditions. Changes in intensity with time were compared using initial analysis of pure paracetamol and caffeine solutions (both 5 $\mu\text{g}/\mu\text{L}$) which were measured separately from glass slides using He added with water vapour in time upon binning of data in 5 seconds intervals. The experimental data of protonated paracetamol and the caffeine molecular ion (both 5 $\mu\text{g}/\mu\text{L}$) are presented in Figure 5.11. The signal intensities of protonated paracetamol and caffeine molecular ions increased by 1.2x for both, reaching a peak at up to ~35 seconds for protonated paracetamol and caffeine molecular ions. The intensity of protonated paracetamol ($[\text{M}+\text{H}]^+$ m/z 152) was 3x higher compared to that of the caffeine molecular ion (M^+ m/z 194) until the end of acquisition time of 1 minute. The results found dramatic differences in the intensity of protonated paracetamol and caffeine molecular ions between tablets and solutions to be ~ 8x and 3x respectively.

The intensity of M^+ for the caffeine was normalised to the intensity of $[\text{M}+\text{H}]^+$ for paracetamol and $[\text{M}+\text{H}]^+$ for caffeine in order to show the plasma effect for both intensities over interaction time, Figure 5.12. The ratio of intensity signal of m/z 152/194 of pure paracetamol and caffeine solutions (both 5 $\mu\text{g}/\mu\text{L}$) over time using outer He added with water vapour are shown in Figure 5.12. As can be seen from this Figure, this ratio is stable over the first 25 seconds, after which it increases up to 45 seconds then stable to 1 minute. From this, we can see that there is no difference in signal intensity between ($[\text{M}+\text{H}]^+$ m/z

152) for paracetamol and (M^+ m/z 194) for caffeine molecular ion in the beginning of analysis time, after which it increases to 60 seconds. These findings may help us to understand that the samples can be analysed easily by PADI-MS, with rapid analysis of less than 30 seconds giving molecular ion information without strongly affecting the sample due to plasma interaction until 30 seconds. This may be attributed to either thermal desorption of analytes from the surface, degradation or continued excitation of analytes on the surface or in the gas phase. The ratio of the intensity signal (m/z 194/195) remains steady over the first 35 seconds, after which it reduces to 1 minute. This may be due to that the intensity of 194 has decreased more than 195 after 35 seconds, Figure 5.13.

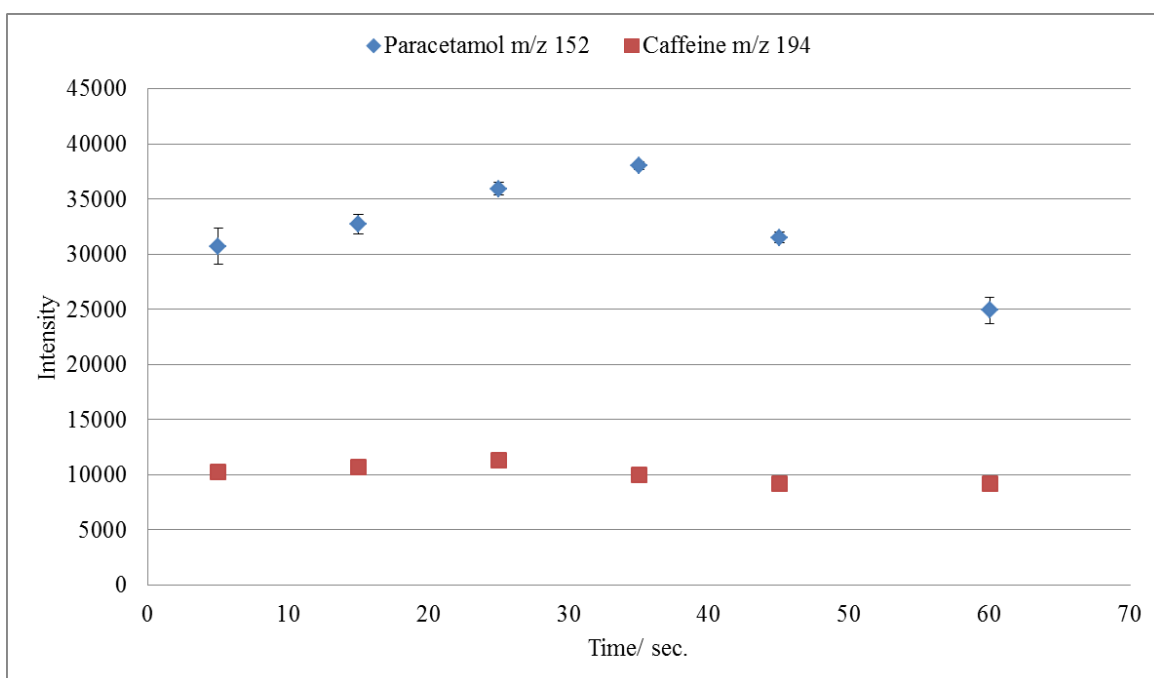


Figure 5. 11. Signal intensity of single paracetamol and caffeine (both $5 \mu\text{g}/\mu\text{L}$) using glass slide with a total acquisition time of 1 minute.

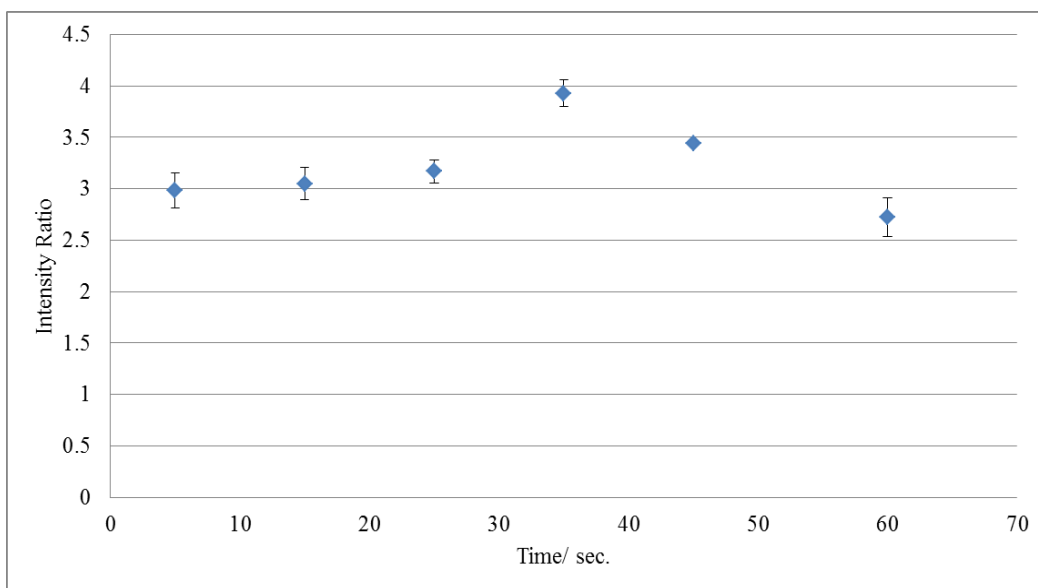


Figure 5. 12. Signal intensity ratios of paracetamol and caffeine solutions (m/z 152/194) (both $5 \mu\text{g}/\mu\text{L}$) applied from the glass slide and measured separately using outer He added with water vapour in 5 seconds intervals 0-5, 10-15, 20-25, 30-35, 40-45 and 55-60 seconds.

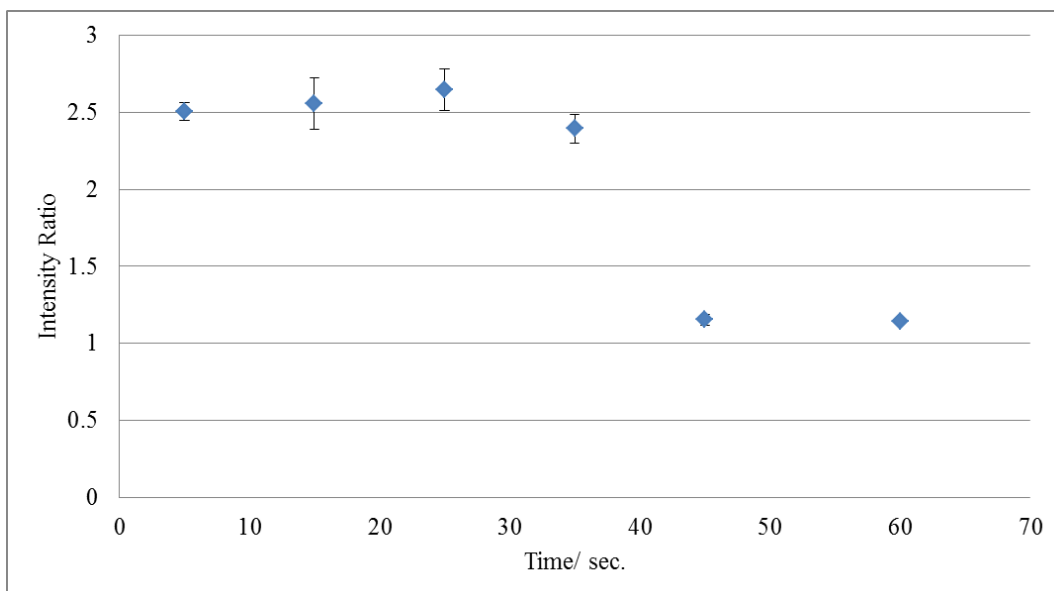


Figure 5. 13. Signal intensity ratios of single protonated caffeine and pure caffeine molecular ion solutions by a factor of (m/z 194/195) (both $5 \mu\text{g}/\mu\text{L}$) applied from glass slide using added with water vapour in 5 seconds intervals 0-5, 10-15, 25-30, 30-35, 40-45 and 55-60 seconds.

Spectra of 1:1 by weight mixtures of paracetamol and caffeine (0.01 $\mu\text{g}/\mu\text{L}$ and 0.1 $\mu\text{g}/\mu\text{L}$) were compared, with acquisition time 30-35 seconds, Figure 5.14. Two diagnostic ions relating to the paracetamol molecular ion were observed at $[\text{M}+\text{H}]^+$ m/z 152 and $[2\text{M}+2\text{H}]^{+2}$ m/z 304. Further diagnostic peaks are very similar to what has been described in Table 5.2. The signal intensities of paracetamol/caffeine mixtures were higher when using 0.1 $\mu\text{g}/\mu\text{L}$ compared to that used by 0.01 $\mu\text{g}/\mu\text{L}$. Additional diagnostic peaks of these compounds were found when using a higher concentration of solutions, such as $\text{M}-\text{CCH}_3$ m/z 124 and $\text{M}-\text{H}+2\text{H}_2\text{O}$ m/z 186. As expected higher concentrations give rise to spectra with higher ion intensities and therefore present more opportunity for lower intensity ions to be observed above the noise. PADI-MS analysis of aqueous 1:1 mixtures of paracetamol and caffeine (both 2.5 $\mu\text{g}/\mu\text{L}$) deposited onto a glass slide showed differences of intensity behaviour between protonated paracetamol and caffeine molecular ion over time, Figure 5.15. An increase in signal intensity of protonated paracetamol and the caffeine molecular ions was observed up to ~35 seconds ($[\text{M}+\text{H}]^+$ m/z 152 is 4x more abundant than M^+ m/z 194), after which they decreased up to 1 minute. The results obtained from the PADI-MS analysis of a Panadol solution with an acquisition time of 1 minute is shown in Figure 5.16. Diagnostic, adduct and fragment peaks are apparent, such as $\text{M}-\text{CCH}_3$ m/z 124, $[\text{M}+\text{H}]^+$ m/z 152, $\text{M}+\text{O H}$ m/z 166 and $[2\text{M}+2\text{H}]^+$ m/z 304 for paracetamol, and M^+ m/z 194 for caffeine. Other diagnostic peaks of paracetamol and caffeine can be identified as listed in Table 5.2.

Important differences between the Panadol solution and aqueous 1:1 mixtures showed increased the signal intensity of protonated paracetamol and caffeine molecular ions being much higher for Panadol. This is due to the concentration differences: the concentrations of paracetamol and caffeine in the Panadol solution were 50 $\mu\text{g}/\mu\text{L}$ and 6.5 $\mu\text{g}/\mu\text{L}$ respectively, control solutions of individual components were each 2.5 $\mu\text{g}/\mu\text{L}$. Figure 5.14

shows very high intensity of protonated paracetamol compared to those that of the caffeine molecular ion. The results showed there was a more intense signal of protonated paracetamol in comparison with caffeine molecular ion and protonated caffeine ions, Figures 5.11 and 5.15.

The observed increase in the intensity of paracetamol in tablets, pure and mixture solutions could be attributed to pK_a effect. The pK_a for paracetamol and caffeine are 9.5 and 14 respectively, therefore, caffeine is more basic than paracetamol. Although caffeine would be expected to give the high-intensity signal, paracetamol can gain proton easier and gives a higher signal. This maybe due to the fact that caffeine did not desorb enough like paracetamol. Another contributing factor might be related to the molecular mass of each compound. The molecular mass for paracetamol is 151 g/mol while for caffeine is 194 g/mol, hence a 1/1 weight ratio means a molar ratio of 1.3 (for more details see Chapter 4).

The results, as shown in all figures, also indicate that intensity of the caffeine molecular ion is bigger than protonated caffeine. This means paracetamol accepts proton easier than caffeine. There are several possible explanations for these results. The first reason for this may be related to pK_a as mentioned before. The second reason could be attributed to the amount of molecule per droplet in the solution of an individual and the mixtures of paracetamol/ caffeine. For example, the number of moles of paracetamol in the individual and mixtures is higher than of caffeine (for more details see Table 5.1). The results also showed that the intensity signal of protonated paracetamol and caffeine molecular ion given by the aqueous 1:1 mixture (both 2.5 $\mu\text{g}/\mu\text{L}$) is similar to that used by the single compounds (both 5 $\mu\text{g}/\mu\text{L}$). This shows that the matrix of analytes does not affect on the results whether individual or mixtures of compounds have been used. The intensity ratio of m/z 152/195 of 1:1 mixture of paracetamol and caffeine (both 0.1 $\mu\text{g}/\mu\text{L}$) was stable until 35 seconds, after which it increases up to 1 minute, Figure 5.17. This factor may explain

the relatively good correlation in intensity between $[M+H]^+$ m/z 152 and $[M+H]^+$ m/z 195 until 35 seconds of analysis time, and the sample can be affected by plasma after this time.

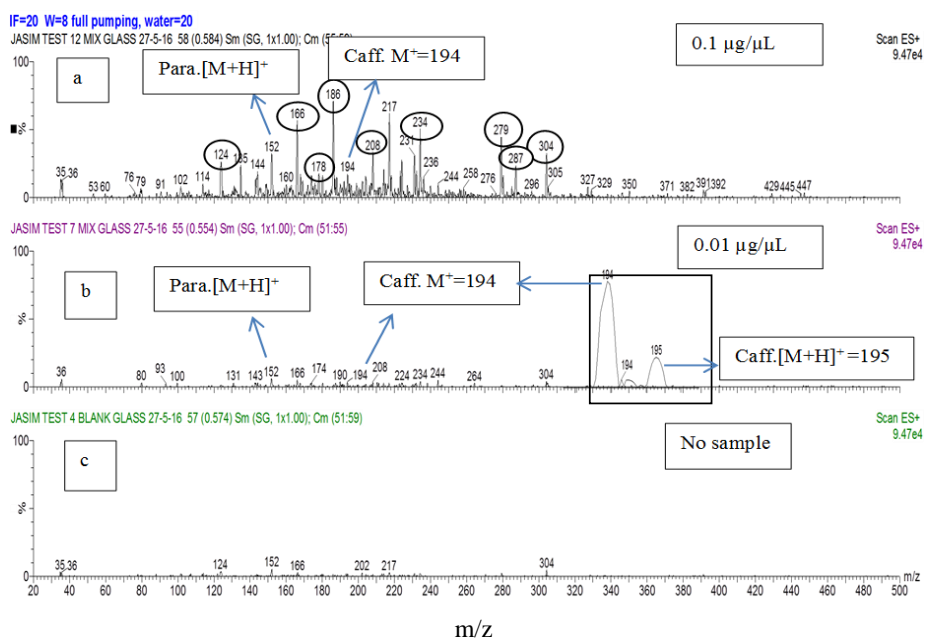


Figure 5. 14. PADI-MS spectra of 1:1 mixed of paracetamol and caffeine of 0.1 $\mu\text{g}/\mu\text{L}$ (a), 0.01 $\mu\text{g}/\mu\text{L}$ (b) and no sample (c), using glass slide with a total acquisition time of 1 minute.

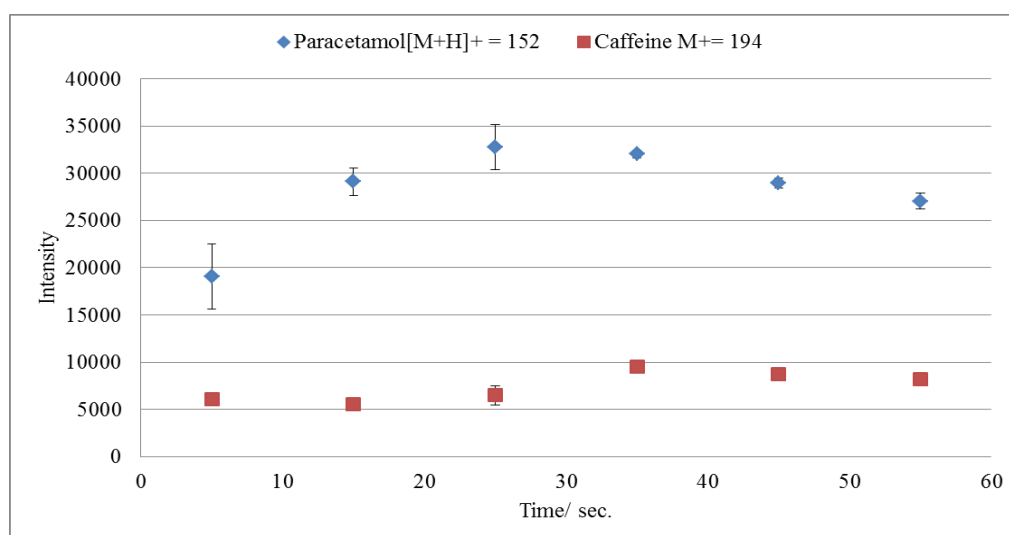


Figure 5. 15. Signal intensity of an aqueous 1:1 mixture of paracetamol and caffeine (both 2.5 $\mu\text{g}/\mu\text{L}$) using a glass slide with a total acquisition time of 1 minute.

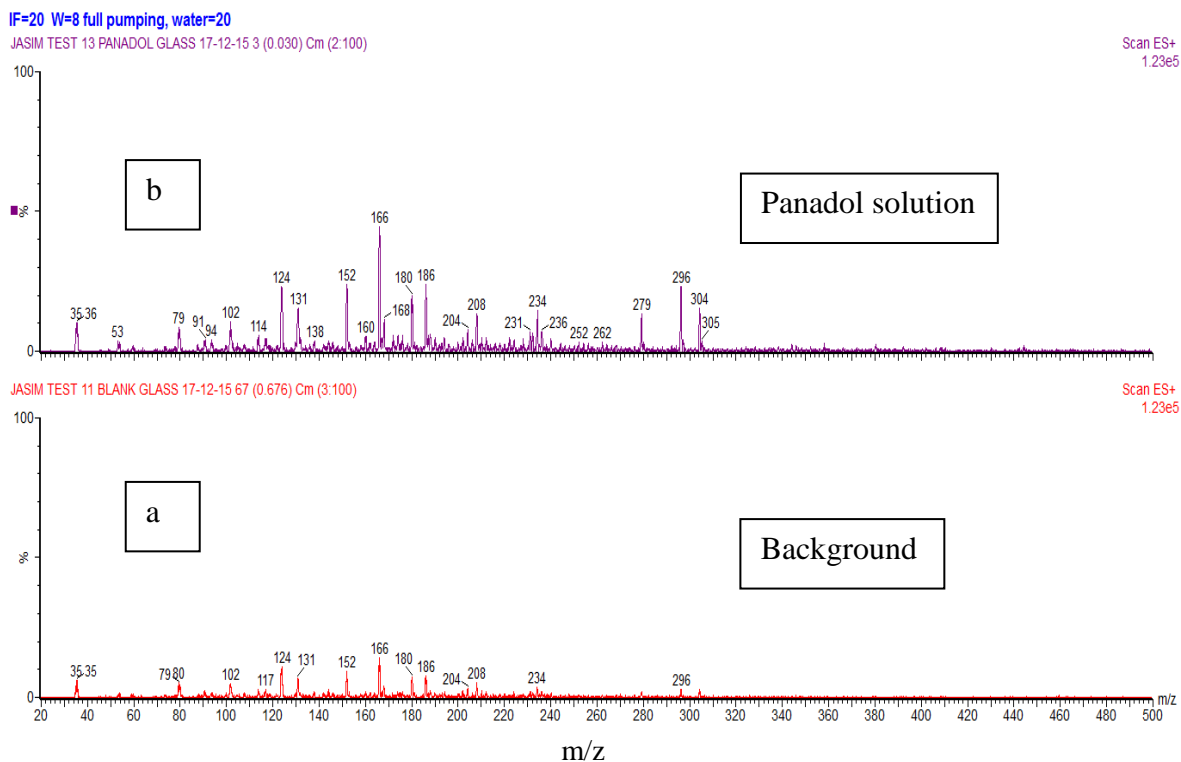


Figure 5. 16. PADI-MS spectra of background (a) and Panadol solution (b) using a glass slide with a total acquisition time of 1 minute.

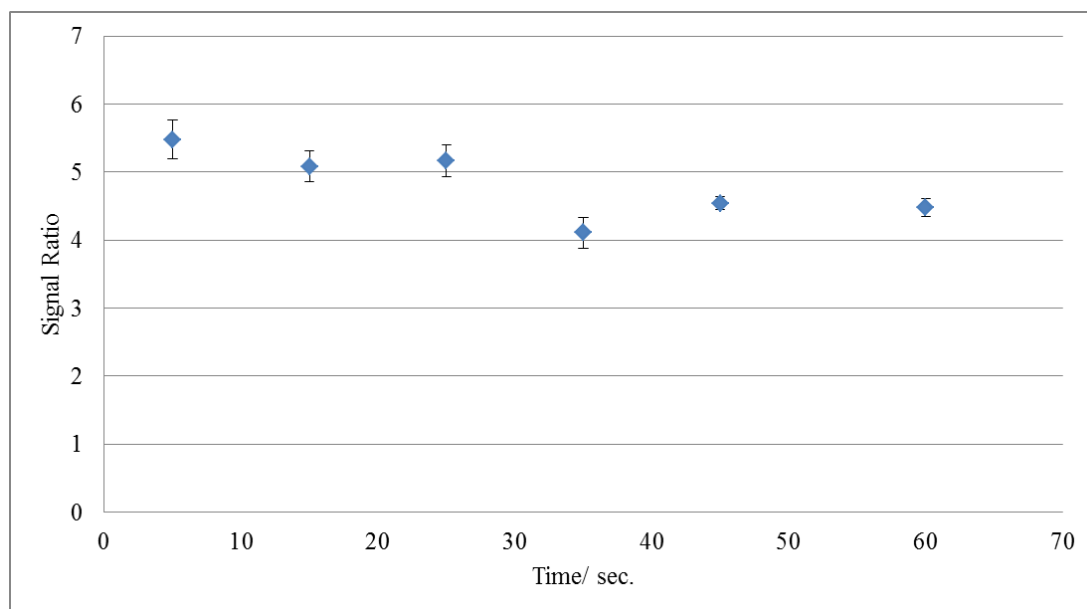


Figure 5. 17. Signal intensity ratio by a factor of 152/195 of 1:1 mixed of paracetamol and caffeine (both $0.1 \mu\text{g}/\mu\text{L}$) applied using glass slides and measured in 5 seconds intervals 0-5, 10-15, 20-25, 30-35, 40-45 and 55-60 seconds.

5.3.4. Analysis of mixtures from cotton swabs

To compare the glass slide with another substrate to analyse paracetamol and caffeine solutions, a cotton swab was used. A cotton swab was chosen in this study for several reasons such as low cost, convenience, an absorbance of liquids and to obtain a better signal. In this part of the analysis, individual solutions and mixtures of paracetamol /caffeine were analysed by PADI-MS using a cotton swab as a substrate with the same optimal conditions as described in Section 5.4.1. In this part, the same solutions were used to those used with glass slides. In the optimised analysis, a cotton swab was dipped in each sample solution of pure paracetamol and caffeine (both 5 $\mu\text{g}/\mu\text{L}$) and then measured by PADI-MS with a total acquisition time of 1 minute.

The experimental data of intensity signals for these pure compounds over time are presented in Figure 5.18. The intensity of protonated paracetamol is higher than the caffeine molecular ion. This may be attributed to either thermal desorption of analytes from the surface, degradation or continued excitation of analytes on the surface or in the gas phase. The intensity of protonated paracetamol and caffeine molecular ions increased by 1.3x and 1.2x respectively, reaching a peak up to ~35 seconds, after which the difference between these intensities decreases to 1x for both until the end of data acquisition to 1 minute. These results are in agreement with glass slides finding which showed the same behaviour of intensities for these compounds over time. However, the intensity signals of protonated paracetamol and the caffeine molecular ion using a cotton swab (Figure 5.18) are higher than that given by the glass slide (Figure 5.11).

The simple analysis was used to analyse the relationship between a factor of m/z 194/195 of pure caffeine solution (5 $\mu\text{g}/\mu\text{L}$) and analysis time. This intensity ratio is relatively constant over the first 25 seconds, and after which it drops and remains stable until the end

of data acquisition at 1 minute, Figure 5.19. The results indicate that the signal intensity of the caffeine molecular ion (M^+ m/z 194) is still higher than protonated caffeine ($[M+H]^+$ m/z 195). The results also indicate that there were no changes in intensities between these ions of caffeine in the first 25 seconds of analysis. The behaviour of the intensity ratio of m/z 194/195 used by the cotton swab (Figure 5.19) is similar to that used by glass slide (Figure 5.13).

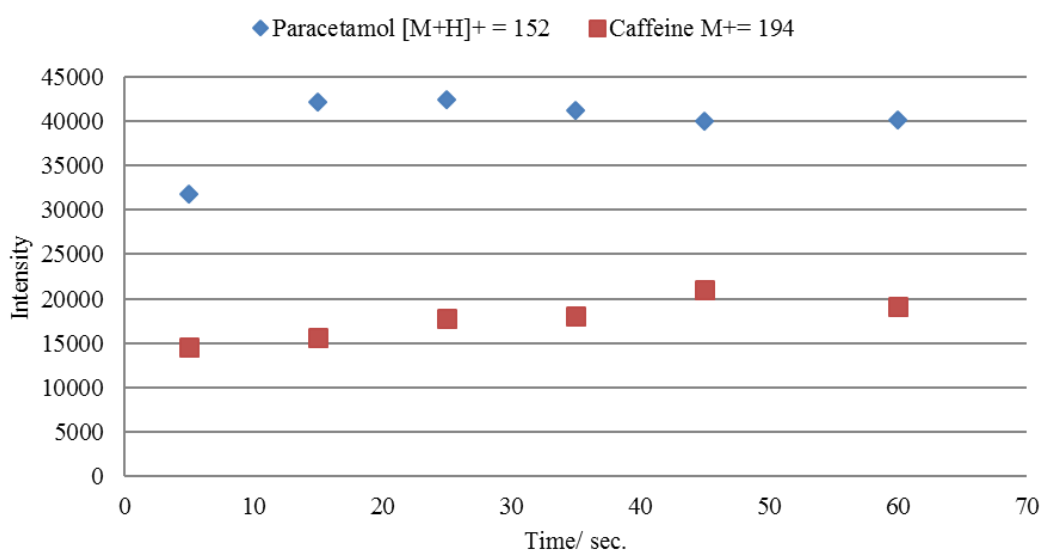


Figure 5. 18. Signal intensity of single paracetamol and caffeine (both $5 \mu\text{g}/\mu\text{L}$) using cotton swabs with a total acquisition time of 1 minute.

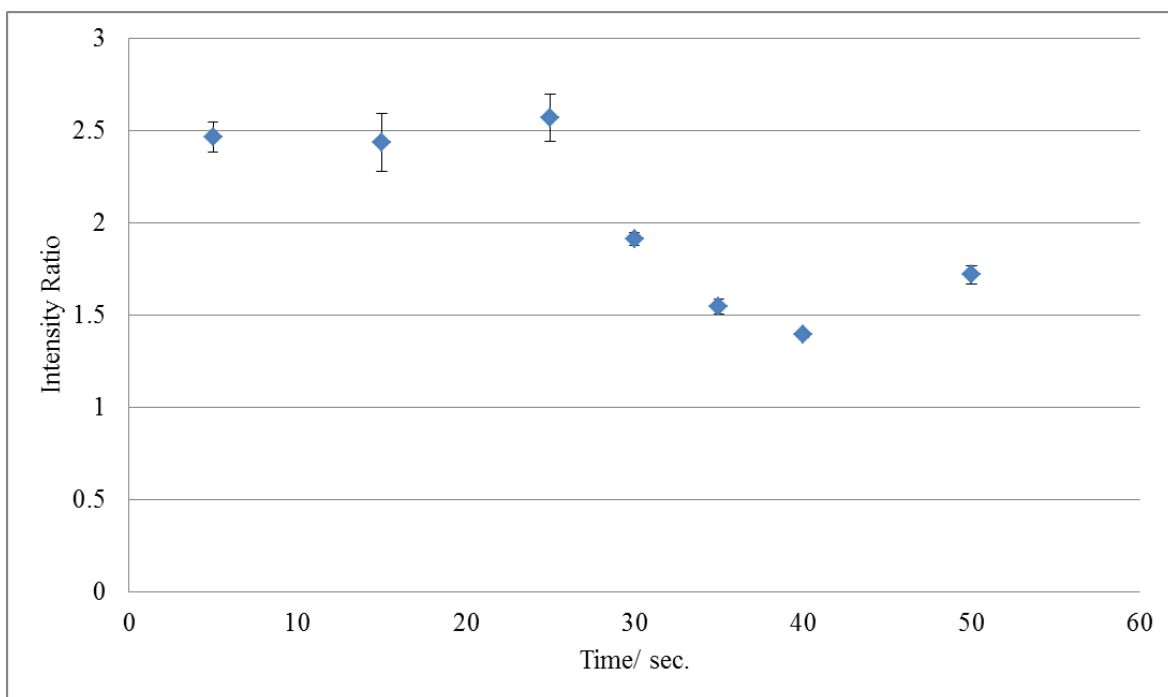


Figure 5. 19. Signal intensity ratios by a factor of (m/z 194/195) of single caffeine molecular ion and single protonated caffeine solutions (both 5 $\mu\text{g}/\mu\text{L}$) applied from cotton swabs using added with water vapour in 5 seconds intervals 0-5, 10-15, 20-25, 25-30, 30-35, 35-40 and 45-50 seconds.

1:1 Mixtures of paracetamol and caffeine solutions with concentrations in the range of 0.01-2.5 $\mu\text{g}/\mu\text{L}$ were prepared and analysed from cotton swabs using PADI-MS with acquisition time up to 60 seconds. As shown in Figure 5.20, two diagnostic peaks relating to paracetamol molecular ion were observed at $[\text{M}+\text{H}]^+$ m/z 152 and $[\text{2M}+\text{2H}]^+$ m/z 304. Other adduct peaks of the paracetamol were observed at $\text{M}+\text{O}-\text{H}$ m/z 166 or $\text{M}+\text{NH}$, $[\text{M}+\text{H}]^+ + \text{CO}$ m/z 180, $\text{M}-\text{H}+\text{2H}_2\text{O}$ m/z 186, $[\text{M}+\text{2H}_2\text{O}]^+$ m/z 187, $[\text{2M}+\text{H}_2\text{O}]^{+2} - (\text{COCH}_3)_2$ m/z 234, $[\text{2M}+\text{H}_2\text{O}]^+ - \text{COCH}$ m/z 279 and $[\text{2M}+\text{2H}_2\text{O}]^+ - \text{COCH}_2$ m/z 296. However, one peak that relates to the caffeine molecular ion was observed at M^+ m/z 194, and another adduct peak was observed at $\text{M}-\text{2H}+\text{O}$ at m/z 208. As expected, intensity signals of all diagnostic, adduct and fragment peaks using high concentrations of

paracetamol and caffeine (both 2.5 $\mu\text{g}/\mu\text{L}$) are higher than using low concentrations (both 0.01 $\mu\text{g}/\mu\text{L}$). For example, the signal intensities of 152 and 194 using 2.5 $\mu\text{g}/\mu\text{L}$ are higher 5x and 1.5x respectively than using 0.01 $\mu\text{g}/\mu\text{L}$. Compared to a glass slide, the intensity signals of protonated paracetamol and caffeine molecular ion tend to be higher with the 0.01 $\mu\text{g}/\mu\text{L}$ using a cotton swab.

The results indicated that paracetamol and caffeine peaks can be detected and identified even at low concentration of mixture solution (0.01 $\mu\text{g}/\mu\text{L}$), Figure 5.21. The signal intensity of protonated paracetamol in all mixture concentrations (0.01- 0.1 $\mu\text{g}/\mu\text{L}$) increased and reached a peak at 35 seconds, after it they decreased up to 1 minute. The results also showed that the behaviour of intensities over time for protonated paracetamol in the mixtures is quite similar to that found with TLC plates after separation of spots, but it was higher when using a cotton swab than TLC plate (see the results in Chapter 4).

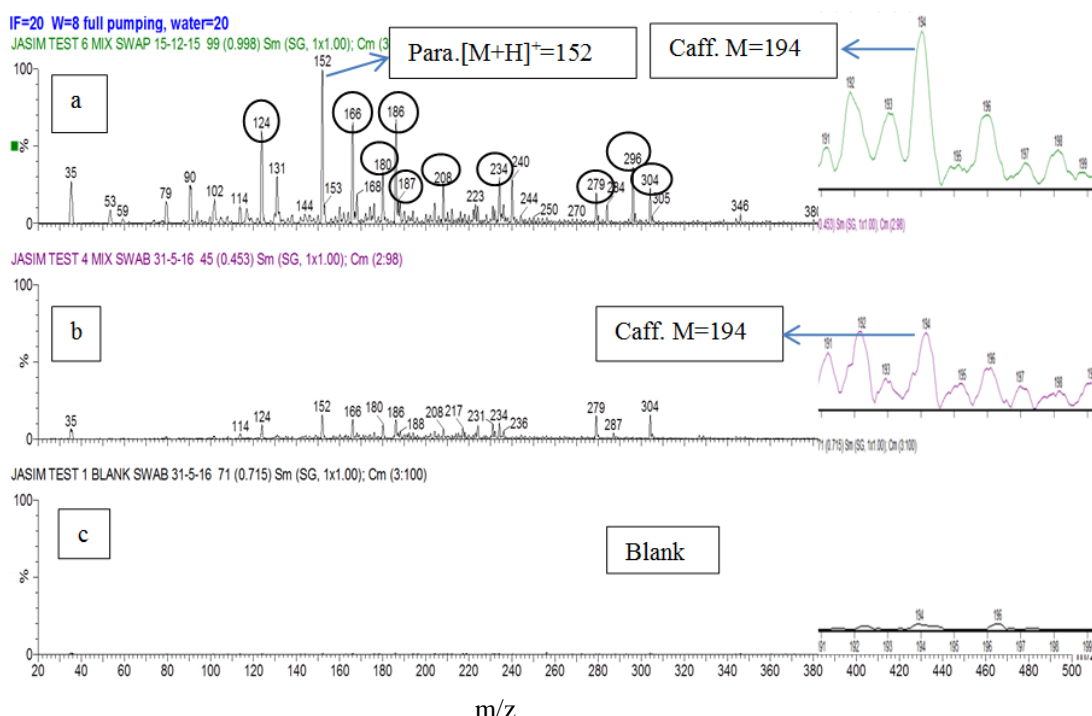


Figure 5. 20. PADI-MS spectra of 1:1 mix with paracetamol and caffeine of (a) 2.5 $\mu\text{g}/\mu\text{L}$, (b) 0.01 $\mu\text{g}/\mu\text{L}$ and (c) blank using cotton swabs with a total acquisition time of 1 minute.

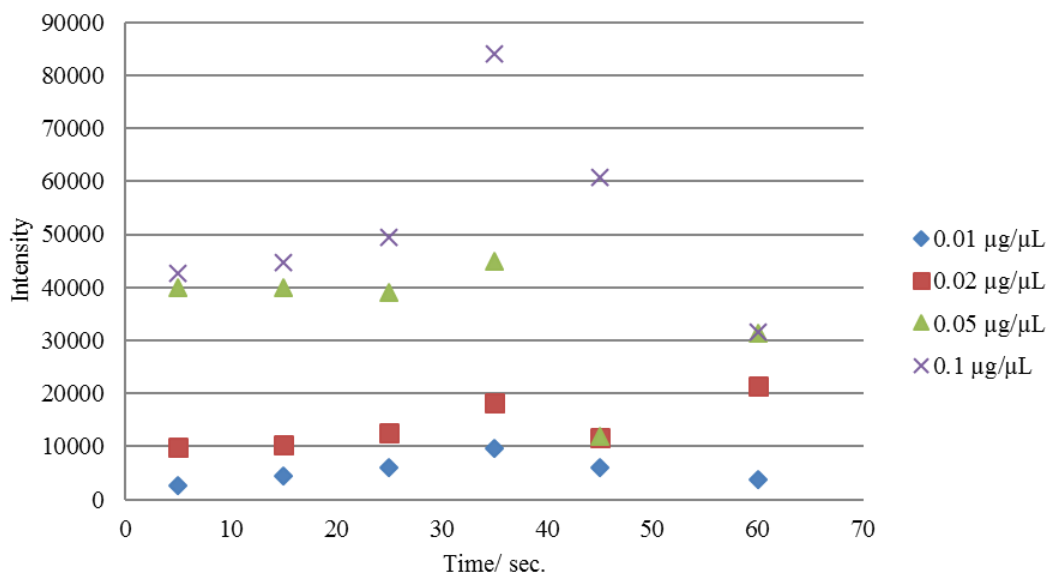


Figure 5. 21. Signal intensity of various concentrations of paracetamol in mixture solutions from cotton swabs with a total acquisition time of 1 minute.

Intensity signal ratios by a factor of m/z 152/195 of the mixture solution of paracetamol and caffeine (both $2.5 \mu\text{g}/\mu\text{L}$) applied from cotton swabs using added water vapour in 5 seconds intervals 0-5, 10-15, 20-25, 30-35, 40-45, 55-60 were plotted. Further analysis was used to analyse the ratios of signal intensity by a factor of m/z 152/195. 1:1 Mixture of paracetamol and caffeine solution (both $2.5 \mu\text{g}/\mu\text{L}$) was used as a model to investigate this ratio. No difference was found in this ratio over the first 25 seconds, after which it decreased up to 60 seconds, Figure 5.22. The behaviour of the intensity ratio of m/z 152/195 used by the cotton swab (Figure 5.22) was similar to that used by glass slide (Figure 5.17).

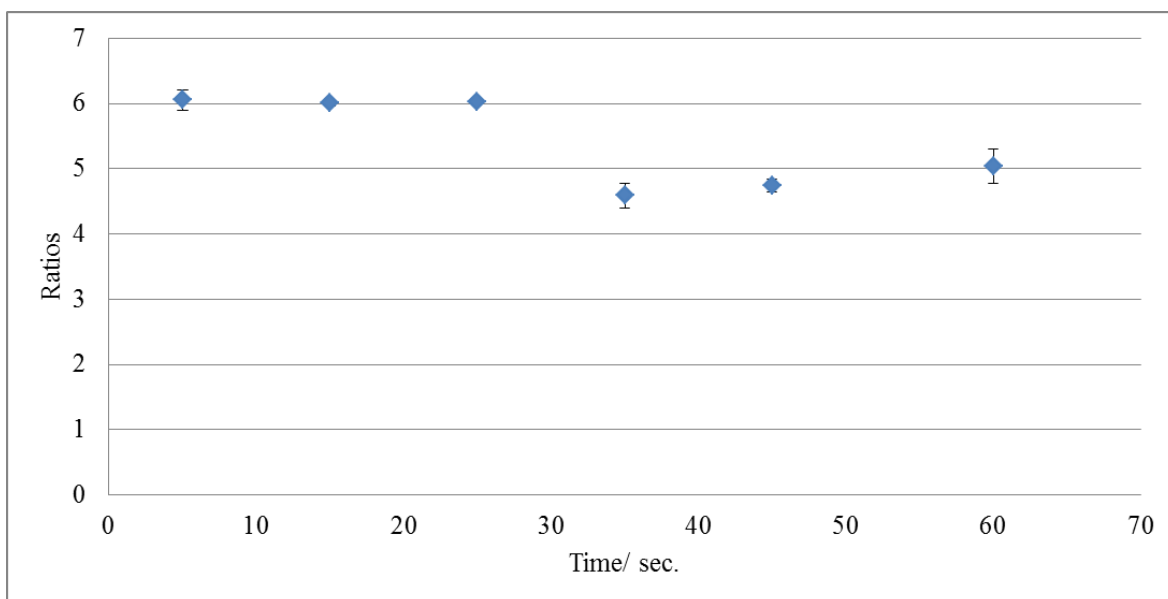


Figure 5. 22. Signal intensity ratios by a factor of m/z 152/195 of the mixture of paracetamol and caffeine solution (both $2.5 \mu\text{g}/\mu\text{L}$) applied from cotton swabs using added with water vapour in 5 seconds intervals 0-5, 10-15, 20-25, 30-35, 40-45 and 55-60 seconds.

PADI-MS analysis of a 1:1 mixture of paracetamol and caffeine solution (both $2.5 \mu\text{g}/\mu\text{L}$) in 5 second intervals with a total acquisition time of 1 minute using cotton swabs are presented in Figure 5.23. The main characteristics of the diagnostic, adduct and fragment peaks of paracetamol and caffeine can be identified as listed in Table 5.2. The intensity of M^+ m/z 194 for the caffeine and $M\text{-CCH}_3$ m/z 124, $[M+H]^+$ m/z 152 diagnostic $M+O\text{-H}$ m/z 166 for paracetamol increased over time, reaching a peak up to ~ 45 seconds, after which they decreased up to 1 minute, and this is consistent with the results that are shown in Figure 5.24. This indicates the length of analysis time up to ~ 45 seconds is the best time to get good spectra and the analysis can be stopped after this time.

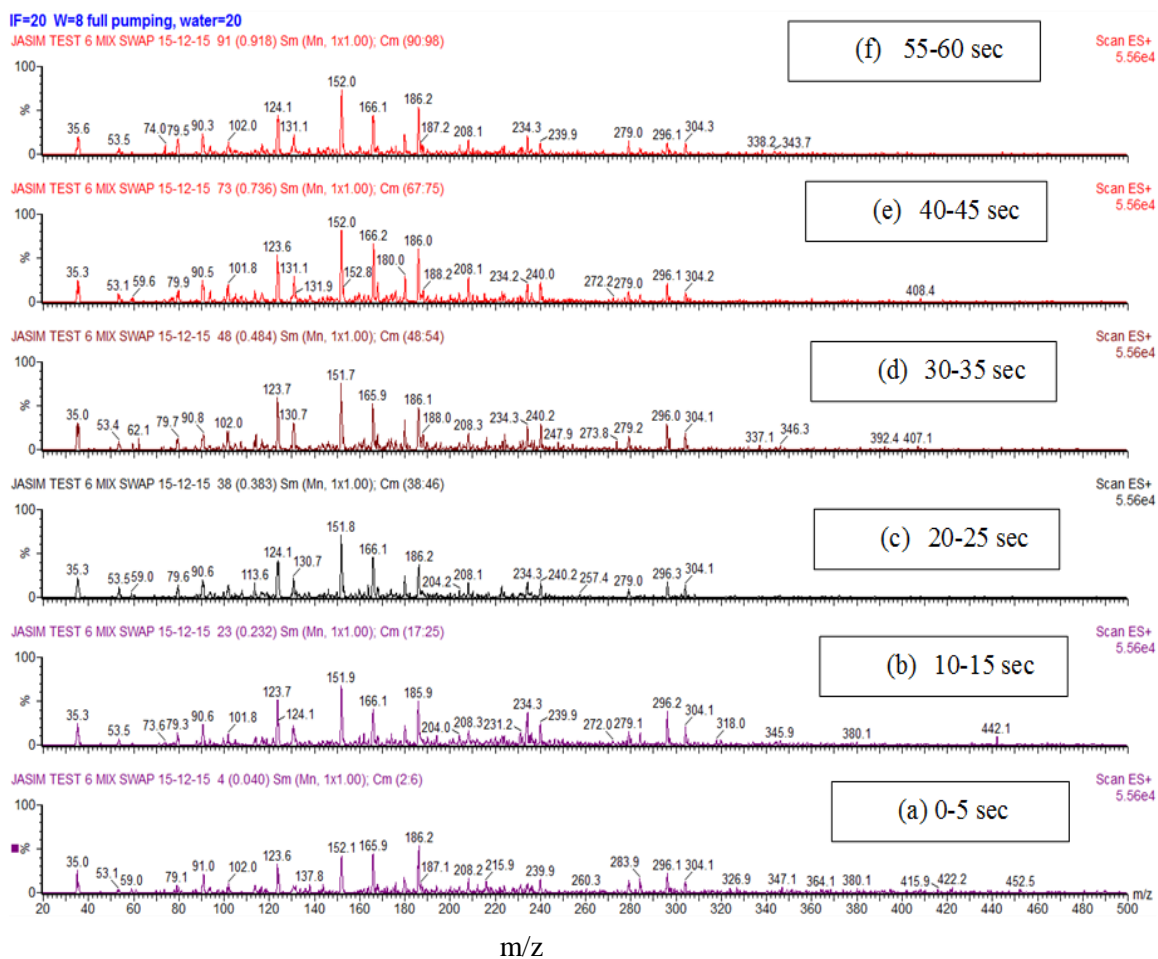


Figure 5. 23. PADI-MS spectra of a 1:1 mixture of paracetamol and caffeine (both 2.5 $\mu\text{g}/\mu\text{L}$) in 5 seconds intervals 0-5 (a), 10-15 (b), 20-25 (c), 30-35 (d), 40-45 (e) and 55-60 seconds (f) using cotton swabs.

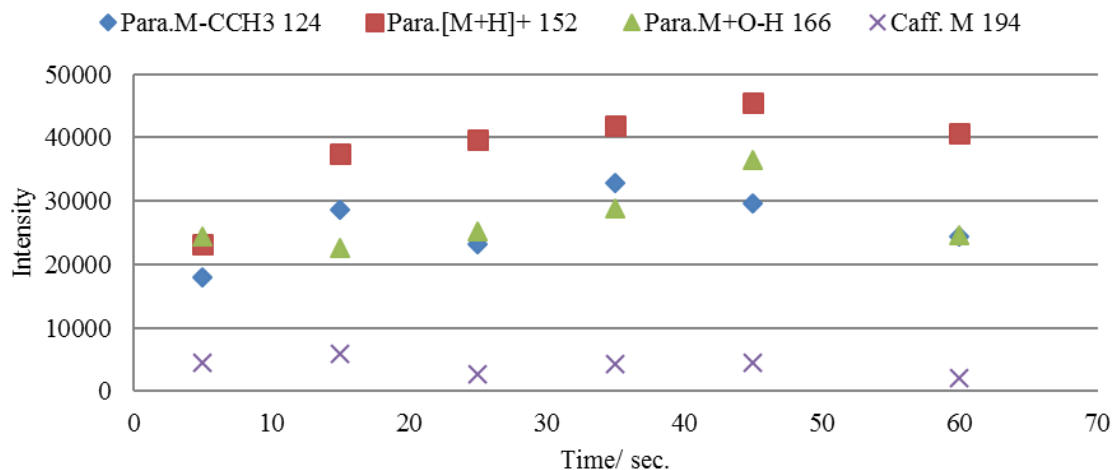


Figure 5. 24. Signal intensity of diagnostic peaks of a paracetamol/caffeine mixture (both 2.5 $\mu\text{g}/\mu\text{L}$) applied using cotton swabs and measured in 5 seconds intervals 0-5, 10-15, 20-25, 30-35, 40-45 and 55-60 seconds.

A mixture solution of Panadol tablet containing different concentrations of paracetamol and caffeine in (50 $\mu\text{g}/\mu\text{L}$ and 6.5 $\mu\text{g}/\mu\text{L}$) was also analysed by PADI-MS with a total acquisition time of 1 minute using a cotton swab, Figure 5.25. There are good signals of diagnostic, adduct and fragment peaks of paracetamol and caffeine in this mixture as identified and listed in Table 5.2. These identified peaks have been compared with those given by 1:1 mixture solutions and found that they are similar in terms of diagnostic, although the concentrations of compounds were not the equal. This indicates that the diagnosis of peaks can not be affected whether using equal or different mixture concentrations. There are a number of similarities and differences between intensities of paracetamol and caffeine over time. Protonated paracetamol and caffeine molecular ions differ not only in intensity but also in behaviour. There is a dramatic increase in intensity for protonated paracetamol by 2x, whereas it a slight by 1x for caffeine molecular ion ~ 25 seconds, after which they decrease by the same amount to 1 minute, Figure 5.26.

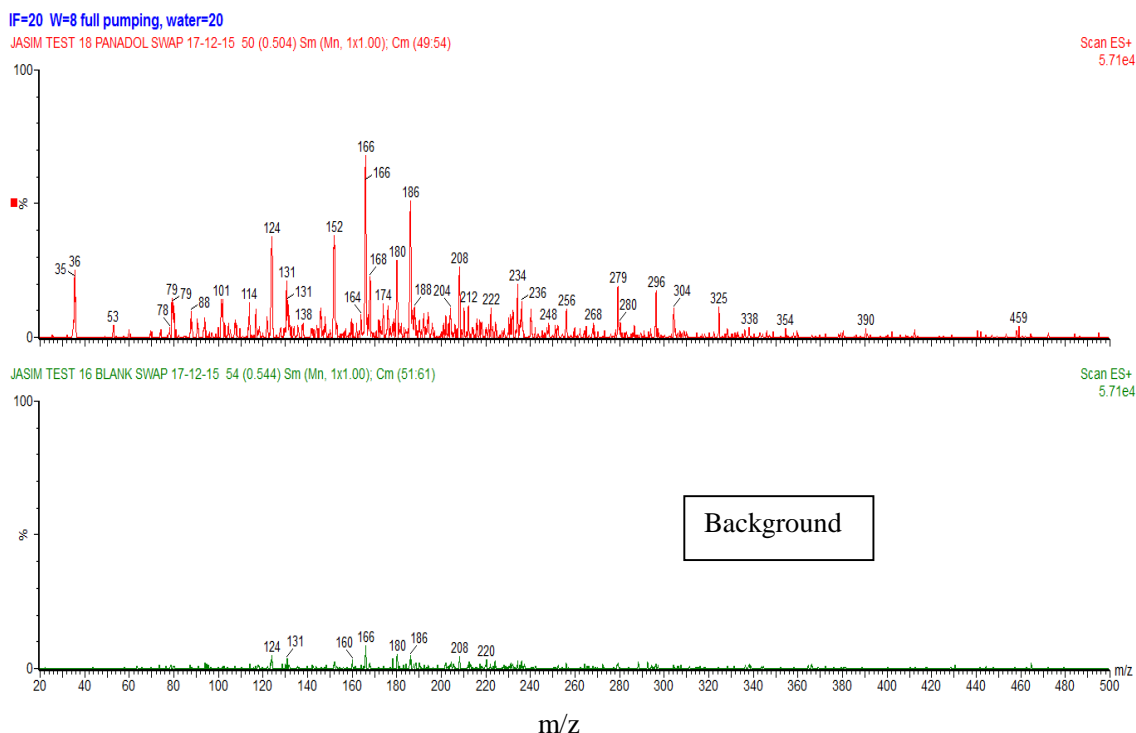


Figure 5. 25. PADI-MS spectrum of Panadol solution (containing paracetamol and caffeine 50 $\mu\text{g}/\mu\text{L}$ and 6.5 $\mu\text{g}/\mu\text{L}$) using cotton swab and measured in 5 seconds intervals 30-35 seconds.

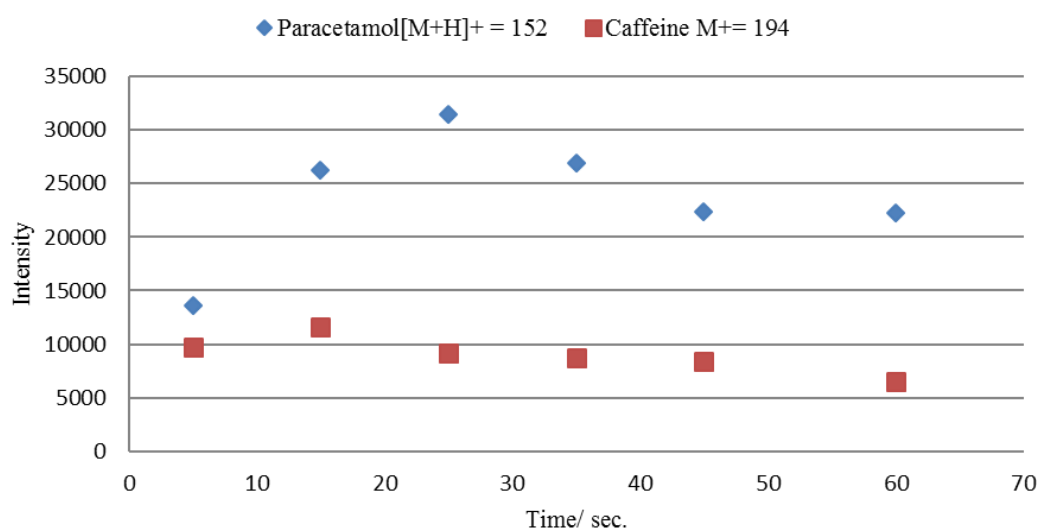


Figure 5. 26. Signal intensity of protonated paracetamol and caffeine molecular ions in Panadol solution from cotton swab using added with water vapour in 5 seconds intervals 0-5, 10-15, 20-25, 30-35, 40-45 and 55-60 seconds.

The results showed that PADI-MS is a fast and easy method to analyse compounds of a sample with no additional sample preparation. Although extensive research has been carried out in this field of analysis, no single study exists which focuses on this method by using these simple and inexpensive substrates to use in the pharmaceutical industry. The main task here is that use these substrates to identify chemical compounds in the different pharmaceutical forms.

5.3.5. Quantification

The correlation between signal intensity and concentrations of standard mixture solutions in this study was tested. A positive linear correlation was found between intensity and concentrations of paracetamol /caffeine mixture using glass slides and cotton swabs. The results showed that a small amount of component can be detected in pharmaceutical mixtures using PADI-MS, via either sampling method tested. The correlation between signal intensity and concentration of paracetamol and caffeine was determined for the concentration range of 0.01 to 0.1 $\mu\text{g}/\mu\text{L}$ in 5 second intervals 30-35 seconds. The correlation coefficients (R^2) values of paracetamol and caffeine were found to be 0.9977 and 0.9588 using glass slide (Figure 5.27), and 0.998 and 0.995 using cotton swabs (Figure 5.28) respectively. The limit of detection (LOD) and limit of quantification (LOQ) were also determined by considering standard deviation to the slope:

$$LOD = \frac{STEYX}{Slope} \times 3$$

$$LOQ = \frac{STEYX}{Slope} \times 10$$

STEYX means the standard deviation of the y-value and x-value.

There are differences in the PADI-MS data collected via these methods. The limits of detection for paracetamol using a glass slide and cotton swab were found to be 6 $\mu\text{g/mL}$ and 5 $\mu\text{g/mL}$ respectively, while for caffeine were 29 $\mu\text{g/mL}$ and 12 $\mu\text{g/mL}$ respectively. The limits of quantification (LOQ) for paracetamol using a glass slide and cotton swab were found to be 22 $\mu\text{g/mL}$ and 18 $\mu\text{g/mL}$ respectively, while for caffeine 96 $\mu\text{g/mL}$ and 42 $\mu\text{g/mL}$ respectively. As can be seen from the values above, the LOD and LOQ for paracetamol can be improved using a cotton swab. However, the linearity is limited using high concentrations of the mixture ($> 0.1 \mu\text{g}/\mu\text{L}$) for both glass slides and cotton swabs because it causes nonlinearity including deviation in the calibration curve.

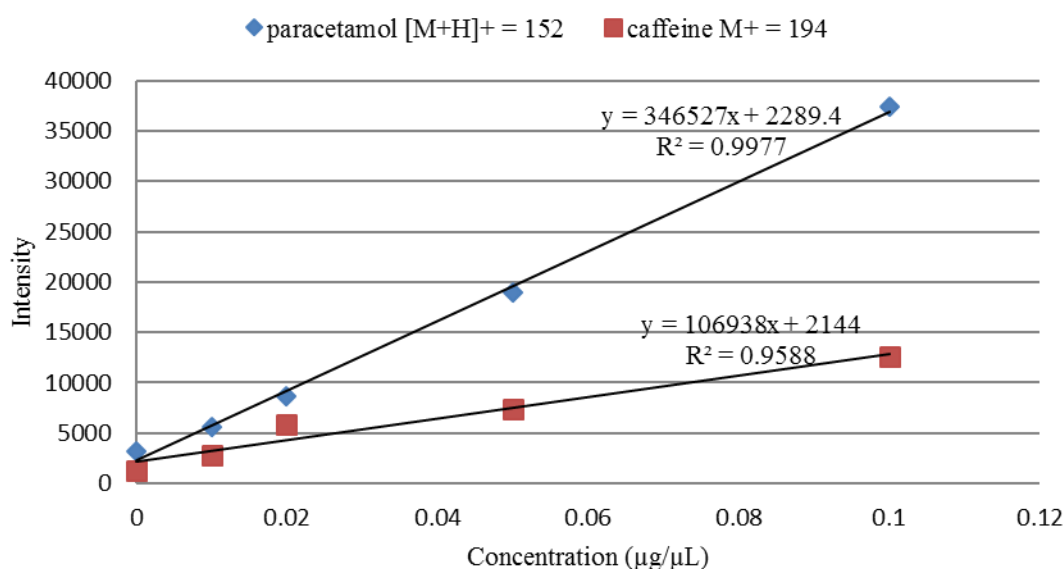


Figure 5. 27. Calibration plot of mass intensity versus concentrations of standard mixture solutions of protonated paracetamol and caffeine molecular ion using glass slides.

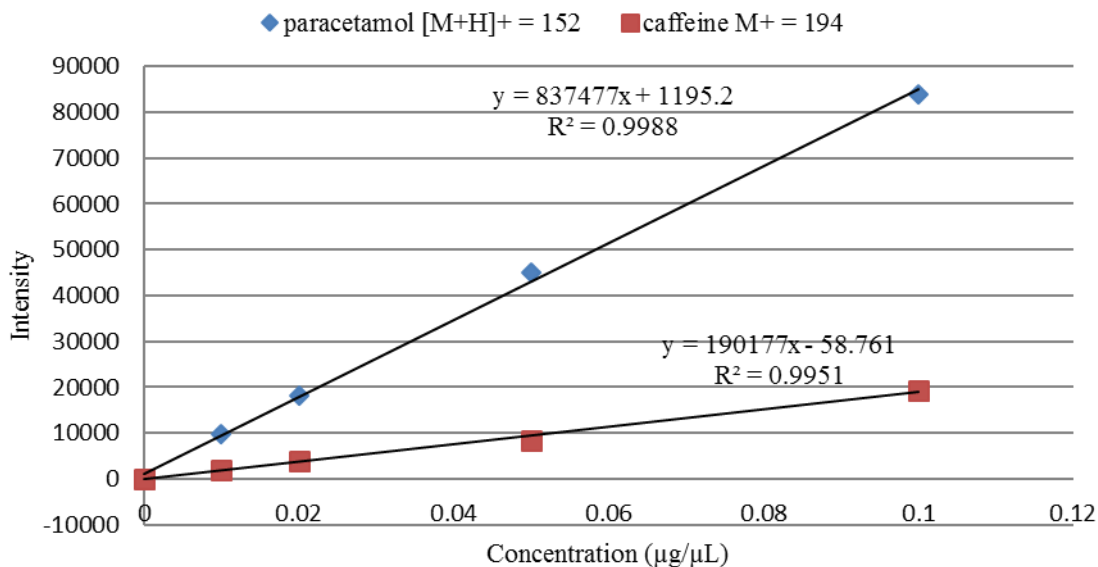


Figure 5. 28. Calibration plots of mass intensity versus concentrations of standard mixture solutions of protonated paracetamol and caffeine molecular ion using a cotton swab.

5.4. Conclusions

The present study was designed and developed to understand if PADI-MS could be used to analyse, identify and gain quantification information for pharmaceutically relevant samples either directly from solids or liquids; with liquids being assessed on glass slides or by cotton swabs. Paracetamol and caffeine were used as model compounds, with mixtures of these commonly found in over the counter drugs such as Panadol. This study has demonstrated, for the first time that the PADI-MS technique is able to be used for direct analysis of solids and pharmaceutical liquids using these simple and cheap substrates. The results showed that the method is simple, sensitive, fast, has good linearity and small amounts of samples are required for analysis compared to other methods. This study has shown that 5 second intervals 30-35 seconds were decided as the optimal time for the high-intensity signal of adduct and fragment peaks for paracetamol and caffeine in the solid and liquid sample. This confirmed that PADI-MS is able to measure samples in single or mixture solutions in 5 seconds. This is an important issue for future research because the

present study raises the possibility that can save time and cost using this method. The main goal of the current study was to develop a novel method that can be used for identification of components in complex mixtures that are not resolved by other methods such as chromatographic and spectroscopic techniques.

The intensity of protonated paracetamol (152) is 7x more abundant than caffeine molecular ion (194) in the Panadol tablet. This study has found that the differences in the intensity of protonated paracetamol and caffeine molecular ion between tablets and solutions are 8x and 3x respectively. The results of this study show that the behaviour of the intensity ratios of 152/195 and 194/195 used by the cotton swab is similar to that used by the glass slide. The research has also shown that the limits of detection for paracetamol in the 1:1 mixture solution using glass slides and cotton swabs were lower than caffeine and it was found to be 6 μ g/mL and 5 μ g/mL respectively. There was evidence that the type of substrate has an influence on the signal intensity of ions observed.

It would be interesting to compare the analysis of this study including individual and paracetamol /caffeine mixtures which used glass slides and cotton swabs to those used by TLC plates in the previous chapter (Chapter 4). There are important similarities and differences between these substrates for quantification analysis of paracetamol and the caffeine. No significant differences were found between the R^2 of paracetamol and the caffeine whether use glass slides, cotton swabs or TLC plates. They found to be 0.9977, 0.998 and 0.999 for paracetamol, and 0.9588, 0.995 and 0.996 for caffeine respectively. On the other hand, the differences between the LOD and LOQ were significant. Compared with the glass slide and TLC plate, the cotton swab was the best substrate to optimise the LOD and LOQ for these compounds. The LOD and LOQ were improved using the cotton swab and found to be 5 μ g/mL and 18 μ g/mL for paracetamol, and 12 μ g/mL and 42 μ g/mL for caffeine respectively. The LOD and LOQ were 6 μ g/mL and 22 μ g/mL for paracetamol,

and 29 $\mu\text{g}/\text{mL}$ and 96 $\mu\text{g}/\text{mL}$ for caffeine using glass slides, whereas they were 15 $\mu\text{g}/\mu\text{L}$ and 49 $\mu\text{g}/\mu\text{L}$ for paracetamol and 50 $\mu\text{g}/\mu\text{L}$ and 165 $\mu\text{g}/\mu\text{L}$ for caffeine using TLC plates respectively. In addition to these results, the cotton swab is cheap, convenient and gives better signal compared to a glass slide and TLC plate.

The findings of this study have a number of important implications for future practice. In the future work, the technique may be applied for identification and monitoring of other pharmaceutical tablets and mixture solutions using these substrates. Although this study focuses on qualitative analysis, the findings may well have a bearing on quantitative analysis. Further studies on the current topic are therefore recommended. Recommendation for further research work is that should focus on determining components in solids/ liquids mixtures. It is also recommended that further research is undertaken in the following areas: pharmaceuticals, biomedicine and environmental pollution. The method used for this analysis may be carried out to other pharmaceutical applications elsewhere in the world. Despite the current study being based on small and simple pharmaceutical molecules, the findings suggest this novel method can be used to analyse big and complex pharmaceutical molecules. This research extends our knowledge of using this simple and easy method to analyse complex mixtures in many fields. The challenge now is to use this method confidently to identify compounds in air, breath and other gas samples.

References

1. Hansen, S. Pedersen-Bjergaard, S. and Rasmussen, K. (2012) 'Introduction to pharmaceutical chemical analysis', UK, John Wiley & Sons, Ltd.
2. Chieng, N. Rades, T. and Aaltonen, J. (2011) 'An overview of recent studies on the analysis of pharmaceutical polymorphs', *Journal of Pharmaceutical and Biomedical Analysis*, 55, pp. 618–644.
3. Sun, S. F. Lui, G. R. and Wang, Y. H. (2006) 'Simultaneous determination of acetaminophen, caffeine, and chlorphenamine maleate in paracetamol and chlorphenamine maleate granules', *Chromatographia*, 64 (11–12), pp. 719–724.
4. El-Gindy, A. Emar, S. Mesbah, M. K. and Hadad, G. M. (2006) 'New validated methods for the simultaneous determination of two multicomponent mixtures containing guaiphenesin in syrup by HPLC and chemometrics-assisted UV-spectroscopy', *Anal. Lett.*, 39 (13–15), pp. 2699–2723.
5. Burge, L. J. Raches, D. W. (2003) 'A rapid HPLC assay for the determination of a dextropropoxyphene related substance in combination with aspirin, acetaminophen, and caffeine in tablet and capsule formulations', *Journal of Liquid Chromatography* R. T., 26 (12), pp. 1977–1990.
6. Qi, M. L. Wang, P. Leng, Y. X. Gu, J. L. and Fu, R. N. (2002) 'Simple HPLC method for simultaneous determination of acetaminophen, caffeine and chlorpheniramine maleate in tablet formulations', *Chromatographia*, 56 (5–6), pp. 295–298.
7. Franeta, J.T. Agbaba, D. Eric, S. Pavkov, S. Aleksic, M. and Vladimirov, S. (2002) 'HPLC assay of acetylsalicylic acid, paracetamol, caffeine and phenobarbital in tablets', *Il Farmaco*, 57 (9), p.p. 709–713.

8. Sawyer, M. and Kumar, V. (2003) 'A rapid high-performance liquid chromatographic method for the simultaneous quantitation of aspirin, salicylic acid, and caffeine in effervescent tablets', *J. Chromatograph. Sci.*, 41 (8), p.p. 393–397.
9. Lim, C.K. and Lord, G. (2002) 'Current developments in LC-MS for pharmaceutical analysis', *Biological and Pharmaceutical Bulletin*, 25(5), p.p. 547–557.
10. De Lima Gomes, P.C. Barletta, J.Y., Nazario, C.E., Santos-Neto, A.J., Von Wolff, M.A. Coneglian, C.M. Umbuzeiro, G.A. and Lancas, F.M. (2011) 'Optimisation of in situ derivatization SPME by experimental design for GC-MS multi-residue analysis of pharmaceutical drugs in wastewater', *Journal of Separation Science*, 34(4), p.p. 436–445.
11. Wollein, U. and Schramek, N. (2012) 'Simultaneous determination of alkyl mesitates and alkyl besitates in finished drug products by direct injection GC/MS', *European Journal of Pharmaceutical Sciences*, 45(1-2), p.p. 201–204.
12. Wang, X.M. Zhang, Q.Z. Yang, J. Zhu, R.H. Zhang, J., Cai, L.J. and Peng, W.X. (2012) 'Validated HPLC-MS/MS method for simultaneous determination of curcumin and piperine in human plasma', *Tropical Journal of Pharmaceutical Research*, 11(4), p.p. 621–629.
13. Nandakumar, S. Menon, S. and Shailajan, S. (2012) 'A rapid HPLC-ESI-MS/MS method for determination of β -asarone, a potential anti-epileptic agent, in plasma after oral administration of *Acorus calamus* extract to rats', *Biomedical Chromatography*, 27(3), p.p. 318–326.
14. Wolfender, J.L. Queiroz, E. F. and Hostettmann, K. (2006) 'The importance of hyphenated techniques in the discovery of new lead compounds from nature', *Expert Opinion on Drug Discovery.*, 1(3), p.p. 237–260.

15. Lee, P.J. Murphy, B.P. Balogh, M.P. and Burgess, J.A. (2010) 'Improving organic synthesis reaction monitoring with rapid ambient sampling mass spectrometry', Waters Corporation, Milford, MA, USA.
16. Lebedev, A. T. (2015) 'Ambient ionization mass spectrometry', *Russian Chemical Reviews*, 84 (7), p.p. 665 – 692.
17. Madhusudanan, K. P. (2007) 'Direct analysis in real time (DART) – a new ionization technique', 12th ISMAS Symposium cum, Workshop on Mass Spectrometry, p.p. 25–30.
18. Hajslova, J. Cajka, T. and Vaclavik, L. (2011) 'Challenging applications offered by direct analysis in real time (DART) in food-quality and safety analysis', *Trends in Analytical Chemistry*, 30 (2), p.p. 204–218.
19. Bridoux, M.C. and Machuron-Mandard, X. (2013) 'Capabilities and limitations of direct analysis in real time orbitrap mass spectrometry and tandem mass spectrometry for the analysis of synthetic and natural polymers', 27(18), p.p. 2057–2070.
20. Ratcliffe, L.V. Rutten, F.J.M. Barrett, D.A. Terry Whitmore, T. Seymour, D. Greenwood, C. Gonzalvo, Y.A. Robinson, S. and McCoustra, M. (2007) 'Surface analysis under ambient conditions using plasma-assisted desorption/ ionisation mass spectrometry' *Analytical Chemistry*, 79 (16), p.p. 6094–6101.
21. P. Roach and F.J.M. Rutten, to be published

CHAPTER 6: PADI mass spectrometry for the monitoring of imine (Schiff base) formation as a model of pharmaceutical reaction mixtures

Abstract

In this chapter a novel analytical approach for monitoring of pharmaceutically relevant reactions using PADI-MS with cotton swabs as a substrate is reported. TLC, HPLC, FTIR and PADI-MS were all evaluated for the monitoring of an imine formation reaction. Even after extensive optimisation of the separation on TLC using ethyl acetate and petroleum ether (80:20 w/w) as a solvent, not all starting materials and reaction products were satisfactorily detected using UV illumination. RP-HPLC was successful in identifying the reactants 4-nitrobenzaldehyde and para-anisidine with well-resolved peaks and distinct retention times for each compound, but it failed to detect imine formation. This was arguably due to that the reaction being driven back in the direction of the reactants during HPLC analysis. HPLC did not detect product, FTIR then revealed it was definitely formed. This result may be explained if in the HPLC process the reaction may have been reversed as the imine should have been detected if present. FTIR has been used to identify the appearance and disappearance of functional groups for products and reactants. The results showed that ($\nu_{C=O}$) stretching peak of 4-nitrobenzaldehyde and imine (N-H) stretch of para-anisidine decreased in intensity with time and completely disappeared after 45 minutes. At the same time, they show an increase in area for the $\nu_{C=N}$ and $\nu_{C=C}$ stretching peaks indicating the formation of the imine reaction product up to approximately 60 minutes. PADI-MS has been optimised for monitoring of the imine formation using a cheap and simple substrate. Samples of reaction as aqueous solutions were taken as swabs and analysed directly from the cotton tip. The results of this study indicate that the PADI-MS technique is simple, sensitive, fast and suitable for monitoring of pharmaceutical reaction mixtures via cotton swabs.

6.1. Introduction

Reaction monitoring is important for a wide range of scientific and industrial processes. Process analytical technologies (PAT) have been developed to follow a wide range of reaction processes in the pharmaceutical and chemical industries (1). Monitoring methods provide important aspects of reaction pathways of chemical synthesis during the reaction process. Imine synthesis from aldehydes or ketones is an important chemical reaction due to its relevance to biological processes (2, 3), role as an intermediates in the organic synthesis of compounds, and directly to manufacture compounds for several applications (4). Therefore, it is very important to monitor this reaction. The reaction between carbonyl group in aldehyde and primary imine, known as Schiff base, was discovered by German chemist Hugo Schiff in 1864 (5). Schiff base formation is important in organic synthesis because it is used to make carbon-nitrogen bonds. Intermediate compounds of Schiff bases that are formed by enzyme reaction with carbonyl and amino group are also important in the biochemical process (6). Due to the biological activities presented by Schiff bases compounds, they known as antimicrobial agents (7). Schiff bases and their metal compounds have beneficial biological applications, as anticancer, antiviral antimalarial, antimicrobial, antioxidant and antidepressant agents (8-12).

Several analytical techniques such as nuclear magnetic resonance (NMR), infrared (IR), Raman spectroscopy and HPLC have been used to monitor pharmaceutical reaction mixtures (13). In a study by Kim *et al.*, UV-Vis spectroscopy has been used to determine the surface density of imine synthesis which is formed by Schiff's base reaction between the carbonyl group of 4-nitrobenzaldehyde and the amine group of ethylenediamine (14). FTIR spectroscopy has been used to monitor the Schiff's base reaction between the carbonyl group of pyruvic acid and amine group of amino alcohols at different temperatures (15).

However, these methods have crucial limitations and disadvantages. NMR has limited sensitivity and hence requires a relatively a large amount of sample for analysis. FTIR is unable to detect all compounds and it is not well-suited for quantitative analysis (16). In the TLC method, the length of the plate is limited and hence separation takes place only up to a certain length. The TLC method operates in open system, hence the temperature and humidity may effect on the results. The retention factor (R_f) of molecules must be known before. Specificity is another problem in the TLC method. For example, different compounds with comparable polarity may have the same R_f value. HPLC tends to be relatively expensive, consumes chemicals, takes a considerable amount of time and sample preparation is often required.

Mass spectrometry is a fast, sensitive and specific tool for identification and quantification of chemical compounds. MS provides information about molecular weights through (quasi-) molecular ions and chemical structures via fragmentation patterns of the analytes (17). Mass spectrometry techniques have been used to monitor chemical reactions in order to save time, sample amounts and solvents whilst identifying analytes by providing information about the chemical structure of compounds (18, 19). Hyphenated chromatographic mass techniques such as gas chromatography (GC-MS) and liquid chromatography (LC-MS) have been used for the monitoring of chemical reactions combining the strengths of both techniques. However, the chromatographic sample preparation such as extraction, filtration, and separation is needed before analysis by GC-MS and LC-MS (18), which adds a considerable time and cost factor.

During the last decade, ambient mass spectrometry (AMS) has been developed for direct analysis of chemical compounds with no or little sample preparation (20). Desorption electrospray ionisation-mass spectrometry (DESI-MS) is an important AMS method used to analyse samples directly (21). DESI applications involve environmental analysis,

clinical diagnostics and reaction monitoring of drugs manufacture. Direct analysis in real time (DART) was introduced shortly after DESI and can be applied for direct analysis of liquids and solid samples without the need for extraction (22). DART-MS has been used to monitor organic reactions and to confirm the final products in drug discovery (23). Due to consume and spray solvent, DESI is not always practical (24). DART has lower detection selectivity and makes this technique more vulnerable to false finding (25). PADI uses non-thermal visible plasma as a source to produce ions from the surfaces of molecules. It can analyse different kinds of compounds directly from a surface including solids, creams and liquids, at room temperature (26, 27). Compared to DART, PADI uses different plasma that causes minimal damage to the sample surface.

In this study, the Schiff base is formed by reacting 4-nitrobenzaldehyde with para-methoxy aniline (para-anisidine) at room temperature, Figure 6.1. This reaction is easy to follow without the need to isolate the intermediate compound, and it would expect to give a stable amine. This reaction was chosen in this study as a model for pharmaceutically and biological relevant mixtures, as it is readily controlled, requires readily available chemicals, requires no heating and the product can, in principle, readily be analysed by TLC, HPLC and IR.

The specific objective of this study was to develop a fast, versatile yet simple, sensitive and cost-effective analytical method for monitoring the imine synthesis, including identification of a suitable substrate. In this work, several analytical techniques namely TLC, HPLC and FTIR, in addition to PADI-MS, have been used to monitor the reaction of 4-nitrobenzaldehyde with para-anisidine over time. Another objective of this study was that using a cotton swab as a substrate in this reaction can give better signals in the PADI spectra in comparison with TLC plates and glass slides. The aim of this study was to find out which technique is best to monitor the reaction.

6.2. Materials and methods

6.2.1. Apparatus:

6.2.1.1. UV-Vis spectrophotometer

A Cary 50 Bio (Varian UK), version 3.00, dual beam spectrophotometer was used. Absorbance spectra of blank (solvent) and samples were recorded using quartz cells. The wavelength ranges used for all samples was 200-800 nm. The scan rate was 600 nm/min, with a 1.00 nm data interval and an average acquisition time of 100 milliseconds. The wavelengths of maximum absorbance of the starting materials and the final product were measured and observed at 265 nm for 4-nitrobenzaldehyde, 241 nm for para-anisidine and 258 nm for the product.

6.2.1.2. Thin layer chromatography (TLC)

Silica gel TLC plates were used (for more details see Chapter 4), and developed using ethyl acetate and petroleum ether ratio as mobile phase. TLC spots were visualised by means of a handheld UV lamp (Upland CA, City, U.S.A).

6.2.1.3. High performance liquid chromatography (HPLC)

HPLC was carried out using a Perkin Elmer system consisting of Flexar LC Autosampler, Flexar LC Detector, Flexar Quaternary LC pump and ODS-C₁₈ column 150 mm × 4.6 mm (Matlab, UK). After thorough optimisation, the following settings were used throughout: all chromatographic experiments were performed in the isocratic mode. The mobile phase consisted of acetonitrile and deionised water (25%: 75%, v/v). The flow rate and detection wavelength were set to be 1 mL/min and 300 nm respectively.

6.2.1.4. Fourier transform infrared spectroscopy (FTIR)

FTIR spectroscopy was carried out using a Thermo Fisher Scientific iS10 instrument (Hemel Hempstead, UK) fitted with a DTGS detector and a single bounce germanium ATR smart accessory. The number of scans and the resolution were optimised to 64 and 4 cm^{-1} respectively.

6.2.1.5. Plasma assisted desorption ionisation mass spectrometry (PADI-MS)

In the PADI-MS instrumentation, a single quadrupole (Waters Micromass ZQ, Manchester, UK) was used with the front end removed to accept a modified Stoffels-design plasma pen ionisation source using a 13.56 MHz RF power source (27). The plasma pencil was fabricated to provide coaxial dual gas flow; an inner ceramic tube was encompassed within a quartz glass tube. Helium gas was flown through both tubes controlled using separate flow meters, the flow inside the ceramic tube will henceforth be referred to as inner flow, the flow between the ceramic and quartz tube as outer flow. Mass conditions including inner flow, flow gas and plasma power were set up for all experiments. The conditions for PADI-MS were optimised and the same settings used for all samples in this study: plasma power of 8 W, helium inner flow of 224 mL/min and the distance between the plasma flame and sample of 5 mm. The effect of water vapour on ionisation efficiency was investigated by flowing the helium through a water vapour added environment (outflow) before the plasma pencil (for more information see Chapter 2).

6.2.2. Chemicals:

4-nitrobenzaldehyde was supplied by AVOCADO Research Chemicals Ltd (purity 99%). Para-anisidine was obtained from Alfa Aesar, UK. Laboratory reagent grade ethyl acetate (GLC > 99%) was supplied by Fisher Scientific, UK. Petroleum ether and dichloromethane

were supplied by VWR Prolabo BDH chemicals, International SAS, France (impurities < 0.1 %). Acetonitrile was supplied by Sigma–Aldrich Chemical Company, UK (purity 99%). Deionised water was provided through a Pure Lab Option system (ELGA, UK) with conductivity of 0.067 MS/cm. Helium gas was supplied by British Oxygen Company (BOC) gases, UK (purity 99%). Standard glass microscope slides and cotton swabs were supplied by Fisher Scientific, UK.

6.2.3. Schiff base reaction

Schiff base formation was carried out at room temperature in around-bottom reaction flask of 100 mL using a magnetic stirrer. 10 mmol of each starting material (4-nitrobenzaldehyde and para-anisidine) was prepared by dissolving 75.5 mg and 61.5 mg respectively in 50 mL of dichloromethane. A schematic of the chemical reaction used for the synthesis of the imine is shown in Figure 6.1. It illustrates the synthesis of N-(4-methoxyphenyl)-1-(4-nitrophenyl) methanimine (N-4-MP-1-4-NPM). The reaction progress was monitored by TLC, HPLC, FTIR and PADI-MS.

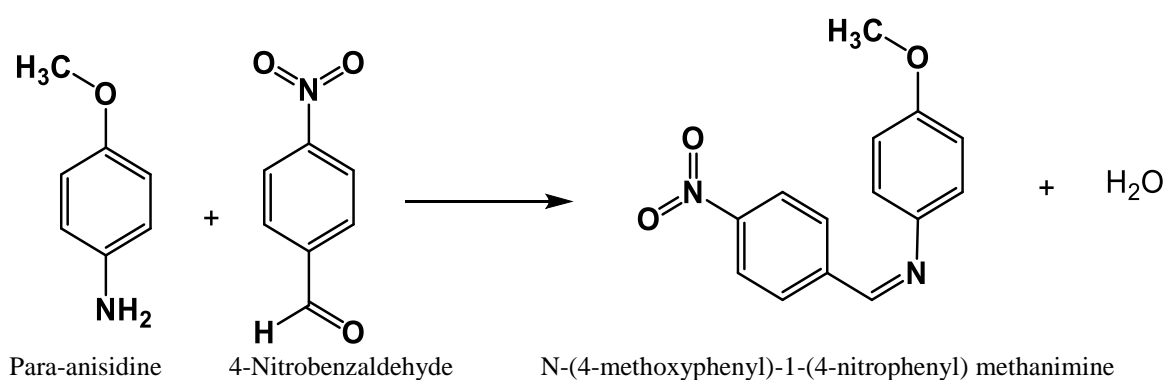


Figure 6. 1. The schematic reaction of the imine formation.

6.2.4. Monitoring Methods

6.2.4.1. Monitoring of the Schiff base formation by TLC

- 1- A large TLC sheet was cut horizontally into plates 6.5 cm by 2.5 cm.
- 2- Small spots of individual compounds of 4-nitrobenzaldehyde and para-anisidine (both 10 mM) were deposited on TLC plate using a spotter tube as a control for identification. The droplet size was 0.8 μL and the amount of reactant per droplet was 4 μg .
- 3- The spots were developed using a mixture of ethyl acetate and petroleum ether as mobile phase, with optimal separation requiring a 80:20 (w:w) mixture.
- 4- The separated spots were identified under the UV light after drying before any further analysis.
- 5- The reaction was carried out for a total time of 1 hour. After this time no further changes were observed. The reaction mixture samples were taken every 10 minutes.
- 6- All samples including starting materials and reaction mixture were deposited immediately on TLC plates and separated.

6.2.4.2. Monitoring of the Schiff base reaction by HPLC

- 1- The wavelengths of the starting materials and product were measured by UV-Vis spectrophotometry.
- 2- Both pure reactants 4-nitrobenzaldehyde and para-anisidine were detected after conditions were optimised.
- 3- The reaction was repeated and run for 2 hours and the reaction mixture was sampled every 15 minutes using a Pasteur pipette.

4- Each sample of the reaction mixture was injected (20 μ L) immediately into the HPLC instrument for analysis.

6.2.4.3. Monitoring of the Schiff base reaction by FTIR

1- Single compounds of the starting materials were analysed by FTIR.

2- The reaction was repeated and run for 2 hours and the reaction mixtures were taken every 15 minutes.

3- The collected samples of the reaction mixtures were analysed immediately by FTIR, without drying.

6.2.4.4. Monitoring of the Schiff base reaction by PADI-MS

1- Both pure reactants were analysed by PADI-MS using the optimal conditions using different substrates such as TLC plate, glass slide and cotton swab in order to find out the best one.

2- The reaction was repeated and run for 2 hours and the reaction mixtures were taken every 15 minutes.

3- The reaction mixtures were analysed immediately (without drying) by PADI-MS using a cotton swab.

6.3. Results and discussion

6.3.1. Wavelength measurements of the starting materials and product using UV-Vis spectrophotometry

The λ_{\max} values of the starting materials (4-nitrobenzaldehyde and para-anisidine) and the product were determined using UV-Vis spectrophotometry, Figure 6.2. The samples were prepared in the same solvent used for the reaction (dichloromethane). Absorbance spectra

of blank (solvent) were recorded before any measurement of the sample. The wavelength ranges were set between 200-800 nm. Because the absorbance of 4-nitrobenzaldehyde and product were too high (off-scale), their concentrations were diluted to 50 times in a comparison with para-anisidine.

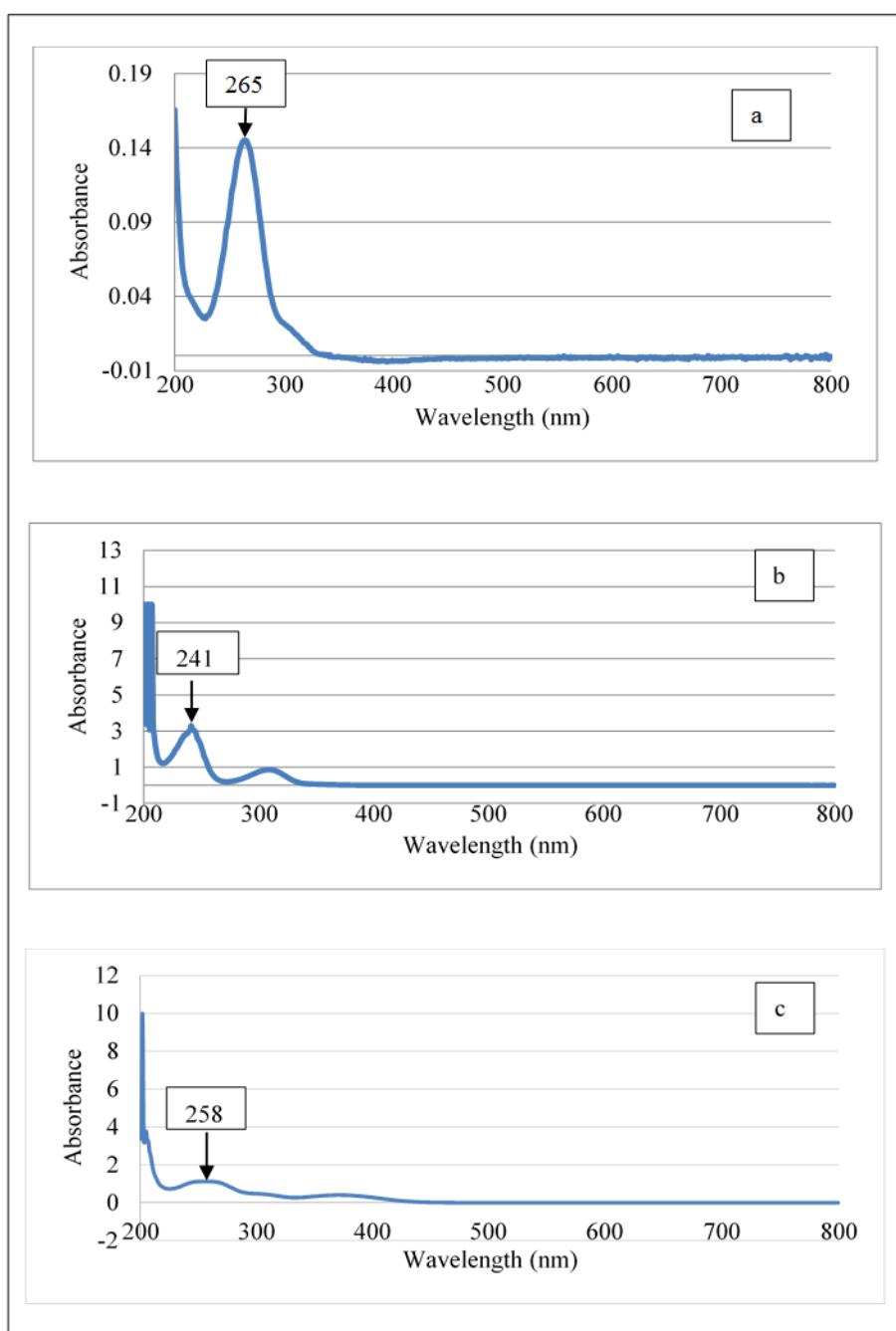


Figure 6. 2. UV/Vis spectra of 4-nitrobenzaldehyde (a), para-anisidine (b) and product (N-4-MP-1-4-NPM) (c) (10 mmol each).

6.3.2. Reaction monitoring of imine formation using TLC

TLC method is in principle a convenient choice to monitor the reaction between 4-nitrobenzaldehyde and para-anisidine for several reasons. It is simple, fast, inexpensive, and very little equipment is required. TLC is one of the most widely used analytical techniques and has been used extensively for the separation and detection of components in a mixture. In addition, it can be used to monitor the progress of a reaction. The solvent is removed before detection of the analyte molecules, and hence the solvent cannot interfere with the measurements.

The samples were taken during the reaction (0 min, 10 min, 20 min, 30 min, 40 min, 50 min and 60 min) and checked by comparing with starting materials spots. UV light was used to visualize compounds on a TLC plate after developing the plates. Several solvents including methanol, ethanol, hexane, petroleum spirit, dichloromethane and ethyl acetate were trialled as mobile phase to separate the mixtures. A mixture of ethyl acetate and petroleum ether with a ratio of 80:20 (w:w) was found to be the most suitable solvent for this purpose. Although equimolar solutions (10 mM) of the starting materials were used, the TLC plate showed an unclear spot of para-anisidine compared to a well-defined 4-nitrobenzaldehyde spot. In addition, all reaction mixture samples showed only one spot on TLC plate with the same R_f value as for the 4-nitrobenzaldehyde spot. A possible explanation for this might be that the imine is unstable on silica or TLC using UV detection is not sensitive enough for para-anisidine. Although the para-anisidine solution was concentrated, no spot was seen on the plate. Therefore, TLC analysis was not successful to monitor the progress of this reaction because not all reaction components could be identified. The problem with this work is that all samples of the reaction mixtures showed the same results with a single spot.

6.3.3. Reaction monitoring of imine formation using HPLC

HPLC is a more advanced chromatographic method that was used in this study to monitor the imine synthesis. The advantages of HPLC over TLC method are: significantly higher resolution and sensitivity and capability for quantitative analysis. HPLC has a range of variables that can be optimised, things such as mobile phase, column, detector, separation method (normal or reverse phase column), mobile phase modifier (isocratic or gradient), flow rate, buffer concentration and wavelength. There is a wide range of stationary phases and detectors available to use with HPLC. In addition, mass spectrometry can be coupled with HPLC to significantly improve specificity and sensitivity. The ratio of mobile phase (acetonitrile and deionised water) was iteratively modified and optimised (25%: 75%, v/v). Although different wavelengths were used, 300 nm was chosen to identify concentrations of starting materials in solutions with good resolution. RP-HPLC was carried out using the optimal conditions (as detailed in the Materials and Methods section) to monitor the reaction between 4-nitrobenzaldehyde and para-anisidine. All peaks were detected in 15 minutes. The solutions of starting materials (4-nitrobenzaldehyde and para-anisidine) and all reaction samples were injected immediately into the column at the same time. The HPLC results showed that the method is able to identify the starting materials easily from the retention time for each peak in the chromatogram, Figure 6.3. Para-anisidine had a peak absorbance of 485 mAU (milli-Absorbance Units) and retention time at 1.8 min, while 4-nitrobenzaldehyde has a peak of 261 mAU and retention time at 5.8 min. The peak areas were also measured for para-anisidine and 4-nitrobenzaldehyde, and they were 6169167 mV and 9067008 mV respectively. These results are likely to be related to the molecular mass of each compound. The molecular mass for para-anisidine is 123 g/mole while for 4-nitrobenzaldehyde is 151 g/mole. Both reactants are polar, therefore, they spent

less time in the column. Para-anisidine, as expected, elute from the column first and this due to the difference between their molecular mass.

Although HPLC could determine para-anisidine, and 4-nitrobenzaldehyde, Figure 6.3, it was unable to determine the presence of the product in any of the reaction mixture samples. HPLC appeared to indicate that the reaction was not proceeding, as the chromatograms were reproducible only showing the reactants. The results in fact did not show any change during reaction until the end of acquisition time of 2 hours, Figure 6.4. Efforts at overcoming this through changing mobile phase and UV detection wavelength were unsuccessful. HPLC measurements were repeated on a 7 day old sample, for which the reaction was known from FTIR results to be complete and contain no remaining reactants, in accordance with the use of equimolar amounts (see section 6.3.4). The HPLC still showed only the reactants, and no evidence for the reaction even taking place. This indicates that the reaction was difficult to monitor by HPLC method. A possible explanation for this might be that the chemical equilibrium of the reaction was changed. The reaction could be driven back in the direction of the reactants during HPLC. The high pressure of the HPLC column is one of the factors that could affect to change in conditions of chemical equilibrium for this reaction. Using water 75% as mobile phase and the reaction contains water could be another reason to drive back the reaction in the direction of the reactants. Regardless of the underlying cause, the results clearly indicate that this reaction could not be monitored by HPLC.

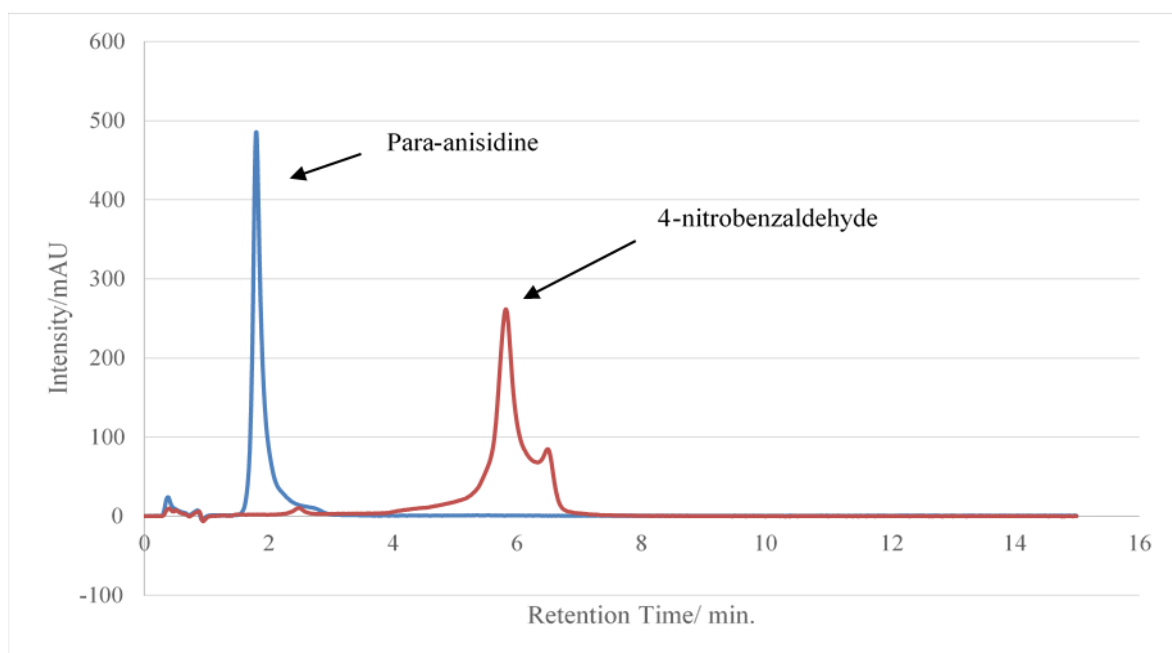


Figure 6. 3. HPLC chromatogram for para-anisidine and 4-nitrobenzaldehyde (both 5 mmol) using ODS-C18 column 150 mm \times 4.6 mm, acetonitrile and deionised water (25%: 75%, v/v) mobile phase, flow rate of 1 mL/min and detection at a wavelength of 300 nm.

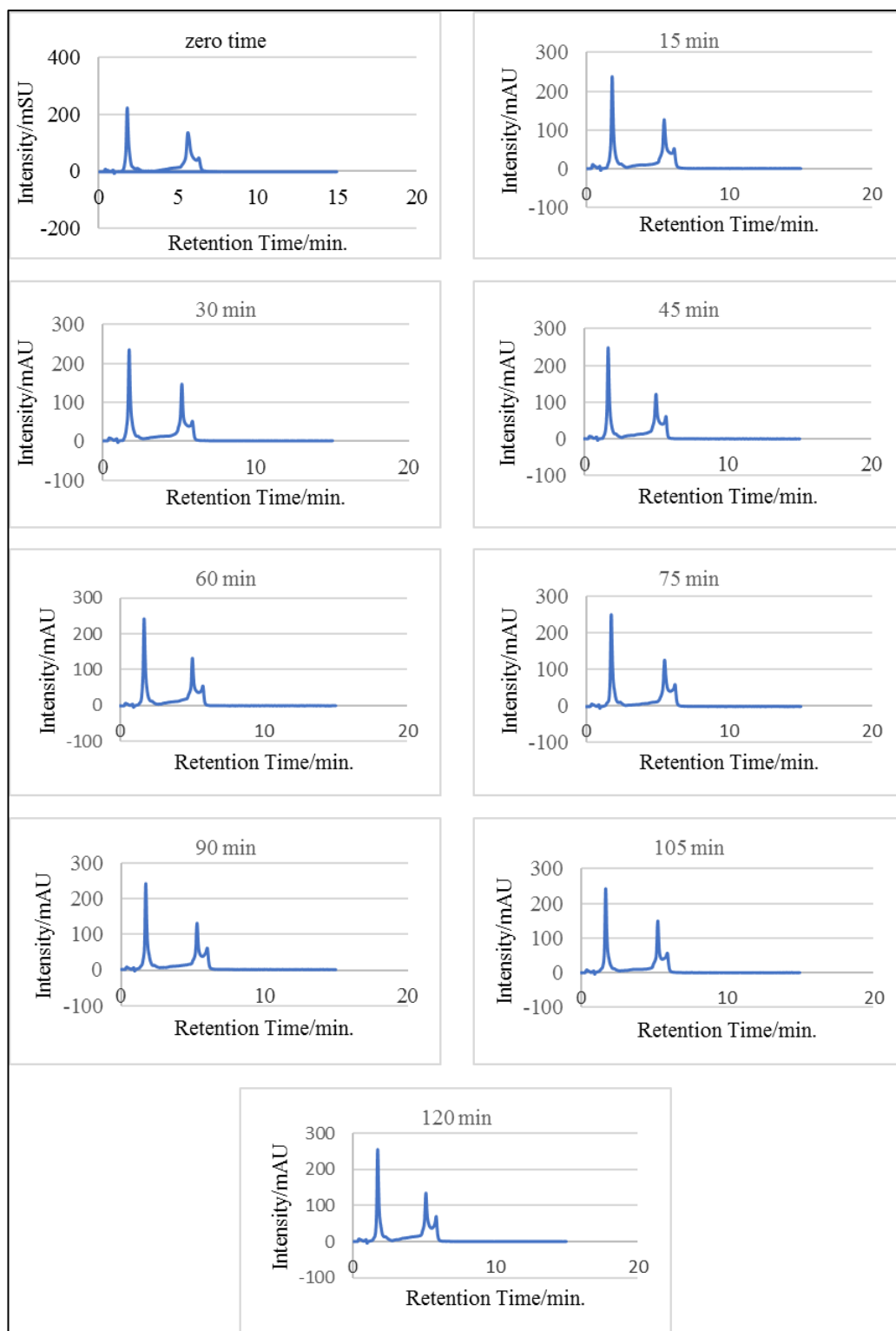


Figure 6. 4. HPLC chromatograms for the reaction mixtures (both 2.5 mmole) at different reaction times using conditions as for Figure 6. 4.

6.3.4. Reaction monitoring of imine formation using FTIR spectroscopy

FTIR as a vibrational technique has been extensively used to identify the functional groups of molecules. Compared to other techniques such as HPLC and NMR, FTIR is fast, cheap and can measure the samples immediately without drying such as solids and liquids. Therefore, FTIR was used in this study to provide some details of the monitoring for this reaction.

FTIR was carried out to establish whether it would be possible to monitor the imine formation reaction. The model reaction of the imine formation is shown in Figure 6.1. To monitor the intensity changes of the vibration peaks during the reaction, FTIR spectra were taken every 15 minutes over 2 hours. The results showed that the method is able to monitor the reaction by identifying the vibrations for the starting materials and the reaction mixtures. Solids and solutions samples of 4-nitrobenzaldehyde and para-anisidine were analysed as a control sample. Diagnostic peaks for 4-nitrobenzaldehyde and para-anisidine were observed and identified. The FTIR spectra of solid 4-nitrobenzaldehyde and solid para-anisidine are shown in Figures 6.5 and 6.6 respectively.

The FTIR spectrum of 4-nitrobenzaldehyde shows the intensity changes of the peaks at 1700 cm^{-1} for carbonyl group (C=O stretch) and 2850 cm^{-1} for C-H stretch (aldehyde). Other vibrations were observed at 1110 cm^{-1} for C-C, 1190 cm^{-1} for C-N, 1615 cm^{-1} for C=C. The nitro group (N=O stretch) was also observed at 1530 cm^{-1} and 1340 cm^{-1} , Figure 6.6. The main vibrations of para-anisidine were also detected and identified. These peaks were observed at 1180 cm^{-1} for C-N, 1230 cm^{-1} for C-O, 1630 cm^{-1} for C=C and 3350 cm^{-1} for N-H, Figure 6.7.

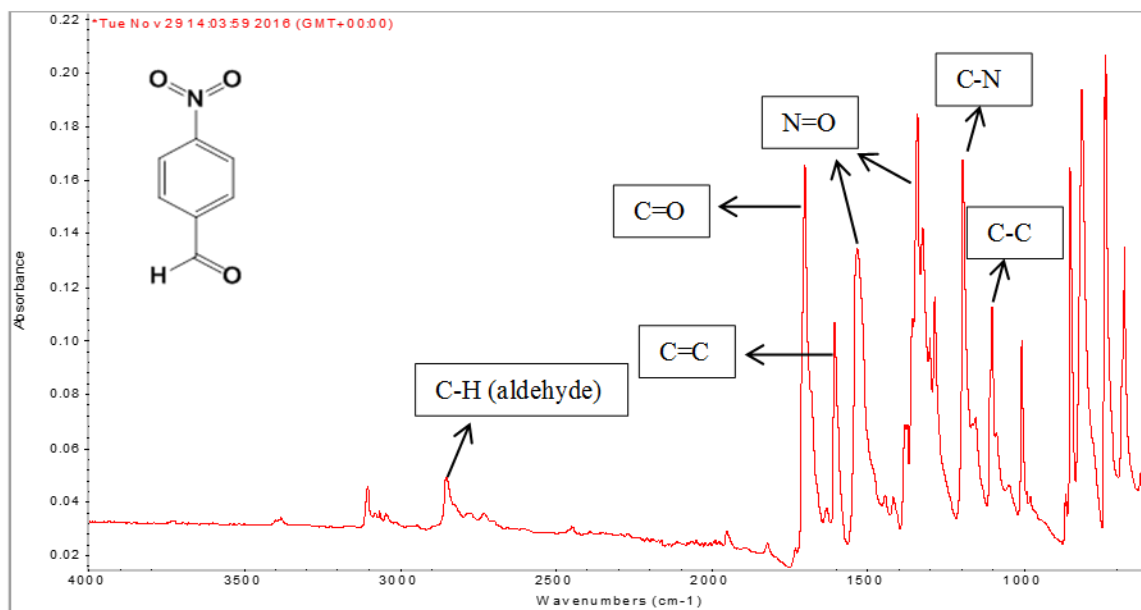


Figure 6. 5. FTIR spectrum of 4-nitrobenzaldehyde (solid).

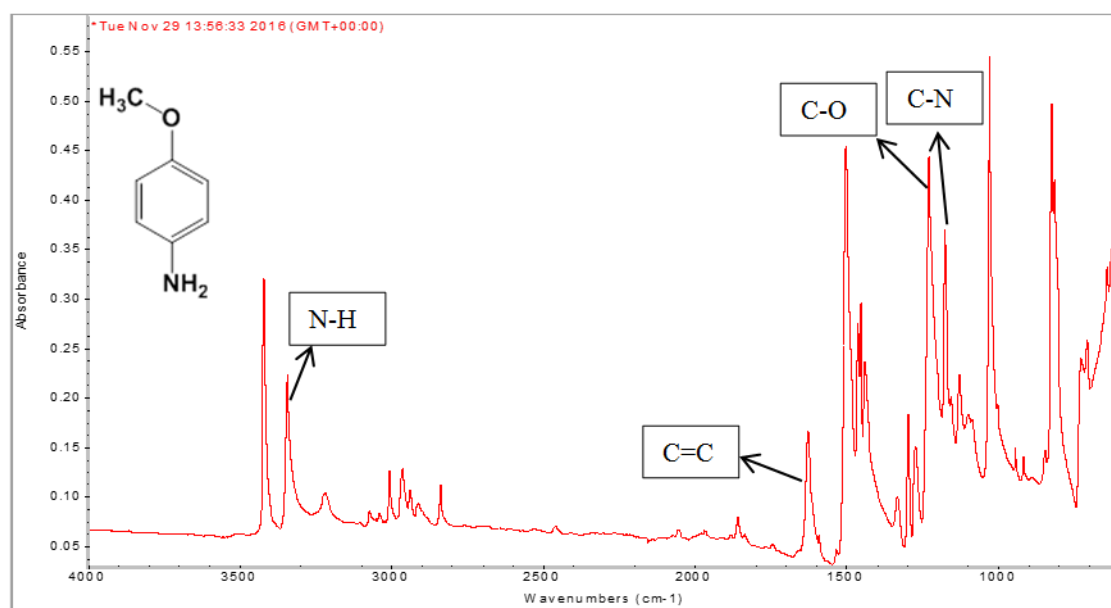


Figure 6. 6. FTIR spectrum of para-anisidine (solid).

To compare the results with the solid materials, single solutions of 4-nitrobenzaldehyde and para-anisidine (both 5 mM) were analysed as a liquid. The spectra did not show any differences between the solids and solutions for identified peaks. However, vibrations of solid compounds showed higher signal intensity in comparison with those in solutions. For example, the intensity of C=O group of solid 4-nitrobenzaldehyde was higher ~15x compared to that of the solution, while the intensity of N-H group of solid para-anisidine was also ~15x more intense compared to that of the solution, reflecting the higher amount of material sampled. Compared with the intensities of the reference solutions of pure 4-nitrobenzaldehyde and para-anisidine (both 5 mM), the reaction mixture samples display the expected changes, Figure 6.7. The spectra show that the C=O stretch of 4-nitrobenzaldehyde and imine stretch (N-H) of para-anisidine decreased in intensity with time and completely disappeared after 45 minutes. The spectra indicate no further changes for the reaction samples between 60 minutes and 120 minutes. Hence 1 hour was decided as the time for the imine formation to complete.

The peak area ratios of some vibrations of the starting materials and product were further studied as a function of reaction time in order to confirm that the reactants were indeed fully converted to the product. Decreases of the peak area for C=O stretch and increases of the peak area for C=N stretch and C=C stretch over reaction time indicate the reaction was fully completed towards imine formation. The ratios of the peak area for C=O/C=C and C=O/C=N for the reaction mixtures were calculated and plotted versus reaction time, Figures 6.8 and 6.9. The results showed that the peak area for C=O decreases up to ~ 60 minutes while it increases for C=C and C=N up to this time. These plots do not show any changes for the reaction samples between 1 hour and 2 hours. These results consistent with the fact that the reaction between 4-nitrobenzaldehyde and para-anisidine was achieved in less than 1 hour and the reactants are fully converted to the product (N-4-MP-1-4-NPM).

The increases in intensity and area for the C=C stretching peak, in principle, be attributed to the ring stretching virtually affected by the conjugation of π electrons, and this is maximised in the product (see Figure 6.1).

FTIR measurement was also re-done on a 7 days old sample for which the reaction was expected to be complete and no reactants should be present given that an equimolar amount was used. The FTIR results indicated the reaction was complete which means there is an issue with the HPLC results. However, compared to MS techniques, FTIR is difficult and often indeed not possible to determine what precise molecules are present, in particular in complex mixtures. In FTIR, not all molecules can be detected. For example, the different samples can have the same functional group and that IR peaks are inherently fairly broad hence overlap is an issue. Moreover, water strongly absorbs IR radiation, so direct analysis of aqueous solutions is a problem for IR.

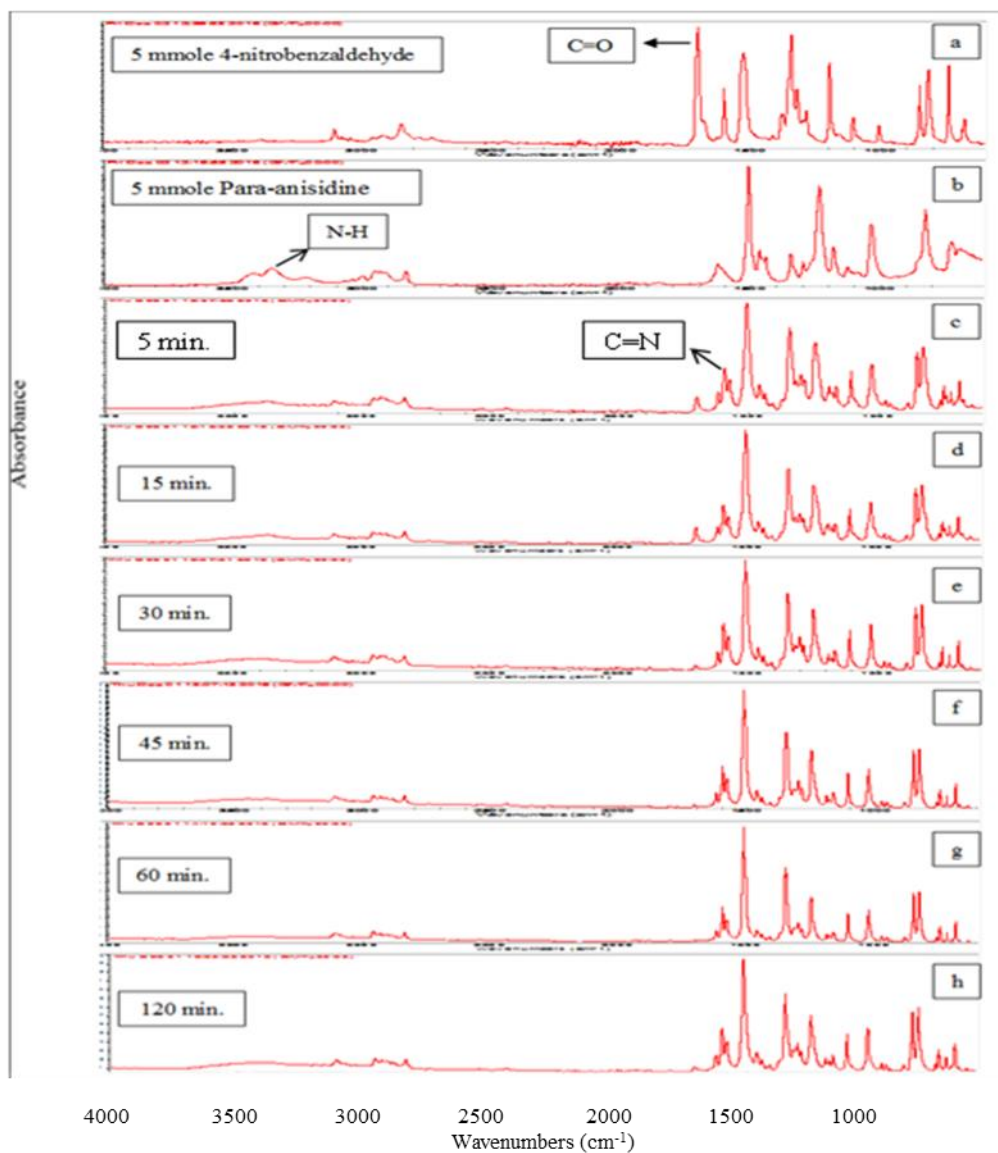


Figure 6. 7. FTIR spectra for reactants 4-nitrobenzaldehyde (a) , para-anisidine (b) and reaction mixtures during reaction times: 5 min (c), 15 min (d), 30 min (e), 45 min (f), 60 min (g) and 120 min (h).

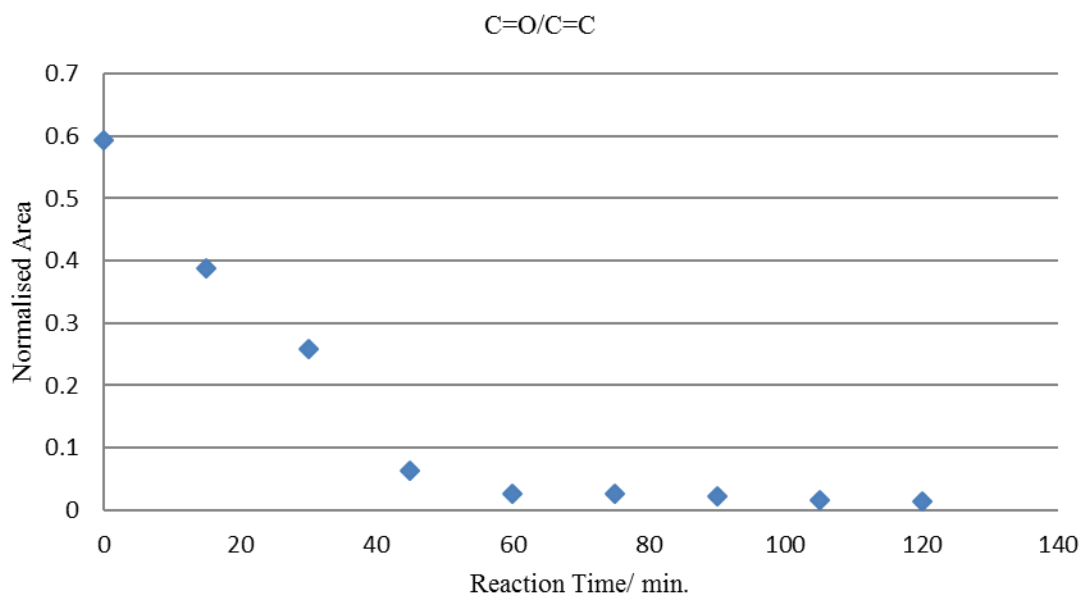


Figure 6. 8. Ratios of the normalised area for C=O/C=C during reaction time.

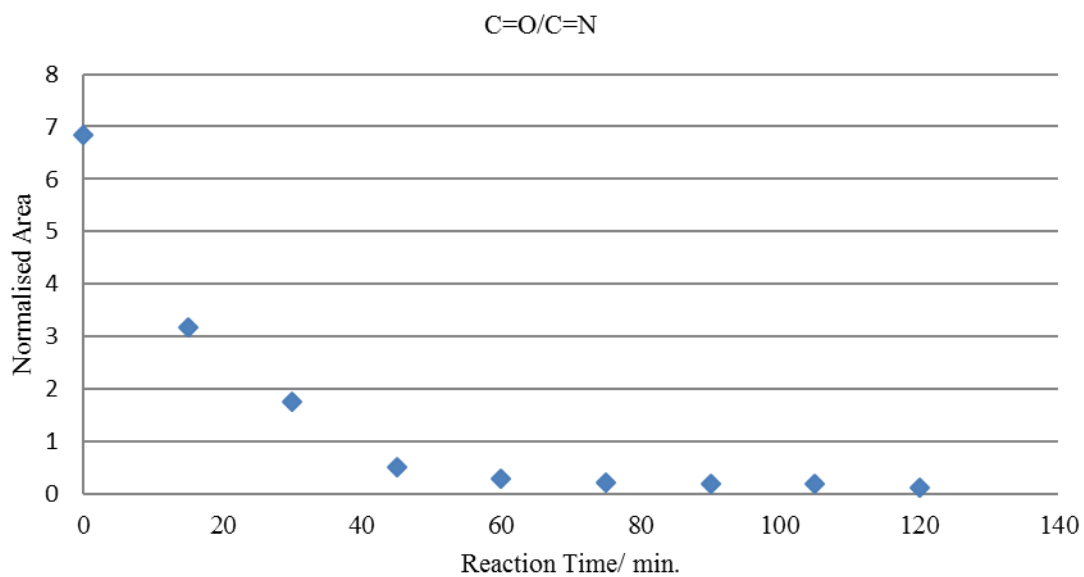


Figure 6. 9. Ratios of the normalised area for C=O/C=N during reaction time.

6.3.5. Reaction monitoring of imine formation using PADI-MS

6.3.5.1. Para-anisidine and 4-nitrobenzaldehyde standards

PADI-MS was selected and developed for AMS monitoring of the imine formation reaction and compared to the TLC, HPLC and FTIR results. In a qualitative approach, PADI-MS was used for identifying starting materials and reaction products. In order to identify the optimal substrate to analyse the samples, the following substrates were tested: TLC plate, glass slide and a cotton swab. Pure samples of 4-nitrobenzaldehyde and para-anisidine were used as a standard to identify and optimise methodology by maximising the (quasi-) molecular ion peaks for both compounds. The conditions of PADI-MS were optimised for all samples in this study (see the materials and methods section). These samples were all analysed directly by PADI-MS using these three substrates without drying and with a total acquisition time of 1 minute.

Different substrates such as a TLC plate, glass slide and cotton swab were used in this work in order to increase the sensitivity and minimise the contamination. The results showed that using a cotton swab can give a higher signal-to-noise ratio (S/N). The peak heights of 4-nitrobenzaldehyde m/z 152 and para-anisidine m/z 124 using cotton swab are higher and more useful and easy to use in the analysis of the reaction components compared to those of a TLC plate and glass slide, Figure 6.10. This could be attributed to the solvent (dichloromethane) absorb very quickly by the cotton. Changes in signal intensity of the starting materials with time were compared to that measured in the reaction mixtures. 4-nitrobenzaldehyde and para-anisidine were analysed directly from cotton swabs using PADI-MS with a total acquisition time of 1 minute, Figure 6.11. The spectra in this Figure show clear and high-intensity signals of these compounds. They showed that $[M+H]^+$ m/z 123 for para-anisidine is 4x more abundant than $[M+H]^+$ m/z 152 for 4-

nitrobenzaldehyde. The observed increase in the intensity of para-anisidine in pure and mixture solutions could be explored by considering their molecular mass values. The molecular mass for para-anisidine is 123 g/mol while for 4-nitrobenzaldehyde is 151 g/mol, so each gramme of para-anisidine contains 0.0081 moles whereas each gramme of 4-nitrobenzaldehyde contains 0.0066 moles. Hence a 1/1 weight ratio means a molar ratio of (81/66), and then $[M+H]^+$ m/z 152 for 4-nitrobenzaldehyde could be expected to give a small signal intensity. Another possible explanation for this is that desorption and ionisation of molecules could well be different for different molecules. Para-anisidine showed a bigger (quasi-) molecular ion peak and lower level of fragmentation compared to those for 4-nitrobenzaldehyde.

Interestingly, there were differences between the results from PADI-MS analysis and TLC, HPLC and FTIR. The samples could be analysed easily by PADI-MS, with rapid analysis of fewer than 35 seconds giving molecular ion information, while the samples required a total acquisition time of 15 minutes for each sample using HPLC. These findings also showed that PADI-MS is very sensitive particularly for para-anisidine, while the TLC method was not sensitive enough to detect this compound, even for the standard. PADI-MS showed a general increase in all peak intensities over the first ~35 seconds, after which the intensity of all peaks reduced, Figure 6.12. The observed increase in intensity with time could be attributed to thermal desorption of analytes from the surface, while decreases in intensity may be attributed to degradation of analytes on the surface or in the gas phase. As expected, the temperature could cause heating of the sample during the interaction between the plasma flame and the sample. Therefore, during this acquisition period, the temperature increased and reached a peak when the analysis time reached 45 seconds, after which it decreased until the end of acquisition time of 1 minute. Because the samples were analysed immediately without drying, it also may be that de-solvation could be an issue.

Adduct peaks relating to 4-nitrobenzaldehyde were observed an m/z 166 for $[M-H]+O$ and m/z 304 for $[2M+2H]^{+2}$, while only one adduct peak that could be related to para-anisidine was observed at m/z 135 for $M-2H+N$, Figure 6.11. The intensity of $[M+H]^+$ m/z 123 for para-anisidine was higher by $\sim 2x$ compared to that of $[M+H]^+$ m/z 152 for 4-nitrobenzaldehyde in 5 second intervals 0-5, 10-15, 20-25, 30-35, 40-45, 55-60 seconds.

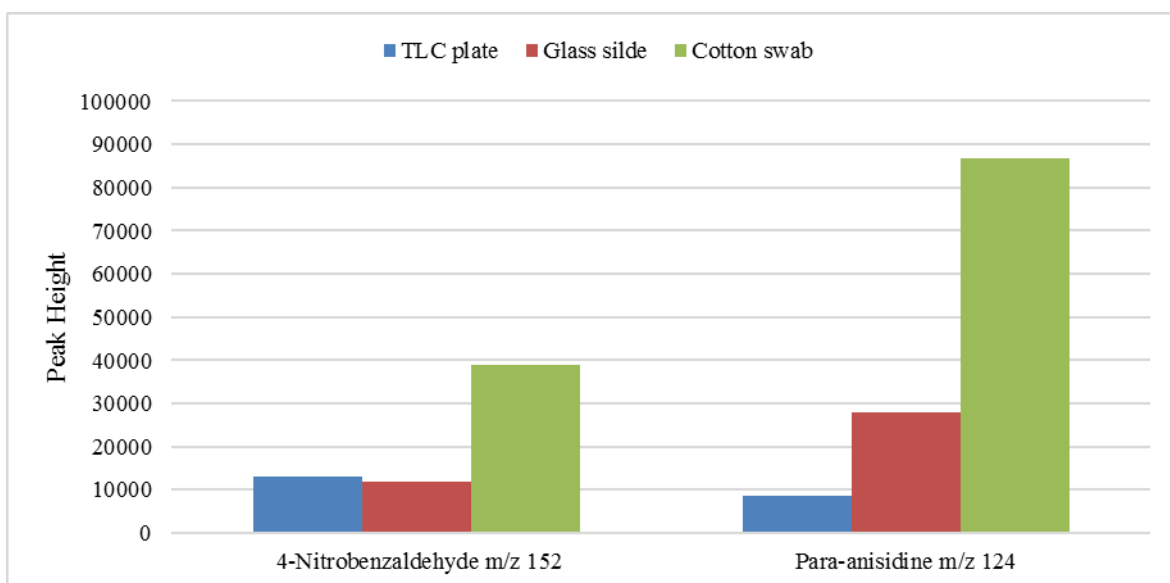


Figure 6. 10. Peak height for 4-nitrobenzaldehyde m/z 152 and para-anisidine m/z 124 using different substrates with a total acquisition time of 1 minute.

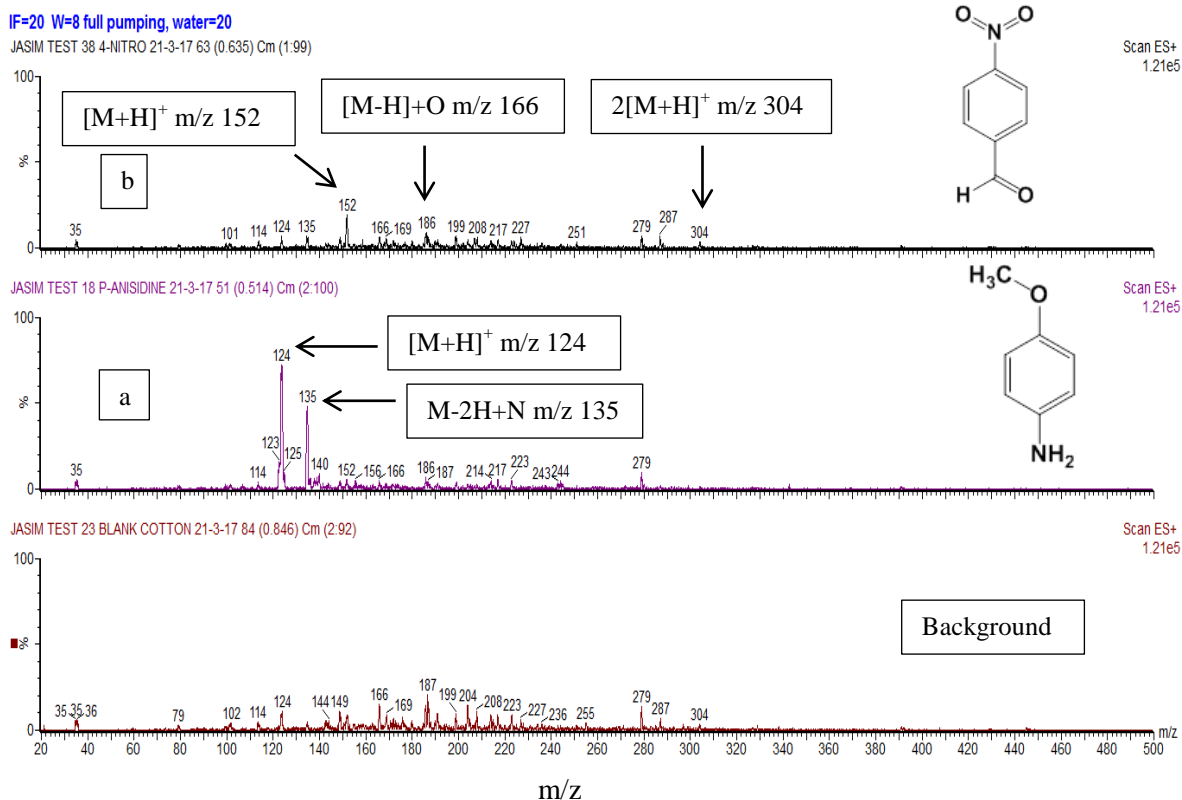


Figure 6. 11. PADI-MS spectra of 4-nitrobenzaldehyde (a) and para-anisidine (b) using cotton swabs with a total acquisition time of 1 minute.

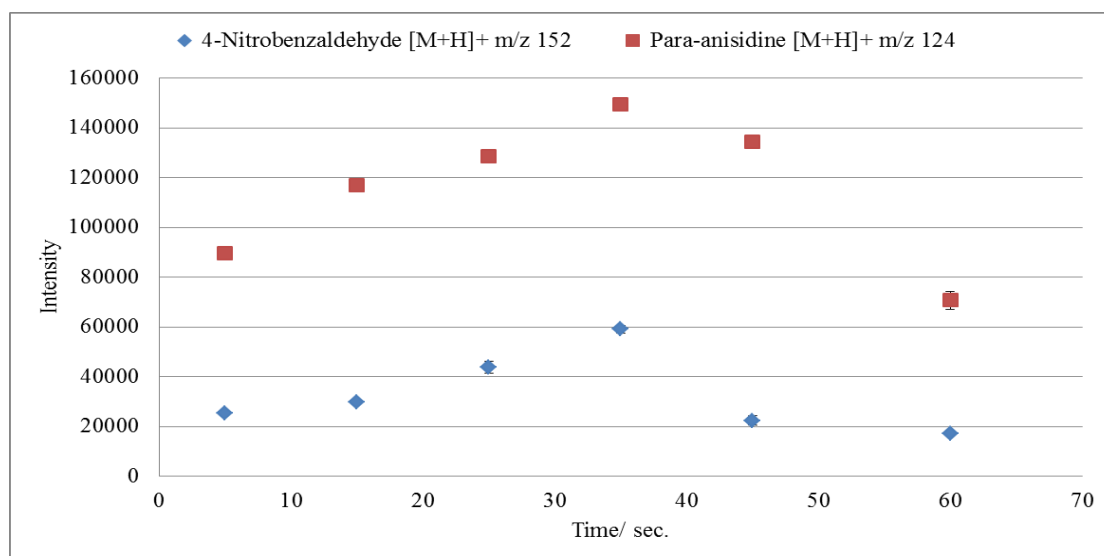


Figure 6. 12. Signals intensity of protonated 4-nitrobenzaldehyde and protonated para-anisidine using cotton swabs in 5 second intervals 0-5, 10-15, 20-25, 30-35, 40-45 and 55-60 seconds.

6.3.5.2. Analysis of reaction mixtures

The reaction of imine formation was monitored as a model system for pharmaceutical reaction mixtures. The reaction was achieved between 4-nitrobenzaldehyde and para-anisidine for 2 hours at room temperature. Samples were taken every 15 minutes during the reaction. This part aimed to monitor the imine formation directly by PADI-MS without the need for preparation or pre-concentration of sample solutions. Reaction mixtures were sampled using cotton swabs as the best substrate as indicated before, and analysed directly from the cotton tip. The PADI-MS analysis of the reaction mixtures over reaction times in 5 second intervals of 30-35 seconds using cotton swabs are presented in Figure 6.13. The intensity of $[M+H]^+$ m/z 152 for the reactants decreased over reaction times, while the product signal increased (N-4-MP-1-4-NPM) up to 1 hour. These results confirm that the reaction between 4-nitrobenzaldehyde and para-anisidine was complete in 45 minutes and the reactants are fully converted to the product. The results show that the $[M+H]^+$ peaks for both 4-nitrobenzaldehyde and a para-anisidine decrease in intensity up to ~ 45 minutes, and then settle at a constant value up to 2 hours, Figure 6.14. Even though the signals for reactants drop by less than 50%, the reaction does not appear to be complete and this due to contamination of the sniffer tube, although the sniffer tube was cleaned several times to minimise contamination effects. The observed peaks here at m/z 124 and m/z 152 might be related to the diagnostic peaks for paracetamol $M-CCH_3$ and $[M+H]^+$ respectively (for more details see Chapter 5). However, the signal intensity of the product increased and reached a peak up to ~ 45 minutes, and then remained steady until the end of data acquisition at 2 hours.

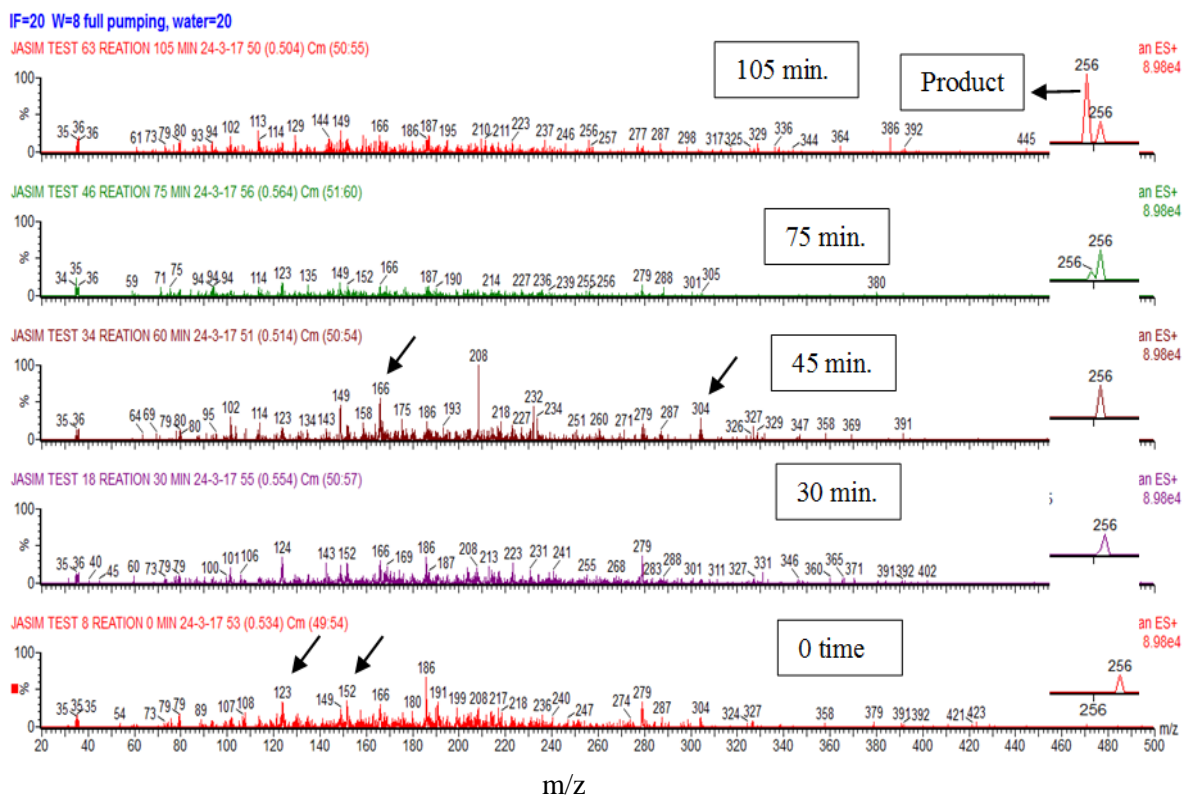


Figure 6. 13. PADI-MS spectra of the reaction mixtures over reaction times in 5 seconds intervals of 30-35 seconds.

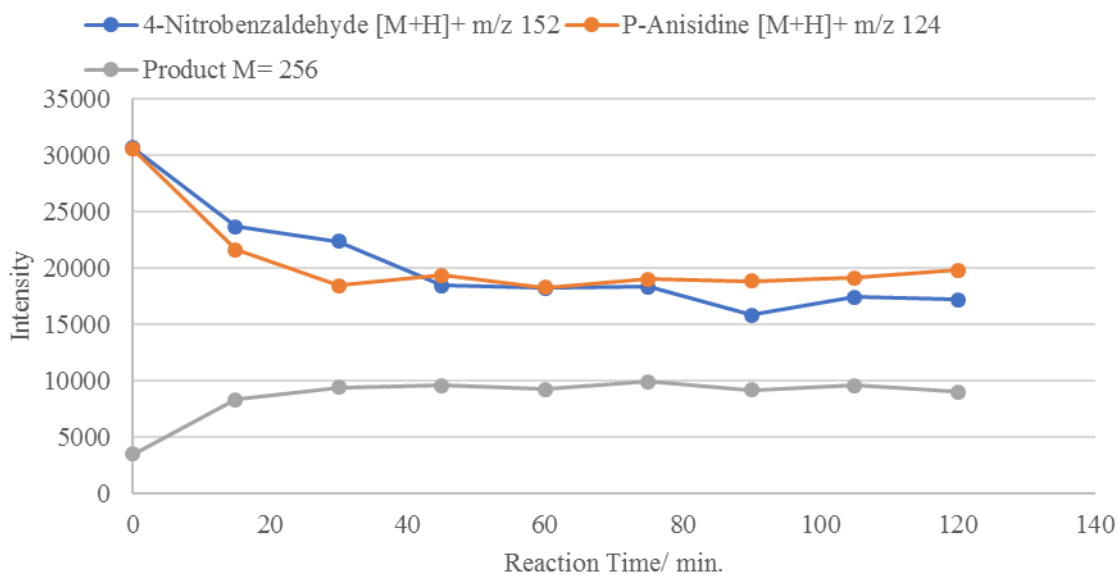


Figure 6. 14. Reaction progress of the synthesis of N-4-MP-1-4-NPM over reaction time in 5 seconds intervals of 30-35 seconds.

The values of the peak height of the product and starting materials were normalised by determining peak height / peak area ratios for the following masses and plotting this against reaction time for an acquisition time of 30-35 seconds: 256/152 and 256/124, Figure 6.15. It can be seen that the ratios of these intensities increased over the first 1 hour of the reaction time, after which they remain steady up to 2 hours. These results also indicate that the reaction between 4-nitrobenzaldehyde and para-anisidine was completely finished in 45 minutes and the imine was formed. The intensity of $[M+H]^+$ for both 4-nitrobenzaldehyde and para-anisidine decreased over reaction times (from 0 to 2 hours) by a factor of 2x and 3x respectively, while it increased for the product by approximately 6x, Figures 6.16, 6.17 and 6.18. These results indicate that the time up to 1 hour is enough to complete the reaction. The length of time up to 35 seconds also is enough to detect and identify the reaction mixtures using PADI-MS. In addition, the results showed that PADI-MS using the optimal conditions was a convenient and simple and fast technique to monitor the reaction of imine formation. The results also found that cotton swabs gave better spectra and were more practical in comparison with the TLC plate and glass slide, hence it was used in the PADI-MS analysis to monitor the reaction.

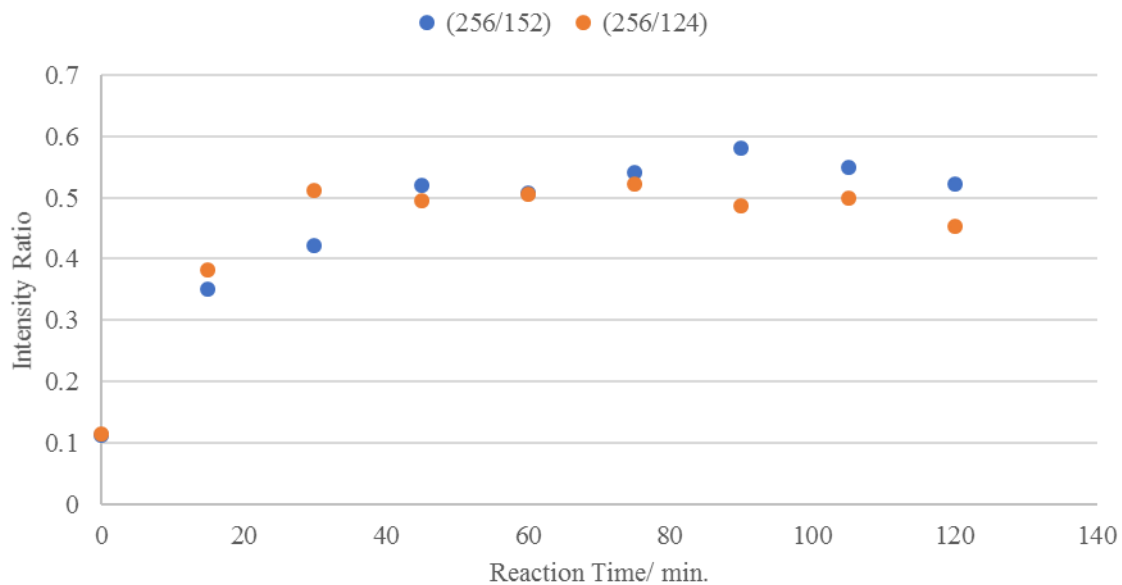


Figure 6. 15. Peak intensity ratios of 4-nitrobenzaldehyde, para-anisidine and the product by a factor of 256/152 and 256/124 over reaction time with an acquisition time of 30-35 seconds.

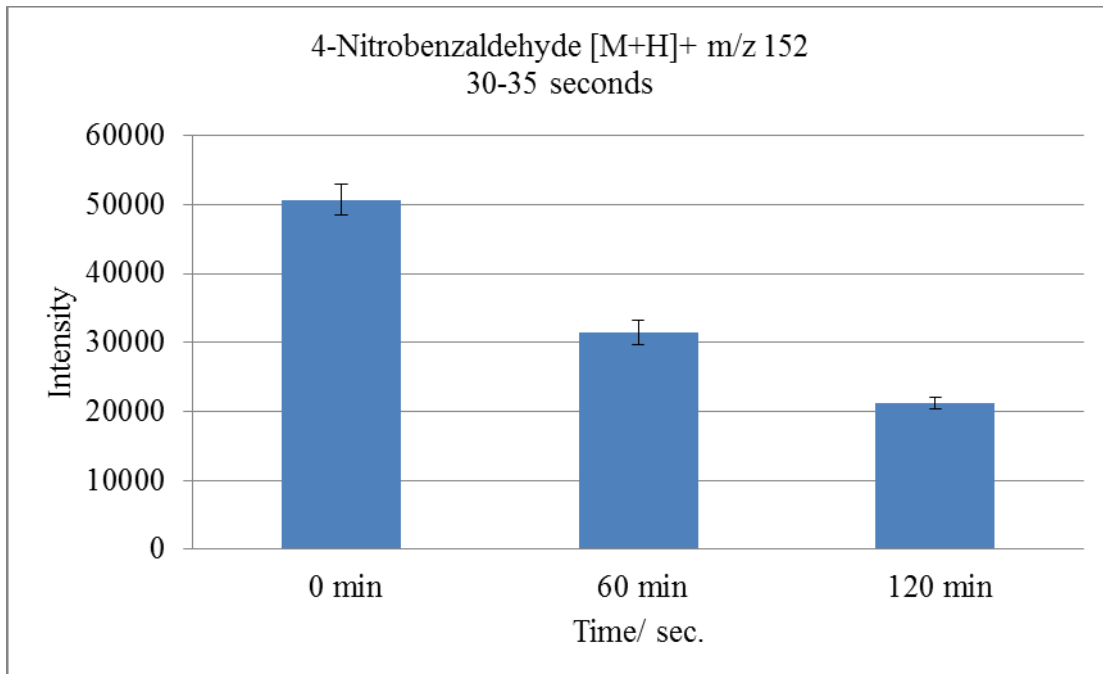


Figure 6. 16. Signal intensity of [M+H]⁺ m/z 152 for 4-nitrobenzaldehyde over different reaction times with an acquisition time of 55 seconds.

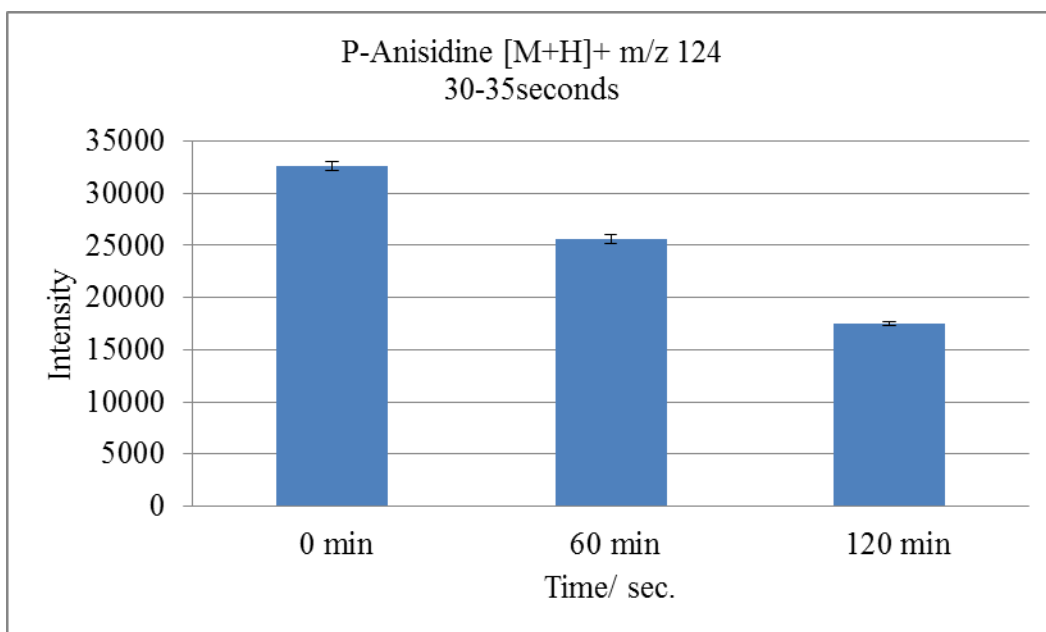


Figure 6. 17. Signal intensity of [M+H]⁺ m/z 124 for para-anisidine over different reaction times with an acquisition time of 55 seconds.

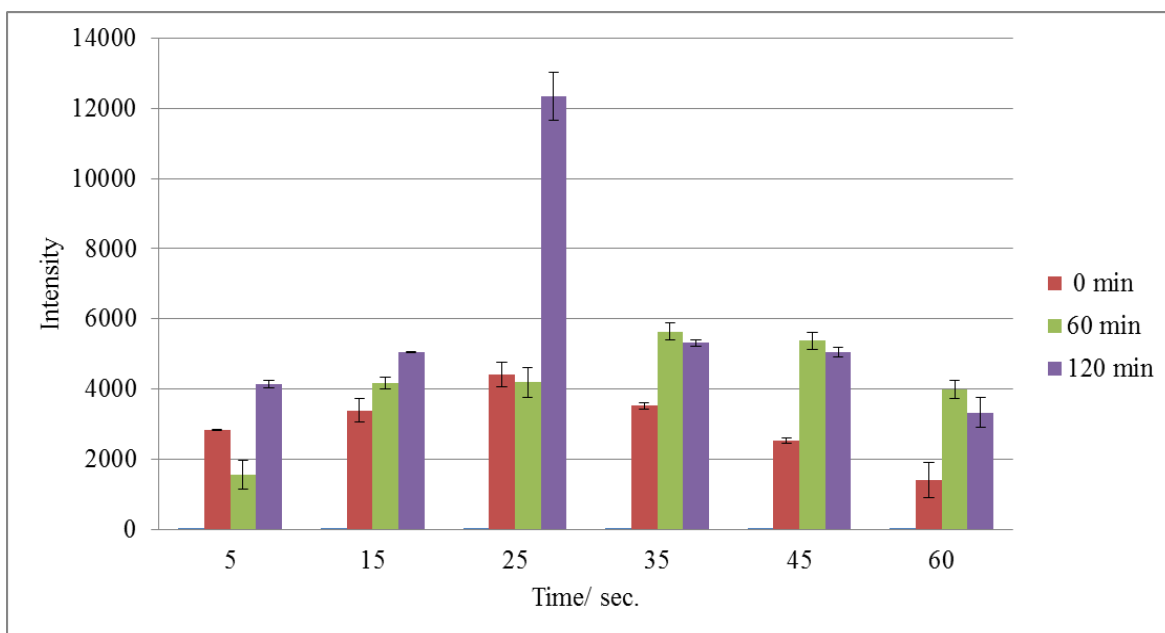


Figure 6. 18. Signal intensity of N-4-MP-1-4-NPM with an acquisition time of 60 seconds at different reaction times.

6.4. Conclusions

The aim of the present study was to develop a novel, fast and sensitive method for monitoring of pharmaceutical synthesis reactions. A relevant model reaction was used to do this. Chromatographic, spectroscopic and ambient mass spectrometric methods have been used for monitoring imine formation. HPLC was found to be unsuitable to monitor the reaction, possibly because the process of HPLC analysis drove the reaction back towards the reactants. TLC was found not to be capable to detect all relevant molecules: it could detect all starting materials, albeit with limited sensitivity for one reactant, and could not detect the product at all. All reaction mixture samples showed only one spot on the TLC plate from 0 times to the end of the reaction. The results also showed that the reaction was difficult to monitor by HPLC. It was unable to identify the peaks of the reaction mixtures and all chromatograms of reaction mixtures only showed the reactants. This might be that the reaction could be driven back in the direction of the reactants during analysis. It appears that in this case, the HPLC measurement may have affected the reaction it was supposed to measure. The IR showed that the reaction was complete, and the reaction of imine formation was monitored successfully by identifying the vibrations of the starting materials and the reaction product over reaction times. The FTIR spectra showed that C=O stretching peaks of the 4-nitrobenzaldehyde and a imine groups (N-H) of para-anisidine decreases in intensity with time and completely disappears after 45 minutes. At the same time, they show an increase in area for the C=N and C=C stretching peaks with the formation of the product up to ~ 1 hour. The FTIR spectra of the reaction mixtures after this time including 75 minutes, 90 minutes, 105 minutes and 120 minutes are quite similar to that for 60 minutes. These results indicate that the reaction between 4-nitrobenzaldehyde and para-anisidine was achieved in less than 1 hour and the reactants are fully converted to the product (N-4-MP-1-4-NPM). However, FTIR only identifies

functional groups and when investigating more complex molecules and reactions it may not be possible to determine what precise molecules are present. Sensitivity can also be an issue.

PADI-MS was chosen in this study as an ambient mass technique, that was intended to overcome the shortfalls of TLC, HPLC and FTIR. The PADI-MS method has improved using the optimal conditions including plasma power, helium inner flow and the distance between the plasma flame and sample and found to 8 W, 224 mL/min and 5 mm respectively. All PADI-MS spectra showed good signals of $[M+H]^+$ for both 4-nitrobenzaldehyde and para-anisidine at m/z 152 and m/z 124 respectively. However, the spectra showed a small peak of the product molecular ion at M^+ m/z 256. The $[M+H]^+$ intensity for both 4-nitrobenzaldehyde and para-anisidine decreased over reaction times, while it increased for the M^+ reaction product to 45 minutes, after which they remained steady up to 2 hours. These results can confirm that the reaction does not need more than one hour to convert the full reactants to the product. These results also confirmed that a 5 seconds interval 30-35 seconds is the best time to analyse the starting materials and reaction mixtures from a cotton swab using PADI-MS.

Overall, the results of this study indicate that PADI-MS has been successful for monitoring this reaction due to being highly sensitive, simple, inexpensive and has the ability to detect different kinds of the sample such as solid, liquid and gas. This study has found that PADI-MS has the potential to monitor pharmaceutically relevant reactions, although the observed carry-over issues will need addressing through a redesigned inlet system.

References

1. Elipe, M.V.S. and Milburn, R.R. (2016) 'Monitoring chemical reactions by low-field benchtop NMR at 45MHz: pros and cons' *Magnetic Resonance in Chemistry*, 54 (6), p.p. 437–443.
2. Lee, M. Kim, H. Rhee, H. and Choo, J. (2003) 'Reaction monitoring of imine synthesis using Raman spectroscopy' *Bulletin of the Korean Chemical Society*, 24 (2), p.p. 205–208.
3. Surya Prakash, G. K. Do, C. Mathew, T. and Olah, G.A. (2010) 'Gallium(III) Triflate catalyzed direct reductive amination of aldehydes' *Catal Lett*, 137, p.p. 111–117.
4. Jalhan, S. Jindal, A. Gupta, A. and Hermaj (2012) 'Synthesis, biological activities and chemistry of thiadiazol derivatives and Schiff bases', *Asian Journal of Pharmaceutical and Clinical Research*, 5 (3), p.p. 199–208.
5. Brodowska, K. and Łodyga-Chruscinska, E. (2014) 'Schiff bases – interesting range of applications in various fields of science' 68 (2), p.p. 129–134.
6. Arulmurugan, S. Kavitha, H.P. and Venkatraman, B.R. (2010) 'Biological activities of Schiff base and its complexes: a review"', *Rasayan Journal of Chemistry*, 3(3), p.p. 385–410.
7. Ejiah, F. N. Fasina, T. M. Familoni, O. B. Ogunsola F. T. (2013) 'Substituent effect on the spectral and antimicrobial activity of Schiff bases derived from aminobenzoic acids', *Advances in Biological Chemistry*, 3, p.p. 475-479.
8. Kirubavathy, S. J. Velmurugan, R. Karvembu, R. Bhuvanesh, N.S.P. Enoch, I.V.M.V. Selvakumar, P. M. Premnath, D. and Chitra, S. (2017) 'Structural and molecular docking studies of biologically active mercapto pyrimidine Schiff bases', *Journal of Molecular Structure*, 1127, p.p. 345–354.

9. Dhar, D.N. and Taploo, C.L. (1982) 'Schiff bases and their applications' *Journal of Scientific & Industrial Research*, 41, p.p. 501–506.
10. Przybylski, P., Huczynski, A., Pyta, K., Brzezinski, B. and Bartl, F. (2009) 'Biological properties of Schiff bases and azo derivatives of phenol' *Current Organic Chemistry*, 13, p.p. 124–148.
11. Fasina, T.M., Ogundele, O., Ejia, F.N. and Dueke-Eze, C.U. (2012) 'Biological Activity of copper(II), cobalt(II), and nickel(II) complexes of Schiff base derived from phenylenediamine and 5-Bromo salicylaldehyde' *International Journal of Biological Chemistry*, 6, p.p. 24–30.
12. da Silva, C. M. Daniel L. da Silva, D. L. Modolo, L. V. Alves, R. B. de Resende, M. A. Martins, C. V. B. and de Fa´tima, A. (2011) 'Schiff bases: A short review of their antimicrobial activities', *Journal of Advanced Research*, 2, p.p. 1–8.
13. Foley, D. A. Wang, J. Maranzano, B. Zell, M. T. Marquez, B. L. Xiang, Y. and Reid, G. L. (2013) 'Online NMR and HPLC as a Reaction Monitoring Platform for Pharmaceutical Process Development', *Analytical Chemistry*, 85, p.p. 8928–8932.
14. Kim, J. Jung, D. Park, Y. Kim, Y. Moon, D. W. and Lee, T. G. (2007) 'Quantitative analysis of surface amine groups on plasma-polymerized ethylenediamine films using UV–visible spectroscopy compared to chemical derivatization with FT-IR spectroscopy, XPS and TOF-SIMS', *Applied Surface Science*, 253, p.p. 4112–4118.
15. Wnorowski, A. and Yaylayan, V. A. (2003) "Monitoring carbonyl-amine reaction between a pyruvic acid and α -amino alcohols by FTIR spectroscopy—a possible route to amadori products", *Journal of Agricultural and Food Chemistry*, 51, p.p. 6537-6543.

16. Kim, J. Jung, D. Park, Y. Kim, Y. Moon, D. W. and Lee, T. G. (2007) 'Quantitative analysis of surface amine groups on plasma-polymerized ethylenediamine films using UV-visible spectroscopy compared to chemical derivatization with FT-IR spectroscopy, XPS and TOF-SIMS', *Applied Surface Science*, 253, p.p. 4112–4118.
17. Wang, H. Liu, J. Cooks, R.G. and Ouyang, Z. (2010) 'Paper spray for direct analysis of complex mixtures using mass spectrometry', *Angewandte Chemie (International Ed. In English)*, 49(5), pp. 877–880.
18. Yang, Y. and Jiewei (2016) 'Analysis of pharmaceutical products and herbal medicines using ambient mass spectrometry', *Trends in Analytical Chemistry*, 82, pp. 68–88.
19. Sparkman, O. D. (2000) 'Mass spectrometry desk reference', Pittsburgh: Global View Pub.
20. Ding, X. and Duan, Y. (2015) 'Plasma-based ambient mass spectrometry techniques: the current status and future perspective', *Mass Spectrometry Reviews*, 34, p.p. 449–473.
21. Cheng, S. Wu, Q. Dewald, H. D. and Chen, H. (2017) 'Online monitoring of methanol electro-oxidation reactions by ambient mass spectrometry', *Journal of The American Society for Mass Spectrometry*, 28 (6), p.p. 1005–1012.
22. Cody, R. B. Laramée, J. A. and Durst, H. D. (2005) 'Versatile new ion source for the analysis of materials in open air under ambient conditions', *Analytical Chemistry*, 77(8), p.p. 2297–2302.
23. Petucci, C. Diffendal, J. Kaufman, D. Mekonnen, B. Terefenko, G. and Musselman, B. (2007) 'Direct analysis in real time for reaction monitoring in drug discovery', *Analytical Chemistry*, 79 (13), p.p. 5064–5070.

24. Madhusudanan, K. P. (2007) 'Direct analysis in real time (DART) – a new ionization technique', 12th ISMAS Symposium cum, Workshop on Mass Spectrometry, p.p. 25–30.
25. Hajslova, J. Cajka, T. and Vaclavik, L. (2011) 'Challenging applications offered by direct analysis in real time (DART) in food-quality and safety analysis', Trends in Analytical Chemistry, 30 (2), p.p. 204–218.
26. Green, F.M. Salter, T.L. Stokes, P. Gilmore, I.S. and Connor, O. (2010) 'Ambient mass spectrometry: advances and applications in forensics' Surface and Interface Analysis, 42, p.p. 347–357.
27. Ratcliffe, L.V. Rutten, F.J.M. Barrett, D.A. Terry Whitmore, T. Seymour, D. Greenwood, C. Gonzalvo, Y.A. Robinson, S. and McCoustra, M. (2007) 'Surface analysis under ambient conditions using plasma-assisted desorption/ ionisation mass spectrometry' Analytical Chemistry, 79 (16), p.p. 6094–6101

CHAPTER 7: General discussions and conclusions

This project was undertaken to develop a novel simple, fast, sensitive and cost-effective ambient mass spectrometric method, that can be used to monitor the progress of chemical reactions. The results of these investigations have shown that PADI-MS has the potential to fill this important gap in the pharmaceutical industry. Analytical methods based on spectroscopy, separation and mass spectrometry were developed for the identification and monitoring of pharmaceutically relevant mixtures. The research has also found distinct differences between PADI-MS and other traditional techniques such as TLC, HPLC, FTIR and Raman spectroscopy. This study has found that generally PADI-MS is easy to set up, little or no sample preparation is required, analysis time is short and can be applied for direct analysis of solids and liquids. In addition, the use of PADI-MS provides structural information on the molecules in seconds. The visible non-thermal plasma plume emerging from a coaxial helium gas flow 13.65 MHz RF plasma pen (modified Stoffel's design) was used.

In the first experimental chapter (Chapter 3), the direct analysis of PADI-MS used helium directly from a cylinder with flow rate of 224 mL/min, and the distance between the plasma flame and sample was 5 mm. Investigation of the use of direct PADI-MS and Raman analysis for paracetamol tablets, as a model for pharmaceutically relevant solids, gave good results without the need for sample preparation. PADI-MS showed that the time exposing of the sample to plasma up to ~50 seconds is enough to avoid damage to the sample, and 30 seconds was the time required to get a reasonable spectrum and the analysis can be stopped after this time. In this investigation, the aim was to determine the effect of non-thermal plasma on the chemical structure of molecules. The results of this investigation showed that the chemistry of tablet can be affected after 50 seconds exposure to visible non-thermal plasma (NTP) as evident from the changes in intensities of the diagnostic, adduct and fragment peaks. Although Raman microscopy was used to analyse

the chemical composition of the top layer of the exposed tablets, changes and behaviours of intensity for the adduct and fragment peaks of these exposed tablets were seen using PADI-MS. Raman showed some changes in an area of vibration peaks for paracetamol after exposure times to plasma, but it did not show any important shift for any peak. This result indicated that the positions of vibrations were not affected by exposure to visible plasma. Therefore, for this purpose, Raman microscopy could not indicate adducts and fragments as that is specific to MS. In this part of analysis, the PADI-MS spectra showed a good signal intensity of $[M+H]^+$ m/z 152 (protonated molecular ion) and other fragment peaks. However, the PADI-MS conditions need to be improved using carrier gas additives such as outer helium flow with water vapour prior to interacting with the plasma plume in order to increase the sensitivity. This was achieved for the next experimental chapters and PADI-MS parameters were optimised to use for following experiments. The plasma was near-contact (5 mm separation) with the sample under investigation, using 8 W and a carrier gas flow of 224 mL/min (inner flow) and (224 mL/min outer flow).

The second aim of this study was to identify chemical components in mixtures of pharmaceutically relevant compounds deposited onto TLC plates (Chapter 4). Paracetamol and caffeine were used as model analytes. The results showed that the separation is not always necessary for identification, and spots can be identified on TLC plates using PADI-MS without separation. However, the separation of the spots can give higher signal-to-noise ratio (S/N) of molecules, and hence the sensitivity of diagnostic, adduct and fragment peaks can be improved. The TLC results indicated that the sensitivity of diagnostic, adduct and fragment peaks for paracetamol without separation of the spots was improved and the damage was reduced when water vapour was added as outer flow gas. In addition, when using water vapour, the protonated caffeine ion ($[M+H]^+$ m/z 195) was detected. In all cases, the sensitivity was better for paracetamol than caffeine in the mixture solution. In

this investigation, degradation excitation of analytes on the surface or in the gas phase was found to cause changes in intensity with time. The temperature was measured using the exact same PADI parameters using a thermocouple (chromel-alumel type) by contact of the visible plasma with under TLC plate, and using a thermal camera by contact the visible plasma with the top of the TLC plate without a sample. The temperature in the middle of the TLC plate was measured for 2 minutes. The temperature increased quickly to 45 °C, after which it increased slowly to 60 °C, and then dropped until 2 minutes. It was below 60 °C when the analysis time reached 45 seconds. This indicated why the $[M+H]^+$ peaks of both paracetamol and caffeine increase in intensity up to ~ 45 seconds, after which they decrease up to 1 minute. Little thermal changes could be detected within the area of the substrate exposed to the plasma, although sample heating does occur slowly up to a maximum of ~45 °C after ~30 seconds interaction.

The study has also identified pharmaceutical solids and liquids from glass slides and cotton swabs using direct mass spectrometric analysis (Chapter 5). This study has found that the differences in the intensity of protonated paracetamol and caffeine molecular ion between tablets and solutions and found to be 8x and 3x respectively. There no differences were observed in the behaviour of intensity ratios of 152/195 and 194/195 between cotton swab and glass slide. Quantification analysis was also showed that no significant differences were found between the R^2 of paracetamol and caffeine whether using glass slides, cotton swabs or TLC plates. However, compared with the glass slide and TLC plate, the LOD and LOQ can be improved when using cotton swabs as a substrate. The results have also shown that the LOD for paracetamol was lower than caffeine in the 1:1 mixture solution using glass slides and cotton swabs. To investigate the heating causes on the sample during the analysis, The temperature was measured using the exact same PADI parameters using a thermal camera by interacting the visible plasma with a tablet. The temperature in the

middle of paracetamol tablet was measured for 5 minutes. The temperature increased dramatically to 75 °C at 45 seconds, after which it increased slowly to 80 °C at 1 minute, and then dropped to 36 °C until 5 minutes. This indicated why the $[M+H]^+$ peak for paracetamol increased in intensity up to ~ 45 seconds, after which they decrease up to 1 minute.

Another important finding of this study was that PADI mass spectrometry can be used for monitoring imine (Schiff base) formation as a model for pharmaceutical production (Chapter 6). This reaction was selected because there is possible to follow the reaction without the need to isolate the intermediate compound, and the reaction between aromatic amine and aromatic aldehyde would expect to give stable imine. The PADI-MS and FTIR results confirmed that the reaction between 4-nitrobenzaldehyde and para-anisidine was complete in less than 1 hour. However, the reaction was difficult to monitor by TLC and HPLC methods. The HPLC only showed the reactants and this may be due to the reaction being driven back in the direction of the reactants during HPLC. There were differences in the results of PADI-MS and FTIR with that by TLC and HPLC. PADI-MS has been used directly to monitor the imine formation using cotton swabs to sample without the need for preparation or pre-concentration. The results indicated the cotton swab to be better than the TLC plate and glass slide, giving good signals in the PADI spectra, which were in accordance with FTIR measurements. PADI-MS was a convenient and simple and fast technique to monitor the reaction of imine formation and provided more details about the chemical structure of the reaction materials. Together these results show that use of an optimised PADI-MS method has been able to monitor the progress of chemical reactions. The results of the study showed that the PADI-MS method is simple, sensitive, fast, has good linearity and small amounts of samples are required for analysis compared to other methods. The PADI-MS conditions were optimised of 8 W and a carrier gas flow of 224

mL/min (inner flow) and (224 mL/min outer flow). It is important to increase protonation as a way to improve sensitivity, and this was achieved by passing the helium flow over a water-filled reservoir. Results suggest that the analysis of paracetamol and caffeine mixture using helium with water vapour as gas flow is indeed more sensitive than using dry helium. In addition, the diagnostic $[M+H]^+$ at m/z 195 peak of caffeine was only observed when using helium with water vapour. This may be explained by referring the pK_a . The pK_a for caffeine is 14 (basic compound), therefore, it can readily gain a proton from water. The results indicate the length of analysis time up to ~ 45 seconds was the optimum time to get good spectra. These findings suggest in general that the samples can be analysed easily by PADI-MS, with rapid analysis in less than 45 seconds giving molecular ion information. Minor effects from the plasma can be seen from 30 s and that it only becomes problematic after 45 seconds. There is no difference observed between the measurement of paracetamol presented in a tablet and when presented in a mixture of caffeine in a Panadol tablet, while a significant difference was observed between tablets and solutions. The observed higher sensitivity for paracetamol in tablets, pure and mixture solutions in comparison with caffeine could be attributed to either pK_a or that the caffeine did not desorb as readily as paracetamol. The amount of molecules per droplet could also be another reason for this. The number of moles for paracetamol in the individual and mixtures is higher than for caffeine. The results did not show any important differences of the signal intensity of $[M+H]^+$ for paracetamol and caffeine whether used pure or mixture solutions, and this indicates that matrix of analytes was not affected.

On the other hand, a limitation of the PADI-MS technique is that the length of interaction time between the visible plasma and sample should be up to 45 seconds. This can give a good signal and more information of molecules, and the samples can be analysed easily by

this technique. With a long analysis time, it can see minor effects from the plasma that starts from 30 seconds, which becomes a problem after 45 seconds.

Quantitative analysis using a TLC plate, glass slide and cotton swab was compared for individual and paracetamol /caffeine mixtures and there were important similarities and differences between these substrates. A positive linear correlation was found between intensity and concentrations of paracetamol /caffeine mixture using glass slides and cotton swabs. No significant differences were found between the R^2 of paracetamol and the caffeine whether use glass slides, cotton swabs or TLC plates. Compared to a glass slide and TLC plate, the cotton swab was the best substrate to optimise the LOD and LOQ for individual and paracetamol /caffeine mixtures due to higher signal intensities compared to glass slide and TLC plate. The results also showed that using a cotton swab can give a higher signal-to-noise ratio (S/N) of 4-nitrobenzaldehyde and para-anisidine compared to those of a TLC plate and glass slide when studying pharmaceutically relevant reactions. This could be attributed to the solvent (dichloromethane) being absorbed very quickly by the cotton.

There are some recommendations for further research work including the findings and contribution of the study. The analysis of analytical methods provided an important opportunity to advance the understanding of the behaviour of molecules tablets with time after exposure to the NTP. These findings enhance our understanding of the plasma interaction with samples and investigation of chemical ionisation methods. The method presented here may be applied for future practice in several areas including biomedical, food industry and environmental. In future work, this NTP of PADI should be compared with other plasmas to analyse pharmaceutical tablets by demonstrating the findings of this study such as numerous micro-discharge produce streamer of LTP and weakly visible plume, discharge gas heated of DART. Future research should also concentrate on the

quantitative analysis of mixture solutions from TLC plates using this method. It would also be useful to use accurate mass and tandem-MS to identify more ions and develop a better understanding of the ionisation process. Further studies using the potential such as induction of chemicals in the carrier gas to aid with chemical ionisation, e.g., formic acid and ammonia need to be carried out in order to ionise samples and stabilise specific fragments due to e.g., proton donor effects. Another possible area of future research would be to investigate use of other plasma sources that are cheaper than helium and have different energy such as argon and nitrogen. The PADI-MS technique may be applied for identification and monitoring of other pharmaceutical tablets and mixture solutions using these substrates. This study has also found that PADI-MS can be applicable to monitor many types of pharmaceutical reactions.